MANUAL ON LOW CYCLE FATIGUE TESTING

STP 465

AMERICAN SOCIETY FOR TESTING AND MATERIALS

MANUAL ON LOW CYCLE FATIGUE TESTING

ASTM SPECIAL TECHNICAL PUBLICATION 465

List price $12.50

AMERICAN SOCIETY FOR TESTING AND MATERIALS
1916 Race Street, Philadelphia, Pa. 19103

Library of Congress Catalog Card Number: 70-97730
SBN 8031-0023-X

NOTE

The Society is not responsible, as a body,
for the statements and opinions
advanced in this publication.

Printed in Baltimore, Md.
December 1969

Foreword

The *Manual on Low Cycle Fatigue Testing* has been compiled by Subcommittee VIII on Fatigue Under Cyclic Strain of ASTM Committee E-9 on Fatigue. The editorial work was coordinated by R. M. Wetzel, Ford Motor Co. L. F. Coffin, Jr., General Electric Co., is chairman of Subcommittee VIII.

Related
ASTM Publications

Fatigue Crack Propagation, STP 415 (1967), $30.00

Electron Fractography, STP 436 (1968), $11.00

Bibliography on Low Cycle Fatigue 1957–1967

(microfiche), STP 449 (1969), $3.00

Fatigue at High Temperature STP 459 (1969) $11.25

Contents

Introduction

In the course of the last 15 years a very considerable interest has developed in the testing of metals where the controlling variable is cyclic strain rather than cyclic stress. Commonly referred to as low cycle fatigue testing, it has now developed to a state of refinement such that a "discipline" exists, at least among those working actively in the field. This special technical publication has been prepared to share the accumulated knowledge on the procedures, techniques, and skills now employed by several experts in the field. It is a collection of individually prepared papers describing the practices and viewpoints which each of the several authors feels best answer his particular testing requirements. Although there is much in common in many of the papers, there is no attempt made here to express a consensus; the reader is left to determine for himself which approach or combination of approaches is best suited to his particular needs. It should be further emphasized that the subject is specimen testing rather than component testing, an important distinction which must be reckoned with in relating the fruits of this work to the design of real parts.

The interest in low cycle fatigue testing stems directly from the need for information on metals when subjected to relatively few cycles of controlled cyclic strain. It may come from a search for methods to study the behavior of metals basically, where the interest is in developing mechanisms for explaining how microstructural and atomic effects can lead to the observed deformation and fracture characteristics, or it may come from the search for quantitative information to predict the life of engineering components subjected to a cyclic history similar to that produced in the laboratory. The latter has become the principal driving force for the development of low cycle fatigue testing methods.

Technological advance in the past 15 years has moved toward the use of higher and higher temperatures in materials for engineering structures, accompanied by an increase in the severity and frequency of thermal transients during operation. This trend is translatable into cyclic thermal stresses, or other cyclic loading, which fall directly in the category of controlled strain behavior. Some examples of components subject to these conditions include steam turbine rotors and shells, aircraft or land gas turbine buckets and wheels, and nuclear pressure vessels and fuel elements. Design procedures based largely on experimental information attained in laboratory testing have evolved for treating these problems. Hence, low

cycle fatigue testing has played an important role in our technological advance.

Since this publication is devoted to fatigue testing in the low cycle regime, it is necessary to distinguish between it and fatigue testing more generally. By definition, failure in low cycle fatigue occurs in fewer than 50,000 cycles. It is further characterized by the existence of a stress-strain hysteresis loop and by the measurement of a plastic strain range in the test specimen. To meet these requirements certain special testing techniques not generally considered in high cycle fatigue testing assume importance. To produce failure in a few cycles, strain rather than stress must be controlled. This places special emphasis on strain-detecting devices and accompanying instrumentation for measurement and control. Further, the loading is nearly always fully reversed, since, with the plastic strain ranges experienced, mean stresses are quickly relaxed. Thus nearly equal tensile and compressive loads are encountered, requiring gripping systems capable of transmitting these loads from machine to specimen without slippage or misalignment. Specimen configuration becomes important, since buckling or bending must be avoided and reliable strain measurements must be made. While these problems exist to some extent in all fatigue testing, they are of special importance in low cycle fatigue.

In selecting subdivisions for this publication, one basis has been the choice of loading, that is, whether it be by uniaxial loading, bending, torsion, or otherwise. Most work was carried out either on uniaxial loading (push-pull) or in bending. More space has been given to push-pull loading, with only one contribution directed to bending. The reader should not infer from this emphasis that a preference in fact exists; rather, he should select the test best suited to individual needs.

Controlled strain testing can also be subdivided into constant temperature and cyclic temperature (thermal fatigue). In cyclic temperature the mechanical strain imposed on the specimen is derived entirely or in part from thermal expansion. Although this is a more complex test to conduct in the laboratory, it may in fact be more realistic in its representation of service conditions. One chapter is devoted to this important subject.

The balance of the papers deal with uniaxial testing: from the viewpoint of metals research, from a mechanics of materials view, and from the viewpoint of high temperature testing. While some duplication in technique appears, we believe this emphasizes the areas of general agreement among the investigators and the laboratories they represent. It also illustrates, the several ways of tackling the same problem: choice of grips, specimen design, strain measurement, instrumentation, testing machine, etc.

This publication is a contribution of Subcommittee VIII on Fatigue Under Cyclic Strain of ASTM Committee E-9 on Fatigue. As chairman of

the subcommittee I should like to acknowledge the contributions made by the several authors. Such a publication could not have been undertaken without the help of many others, among whom I should like to thank R. S. Carey who has prepared the Index, and the editorial committee coordinated by R. M. Wetzel and ably supported by J. A. Dunsby and V. Weiss. Finally, the full support of Committee E-9, H. F. Hardrath, chairman, is gratefully appreciated.

L. F. Coffin, Jr.,
Metallurgy and Ceramics Laboratory,
General Electric Co., Schenectady, N.Y.;
Chairman, Subcommittee VIII,
ASTM Committee E-9

D. T. Raske[1] *and JoDean Morrow*[1]

Mechanics of Materials in Low Cycle Fatigue Testing

REFERENCE: Raske, D. T. and Morrow, JoDean, **"Mechanics of Materials in Low Cycle Fatigue Testing,"** *Manual on Low Cycle Fatigue Testing, ASTM STP 465*, American Society for Testing and Materials, 1969, pp. 1–25

ABSTRACT: The purpose of this paper is to outline a method for evaluating the low cycle fatigue resistance of a metal from the mechanics of materials viewpoint. This includes a discussion of the fatigue properties and the effect of repeated plastic straining on the mechanical properties of metals. The cyclic stress-strain curve is defined as the locus of tips of several stable hysteresis loops obtained at different cyclic strain ranges. An expression is presented for mathematically representing the locus of their tips, and a number of experimental methods are discussed for determining the stable cyclic stress-strain properties.

Experimental techniques for low cycle fatigue testing and methods of interpreting results are presented. The equations which relate the elastic and plastic components of cyclic strain amplitude to fatigue life are developed. A means of approximating the strain-life curve using these relations is presented.

KEY WORDS: tests, fatigue (materials), fatigue tests, stresses, strains, metals, strain cycling, stress cycle, low cycle fatigue, fracture, plastic flow

Nomenclature

- A Actual, instantaneous, area
- A_f Area at fracture
- A_o Original area
- b Fatigue strength exponent, slope of log σ_a-log $2N_f$ plot
- c Fatigue ductility exponent, slope of log $(\Delta\epsilon_p/2)$-log $2N_f$ plot
- D Actual instantaneous diameter
- D_o Original diameter
- e Engineering strain, equal to S/E when the strain is elastic
- E Modulus of elasticity
- K Strength coefficient; true stress to cause a true plastic strain of unity in the equation $\sigma = K \epsilon_p^n$

[1] Research assistant and professor, respectively, Department of Theoretical and Applied Mechanics, University of Illinois, Urbana, Ill. 61801. Dr. Morrow is a personal member ASTM.

L Instantaneous gage length
L_f Gage length at fracture
L_o Original gage length
n Monotonic strain hardening exponent
n' Cyclic strain hardening exponent
N_f Fatigue life, number of cycles to failure
$2N_f$ Number of reversals to failure
P Axial load
P_f Axial load at fracture
S Engineering stress, axial load divided by original area, P/A_o
S_{ty} Tensile yield point, usually taken as the lower yield point
S_u Ultimate tensile strength
S_{ys} Offset yield strength
S'_{ys} Cyclic offset yield strength
ϵ True strain, equal to σ/E when the strain is elastic
ϵ_e Elastic component of strain
ϵ_f True fracture ductility, true strain at fracture in monotonic tension
ϵ_f' Fatigue ductility coefficient, intercept of log $(\Delta\epsilon_p/2)$-log $2N_f$ plot
ϵ_n True strain at necking in monotonic tension
ϵ_p Plastic component of strain
$\Delta\epsilon$ Total strain range
$\Delta\epsilon_e$ Elastic strain range
$\Delta\epsilon_p$ Plastic strain range
ν Poisson's ratio
σ True stress, axial load divided by actual area, P/A
σ_a Stress amplitude
σ_f True fracture strength, true stress at fracture in monotonic tension, P_f/A_f, corrected for necking
σ_f' Fatigue strength coefficient, intercept of log σ_a-log $2N_f$ plot
σ_{ty} True tensile yield point
σ_{ys} True offset yield point

Each research group with experience in low cycle fatigue testing has evolved methods and procedures which fit their particular needs and testing capabilities. Thus, there is as yet no "standard" low cycle fatigue test.

The purpose of this paper is to outline a method for evaluating the low cycle fatigue resistance of a metal from the mechanics of materials viewpoint; that is, representative smooth samples of a particular metal are subjected to known strains and their mechanical resistance is measured. Axial straining is generally used so that the quantitative results can easily be correlated with the monotonic tension properties of the metal.

Influencing factors such as temperature changes, corrosive environments, material inhomogeneity, notches, and so on are avoided or held constant. This is so that a quantitative description of the metal's mechanical resistance to repeated strain and stress can be obtained which is independent of the shape or type of structural member and the service environment in which the metal is to be used.

This approach admittedly ignores or circumvents many of the important features of fatigue behavior that should be of interest to practical engineers; however, it is still believed to be a worthwhile and valid method of characterizing the low cycle fatigue resistance of the *metal itself.*

In this sense our approach is like the usual tension tests that are conducted in great numbers to obtain quantitative measures of the stiffness, strength, and ductility of metals. Tension test results are demanded by design engineers to guide their judgment of the potential resistance of a structural member, even though the metal is seldom subjected to simple tension and even though there are a host of influencing factors present in service which are not assessed in the usual tension test.

Specimens

The overall size and type of specimen used for low cycle fatigue testing is often dictated by the form of the available metal stock. Even when this is not a consideration, there are other factors which may influence the design. Obviously, the specimens must be "sized" to the load capacity of the testing system employed. Also the enlarged threaded ends which are generally used to fasten the specimen to the testing system must be designed to insure failure in the reduced section. A ratio of between 4 to 6 for the areas of the threaded end and the reduced section is usually satisfactory.

Several successful low cycle fatigue specimen configurations are given in Fig. 1 along with comments on their limitations and applicability.

The correct or optimum choice of specimen size and shape also depends upon the strength and ductility of the metal being investigated. Consequently, one should plan to measure the tensile properties of the metal before extensive fatigue testing is performed. If properly designed, the fatigue specimens will also serve as monotonic tension test specimens.

While it is important to machine the samples carefully so they are straight and axial, normally it is not necessary to be as careful about the surface finish in the reduced section as it is for long-life fatigue specimens. Since plastic strain is usually present in low cycle fatigue testing, the scatter in results is usually not as great as in tests where longer lives result. This is illustrated in Fig. 2 for an SAE 4340 steel. One reason is that the plastic action "washes out" many of the scatter-producing factors. This is partic-

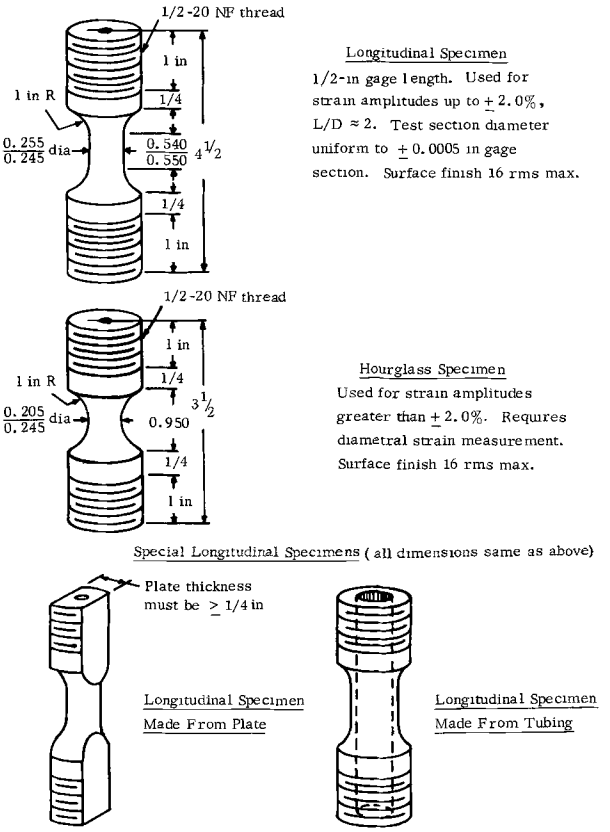

FIG. 1—*Specimen designs.*

ularly true for reasonably ductile metals in the low cycle fatigue region because the large amount of cyclic plastic strain imposed during the fatigue test eliminates initial residual stresses and greatly reduces the influence of small scratches and other stress raisers. Furthermore, at short lives where the slope of the strain-life curve is large, scatter results in small variation in life. When longer lives are expected and when metals have low ductility, the same care should be taken to obtain a smooth surface which is as free of residual stresses as is generally taken with long-life fatigue samples.

After the machining has been completed, the diameter and hardness of the specimens are measured. Normally the specimen diameter is measured at three locations in the gage section. At each location, the diameter is measured at least twice (90 deg apart) and the average of the two values is used to compute the area. If these areas differ greatly, the specimen should be rejected or used only for preliminary or exploratory tests.

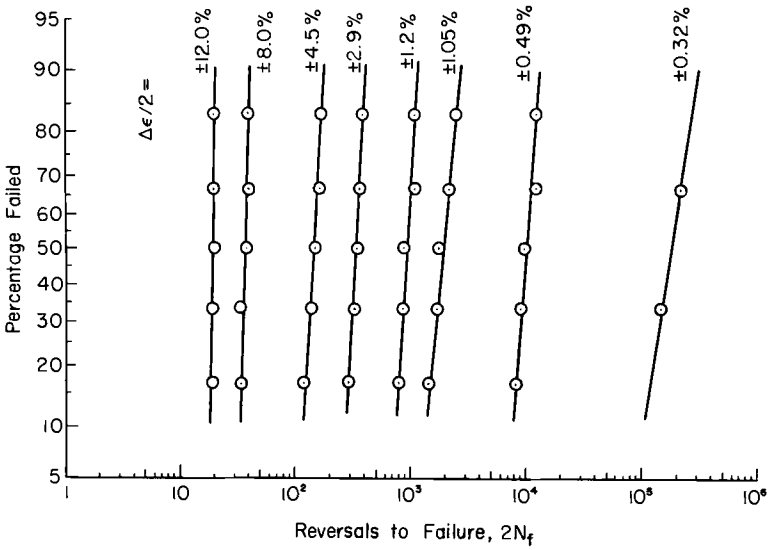

FIG. 2—*Scatter in fatigue life for completely reversed strain cycling—SAE 4340 steel. See Ref.* 11.

Hardness measurements should be made on each specimen to insure uniformity. It is usually satisfactory to use the average of three hardness values from each shoulder adjacent to the gage section. If possible, the Vickers or Brinell hardness number should be employed since these correlate better with the metal's strength [*1*][2]. However, if a large number of specimens of different hardness are to be tested, the Rockwell hardness test will suffice once each hardness group has been categorized.

Once these preliminary steps have been completed, it is desirable to store the specimens in an evacuated bell jar or individually in test tubes containing noncorrosive anhydrous salts.

Tension Testing

It will be seen later that results from the monotonic tension test can be used as the half-cycle fatigue results. In addition to measuring the engineering stress-strain properties listed in Table 1, the true stress-strain properties listed in Table 2 should also be determined. Since most engineers are not accustomed to dealing with true stress and strain and with true stress-strain properties, these are carefully defined in the Appendix. These are also shown on the stress-strain curve in Fig. 3 as well as the usual engineering stress-strain properties.

[2] The italic numbers in brackets refer to the list of references at the end of this paper.

TABLE 1—*Engineering stress-strain properties.*[a]

Property	Definition	Remarks
E, modulus of elasticity, psi	Stress to cause an elastic strain of unity in Hooke's Law, $\sigma = E\,\epsilon$ ($\sigma = E$ when $\epsilon = 1$)	Taken as the slope of the stress-strain curve at low stresses
S_{ty}, tensile yield point, psi	Stress to cause sudden gross yielding; applies only if there is a "flat top" region of yielding	Usually taken as the lower yield point
S_{ys}, tensile yield strength, psi	Stress to cause a specified amount of inelastic strain, usually 0.2%	Determined by constructing an offset line with a slope of E (See Fig. 3)
S_u, ultimate tensile strength, psi	Engineering stress at the maximum load, P_{max}/A_o	Generally governed by necking (engineering stress to cause necking)
$\%RA$, percent reduction in area	Percentage reduction in cross-sectional area required to cause fracture: $100(A_o\text{-}A_f)/A_o$	A_f measured at the minimum section after fracture
ν, Poisson's ratio	Ratio between diametrical strain and longitudinal strain	Taken as the ratio of the longitudinal strain to the diametrical strain at stresses below the yield point

[a] The proportional limit, percent elongation, and engineering toughness have been purposely omitted since their definitions are arbitrary and misleading and they are not directly relevant to fatigue.

Methods of measuring true stress-strain behavior reduce to simultaneous determinations of the load and area of the tensile specimen. In the crudest type of test, a hand-held, ball-tipped micrometer may be used for this purpose. The opening of the micrometer is preset, and load is read at the instant the micrometer can be passed over the diameter of the specimen. With more sophisticated instrumentation, a clip gage may be used to obtain an electrical signal proportional to the diameter. Regardless of the method used to determine true stress and strain during the test, the load and specimen area at fracture must be carefully determined.

Once the monotonic stress-strain properties have been determined, it is possible to estimate the cyclic stress-strain behavior of the metal under investigation.

TABLE 2—*True stress-strain properties.*

Property	Definition	Remarks
E, σ_{ty} and σ_{ys}	Same as E, S_{ty} and S_{ys} in Table 1	At small strains true and engineering values are nominally the same
σ_f, true fracture strength, psi	True tensile stress to cause fracture, P_f/A_f	Should be corrected for influence of lateral stresses due to necking[a]
ϵ_f, true fracture ductility	True plastic strain required to cause fracture, $\ln(A_o/A_f)$	Related to % RA by, $\ln(100/100-\%RA)$
n, strain hardening exponent	The power to which the plastic strain must be raised to be proportional to the stress	Taken as the slope of the $\log \epsilon_p - \log \sigma$ plot[b]
K, strength coefficient, psi	True stress to cause a true plastic strain of unity in the equation,[c] $\sigma = K \epsilon_p^n$	If σ_f is corrected as shown in Fig. 16, $K = \sigma_f/\epsilon_f^n$

[a] The load at fracture divided by the area at fracture is higher (for example, about 20 percent when $\%RA = 70\%$) than the corrected value, depending on the severity of the neck (See p. 250 of Ref *1*)

[b] Can also be shown to be equal to the true strain at which necking occurs (See Appendix).

[c] If $\epsilon_f < 1$ the flow curve is extrapoalted to a plastic strain of unity to obtain K.

For each metal there is a range of potential strength or hardness which can be achieved by cold working, annealing, heat treating, etc. If a metal is initially soft, it will cyclically harden; if it is initially hard, it will probably soften [*2*]. Some intermediate state will be approached which represents a stable condition for the particular metal under the imposed conditions. The initial state is reflected by the *monotonic strain hardening exponent, n.* For most metals subjected to cyclic loadings, the value of the *cyclic strain hardening exponent, n'*, lies between 0.10 and 0.20. Consequently if n is initially low (a "hard" metal), the expected cyclic behavior would be for n' to increase. On the other hand, an initially high n (a "soft" metal) would indicate that n' will decrease. This behavior is schematically illustrated in Fig. 4. These cycle-dependent changes are also reflected by measurable changes in a host of bulk material properties including indentation hardness [*3–5*]. The effects of cycling on the properties determined from the monotonic tension test are shown in Table 3.

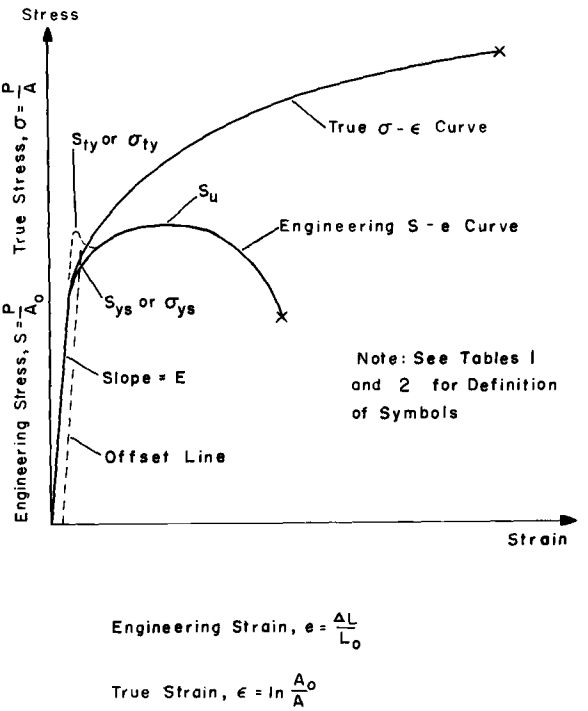

FIG. 3—*Definition of stress-strain properties.*

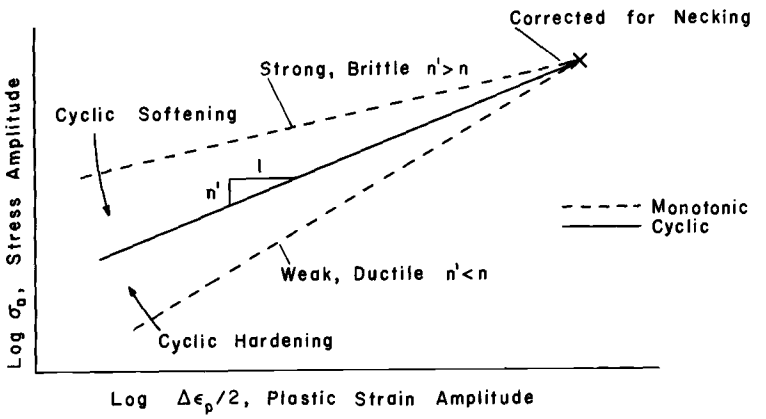

FIG. 4—*Comparison of monotonic and cyclic strain hardening exponents.*

TABLE 3—*Cycle-dependent changes in the mechanical properties.*

Mechanical Property	Effect of Cycling
E, modulus of elasticity	Negligible Effect
Hardness S_{ty}, tensile yield point[a] S_{ys}, offset yield strength S_u, ultimate strength	These are flow properties, since they are related to the ease with which plastic deformation can occur, and are all potentially changed by cycling. They will increase if the metal cyclically hardens, decrease if it cyclically softens, or remain unchanged if the metal is initially in a stable state. The initial n and the ratio S_u/S_{ys} can be used to estimate whether a metal will cyclically soften or harden.
σ_f, true fracture strength ϵ_f, true fracture ductility $\%RA$, percent reduction in area	These properties may be classed as fracture properties, since they are measures of the fracture resistance. They may be changed somewhat by cycling but not to the degree that the flow properties are changed.[b]
n, strain hardening exponent	This is also a flow property and can be greatly changed by cycling. All metals seem to cyclically adjust to a cyclic strain hardening exponent of $0.10 < n' < 0.20$. If n is initially low (a severely hardened metal) n will increase, if n is high it will decrease. Within the range 0.10 to 0.20, n will change only slightly.

[a] The yield point phenomenon may be removed by cyclic stressing. After a number of cycles below the yield point the hysteresis loop may open and the yield point disappear [*4*], indicating a cyclic softening. At higher cyclic strains the same metal may harden.

[b] There have been a number of investigations of "exhaustion of ductility" and loss of "residual strength" of fatigued specimens and components. It has been found that the strength and ductility are not drastically reduced until the later stages of fatigue where large cracks are present.

The preceding discussion indicates that the flow properties determined from the monotonic tension test may not reflect the ability of a metal to resist repeated straining. Consequently, these properties must be determined after the cycle-dependent changes have been completed.

The Cyclic Stress-Strain Curve

The initial cyclic rate of change in properties is greatly influenced by the cyclic strain range. However, the amount of change rapidly diminishes with repeated cycling during the first few percent of the fatigue life. As long as the control conditions are not altered, a metal will quickly adjust to a nearly stable condition which is reflected by a constant terminal hardness and a

TABLE 4—*Fatigue properties*[a] *and their approximate relation to other materials properties.*

Fatigue Property	Definition	Remarks
ϵ'_f, fatigue ductility coefficient	The true strain required to cause failure in one reversal. Taken as the intercept of the $\log(\Delta\epsilon_p/2) - \log 2N_f$ plot at $2N_f = 1$	Can be approximated by $0.002(\sigma'_f/S'_{us})^{1/n'}$; ϵ'_f is between ϵ_f and $\epsilon_f/2$ in magnitude and ranges between nearly 0 and 1^+ for steel.
c, fatigue ductility exponent	The power to which the life in reversals must be raised to be proportional to the plastic strain amplitude. Taken as the slope of the $\log(\Delta\epsilon_p/2) - \log 2N_f$ plot	Nearly a constant for metals between about -0.50 and -0.70 with -0.60 as a representative value; value is reasonably independent of composition hardness, test temperature, etc.
σ'_f, fatigue strength coefficient, psi	The true stress required to cause fracture in one reversal. Taken as the intercept of the $\log \sigma_a - \log 2N_f$ plot at $2N_f = 1$	Proportional to the true fracture strength; $\sigma'_f \approx \sigma_f$, for practical purposes; ranges between about 100 and 500 ksi for heat-treated metals.
b, fatigue strength exponent (also Basquin's exponent [6])	The power to which the life in reversals must be raised to be proportional to the stress amplitude. Taken as the slope of the $\log \sigma_a - \log 2N_f$ plot.	A maximum of about -0.12 for softened metals—decreases to a minimum value of about -0.05 with increasing hardness and may increase again at high hardness in the case of heat-treated metals.

[a] Determined on smooth, carefully prepared, laboratory specimens under controlled, completely reversed cycling.

nearly stable mechanical hysteresis loop. By connecting the tips of several stable loops at different strain ranges, a smooth curve is formed which is called the *cyclic stress-strain curve*. Morrow [6] has shown that this curve can be mathematically expressed as

$$(\Delta\epsilon/2) = (\Delta\epsilon_e/2) + (\Delta\epsilon_p/2) = (\sigma_a/E) + \epsilon'_f(\sigma_a/\sigma'_f)^{1/n'} \quad \ldots\ldots\ldots (1)$$

which is similar to Eq 20 in the Appendix for the monotonic stress-strain curve. From Eq 1, σ'_f and ϵ'_f are defined as the *fatigue strength coefficient* and *fatigue ductility coefficient,* respectively, and their relationship to other material properties is described in Table 4.

For metals which cyclically harden, the cyclic stress-strain curve will be above the monotonic stress-strain curve; for metals which soften, the cyclic stress-strain curve will be below the monotonic curve. By cycling, it is possible to increase the yield strength of a completely annealed pure metal by a factor of 5, or more, and to reduce the yield strength of the same metal by as much as a factor of 2 if it is initially highly cold worked. Figure 5 illustrates this behavior for typical cyclically hardening and cyclically softening metals.

Since most metals stabilize rather quickly after changes in the cyclic strain amplitude, it is possible to determine the cyclic stress-strain curve from one specimen. The following describes three techniques which have been used at the University of Illinois [*6, 7*] to determine this curve.

Multiple Step Tests—Determining the cyclic stress-strain curve from multiple step testing consists of cycling one specimen at several levels of strain amplitude. The number of cycles at each level should be sufficient

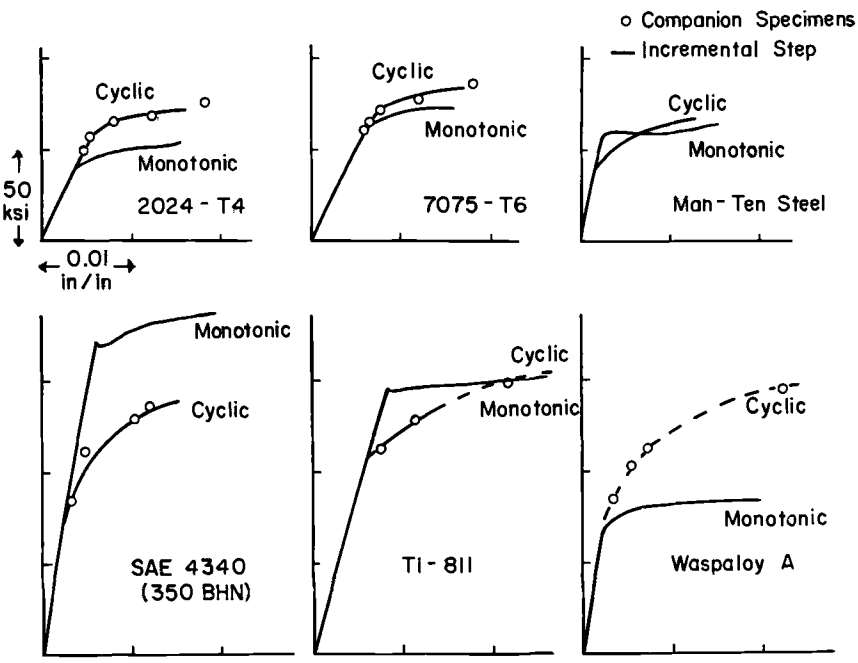

FIG. 5—*Monotonic and cyclic stress-strain curves for several materials. See Ref.* 7.

to achieve stability but small enough to avoid serious fatigue damage. With the stable hysteresis loops superimposed, the cyclic stress-strain curve is obtained by drawing a smooth curve through the tips of the loops.

Incremental Step Tests—Another means of producing the cyclic stress-strain curve consists of subjecting a specimen to blocks of gradually decreasing and then increasing strain amplitudes as shown in Fig. 6. A maximum strain amplitude of ±1.5 to 2.0 percent is usually sufficient to cyclically stabilize the metal quickly without the danger of causing the specimen to neck, fail, or buckle before a stable state is achieved. The cyclic stress-strain curve is then determined by the locus of superimposed hysteresis loop tips.

One means of producing these curves is to use a Data-Trak (MTS Systems Corp., Minneapolis, Minn.) function generator to control the strain level of an MTS electrohydraulic closed-loop testing system similar to that described by Feltner and Mitchell [*8*]. With this equipment, the maximum strain amplitude is set on the testing system and the Data-Trak is used to provide a uniformly decreasing then increasing envelope for the strain amplitude. Figure 7 depicts a typical strip chart record obtained by this technique. Usually the Data-Trak and testing system are coordinated so that the zero strain amplitude is reached after 40 cycles and the maximum strain amplitudes after another 40 cycles. In this way a cyclic stress-strain curve is generated after three or four blocks of decreasing and increasing strain amplitude.

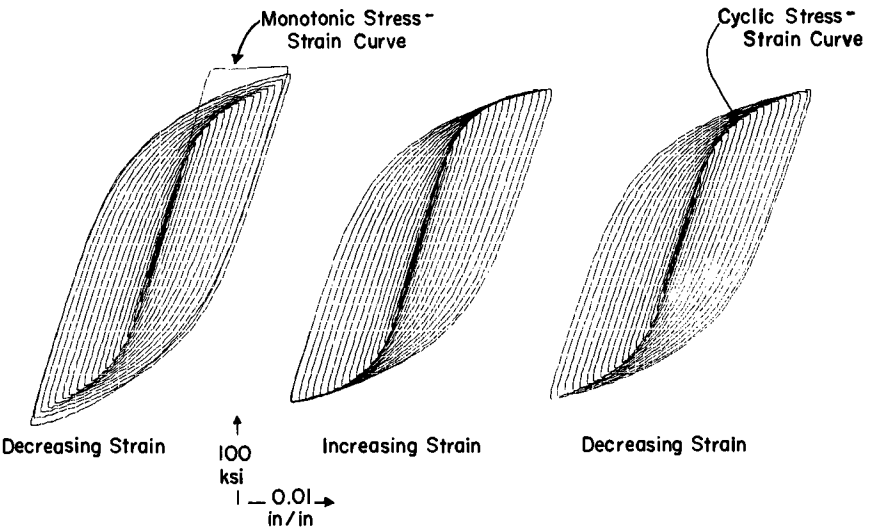

FIG. 6—*Stress-strain record of incremental step test on quenched and tempered SAE 4142, 380 BHN. See Ref.* 7.

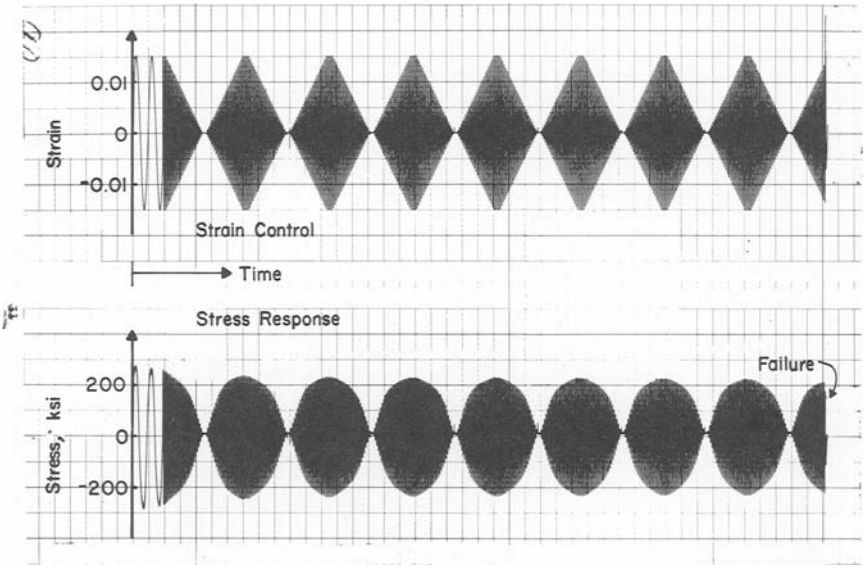

FIG. 7—*Strain-time, stress-time record of incremental step test on quenched and tempered SAE 1045 steel, 450 BHN. See Ref.* 7.

Monotonic Tension After Spectrum Straining—A third means of obtaining a cyclic stress-strain curve is to pull the specimen to fracture after a series of decreasing and increasing strain blocks similar to those described above. The tension test is conducted after a block of decreasing strain amplitude, once cyclic stability has been observed. Test results [7] indicate that this curve will fit reasonably well with the curves determined by the two methods previously discussed. However, since this technique requires separate specimens for the tension and compression curves, the incremental step test is recommended.

Strain-Controlled Low Cycle Fatigue Testing

Testing Sequence—Usually from seven to ten specimens are required to determine the low cycle fatigue resistance of a metal. For most metals this can be adequately described by testing at strain amplitudes between ±2.0 and ±0.2 percent. The result is a strain-life curve similar to that shown in Fig. 8.

The testing should be conducted so that the data points will be uniformly distributed along the log-life axis. To accomplish this, the strain-life curve is approximated so that fatigue lives can be predicted. The initial approximation is made from the results of the tension test, the cyclic stress-strain curve, and one strain-controlled fatigue test. The strain amplitude for this

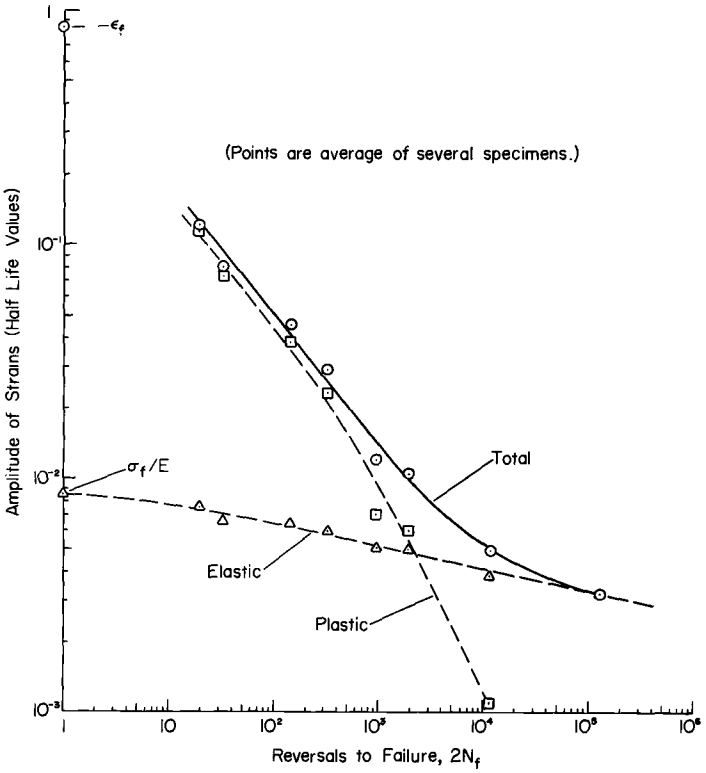

FIG. 8—*Life as a function of elastic, plastic, and total strain—SAE 4340 steel. See Ref.* 11.

fatigue test must be selected so that plastic strains larger than 10^{-3} and failures at about 10^3 reversals[3] result. It has been empirically found that a strain amplitude of ± 1 percent fulfills these requirements for all steels regardless of strength and for most ductile metals. Thus, testing is usually begun at this strain amplitude. Figure 9 shows typical hysteresis loops and strain-life curves for metals of different strength and ductility at this strain amplitude.

Before proceeding with this approximation, it is necessary to develop the equations which relate strain to fatigue life. As shown in Fig. 8, the total strain amplitude can be separated into its elastic and plastic components. In low cycle fatigue testing, the plastic component of the strain amplitude is characterized by the *fatigue ductility properties* and the elastic component by the *fatigue strength properties* of the metal.

[3] The convention adopted at the University of Illinois is to present fatigue results in terms of reversals to failure, $2N_f$, instead of cycles to failure, N_f.

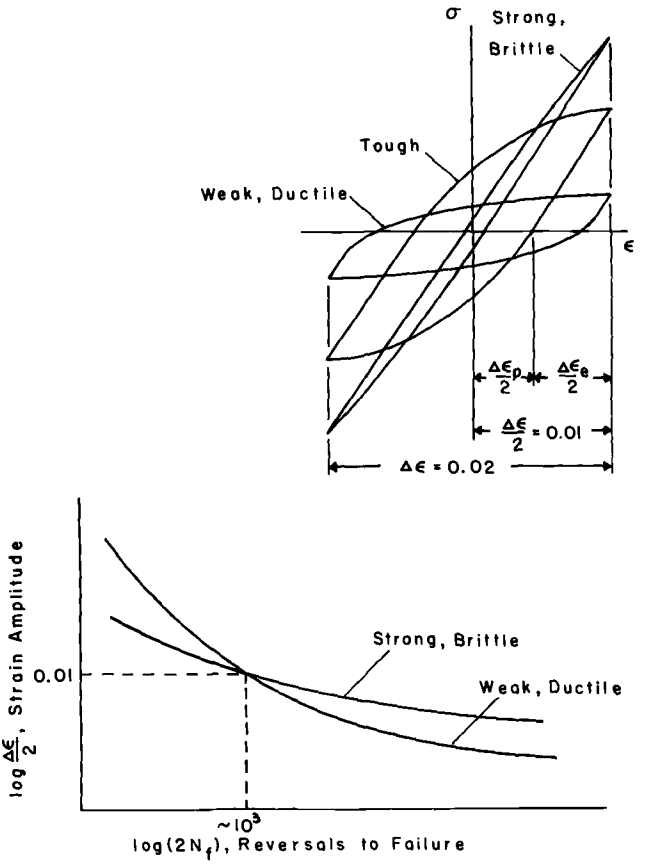

FIG. 9—*Schematic representation of the manner in which ductile and strong metals respond to cyclic strains of ±1 percent.*

Fatigue Ductility Properties—For a series of completely reversed tests at different strain ranges, a log-log plot of the fatigue life versus the stable plastic strain amplitude[4] usually gives a straight line. As illustrated in Fig. 10, the plastic strain intercept at one reversal is defined as the *fatigue ductility coefficient* and can be approximated by

$$\epsilon'_f = 0.002\,(\sigma'_f/S'_{ys})^{1/n'} \quad \ldots\ldots\ldots\ldots\ldots\ldots\ldots\ldots (2)$$

where $\sigma'_f = \sigma_f$ and S'_{ys} is the cyclic 0.2-percent offset yield strength [9]. The slope of the curve in Fig. 10 is also considered a fatigue ductility property. This is defined by the *fatigue ductility exponent, c.* Thus the

[4] Since the plastic strain usually changes in the course of the test, half-life values are used.

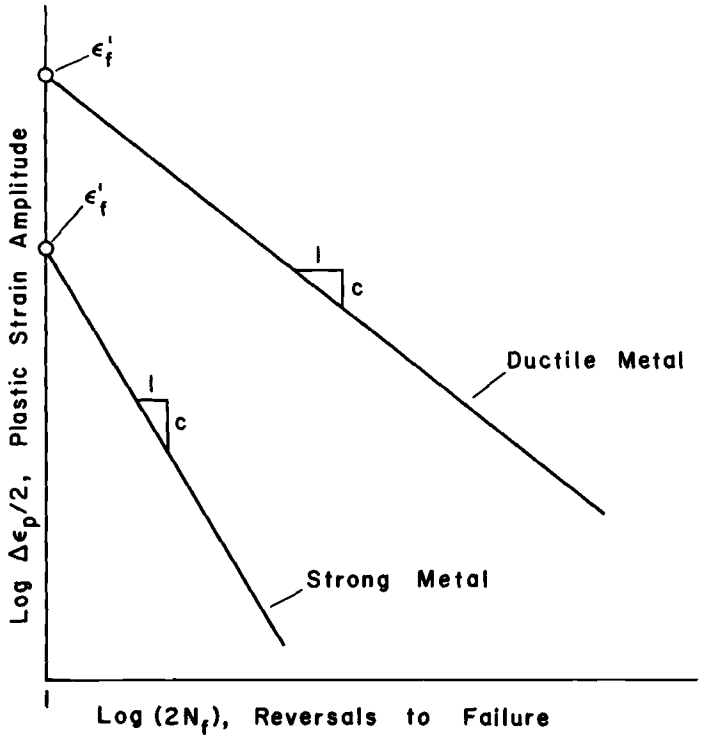

FIG. 10—*Schematic plastic strain-life curves showing the influence of strength and ductility.*

plastic strain amplitude can be written as

$$(\Delta\epsilon_p/2) = \epsilon'_f(2N_f)^c \quad (3)$$

Figure 10 also illustrates the overall level of fatigue ductility for strong and ductile metals. As indicated, the slope of the curve may be slightly different and the curve will be displaced in the upward direction for more ductile metals, and downward for less ductile metals.

Fatigue Strength Properties—In 1910 Basquin [*10*] proposed a linear relationship between the logarithm of the stress amplitude and the logarithm of fatigue life as illustrated in Fig. 11. The intercept at one reversal is defined as the *fatigue strength coefficient*. The *fatigue strength exponent, b*, is defined as the slope of the curve. Hence a relationship similar to Eq 3 can be written for the stress amplitude,

$$\sigma_a = \sigma'_f(2N_f)^b \quad (4)$$

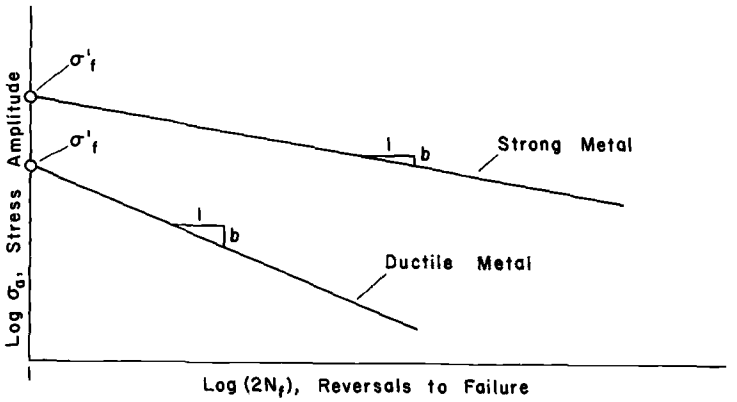

FIG. 11—*Schematic stress-life curves showing the influence of strength and ductility.*

where σ_a is taken as the half-life value of the stress amplitude. Equation 4 can also be derived by combining Eqs 1 and 3 to eliminate $\triangle\epsilon_p$ and letting $n'c = b$.

$$(\Delta\epsilon_p/2) = \epsilon'_f(\sigma_a/\sigma'_f)^{1/n'} = \epsilon'_f(2N_f)^c \quad \ldots\ldots\ldots\ldots\ldots\ldots (5)$$

Since the elastic strain amplitude is given by σ_a/E, the relationship between elastic strain and life is derived as

$$(\Delta\epsilon_e/2) = (\sigma_a/E) = (\sigma'_f/E)\,(2N_f)^b \quad \ldots\ldots\ldots\ldots\ldots\ldots (6)$$

Figure 11 shows that the fatigue strength of a ductile metal is usually less than that for a strong metal. The slope, however, is usually steeper for a ductile metal. The relationship between these properties and other material properties is also described in Table 4.

The strain-life curve can now be approximated as follows: The first reversal intercepts are determined by the *fatigue ductility coefficient* computed from Eq 2 and the *fatigue strength coefficient* approximated by the true fracture strength. The half-life plastic strain amplitude from the ±1-percent test is determined from the hysteresis loops recorded during the test. This results in a datum point on the strain-life curve. A straight line drawn through this point and the *fatigue ductility coefficient* results in the plastic strain-life curve. Similarly the elastic strain-life curve is the line drawn through the half-life elastic strain amplitude and the fatigue-strength coefficient. These curves, represented by Eqs 3 and 6, are then summed to give the total strain-life curve as shown in Fig. 12. The equation of this curve is written as

$$(\Delta\epsilon/2) = (\Delta\epsilon_e/2) + (\Delta\epsilon_p/2) \quad \ldots\ldots\ldots\ldots\ldots\ldots (7)$$

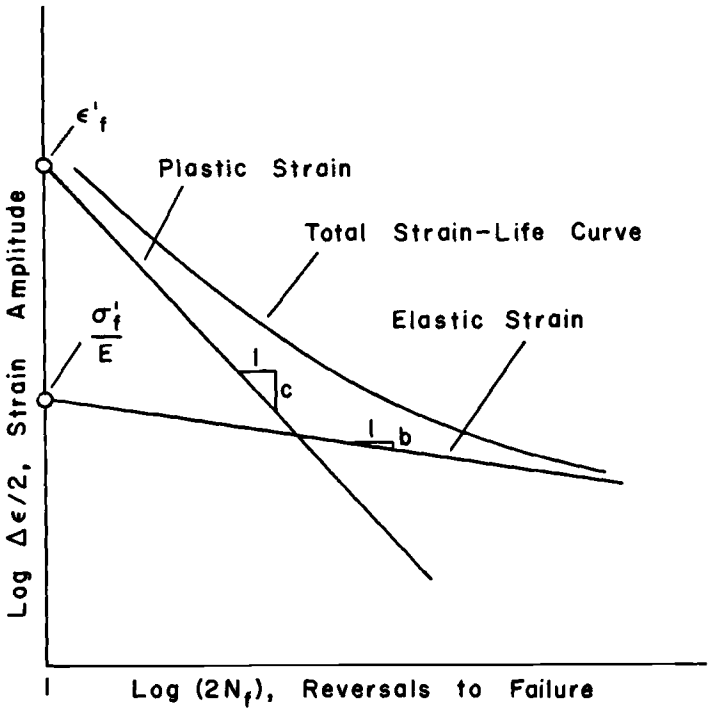

FIG. 12—*Life as a function of elastic, plastic, and total strain amplitude.*

With Eqs 3 and 6 this becomes

$$(\Delta\epsilon/2) = [(\sigma'_f/E)(2N_f)]^b + \epsilon'_f(2N_f)^c \quad (8)$$

The results of subsequent tests can then be used to improve the approximation of the strain-life curve. An accurate strain-life curve is especially important at long lives where a small change in the strain amplitude can change the life of the specimen by several orders of magnitude. Therefore it is best to test at the larger strain amplitudes first. Also, since the scatter is usually less at higher strain amplitudes [*11*], the fatigue lives of subsequent tests can be predicted with more confidence. An exception to this testing sequence would occur if more than one condition of the metal were to be tested. When more than one metal is tested it is usual to complete the testing at each strain amplitude using specimens from each condition. This testing sequence is more expedient because recalibration is usually unnecessary between tests.

Tests at strain amplitudes in excess of ±1.5 percent are usually begun in compression. The reason for this is twofold: First, since many of the

metals of interest cyclically soften, it is advantageous to utilize this behavior to eliminate the possibility of developing a locally necked region in the specimen during the first tensile loading. Starting the test in compression usually allows the metal to soften sufficiently to avoid this difficulty. Secondly, starting a test in this manner provides the initial portion of the monotonic compression curve for the material.

A summary of the testing sequence previously discussed is presented in Table 5. Also included is a brief description of each test and the application of the resulting data.

Testing Procedures

Most of the low cycle fatigue testing at the University of Illinois is conducted with 20-kip MTS closed-loop, servo-controlled hydraulic test systems similar to those described by Feltner and Mitchell [*8*]. Liquid metal grips as shown in Fig. 13 are used to insure proper axial alignment of the specimens. A detailed, pictorial description of one of these test systems is given in Ref *12*.

The first concern, once the testing equipment has been balanced and calibrated, is to select the testing frequency. For cyclic frequencies of 0.1

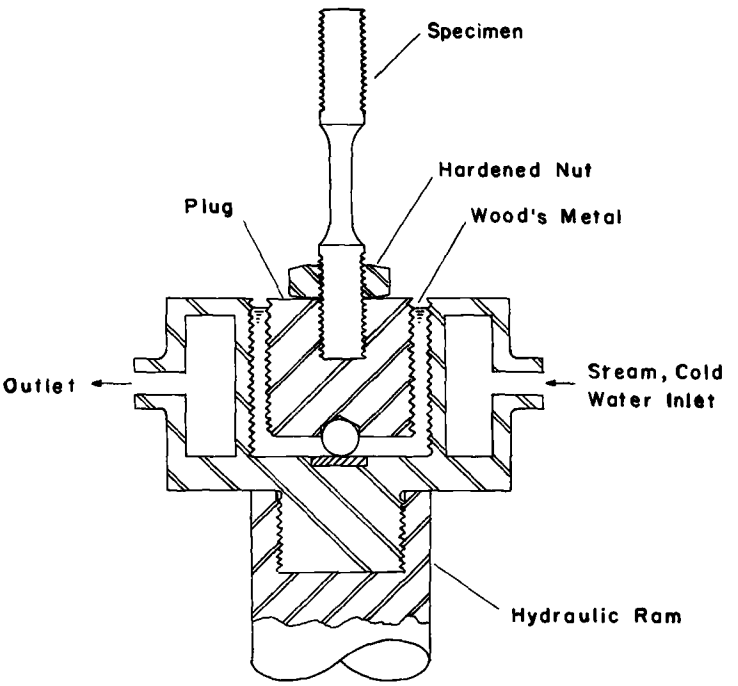

FIG. 13—*Self-aligning grip for low cycle fatigue testing.*

TABLE 5—*Summary of testing sequence and applications.*

Activity	Experimental Results	Application
Tension test	E, modulus of elasticity, psi	General; also used to check proper extensometer mounting
	S_y, tensile yield strength, psi	Compare with cyclic yield strength to determine degree of hardening or softening
	S_u, ultimate tensile strength, psi	Determines strain at which necking occurs, ϵ_u; also used to estimate fatigue strength at 10^6 reversals
	$\%RA$, reduction in area	Used to compute true fracture ductility, ϵ_f
	Stress-strain curve	Used to compute strain hardening exponent, n.
Cyclic strain-strain curve	S'_{ys}, cyclic yield strength, psi	Compare with monotonic yield strength to determine degree of hardening or softening
	Cyclic stress-strain curve	Used to compute cyclic strain hardening exponent, n′, and fatigue ductility coefficient; also used to predict cyclic plastic strain
±1% strain-controlled fatigue tests	$\Delta\epsilon_p/2$, half-life plastic strain amplitude	Used to estimate fatigue ductility exponent, c, and to estimate the plastic strain versus life curve
	$\Delta\epsilon_e/2$, half-life elastic strain amplitude	Used to estimate fatigue strength exponent, b, and to estimate the elastic strain versus life curve
Strain-controlled low cycle fatigue tests	Strain versus life curve	Used to evaluate metals subject to low cycle fatigue; also design data

to about 10 Hz and isothermal conditions, we have found no significant differences in the life of metals of engineering interest at room temperature. If isothermal conditions are not maintained, the heating due to plastic action may induce changes in the metallurgical properties of the metal. But since this is rarely encountered in room-temperature low cycle fatigue testing, the testing frequency is more dependent on system capabilities.

Although the basic MTS electrohydraulic closed-loop testing system is capable of frequencies of about 100 Hz, the recording equipment and the dynamic characteristics of the extensometer usually limit the actual test frequencies which can be employed. Typically, our controlled-strain tests are conducted at a cyclic frequency of from 0.1 to 0.5 Hz when failure is expected in less than 10^3 cycles, and from 1 to 2 Hz for lives greater than this value. Since poor hysteresis records result when the X-Y recorder is driven faster than 0.1 Hz, loops are recorded at fixed intervals at this lower frequency. A typical test record is shown in Fig. 14 for an 18 percent nickel maraging steel [*13*]. Note that this particular metal exhibited considerable softening and that the presence of a large fatigue crack is indicated by the shape of the hysteresis loop taken at 1050 cycles. Strip chart records of the entire test are used to provide a measure of the relative changes in stress when the strain is controlled.

At strain amplitudes where the life is expected to exceed 10^6 cycles, the stress rather than strain is usually controlled allowing a higher cyclic frequency. Moreover, if the cyclic stress-strain curve indicates that the material will remain elastic throughout the test, the clip gage extensometer may be omitted allowing even higher frequencies. Since the response of strip chart recorders decreases at high frequencies (the critical frequency may be between 20 to 40 Hz depending on the unit) they are also omitted from the system.

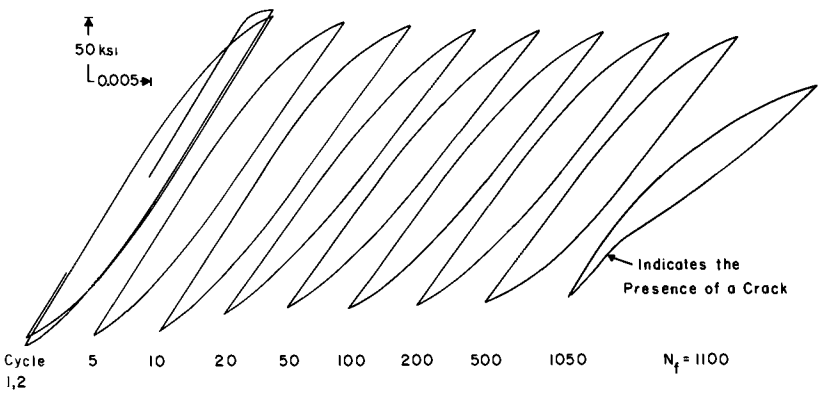

FIG. 14—*Stress-strain hysteresis loops during strain. Cyclic for 18 percent nickel maraging steel,* $\Delta\epsilon/2 = 0.010$. *See Ref.* 13.

During these high frequency tests (20 to 100 Hz), the output signal from the load cell is compared with a known voltage, corresponding to the desired load, on an oscilloscope. In this way any frequency-dependent changes in the system can be detected. Also, to discourage the heating effects discussed previously, cold water can be periodically flushed through the grip. As shown in Fig. 13, the proximity of the specimen to the cold grip maintains it essentially at room temperature.

One of the most critical aspects of fatigue testing, particularly at long lives, is the alignment of the specimen. Although the liquid metal grip allows the specimen to align itself, the location of the fatigue crack in the specimen with respect to a fixed direction should be monitored. Then if a majority of specimens exhibit cracks in the same relative location, misalignment is indicated.

Another problem associated with strain-controlled low cycle fatigue testing is slipping of the clip gage on the specimen. A small piece of cellophane tape between the specimen and clip gage reduces this problem. However, the knife edges of the gage, either through wear or because of the weight of the gage, may tend to slide downward on the specimen. Clip gage slipping will show up on the strip chart record as a steady increase in tensile stress and an accompanying decrease in compressive stress. Carefully remounting the clip gage usually eliminates this problem although a similar change in stress can be due to material behavior.

The liquid metal grip can also be a source of testing difficulties. If the Wood's metal has not wet the plug (Fig. 13), it is probable that it will become loose in the course of a test. This may be detected by an audible "click" on each cycle. To avoid a loose grip, every effort must be made to insure the cleanliness of the plug and the Wood's metal itself. If these precautions prove fruitless and the plug is still not wetting, we have found that spraying the plug with a high temperature automotive engine enamel will eliminate the problem.

Data Interpretation and Presentation

The basic purpose of low cycle fatigue testing is to determine the resistance of a metal to repeated straining. Results of these tests are presented as a plot of the total strain amplitude versus life in reversals as shown in Fig. 8. In addition to the total strain amplitude, the half-life values of elastic and plastic strain amplitudes are also recorded. These components of the strain amplitude are used to determine the transition fatigue life.

The transition fatigue life is defined as the life where the total strain amplitude consists of equal elastic and plastic components, that is, the life at which the elastic and plastic strain curves intersect. As can be seen in Fig. 8, the elastic strain is predominant for lives greater than the transition

life. Thus at long lives the fatigue resistance of a metal is determined by its strength. For lives less than the transition life, the plastic strain is predominant indicating that the ductility of the metal will determine its fatigue resistance. This is also apparent from the strain-life curves shown in Fig. 9. Notice that a strong metal generally exhibits superior fatigue resistance in terms of strain at long lives while a ductile metal is usually superior at short lives.

In addition to the strain-life curve, plots of other data are useful in interpreting the response of a metal to repeated straining. For example, a logarithmic plot of the plastic strain amplitude versus reversals to failure provides an indication of a metal's response to different amplitudes of total strain. An alternative would be to plot the stress amplitude versus the logarithm of reversals to failure. As shown in Fig. 4, the logarithmic plot of the cyclic stress amplitude versus the plastic strain amplitude is used to determine the cyclic strain hardening exponent. Values for stress and plastic strain are taken from the cyclic stress-strain curve.

Other data plots are useful if the purpose of testing is to optimize the processes which affect the fatigue resistance of a metal. For example, a plot of hardness versus life can be used to optimize the heat treatment of a metal.

Acknowledgment

The authors are indebted to the many people who, during their past association with the H. F. Moore Research Laboratory of the Department of Theoretical and Applied Mechanics, University of Illinois, have been instrumental in developing these testing procedures. Included are C. E. Feltner, R. W. Landgraf, and R. M. Wetzel of the Scientific Laboratory, Ford Motor Company, G. R. Halford, Lewis Research Center, National Aeronautics and Space Administration, B. I. Sandor, University of Wisconsin, T. H. Topper, University of Waterloo, Ontario, Canada, and F. R. Tuler, Sandia Corp.

In addition, T. J. Dolan, head of the Department of Theoretical and Applied Mechanics, has for many years actively supported and encouraged the development of our cyclic deformation and fracture research facility. The development of this facility would not have been possible without the continued interest and valuable assistance of H. C. Johnson, president of MTS Systems Corp., and numerous members of his staff.

Financial support of this research has been provided by grants and contracts with the Naval Air Development Center (Contract Nos. N0156-46083 and N00-156-67-C-1875), the National Aeronautics and Space Administration (Grant NGR 14-005-025), and by Caterpillar Tractor Co., LaSalle Steel Co., and United States Steel Corp.

APPENDIX

Engineering and True Stress-Strain Definitions

From Fig. 15, the engineering and true stress-strain values are defined as follows:

Engineering Stress-Strain Values

The engineering stress is defined as

$$S = (P/A_o) \quad (9)$$

and the engineering strain,

$$e = (L - L_o/L_o) = (\Delta L/L) \quad (10)$$

True Stress-Strain Values

True stress is defined as

$$\sigma = (P/A) \quad (11)$$

and the true tensile stress to cause fracture as

$$\sigma_f = (P_f/A_f) \quad (12)$$

Note that σ_f should be corrected for the influence of lateral stresses due to necking (see p. 250 of Ref *1*). True strain is defined as

$$\epsilon = \ln(L/L_o) \quad (13)$$

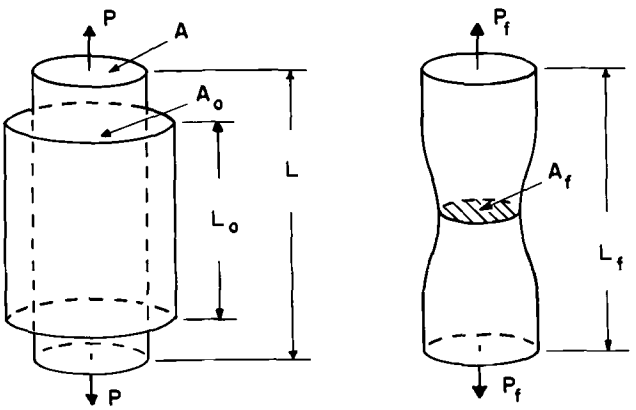

(a) Original Gage Section (b) Gage Section after Fracture

FIG. 15—*Gage section from a longitudinal tensile specimen.*

If constancy of volume is assumed, then $A_oL_o = AL$ and Eq 13 may be rewritten as

$$\epsilon = \ln(A_o/A) = 2\ln(D_o/D) \quad (14)$$

The true fracture ductility is defined as

$$\epsilon_f = \ln(A_o/A_f) = \ln(100/100 - \%RA) \quad (15)$$

where RA is the reduction in area of the specimen. Also since $\epsilon = (L/L_o) - 1$ then

$$\epsilon = \ln(1 + e) \quad (16)$$

up to necking. Similarily,

$$\sigma = S(1 + e) \quad (17)$$

up to necking.

The strain can also be written in terms of the elastic and plastic components

$$\epsilon = \epsilon_e + \epsilon_p \quad (18)$$

Now $\epsilon_e = \sigma/E$ and from Table 2, $\epsilon_p = (\sigma/K)^{1/n}$ therefore the strain may be rewritten as

$$\epsilon = (\sigma/E) + (\sigma/K)^{1/n} \quad (19)$$

Also $\sigma_f = \epsilon_f{}^nK$, therefore eliminating K from Eq 19 results in

$$\epsilon = (\sigma/E) + \epsilon_f(\sigma/\sigma_f)^{1/n} \quad (20)$$

Monotonic Strain Hardening Exponent

The monotonic strain hardening exponent, n, is defined as the slope of the log σ − log ϵ_p curve as shown in Fig. 16. Thus,

$$n = [(\log \sigma_f - \log \sigma)/(\log \epsilon_f - \log \epsilon)] = [(\log\sigma_f/\sigma)/(\log\epsilon_f/\epsilon)] \quad (21)$$

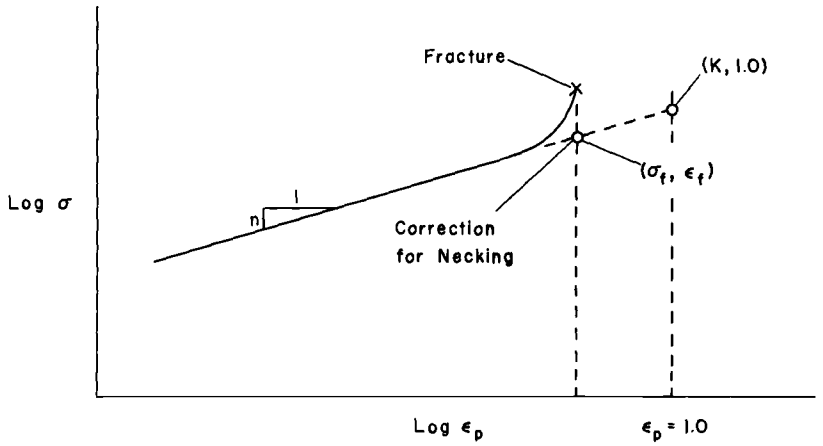

FIG. 16—*Schematic illustration of the relationship between stress, plastic strain, and the monotonic strain hardening exponent.*

Or, using K,

$$n = -(\log(K/\sigma)/\log \epsilon) \quad (22)$$

Also since $dP = 0$ at the maximum load and $P = \sigma A$, then $dP = \sigma dA + A d\sigma = 0$. With constancy of volume this becomes

$$-(dA/A) = (dL/L) = (d\sigma/\sigma) \quad (23)$$

and by definition $d\epsilon = dL/L$, therefore

$$(d\sigma/d\epsilon) = \sigma \quad (24)$$

But $\sigma = K \epsilon^n$, which gives

$$(d\sigma/d\epsilon) = nK\epsilon^{n-1} \quad (25)$$

Comparison with Eq 24 indicates that the strain hardening exponent is equal to the true strain at necking (point of maximum load).

$$n = \epsilon_n \quad (26)$$

References

[1] Dieter, G. E. *Mechanical Metallurgy,* McGraw-Hill, New York, 1961, p. 287.

[2] Polakowski, N. H. and Palchoudhuri, A., "Softening of Certain Cold-Worked Metals Under the Action of Fatigue Loads," *Proceedings,* American Society for Testing and Materials, ASTEA, Vol. 54, 1954, pp. 701–716.

[3] Benham, P. P., "Fatigue of Metals Caused by a Relatively Few Cycles of High Load or Strain Amplitude," *Metallurgical Review,* Vol. 3, No. 11, 1958, pp. 203–234.

[4] Lazan, B. J. and Wu, T., "Damping, Fatigue, and Dynamic Stress-Strain Properties of Mild Steel," *Proceedings,* American Society for Testing and Materials, ASTEA, Vol. 51, 1951, p. 649.

[5] Coffin, L. F., Jr., "A Study of the Effects of Cyclic Thermal Stresses on a Ductile Metal," *Transactions of the American Society of Mechanical Engineers,* Vol. 76, Aug. 1954, pp. 931–950.

[6] Morrow, JoDean, "Cyclic Plastic Strain Energy and Fatigue of Metals," *Internal Friction, Damping, and Cyclic Plasticity, ASTM STP 378,* American Society for Testing and Materials, 1965, pp. 4–83.

[7] Landgraf, R. W., Morrow, JoDean and Endo, T., "Determination of the Cylic Stress-Strain Curve," *Journal of Materials,* JMLSA, Vol. 4, No. 1, March 1969, pp. 176–188.

[8] Feltner, C. E. and Mitchell, M. R., "Basic Research on the Cyclic Deformation and Fracture Behavior of Materials," *Manual on Low Cycle Fatigue Testing, ASTM STP 465,* American Society for Testing and Materials, 1969, pp. 27–66.

[9] Feltner, C. E. and Landgraf, R. W., "Selecting Materials to Resist Low Cycle Fatigue," *ASME Publication No. 69-DE-59,* American Society of Mechanical Engineers, 1969.

[10] Basquin, O. H., "The Exponential Law of Endurance Tests," *Proceedings,* American Society for Testing and Materials, ASTEA, Vol. 10, 1910, pp. 625–630.

[11] Endo, T. and Morrow, JoDean, "Cyclic Stress-Strain and Fatigue Behavior of Representative Aircraft Metals," *Journal of Materials,* JMLSA, Vol. 4, No. 1, March 1969, pp. 159–175.

[12] "Building a System for Testing Small Metal Specimens," *Closed Loop,* MTS System Corp., Minneapolis, Minn., Vol. 1, No. 8, 1968, pp. 3–6.

[13] R. W. Landgraf, "Cyclic Deformation and Fatigue Behavior of Hardened Steels," *TAM Report No. 320,* Department of Theoretical and Applied Mechanics, University of Illinois, Urbana, Ill., November, 1968.

ERRATA

STP 465 Manual on Low Cycle Fatigue Testing

p. 18 Eq. 8

$$(\Delta\epsilon/2) = (\sigma_f'/E)(2N_f)^b + \epsilon_f'(2N_f)^c$$

C. E. Feltner[1] *and M. R. Mitchell*[2]

Basic Research on the Cyclic Deformation and Fracture Behavior of Materials

REFERENCE: Feltner, C. E. and Mitchell, M. R. **"Basic Research on the Cyclic Deformation and Fracture Behavior of Materials,"** *Manual on Low Cycle Fatigue Testing, ASTM STP 465*, American Society for Testing and Materials, 1969, pp. 27–66.

ABSTRACT: This paper describes the experimental methods that we employ for low cycle fatigue studies. Techniques associated with two test systems, an MTS[3] system and an Instron[4] machine, are described. In particular, the following subjects are treated: principles underlying low cycle fatigue testing; load frames, load cells, and load applying devices; design of specimens; specimen gripping methods; measurement of strain; selection of test program; strain control during a test; recording of data; determination of failure; analysis, reduction, and presentation of test results; and metallographic techniques associated with low cycle fatigue testing.

KEY WORDS: mechanical properties, low cycle fatigue, extensometry, strain measurement, fatigue (material), specimen gripping, specimen design, tests

Low cycle fatigue is generally considered to be the failure of materials under cyclic strains in less than about 10^5 cycles. The purpose of this paper is to describe the methods that we employ for low cycle fatigue studies in the Metallurgy Department of the Scientific Research Staff, Ford Motor Co. The paper is divided into two parts: The first part is a discussion of our philosophy of low cycle fatigue testing, and the second part describes in detail the operational methods and devices we use in carrying out low cycle fatigue tests. These procedures are constantly changing and have evolved to the present status over a period of the past five years at the Ford Scientific Laboratory.

[1] Metallurgy Department, Scientific Research Staff, Ford Motor Co., Dearborn, Mich. 48121.

[2] Advanced Experimental Technology Dept., Engineering Technology Office, Engineering Staff, Ford Motor Co., Dearborn, Mich. 48121.

[3] MST Systems Corp., Minneapolis, Minn.

[4] Instron Corp., Canton, Mass.

Research Philosophy

The other papers in this book deal mainly with the phenomenological behavior of materials during low cycle fatigue and are concerned primarily with the development of methods to *evaluate* the properties of existing materials and the provision of design information. By contrast, our first goal is to *understand* the mechanistic behavior of materials during low cycle fatigue and to study the response of different metallurgical structures to large strain amplitudes. Studies of this type are carried out in our laboratory to determine which microstructural factors affect the low cycle fatigue behavior of materials, with the eventual aim of using this information to develop new materials which are better able to resist low cycle fatigue. The experimental requirements imposed by our need to obtain fundamental information are often reflected in certain procedures and equipment employed in our low cycle fatigue tests.

It has become clear that plastic strain is the controlling parameter in the alteration of the microstructure of metals during fatigue, therefore, it is important to control the strain limits rather than the load limits. In addition, we prefer to do all of our tests in axial loading since the metallurgy of low cycle fatigue is sufficiently complex without adding further complication by the use of a nonuniform stress distribution (which would be inherent in bending or torsion tests). Having decided for what *purpose* one desires information, let us now consider which *properties* one needs to determine to fulfill the stated purpose.

We would normally determine those low cycle fatigue properties which are defined in the paper by Raske and Morrow [*1*],[5] such as the fatigue ductility coefficient, the fatigue ductility exponent, etc. Refer to Ref *1* for a complete discussion of these properties. The data that we collect to obtain values for these desired properties are: (1) monotonic properties, (2) hysteresis loops, (3) cyclic strain hardening and softening curves (which are plots of the peak flow stress versus cycles or cumulative plastic strain in an experiment in which the strain amplitude is controlled), (4) the cyclic stress-strain curve, and (5) the strain amplitude versus life curves. In addition to these data, we often obtain information associated with microstructural behavior such as: (1) slip band topography and surface damage where one examines the surface of the deformed (or cracked) material both in incidence and in section; (2) fracture surfaces where one again can look at the fracture surface either in incidence or in section; and (3) the dislocation structures developed in the material (determined by transmission electron microscopy). Metallurgical studies of this type often

[5] The italic numbers in brackets refer to the list of references at the end of this paper.

impose a number of restrictions on both the method of testing and the type of specimen employed. These restrictions will become apparent in the discussion of actual test procedures.

In obtaining the above data, the variables that we deal with include stress, strain, strain rate, temperature, and other environmental factors. In our tests, we usually control the strain range and measure the stress response while holding all other variables fixed. Often, as a means of studying certain physical processes in the material, it is useful to control the temperature, and an appreciable portion of our work has been done at temperatures *below* room temperature. In addition to mechanical variables there are several structural variables which we often study. They include: slip character of the material; cold work introduced into the material; variations in grain size; the size, number, and distribution of precipitates in the material; and different combinations of these structural parameters. Again, these structural variables may also impose certain limitations on the experimental methods employed.

Our procedures for low cycle fatigue testing are built around two different systems, which include an MTS electrohydraulic closed-loop system and a screw-driven Instron machine. The problems associated with testing in these two systems are different and therefore we have divided the following description into two parts, the first part dealing with room temperature tests in the MTS and the second part treating low temperature tests in the Instron.

Performing a Low Cycle Fatigue Test in the MTS Test System

Description of Test System

The MTS test system[6] which we have operated for approximately two years (System No. 902.64) consists of a three-bay control console and two hydraulic rams and load frames. The capacities of the two rams are 20 kips (89 kN) and 2.5 kips (11.1 kN) and these rams, mounted in load frames, are shown in Figs. 1 and 2 respectively. An overall view of the control console is shown in Fig. 3. In addition to this two-station test system we also have a third station which is a 10-kip (44.5-kN) ram on a standard MTS frame and a two-bay control console. This third system is used for normal tension testing and as a backup fatigue test system.

The loading frames shown in Figs. 1 and 2 are home built and are patterned after a design by R. M. Wetzel, J. Morrow, and their associates of the University of Illinois Department of Theoretical and Applied Mechanics. The frame, Fig. 1, consists of two 3-in. (76-mm)-thick platens *A*,

[6] The details concerning the size and specification of the components that are supplied by MTS Systems Corp. are available in their technical bulletins.

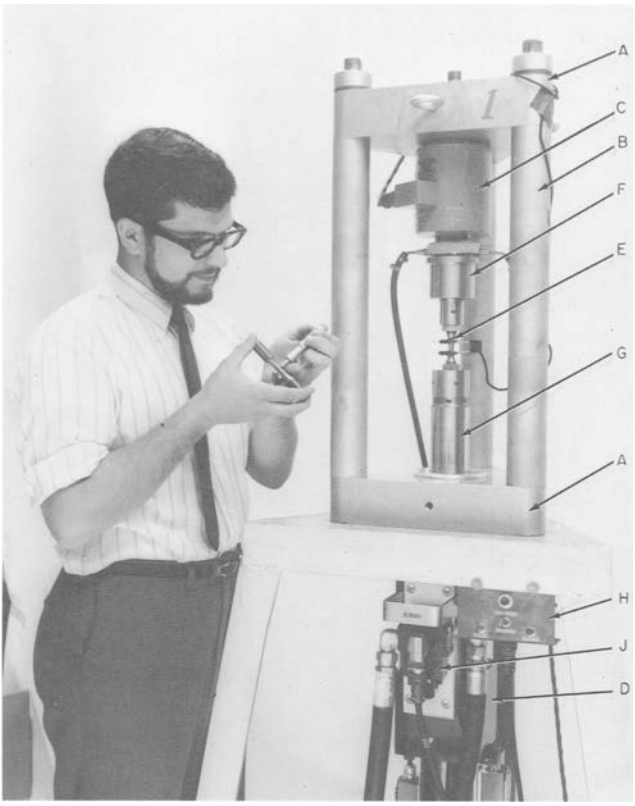

FIG. 1—*Overall view of 20-kip (89-kN) load frame.*

which are separated by three adjustable-height posts *B*. The load cell *C* is mounted to the upper platen and the hydraulic ram *D* is mounted to the lower platen. Specimen *E* and grip *F* are in the loading column between ram head *G* and the load cell. The load frame with attached ram is supported on an angle-iron base frame which positions the loading frame at a working height convenient for the operator (that is, the specimen is located at approximately chest level). The distance between the platens may be adjusted by removing or inserting different lengths of the hollow posts through which threaded rods run. The assembly is held together by tension nuts located at the top of each post. This frame is simple in construction, relatively inexpensive, and is designed for minimum deflection. The deflection characteristics of the frame, grip, and load cell in Fig. 1 have been determined by letting the ram contact the grip and applying incremental loads up to 20 kips (89 kN) while simultaneously measuring

the associated deflection between the head of the ram and the lower platen. A plot of applied load versus measured deflection is shown in Fig. 4, from which a deflection rate of 0.5 μin./lb (5.76×10^{-6} mm/kg) is obtained.

Hydraulic pressure is supplied to the ram by a 20-gal/min (1.26-liters/s) pump which is remotely located in order to reduce the noise and vibration in the vicinity of operation. The hydraulic ram used to apply the load is MTS Model No. 204.24 and is equipped with a 5-gal/min (0.32-liters/s) Moog (Moog, Inc., East Aurora, N. Y.) servovalve No. 73-102. The 20-kip (89-kN) system utilizes a Lebow (Lebow Associates, Inc., Oak Park, Mich.) load cell No. 3116-103 which has a dynamic rating of

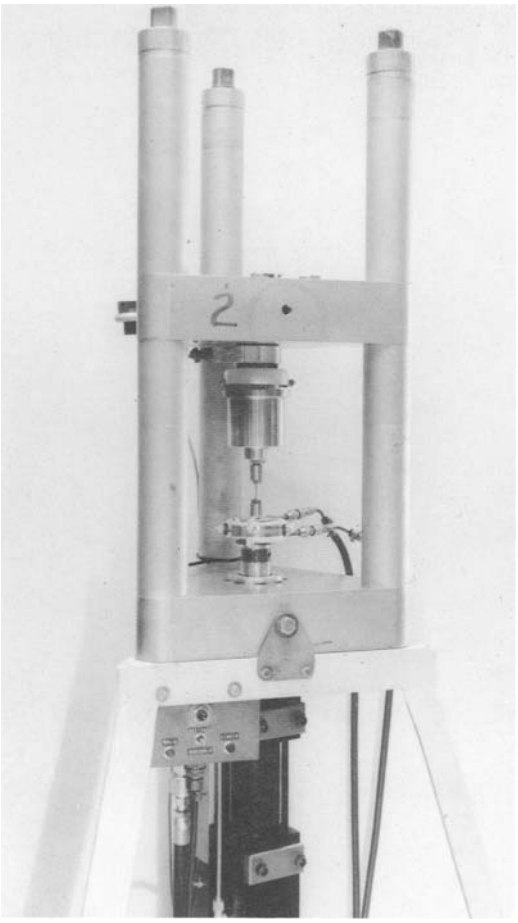

FIG. 2—*Overall view of 2.5-kip (11.1-kN) load frame.*

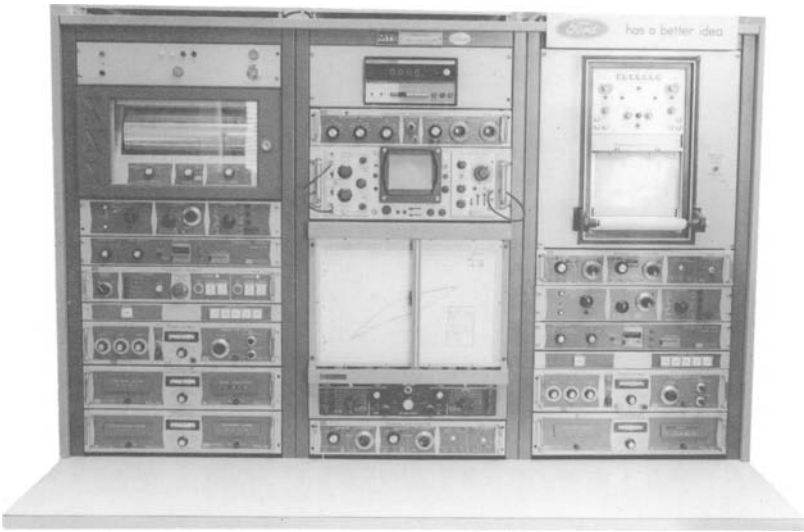

FIG. 3—*Control console for two-channel MTS test system.*

20 kips (89 kN).[7] This capacity is usually adequate for monotonic and cyclic testing of a variety of commercial metals using normal size laboratory specimens.

The load frame shown in Fig. 2 is identical in design to that in Fig. 1 but is of lower capacity, that is, 2.5 kips (11.1 kN). This system utilizes a 2.5-kip (11.1-kN), dynamically rated Strainsert (Strainsert, Inc., Bryn Mawr, Pa.) load cell No. FLU-2.5SG2-0222 and a 1-gal/min (0.06-liter/s) Moog servovalve No. 73-100 on the hydraulic ram Model No. 204.11. The reason for having this low capacity ram is that an appreciable portion of our work entails the testing of single crystals and many polycrystalline pure metals of low yield strengths. It is preferable for materials of this type to use a more sensitive loading system.

In much of our work we study surface slip bands developed during fatigue and the processes of crack initiation and propagation. Figure 5 shows a special loading frame that we have designed to make *in situ* observations of surface damage and crack initiation and growth while a test is in progress. It consists of a two-post load frame that pivots and can be operated in either the vertical or horizontal position. The frame and a Leitz Metallux ND microscope are mounted on a work table. With the frame in the vertical position the specimen is mounted and then the frame is rotated into the horizontal position for easy viewing of the specimen during operation.

[7] The load cells are calibrated quarterly to National Bureau of Standards specifications.

This special microscope test frame is used in conjunction with the 2.5-kip (11.1-kN) hydraulic ram. To avoid having an extensometer in the field of view of the microscope, we are using an Optron (Optron, Inc., New Haven, Conn.) optical extensometer for remote strain measurement and control. This instrument is discussed in a subsequent section.

The three-bay console in Fig. 3 comprises the necessary modules and components to operate the two rams independently. Each basic control system has an on-off control panel, command center, Servac (MTS systems), cycle counter, function generator, feedback selector unit and appropriate transducer conditioner modules for load and strain. There are a number of additional components which are shared between each testing station. These include a Data-Trak (Research, Inc., Minneapolis, Minn.), which is an arbitrary function generator, the facilities for recording data, a stroke module, an Optron conditioner module, and a digital voltmeter. Since the running of any one test does not usually require continual usage of these components, we feel it is unnecessary to duplicate them. With this overall picture of our MTS system in mind, we will now proceed with a detailed description of the performance of a low cycle fatigue test with this equipment.

Specimens

Before a test program can be initiated one must have a specimen design which is adequate to provide the desired data. Several factors must

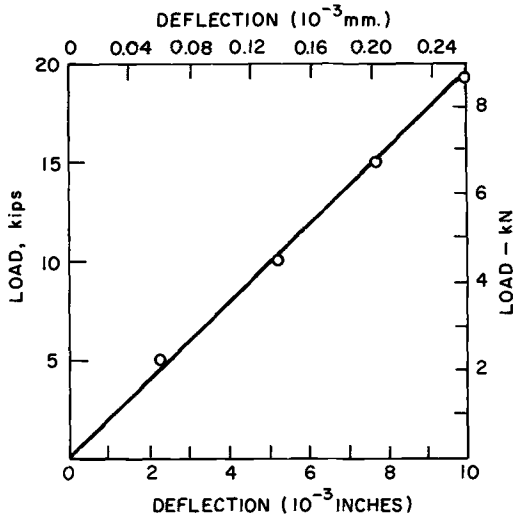

FIG. 4—*Stiffness characteristics of 20-kip (89-kN) load frame.*

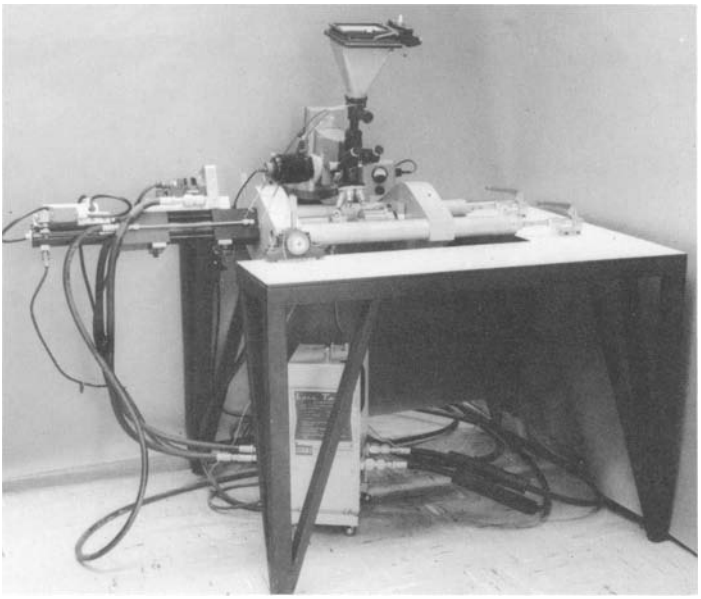

FIG. 5—*Special loading frame for making* in situ *surface studies of fatigue specimens.*

be considered when designing a specimen. These include:

1. *Availability of Material*—This factor often limits the size and shape of a specimen Obvious examples are, (a) studies on expensive metals such as gold or platinum, (b) studies on single crystals which are both limited in size and are more expensive as their size is increased, (c) new or exotic materials which are available in limited quantities and, (d) specimens cut from production parts which may be small to start with and odd shaped, as well as an expensive source of raw material.

2. *Gage Section Shape*—Here consideration must be given to how one prefers to measure strain as well as to the actual type of extensometer used. We prefer to measure longitudinal strain as opposed to diametral strain, and therefore must employ straight gage sections. The types of extensometers we use (see section on *Extensometry*) demand a minimum straight section of about ¼ in. (6.35 mm) with the maximum being determined by a combination of buckling and machine capacity considerations (see Item 4 below).

3. *Buckling*—To minimize buckling, we would normally use specimens having a length-to-diameter ratio (L/D) ranging from about 1.5 to 2.5. Depending on the modulus, we have been able to reach strains in excess of $\pm$ 5 percent with $L/D = 1.5$ without buckling.

4. *Machine Capacity*—If an L/D of 2 is chosen, then the maximum D is determined by the machine capacity and material strength, which in turn sets the value of L. However, consideration of materal availability and type of extensometer may often force compromises to be made.

5. *Avoidance of Threaded End Failures*—In the extreme case materials of low ductility and a high notch sensitivity may require a ratio of grip end area to gage section area of 10 to 15 when threaded end specimens using a lock nut are employed. In more normal circumstances a ratio of 3 to 5 is adequate. If threaded end failures are encountered after a large number of specimens have already been machined, shot peening of the threads may often alleviate the problem.

We have employed a variety of specimens, each being designed for a different purpose. Several of these are shown in Fig. 6. Specimen B in this

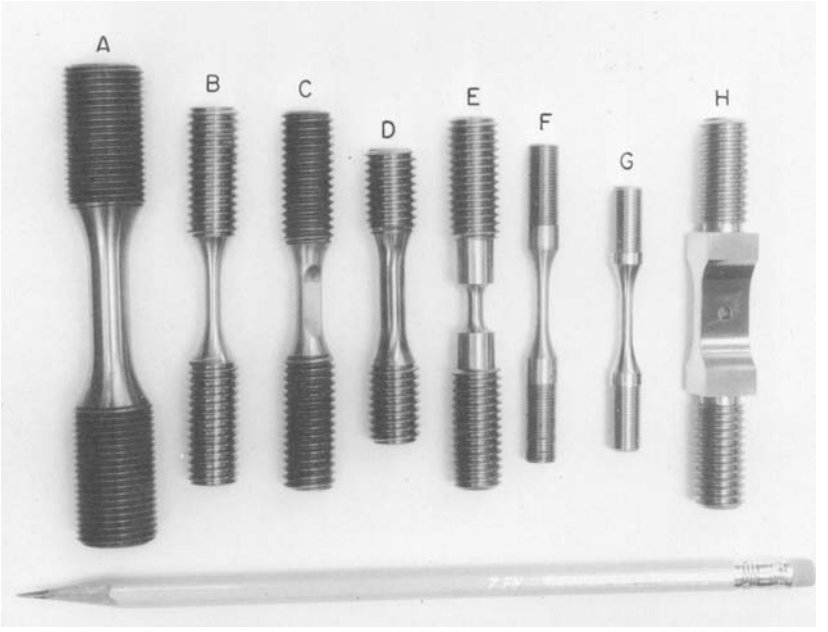

A Normal type specimen for controlled strain tests on lower strength materials.
B Normal type specimen for controlled strain tests on higher strength materials.
C Flat-sided specimen for surface topography studies.
D Used for high amplitude tests with low L/D to minimize buckling.
E Low temperature test specimen.
F, G Special specimens the sizes of which are limited by casting limitations and material availability.
H Plain-notched type specimen.

FIG. 6—*Various types of specimens employed in our fatigue testing.*

figure is a typical specimen which we use for strain control tests. It is approximately 3 in. (76 mm) long and is usually electropolished to provide a good surface for slip line observations. It has a straight gage section of 0.3 in. (7.6 mm) and is 0.150 in. (3.810 mm) in diameter ($L/D = 2$). The straight section is blended into the threaded ends with a generous radius. The ends of Specimen *B* have a ½-13 UNC thread for gripping. A specimen such as this can usually be cycled at plastic strain ranges up to about 5 percent without appreciable buckling.

A specimen with a straight gage section is essential in our work for two reasons: (1) for longitudinal or taper sections for surface topography studies, and (2) to provide ample amount of equally strained, bulk materal which can be used for transmission electron microscopy studies of dislocation structures associated with low cycle fatigue. Some of the variations of Specimen *B* and the reasons for these variations are given in Fig. 6.

All of our specimens have at least 10-rms finish after machining. No attempt is made to align machining marks parallel to the straight section. If surface observations are not to be made, the specimens are tested in the

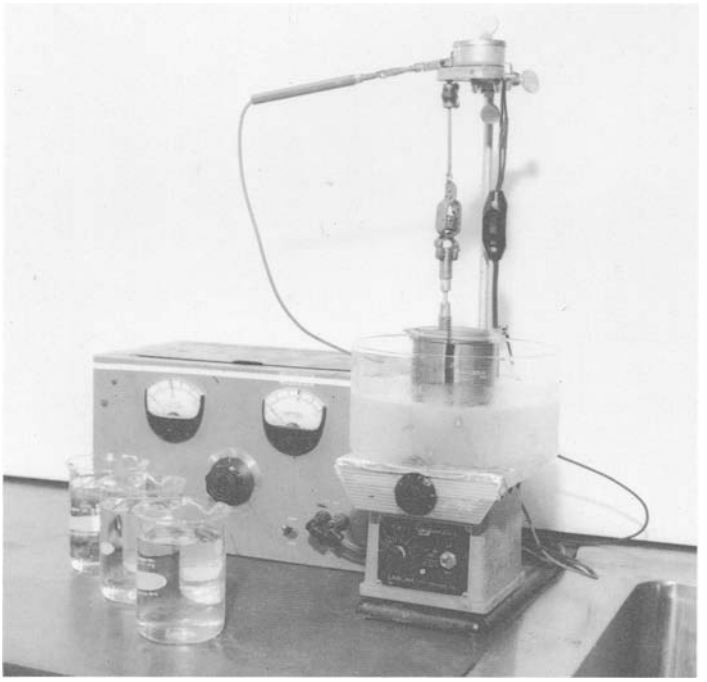

FIG. 7—*Electropolishing apparatus.*

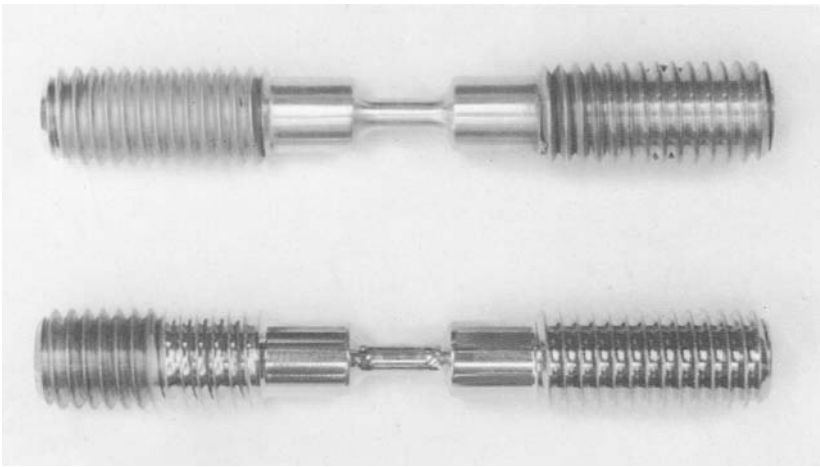

FIG. 8—*As-machined and electropolished test specimens.*

as-machined condition. When surface observations are to be made, the specimen is electropolished using an apparatus such as that shown in Fig. 7. The usual metallographic laboratory practices are employed in electropolishing [*2*,*3*] to obtain an adequate surface finish for slip line observations. The appearance of as-machined and electropolished copper specimens are compared in Fig. 8. The diameter of as-machined specimens is usually measured with a micrometer while that of specimens with an electropolished surface is determined by optical methods. The resolution of the devices employed to measure specimen diameters is 0.0001 in. (0.0025 mm).

Mounting a Specimen

Now that we have an appropriate test specimen, the next step is to mount the specimen in the loading frame. To appreciate fully the mounting procedure it is necessary to have an understanding of how the upper grip *F* in Fig. 1 is constructed.

A picture of the disassembled upper grip is shown in Fig. 9. It consists of the hollow inner chamber *B* which is attached to the load cell via stud *D*, and an outer pot *A* which fits over the inner chamber and accepts the specimen *F* at point *C*. These two pieces are held together by a Wood's metal joint. The mating parts in the joint have annular V-grooves, *E*, machined in them and have a total shear area of approximately 15 in.^{2} (9.67×10^{-3}m^2). This grip design has been used to a capacity of 20 kips (89 kN) with no difficulty. The upper chamber *B* is hollow and steam or

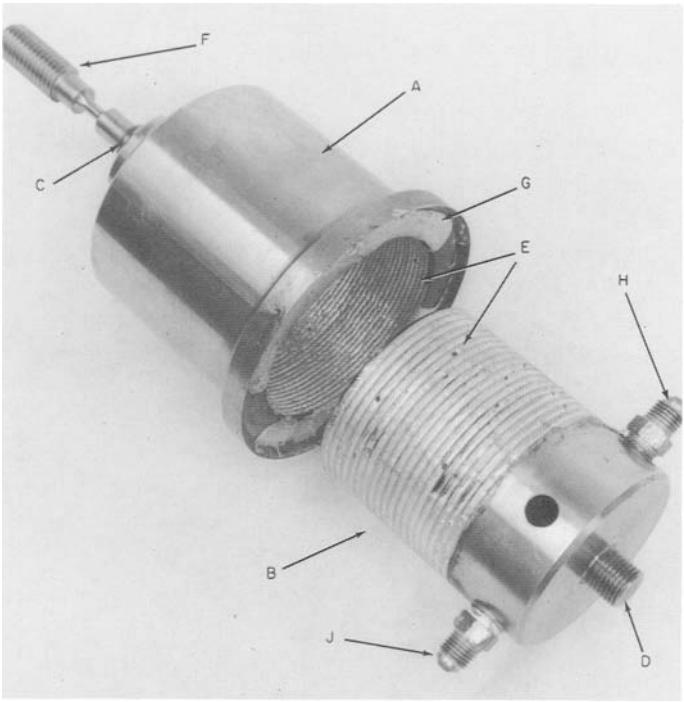

FIG. 9—*Wood's metal grip.*

water can be passed through it (inlet *J* and outlet *H*) to liquefy or solidify the joint. Lip *G* serves as a reservoir for excess molten Wood's metal which acts as a hot top. Molten metal can flow into the joint from this hot top to compensate for contraction which occurs during solidification. Steam at 50 psi (0.3 MN/m^2) is produced by a small steam generator[8] which employs a resistance heating element. Flow of steam or water through the upper chamber is controlled by a set of solenoid valves[9] which are actuated by switches *H* mounted on the load frame in Fig. 1.

With the head of the hydraulic ram retracted, and the upper pot solidified to the inner chamber, the specimen is screwed into the outer pot and locked down with the lock nut *A* in Fig. 10*a*. The head *B* of the hydraulic ram is then brought to a position about ⅛ in. (3.18 mm) below the lower end of the specimen in Fig. 10*a* and the switches are activated to liquefy the grip. Once the grip is liquefied, the specimen and outer pot assembly

[8] Hot Shot steam generator, Model No. MB-4L, Automatic Steam Products Corp., Long Island City, N.Y.

[9] Skinner valve, No. V5H-37920, Skinner Electric Valve Division, New Britain, Conn.

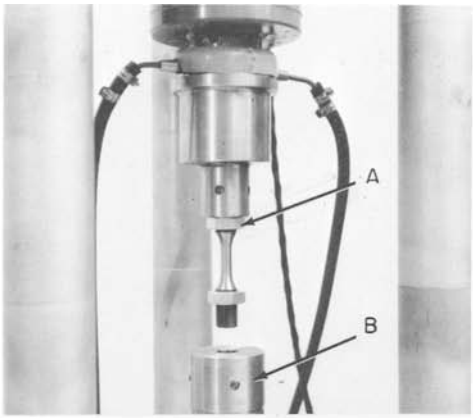

(*a*) Mounting of specimen into bottom of Wood's metal grip.

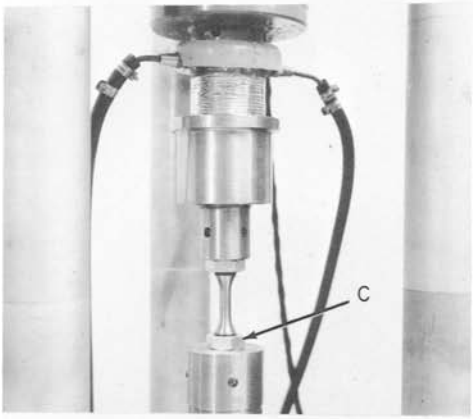

(*b*) Wood's metal grip in liquefied condition and specimen locked into hydraulic ram.

(*c*) Wood's metal grip solidified and specimen prepared for testing.

FIG. 10—*Specimen mounting procedure.*

are threaded into the head of the hydraulic ram and locked down by lock nut *C* shown in Fig. 10*b*. The system is then put in load control and the hydraulic pressure turned on. Next, the ram, with specimen and pot attached, is raised until the upper pot contacts the inner chamber and a small force of approximately 5 to 10 lb (approximately 22 to 44 N) is developed. The system is then set to maintain this small compressive force and the solenoid valves are activated to pass water through the inner chamber, which results in solidification of the grip. This final condition of mounting is shown in Fig. 10*c*. The specimen is now ready for testing.

Several advantages of this gripping arrangement are: (*a*) the grip is self-aligning, (*b*) there is no backlash in the grip, (*c*) clamping stresses are held to a minimum, (*d*) the total mounting time is less than 5 min., and (*e*) it can be used for a variety of other tests such as monotonic tension, creep, etc.

We have designed and used a number of different versions of this Wood's metal grip. One such version is shown in Fig. 11, in which the liquid grip is located at the lower end of the specimen rather than at the upper end. The advantage in this arrangement is that the specimen *A* (in this case a

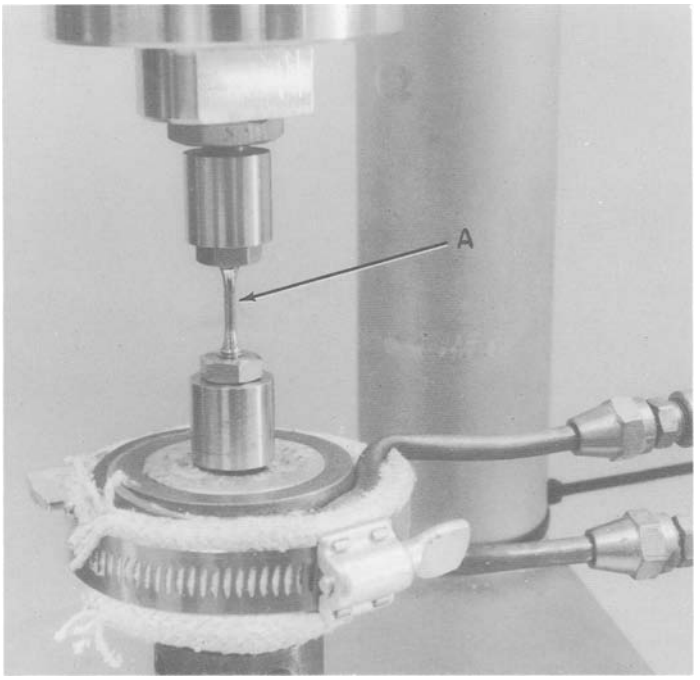

FIG. 11—*Special version of the Wood's metal grip.*

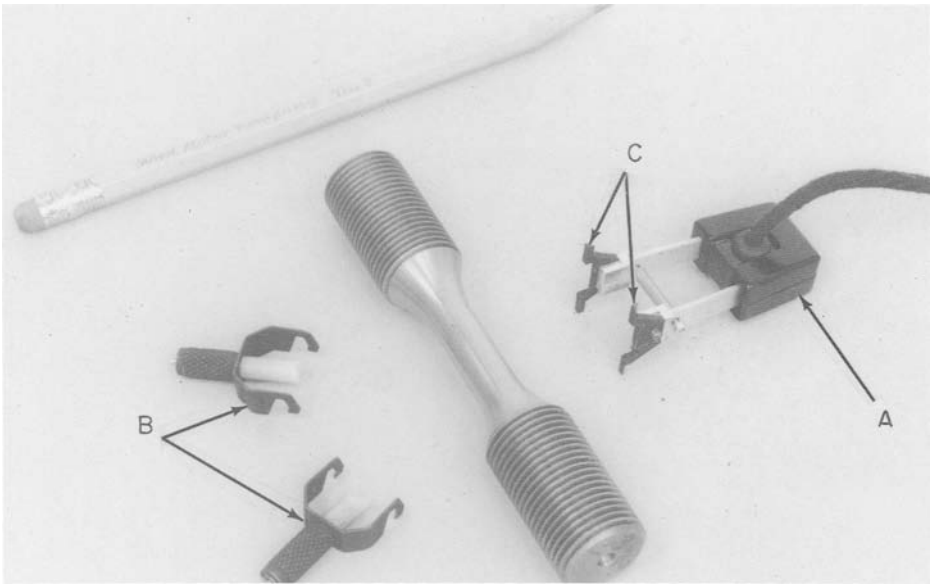

FIG. 12—*Clip gage extensometer commonly employed in our tests.*

molybdenum single crystal) does not have to carry the weight of the upper pot as in the previously discussed design, thereby reducing the possibility of accidentally deforming the specimen during mounting. One disadvantage in this arrangement, however, is that the water and steam lines may have to be moved over large distances when the ram is operated. This disadvantage is minimized through the use of flexible steam and water lines. With the specimen in place, as in Fig. 10*c* or in Fig. 11, we are now ready to attach the extensometer to the specimen.

Extensometry

For the measurement and control of strain we have generally used an Instron clip gage No. G51-16 which is shown detached from a specimen in Fig. 12. The extensometer *A* uses strain gages as sensing elements and is attached to the specimen via the slips *B*, which are spring loaded. The gage length of this extensometer, that is, the distance between the knife edges *C*, is normally ½ in. (12.7 mm); however, these knife edges may be shimmed to give a gage length ranging between ¼ and ¾ in. (6.35 and 19.05 mm). This extensometer has a linear range of 0.50 in. (1.270 mm) and weighs 0.5 oz. (approximately 15 g). It has a resolution of at least 10^{-5} in. (25.4×10^{-5} mm) and a frequency response of about 5 Hz. Prior to mounting, the extensometer is calibrated with the

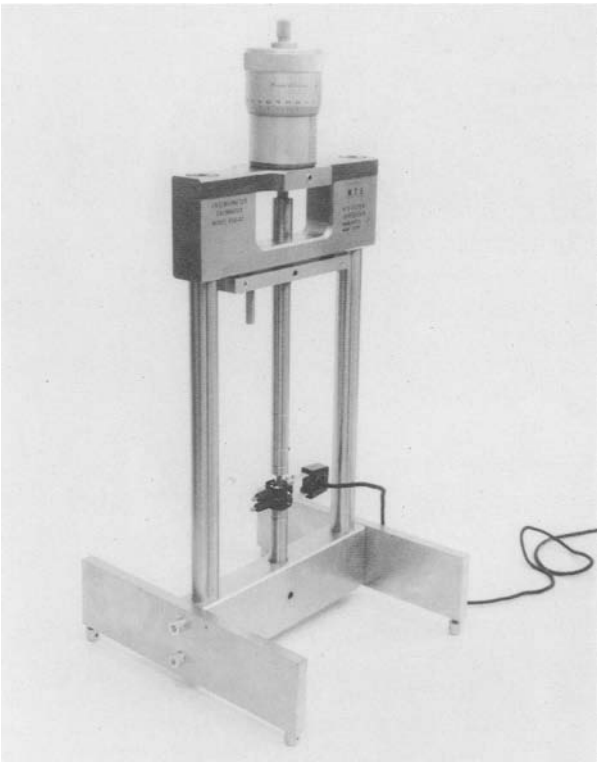

FIG. 13—*Extensometer calibrator.*

MTS extensometer calibrator, Model No. 650.02 shown in Fig. 13, which has a least reading of 0.0001 in. (0.0025 mm).

The first step in attaching the extensometer is to put ¼-inch (6.35-mm) wide strips of Scotch Brand Magic Tape around the diameter of the specimen at the points where the knife edges will contact the specimen. This is done to prevent slippage of the knife edges and to reduce the contact stresses. The upper knife edge is first affixed with a clip to the sample. The desired gage length is then obtained by hand positioning of the lower knife edge and clip until a zero reading is observed on the *X-Y* recorder. The gage length can usually be set by this method to within approximately ¼ percent of the desired value. Often the extensometer will undergo some drift as the knife edge settles into the tape. Sometimes a waiting period of 5 to 15 min may be required before this creep effect disappears. The extensometer in its finally mounted condition is shown in Fig. 14.

A new optical extensometer system which is currently in the experimental stages is shown in Fig. 15. This electrooptical transducer system

consists physically of two optical tracking heads *A* and a control unit *B*, interconnected by a cable. The optical tracking heads *A* are mounted on a 3-way positioning seismic stand *C*. The system we are using is Optron Model No. 800, which operates on a servo control principle. This system will resolve between ten millionths and two hundred and fifty millionths of an inch (2.54×10^{-4} mm and 6.35×10^{-2} mm) depending upon the data frequency bandwidth.

The working distance of this particular noncontacting displacement measuring device is 18 in. (457 mm) and a dull, black-white target must be attached to the specimen as shown in Fig. 16. The full scale frequency response is 40,000 Hz. The full scale displacement range of our lens system, Model No. 800-01, is 0.100 in. (2.54 mm). MTS Systems Corp. has designed, constructed, and installed in our system a transducer conditioner module which allows us to use this device in the feedback control loop. Although it is still in the trial stages of operation, we have conducted several strain control tests, for example, in which the total strain range was 0.002 at a frequency of 10 Hz and a square wave form.

Selection of Program

With the specimen and extensometer in place as shown in Fig. 14, the next step is to select the desired strain-time wave form and the frequency at which the test will be run. This is done by making the proper settings on the function generator *A*, shown in Fig. 17. The preset cycle counter *B*

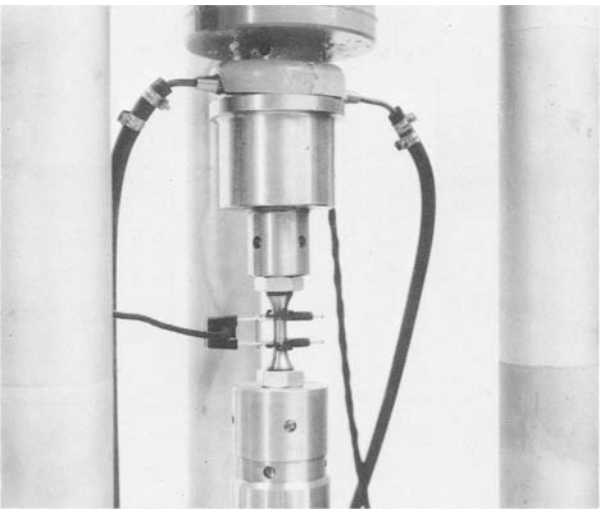

FIG. 14—*Extensometer in mounted position.*

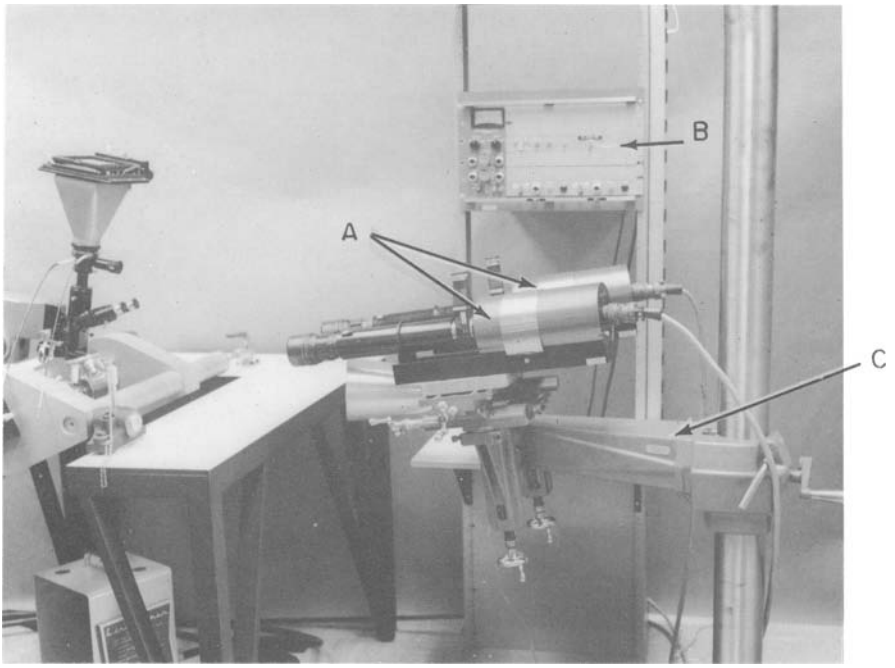

FIG. 15—*Optical extensometer tracking heads and control unit.*

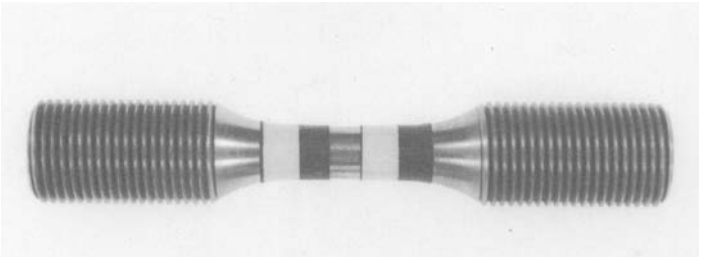

FIG. 16—*Specimen with targets used for optical extensometer.*

can be used to stop this program after the application of a desired number of cycles. The Data-Trak *C* may be used to develop special programs not available on a standard function generator. The Data-Trak is set up to be operated with either system in two possible modes: (*a*) It can be used independently as an arbitrary function generator, or (*b*) it can be used to develop a composite program when connected with either of the stand-

ard function generators. As a composite programming center, the Data-Trak can be used to modulate either the amplitude or frequency of the particular wave form that is selected on the standard function generator. In addition, it can be used to control the mean value of the chosen wave form.

For materials that are relatively insensitive to strain rate, we would normally employ a sine strain-time wave form. The usage of a sine wave for the strain wave form results in a continually varying strain rate during the course of one cycle, which is undesirable for strain-rate sensitive materials. For these materials, we would use a triangular wave form, so that the strain rate is constant throughout a cycle. Furthermore, the frequency of the wave would be adjusted such that the strain rate is constant in companion tests at different strain amplitudes.

The consequence of using a *sine* strain-time wave form for a highly strain-rate sensitive material, that is, pure iron, is shown in Fig. 18*a*. Note that as the strain limit is approached, in either tension or compression, the stress amplitude begins to decrease. This occurs because the strain rate approaches zero as the peak strain amplitude is approached. At some point prior to the peak amplitude the relaxation rate exceeds the strain

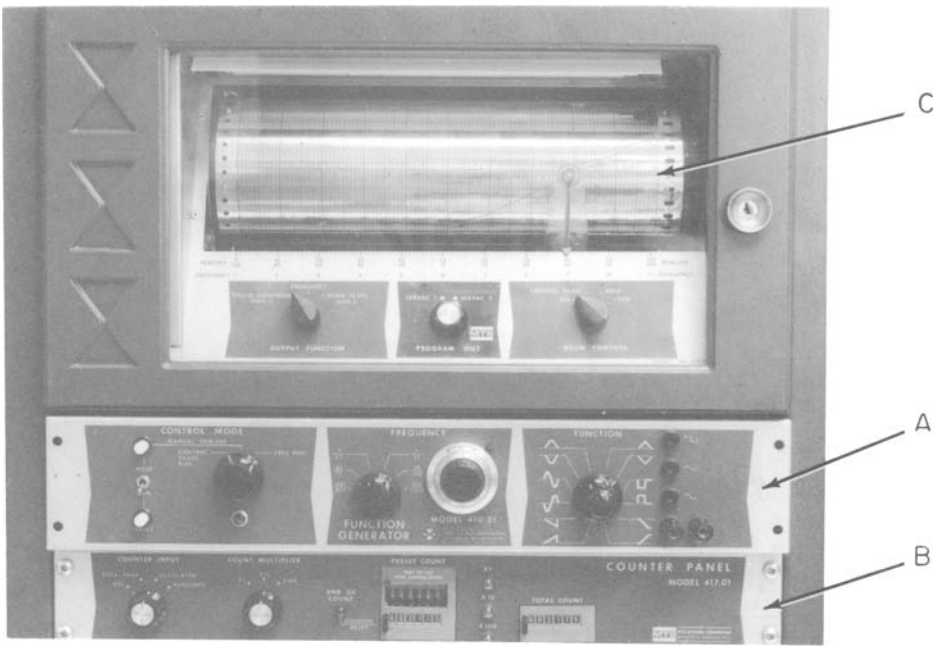

FIG. 17—*Programming equipment.*

rate resulting in a round tip hysteresis loop. Using a triangle strain-time wave form, the same specimen gives the hysteresis loop in Fig. 18*b*. In this case the strain rate is constant throughout the tensile and compressive strokes of the cycle and the hysteresis loop has sharp tips.

In the selection of frequencies for a sine wave form, we normally use increasing frequencies as the strain amplitude is decreased. This has two advantages. First, the lower strain amplitude tests require a greater number of cycles to produce failure, and therefore higher frequencies allow the test to be conducted in a reasonably short period of time. Second, with decreasing strain amplitude and increasing frequency, the tendency is to maintain the strain rate approximately the same in both the long- and short-life tests. Thus, in the case of strain-rate insensitive materials, the choice of frequency is a compromise between convenience of test length and not too excessive a variation in the average strain rate. To set the strain amplitude to the desired value we must first select a full scale range on the strain module, *B* in Fig. 19, which encompasses the strain range of the test. The span pot *D* can then be adjusted to give between 0 and 100 percent of the full scale range selected on the module thereby giving the desired strain amplitude. Finally, if a mean strain is desired, it may be set with the mean level control pot *E*.

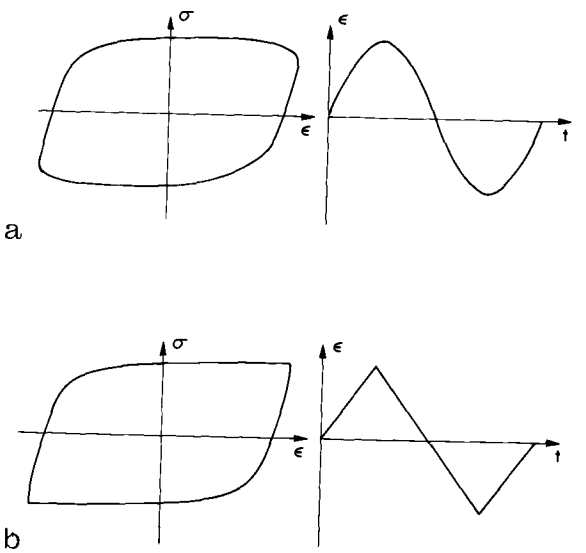

FIG. 18—*Stress-strain response of the same specimen to different* ϵ-t *waveforms.*

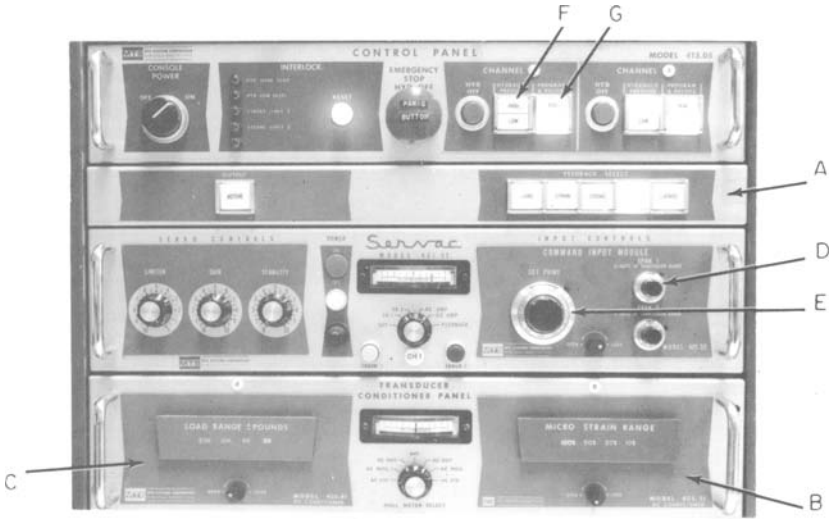

FIG. 19—*Control panel and command input system.*

Recording of Data

Prior to commencement of a test the appropriate range must be selected on the load module and the recorders must be set on ranges which will accommodate the quantities to be measured. This is done in a standard fashion and we wish to use this section to describe the types of recorders we normally employ.

The Varian (Varian Associates, Palo Alto, Calif.) Model F80 recorder *A*, shown in Fig. 20, is used to record stress-strain hysteresis loops up to a frequency of about 1 Hz. Associated with the *X-Y* recorder is a recorder input selector *B* which allows the selection of load or strain inputs from either of two channels. The recorder input selector is also equipped with a zero suppression control for both the *X* and *Y* axes.

The Tektronix (Tektronix, Inc., Beaverton, Ore.) Model No. RM564 storage oscilloscope *A*, shown in Fig. 21, is used for two recording purposes: first to record hysteresis loops at frequencies greater than 1 Hz, and second, it can be used in conjunction with the amplitude measurement panel *B* to monitor the amplitude of a particular variable to a precision of 0.2 percent of full scale.

The Brush (Brush Instruments Div., Clevite Corp., Cleveland, Ohio) recorder Mark 280, *A*, and recorder input selector *B* in Fig. 22, allow the recording of variables from either channel versus time at a frequency up to about 50 Hz. This two-channel strip chart recorder is used to monitor the progress of a test and is not usually employed for precision measurements (mainly because of the small paper width and consequent low resolution).

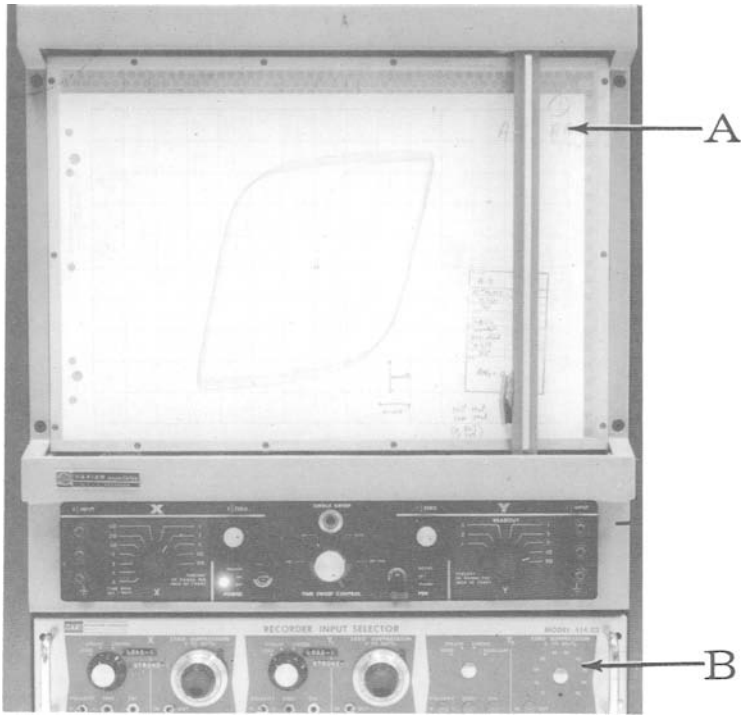

FIG. 20—X-Y *recorder and input selector.*

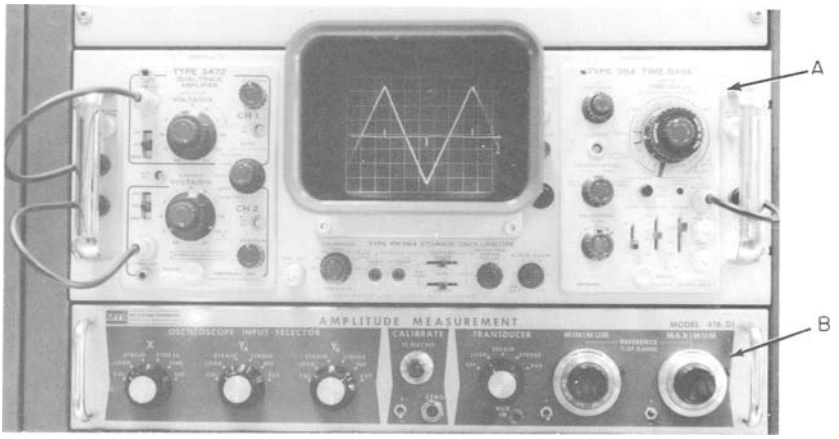

FIG. 21—*Oscilloscope, oscilloscope input selector, and amplitude measurement device.*

Test Start-Up and Test Control

In initiating a test we first select the appropriate feedback signal on the feedback select panel *A* in Fig. 19, which in this case is the strain signal. The Servac is then balanced for zero feedback with the set point control *E*. The hydraulic pressure button *F* is then turned on and small adjustments in the mean valve of the strain are made to ensure that the specimen is at zero mean load. Next all of the charts are checked to see that the pens are writing and the recorders are set to the appropriate scales. For higher frequency tests, where the oscilloscope is used to monitor the amplitude, the appropriate amplitude levels are set in the amplitude measurement panel *B*, shown in Fig. 21. The test is commenced by pushing run button[10] *G*, in Fig. 19. The strain limits and the load response are monitored on the recorders and minor adjustments can be made via the span control *D* and set point *E* to ensure the proper strain limits. Strain-time and load-time records are made virtually continually on the Brush recorder. The first ten hysteresis loops are usually recorded continually and subsequent recordings are made periodically when significant changes have occurred in shape or size of the loop. The test is continued until specimen failure occurs.

Determination of Failure

We define failure as having occurred when the specimen is in two separate pieces. However, in strain control, a specimen that is broken into two pieces may continue to cycle even though there is a zero tensile load response. Therefore, in order to obtain the proper number of cycles to failure and prevent hammer damage to the fracture surfaces, either an operator must be present when the specimen separates or provisions must be made for stopping the specimen prior to its complete separation. The shutoff device which we use is a load peak counter which requires that a predetermined tensile load be reached on each successive cycle for the test to continue. The present load which must be reached is usually set at about 50 percent of the steady state stress response of the specimen. Thus, when a crack develops in a specimen and the tensile load falls below the preset value the machine will stop, allowing the operator to run the final few cycles while carefully observing the specimen. The indication of a crack

[10] Although this may seem trivial, it is the "moment of truth" when operating a *closed-loop* system, for once the run button is pushed the operator effectively gives up control of the machine and must stand by and watch the machine carry out its preselected program. What might seem to be minor errors in programming or switch settings often end in disaster (accidentally broken specimens, mangled extensometers, etc.) long before the operator has time to override the machine. Thus, it is not uncommon to see an MTS operator hesitate for several minutes before nervously depressing the run button. One must conclude that the allowable margin of error in test setup is far less in a closed-loop system as opposed to an open-loop system.

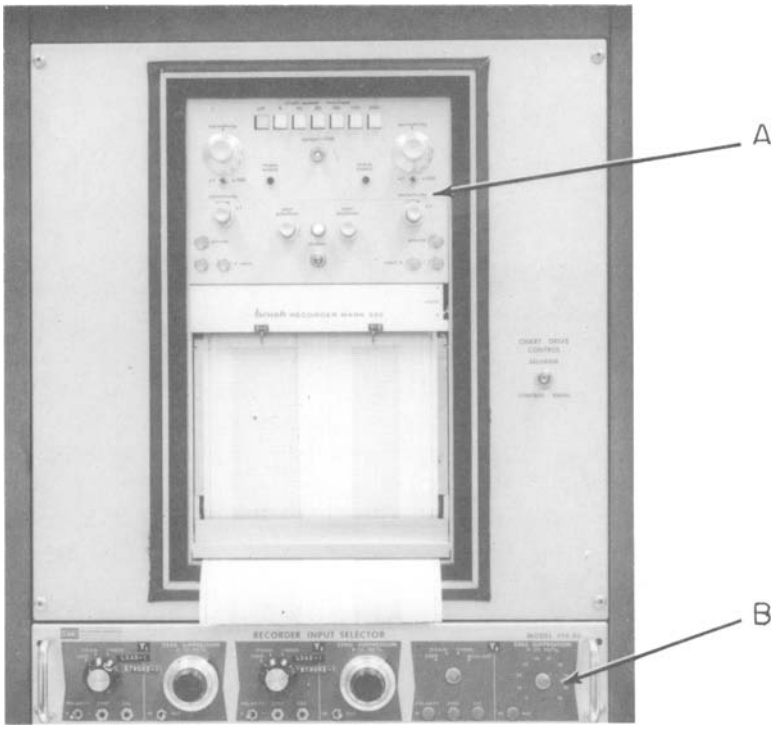

FIG. 22—*Strip chart recorder and input selector.*

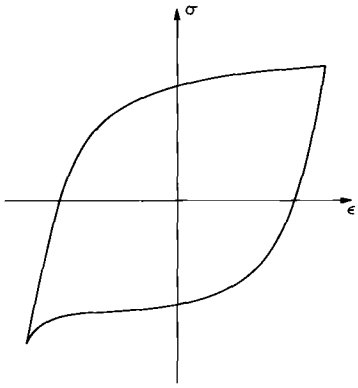

FIG. 23—*Indication of cracked specimen by irregularity in compressive half of hysteresis loop.*

may also be noted by the development of an inflection point in the compressive half of the hysteresis loop. An example of this behavior is shown in Fig. 23.

Additional Procedures Associated with MTS Low Cycle Fatigue Tests

Although most of our work is completely reversed strain- or stress-controlled fatigue testing, we also conduct, as a matter of routine, monotonic tension and compression tests. In addition, to ascertain quickly a material's cyclic stress-strain behavior or to rank a material's fatigue resistance relative to several others [*4*], we often employ the incremental step strain test devised by Landgraf et al [*5*]. This test incorporates a modulated strain-time program which is developed in the following way:

1. The function generator in Fig. 17*a* is set to a sine wave form. The maximum amplitude of the wave form is set by the span control (Fig. 19*d*).
2. The Data-Trak (Fig. 17*c*) is programmed with a linearly increasing-decreasing ramp function.
3. The programs from the function generator and Data-Trak are combined in such a way as to produce a modulated sine wave program, for example, the strain-time program shown in Fig. 24. The associated cyclic stress-strain response (that is, hysteresis loops) is shown in Fig. 25.

After the application of several blocks of this increasing-decreasing strain-time history, a stabilized stress-strain response develops. The curve drawn through the tips of these stabilized hysteresis loops have been found to represent adequately the cyclic stress-strain curve [*5*].

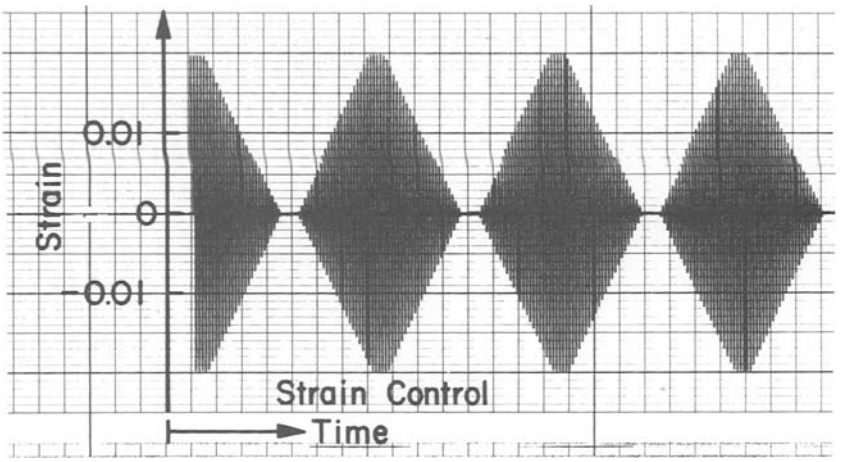

FIG. 24—*Strain-time record of incremental step strain test.*

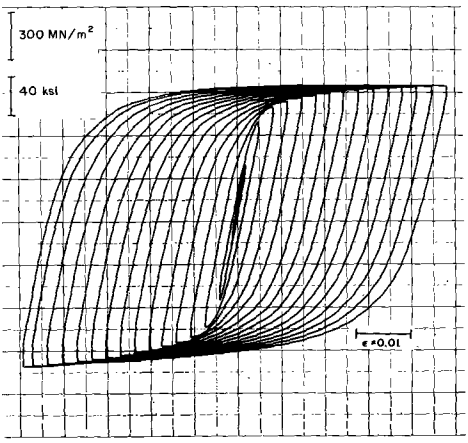

FIG. 25—*Stress-strain response of incremental step strain test.*

Analysis, Reduction, and Presentation of Data

From the recordings of hysteresis loops made in the progress of a test, for example, Fig. 26, data is reduced in the following manner:

1. The total of the strain range and cycles to failure for the specimen is recorded. This becomes a single point on a strain-life curve.

2. The plastic strain range and stress amplitude at one half of the life are determined from the hysteresis loops recorded at this point. This becomes a single point on the cyclic stress-strain curve.

3. A cyclic strain hardening or softening curve is constructed by plotting the stress amplitude, that is, $\triangle\sigma/2$, Fig. 26, versus cycles. Several such curves are shown in Fig. 27.

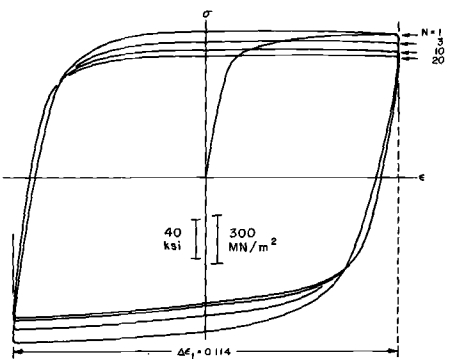

FIG. 26—*Typical mechanical hysteresis loops of cyclically work softening material.*

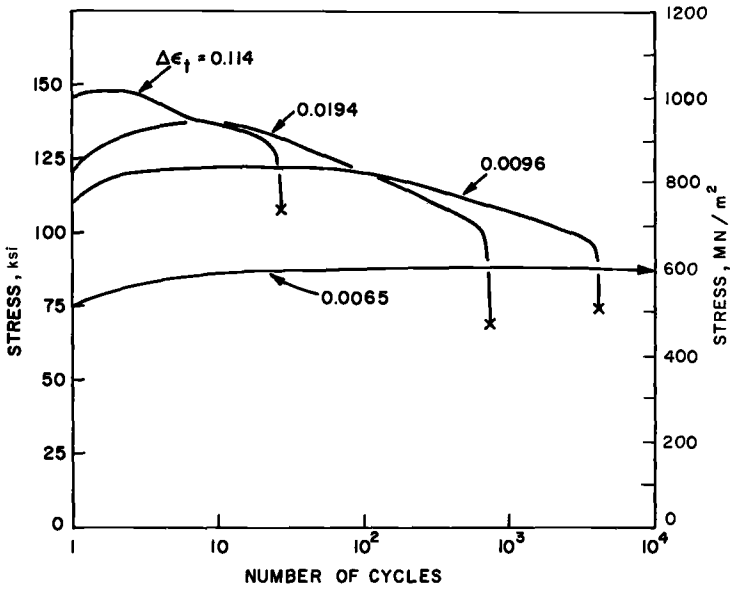

FIG. 27—*Stress amplitude-cycles curve showing stress response of a material.*

Once a series of companion specimens have been tested at various strain amplitudes the following plots are constructed:

1. A total strain range, $\triangle\epsilon_t$ versus cycles to failure, N_f curve (or reversals to failure, $2N_f$) Fig. 28. Comparison of this life behavior is usually made with the predictions of life based on the empirical methods of Manson [*6*] and Morrow [*7*] which utilize only monotonic properties. Calculations for these predicted curves are usually made on computer.

2. A cyclic stress-strain curve, that is, a plot of $\sigma_a = \triangle\sigma/2$ versus $\triangle\epsilon_p/2$, both determined at $N_f/2$, for example, Fig. 29. This data is usually fitted by a computer with an equation of the form, $\triangle\sigma/2 = k(\triangle\epsilon_p/2)^{n'}$.

3. A stress amplitude, $\sigma_a = \triangle\sigma/2$ versus cycles to failure, N_f (or reversals to failure, $2N_f$) curve. This data is usually fitted by computer with an equation of the form $\sigma_a = \sigma_f'(2N_f)^b$.

These curves, along with the hysteresis loops, are used in conjunction with studies of slip band damage and crack morphology to interpret the deformation and fracture processes occurring during low cycle fatigue.

Performing a Low Cycle Fatigue Test in an Instron Test System

An appreciable portion of our low cycle fatigue research has been carried out at low temperatures, that is, below room temperature and down to liquid nitrogen temperatures [*8–13*]. In this section we shall treat in de-

tail the techniques which we have employed for this type of testing. However, much of the equipment and methods may also be used for room temperature work as well.

Description of Test System

The Instron test system that we employ is a standard system (Model No. TTCL) except for several special purpose modifications. A general view of this machine is shown in Fig. 30. The load is applied by the crosshead *A*, which is screw driven. Load cell *B*, which is a ± 10-kip (44.4-kN)

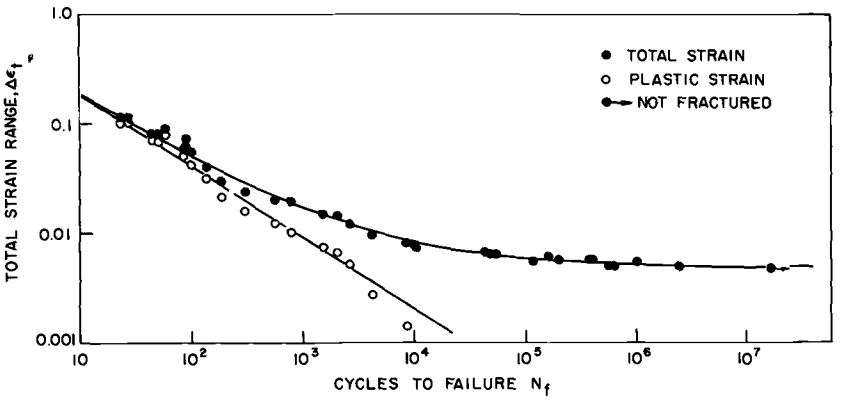

FIG. 28—*Strain range-cycles to failure curve.*

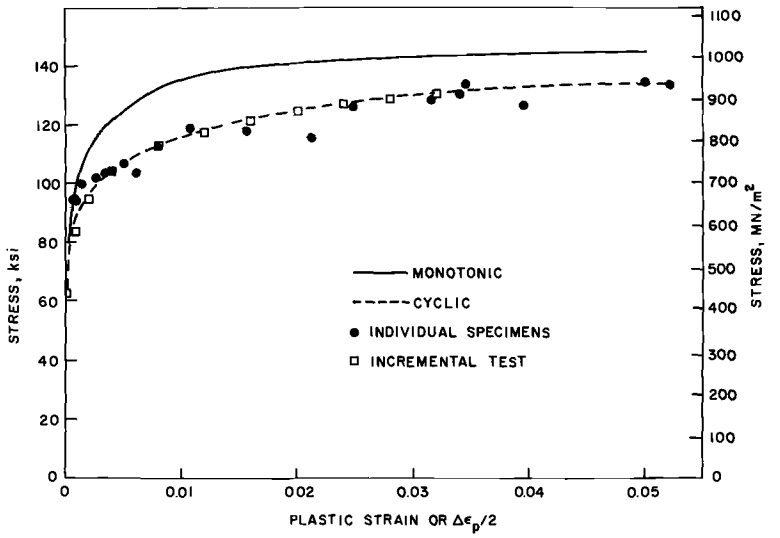

FIG. 29—*Cyclic stress-strain curve.*

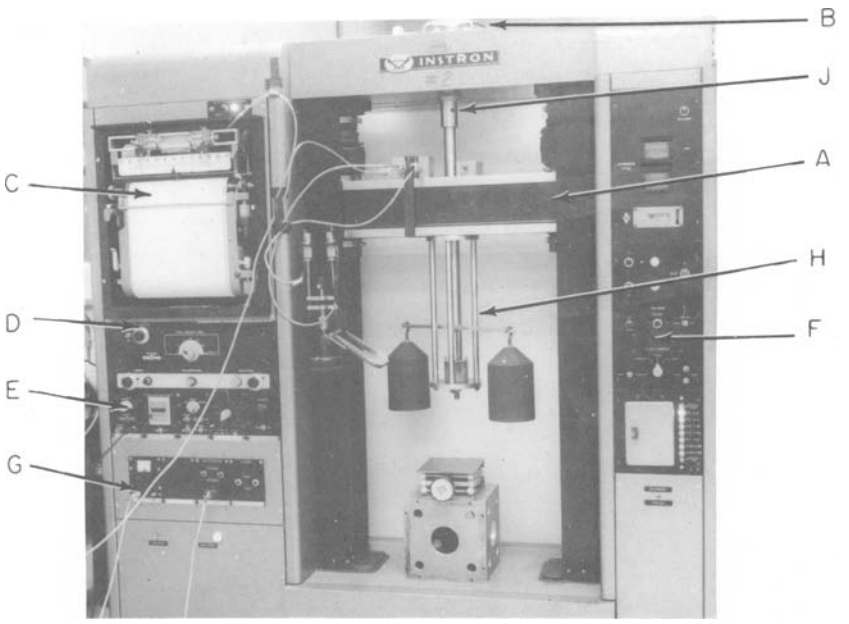

FIG. 30—*Overall view of Instron testing system.*

reverse stress load cell, measures the load which is recorded on the strip chart *C*. The range selector panel *D* allows the selection of full scale ranges between 0.2 and 10 kip (0.89 and 44.4 kN). Panel *E* contains several assorted standard Instron options (such as area compensator, event marker, decade zero suppression, etc.). Panel *F* on the right side contains all the run controls, that is, stop, start, and crosshead speed controls. Panel *G* on the lower left contains several special modifications which we have made in order to carry out strain control low cycle fatigue tests. The carriage *H* is attached to the moving crosshead and has a Wood's metal pot attached to the lower carriage plate. A Dewar flask may be fitted around the carriage for low temperature tests. The load train is completed by bar *J*, which attaches to the top end of the specimen, passes through a hole in the crosshead, and attaches to the load cell.

Assorted electronic devices used for control and recording of low cycle fatigue tests are shown in Fig. 31. The exciter, demodulator, amplifier unit, *K*, is a Daytronic (Daytronic, Inc., Dayton, Ohio) Model No. 300 CL-60 which powers the linear variable differential transformers (LVDT) used on the extensometer. This unit has been integrated into the crosshead cycling circuit of the Instron machine for strain control testing. The Daytronic unit has been modified by replacing the standard-limit setting pots by more sensitive and accurate pots which allow calibrated settings.

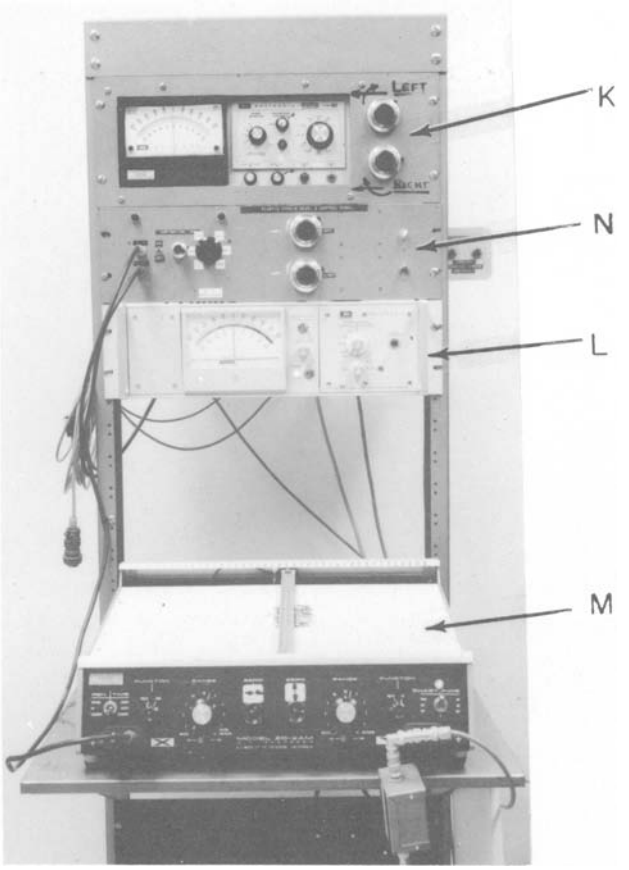

FIG. 31—*Special electronics and recording equipment.*

Strain gage type extensometers, which we occasionally use for strain control testing in the Instron system, are powered by the transducer, conditioner unit, *L*, which is a Daytronic Model 300D-91. The Moseley (Moseley Div., Hewlett-Packard Corp., Palo Alto, Calif.) Model 2D2 *X-Y* recorder *M* is used to make load-extension recordings (hysteresis loops). Unit *N* is a special device for the direct measurement and control of the plastic strain [*14*]. This device and other modifications will be discussed in detail in later sections.

Specimens

The specimen that we have generally used for low temperature work in the Instron system is shown in Specimen *E* of Fig. 6 and in Fig. 8. The discussion given on the design and machining of specimens (pp. 33–

37) applies as well to this specimen. The main difference in this specimen, compared to those used in the MTS system, is that shoulders are used for the attachment of a special low temperature extensometer. The extension is therefore measured across shoulders and not directly on a straight gage section. An effective gage length may be determined by the simultaneous measurement of extension and diameter (see Ref. *15*). The specimen shown in Fig. 8 has a 0.150-in. (3.810-mm) diameter with a 0.20-in. (5.08-mm) straight section giving an L/D of 1.3. The shoulders, which carry the extensometer, are ⅜ in. (9.53 mm) in diameter and the threaded ends are ½-13 UNC threads.

Mounting a Specimen

To mount a specimen (Fig. 32) we first place a 1½-in. (38.1-mm) diameter threaded washer *A* on the lower end of the specimen *B*. Next, a pot cover plate *C* is slipped over the specimen and is allowed to rest against the washer. Nut *D* is threaded onto the top of the specimen and this assembly is then screwed into the bar *H* and locked down tightly by the nut. The Wood's metal pot *E* is then melted with a torch and the specimen

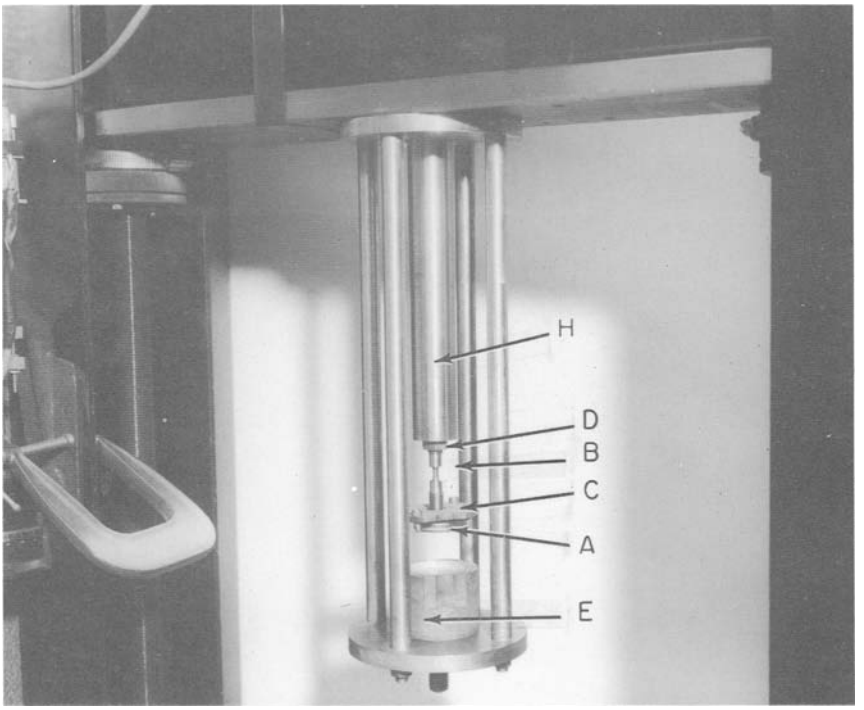

FIG. 32—*Mounting of specimen into Instron test fixture.*

assembly is lowered into the molten pot. The cover plate *C* is bolted to the pot. With the specimen in this position, a vessel containing cold water is placed around the pot to solidify the Wood's metal. During solidification the Instron machine is set to maintain virtually zero load. The specimen, in its final mounted position, is shown in Fig. 33.

Extensometry

The extensometer employed for low temperature testing is shown in Fig. 34 and is described in detail in Ref. *16*. The extensometer is calibrated using the fixture *A* shown in Fig. 35, which has a least reading of 0.0001 in. (0.0025 mm). The Schaevitz (Schaevitz Engineering, Camden, N. J.) LVTD's that we have normally employed are Model No. 60SSL, which have a range of $\pm$ 0.06 in. ($\pm$ 1.52 mm). With these transducers we have been able to resolve easily strains of the order of 10^{-5}.

The final configuration of the extensometer mounted on the specimen is shown in Fig. 36. The carriage, specimen, and extensometer arrangement is compact and contained within a 6-in. (152-mm)-diameter circle. This allows a Dewar flask with liquids, such as liquid nitrogen, to be placed around the specimen with the LVDT's extending above the liquid level.

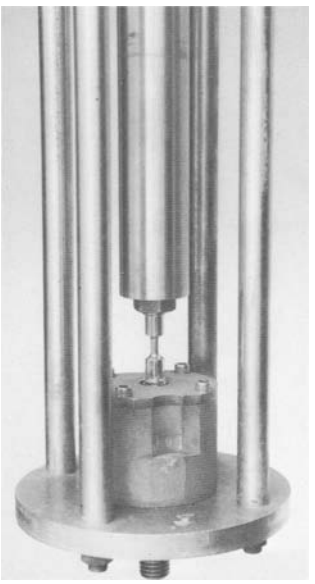

FIG. 33—*Specimen in final mounted position.*

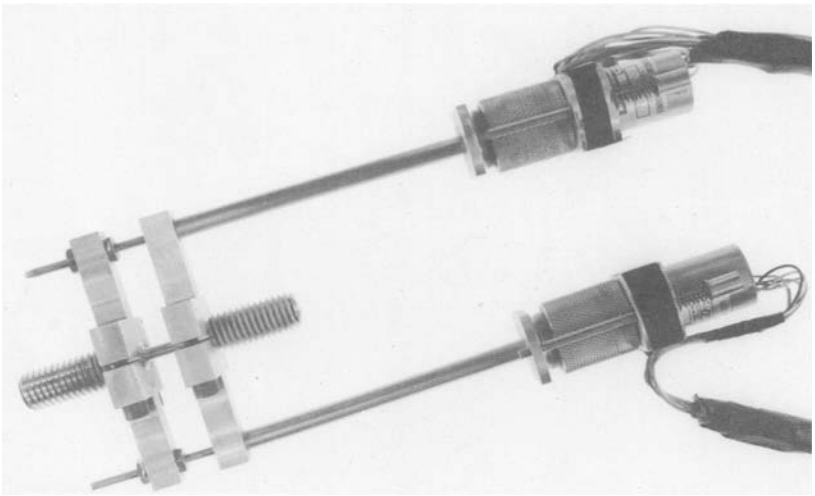

FIG. 34—*Extensometer for low temperature testing.*

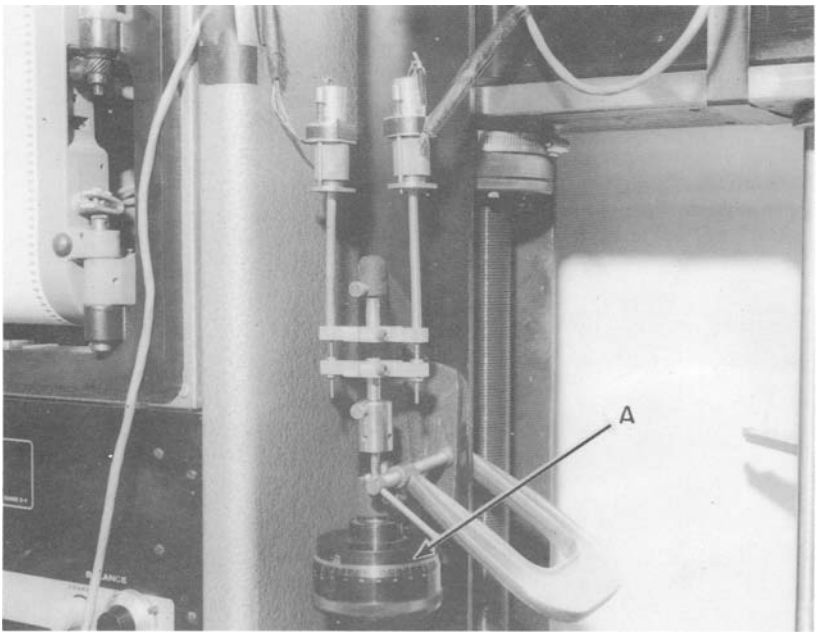

FIG. 35—*Calibration fixture for extensometer.*

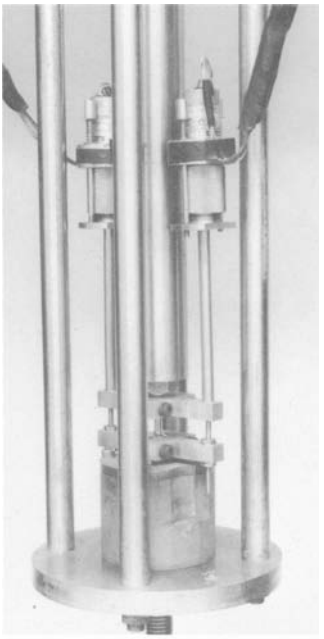

FIG. 36—*Extensometer mounted on specimen.*

Program Selection, Test Start-Up, and Recording of Data

In conducting a controlled total strain range test, we first set the preselected strain limits on the Daytronic instrument *A*, Fig. 37, by means of the calibrated dials *B*.[11] Next the appropriate scales are selected for the Instron load-time chart and the *X-Y* recorder.

If one desires to conduct a controlled *plastic* strain range test, it can be performed in either of two ways: manually or automatically. Both of these methods as well as the principle of operation of the automatic plastic strain unit are described in Ref. *14*.

Once the strain limits, whether total strain or plastic strain, have been selected and the charts set on the appropriate scales for recording, the test is commenced. We generally make continual recordings of load time on the Instron recorder and periodic recordings of hysteresis loops on the *X-Y* recorder. It is often necessary to make occasional adjustments to the control dials to maintain the strain limits at their preselected value. The test is then allowed to continue until the specimen fails.

[11] The wiring diagram for connecting the Daytronic limit circuit into the extension cycling circuit of the Instron machine may be obtained from the authors upon request.

Determination of Failure and Machine Shutoff

The discussion concerning the definition of failure (p. 49) and the problems encountered in the MTS system, also applies to the Instron system. The shutoff device also works on the same principle as before, that is, it is required that a predetermined tensile load be reached on each successive cycle for the test to continue. However, the manner of obtaining the shutdown command is different in this case. The device used to sense the predetermined tensile load is an external load limit system (which we have constructed) shown in Fig. 38. These external load limit switches are connected to an internal set of load limit switches normally supplied with the Instron. For machine shutoff, the tensile load limit switch is connected to the Instron cycle-stop circuit.[12]

Usually, the predetermined tensile load, set by means of limit switch *A* (Fig. 38), is not selected until the specimen has reached a steady-state stress response. After the test is completed, the analysis, reduction, and presentation of data are normally done in the same manner as discussed previously (p. 52).

Metallographic Techniques Associated with Low Cycle Fatigue Testing

As pointed out earlier, much of our work is concerned with microstructural changes occurring during fatigue. Consequently, several techniques have been developed for the study of (1) slip band damage and cracking behavior, (2) fracture surfaces, and (3) dislocation structures of metals.

The chief problem associated with surface damage studies is knowing a priori where the main crack will start. Of almost equal importance is the fact that it is undesirable to remove and remount the specimen for observation several times during a test. We have circumvented these problems in two ways. The first method may be used in either the MTS or the Instron and employs the flat-sided specimen shown in Fig. 6*c*. The specimen, electropolished by conventional methods, is mounted in either test system and two sets of plastic replicas[13] are then made of each flat side in the "virgin" condition. After allowing 20 to 30 min. for drying, the replicas are stripped off, mounted on glass slides, and labeled. Next, the specimen is cycled at the amplitude of interest for a percentage of its estimated life. With the specimen still in the machine, another set of surface replicas is made and labeled. This sequence of events (that is, cycle-replicate) is repeated until a major crack develops and fracture of the specimen is emi-

[12] The wiring diagram for these modifications may be obtained from the authors upon request.

[13] The replicating tape is a cellulose acetate tape which is softened in acetone prior to application.

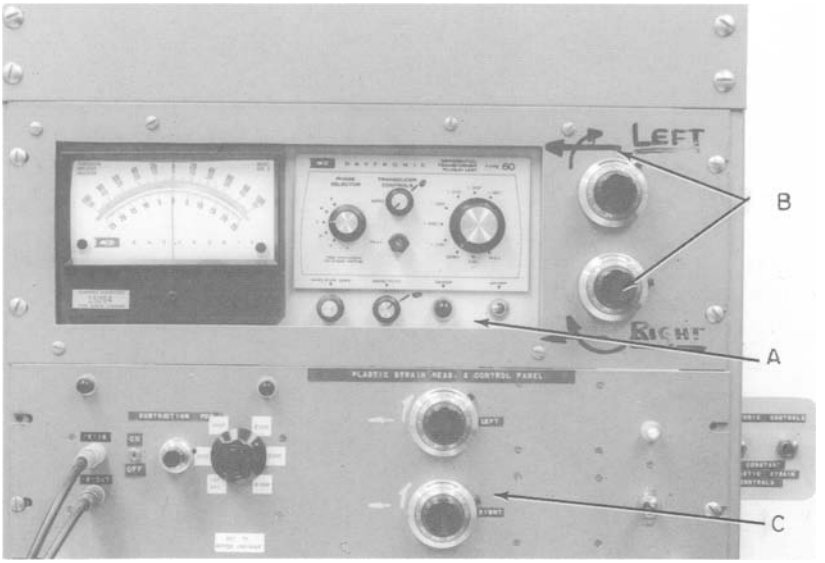

FIG. 37—*Associated electronics for strain-controlled tests.*

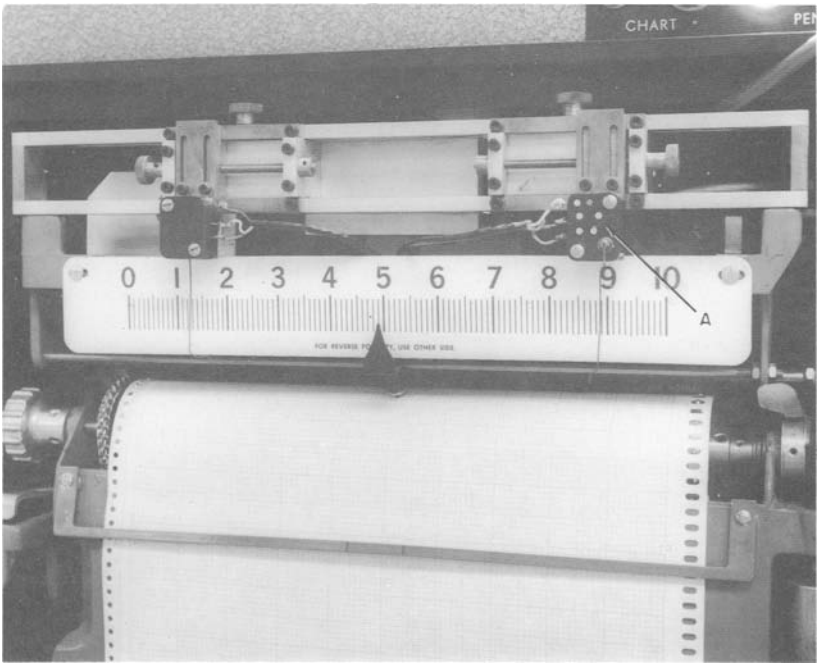

FIG. 38—*Load limiting switches.*

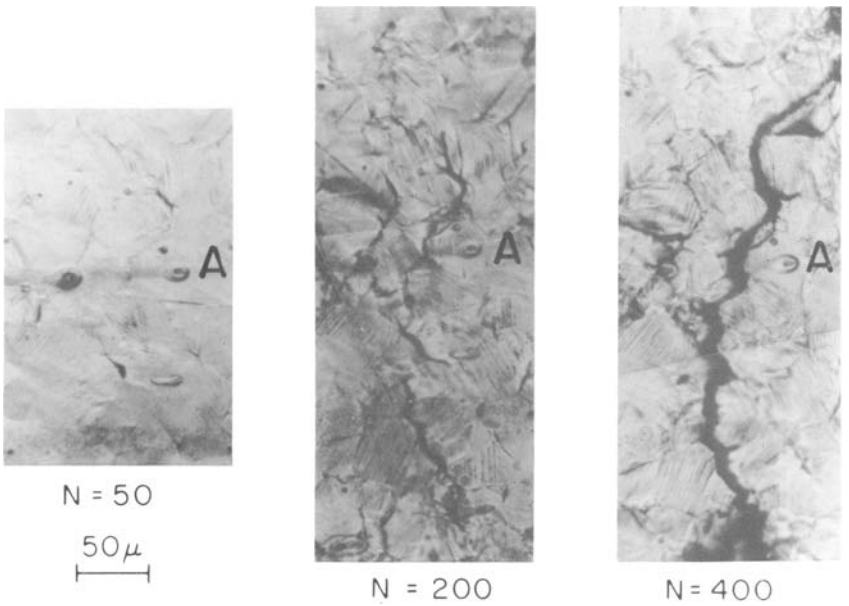

FIG. 39—*Micrographs obtained from replicas showing the development of the main fatigue crack on the surface of a flat-sided Ni_3Mn specimen. Pit at point* A *may be used as a reference marker.* $N_f = 460$ *cycles.*

nent. The specimen is then removed from the machine and a photographic montage is made of the main crack. One of the two sets of replicas is shadowed with vaporized chromium for observation with a light microscope and the second set is saved in the event a more detailed study using an electron microscope is required. With the main crack identified, it is a relatively simple procedure to retrace and photograph at various stages of the life, the cracking sequence from the replicas. A typical example of photographs taken in this way of the cracking sequence in a Ni_3Mn alloy is shown in Fig. 39.

Although the above technique does provide an adequate approach to the study of the topography of fatigued specimens, it is time consuming and tedious. The second technique requires less effort and utilizes the specially designed microscope—MTS load frame shown in Fig. 5. Using a specimen similar to Specimen *H* shown in Fig. 6, the main crack is "forced," on account of the stress concentration, to initiate and propagate from a predetermined site, that is, the edge of the hole. Thus, *in situ* photographs may be taken with ease of the development of surface damage as a function of cycles. Such a series of photographs taken in a recent study of the fracture behavior of gray cast iron [*17*] is shown in Fig. 40. Both of the above

methods have the advantage of being able to record surface damage at any point during a cycle (for example, at the maximum tensile stress) since the specimen remains in the machine. However, in the second method, dynamic as well as static observations may be made.

Fracture surface observations, as opposed to surface damage studies, require that the failed specimen be removed from the test fixture and observed directly on its fractured faces. The primary consideration in this phase of our testing is to prevent the faces of the failed specimen from "hammering" together and thereby destroying fatigue markings on the fracture surface. To prevent such occurrences, we rely on the automatic shutoff devices already discussed (pp. 49 and 61).

For dislocation structure studies, the first consideration is to have available an ample amount of equally strained bulk material. This can only be accomplished by using a straight gage section specimen such as that shown in Fig. 8. The specimen is cycled at a given amplitude and number of cycles, removed from the test machine, and mounted in a holding fixture. Wafers, approximately 0.05 in. (1.27 mm) thick, are carefully cut from the gage section of the specimen using a jeweler's saw. Further reduction of the wafers to a thickness of about 0.01 in. (0.25 mm) is then done by hand on No. 600 emery paper using methyl alcohol as a coolant and lubricant. Next, the wafer is masked off on its edges with electroplater's lacquer and electropolished from both sides to local thicknesses (hopefully) of about 2000 Å. Transmission electron microscope specimens are then cut from the electropolished wafers and viewed in the microscope to ascertain if sufficient thin regions are available for study. If not, then a second attempt must be made. Several such attempts may be required before an adequate microscope specimen is obtained. The need, therefore, for a specimen with a straight gage section at least ¼ in. (6.35 mm) long

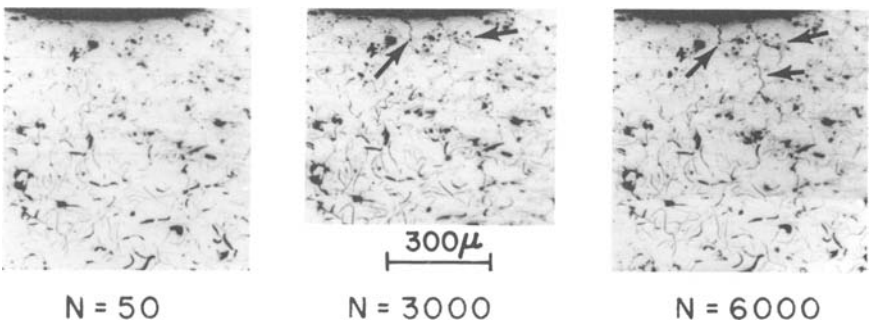

FIG. 40—*Micrographs obtained from direct observations with microscope—load frame showing the development of the main fatigue crack at the edge of a hole in a gray cast iron specimen.* $N_f = 14{,}000$ *cycles.*

is obvious. Typical results obtained by the above procedure are given in Ref. *12*.

Summary

We have presented a description of the systems and techniques we *have* employed for low cycle fatigue studies. We are constantly striving to improve our existing methods and to develop new and better techniques. Thus, we hope to expand our capability to attack complex problems which demand techniques beyond the current state of the art. At the time of this writing, for example, we are installing in one of our MTS systems a pseudo-random noise generator and a digital block/random programmer which will enable us to study cumulative (low cycle) fatigue damage under complex strain (or stress) histories. The use of these, and other innovations, may provide the means to obtain new insight and results on the fatigue behavior of materials.

Acknowledgments

The authors wish to thank R. M. Wetzel, formerly at the University of Waterloo, Waterloo, Ontario, and now at our laboratory, for helping us with the original design of our MTS load frames and grips. His capable assistance in the initial operation of our MTS test system during his stay in our laboratory in the summer of 1967 is gratefully acknowledged. G. Mabee has provided continued assistance in the maintenance and upgrading of this equipment.

The test procedures we describe in this paper have been strongly influenced by the senior author's past association with the staff of the H. F. Moore Fracture Research Laboratory of the Department of Theoretical and Applied Mechanics, University of Illinois. In particular, the senior author wishes to acknowledge his continued association with JoDean Morrow of the University of Illinois, who has offered considerable advice and encouragement.

We also wish to thank P. Beardmore, T. L. Johnston, and R. Landgraf for their comments on this manuscript.

References

[*1*] Raske, D. T. and Morrow, JoDean, "Low Cycle Fatigue Testing from the Viewpoint of Mechanics of Materials," *Manual on Low Cycle Fatigue Testing, ASTM STP 465*, American Society for Testing and Materials, pp. 1–26.

[*2*] Kehl, G. L., *The Principles of Metallographic Laboratory Practice*, McGraw-Hill, New York, 1949.

[*3*] Tegart, W. J. McG., *The Electro-Polishing and Chemical Polishing of Metals*, Pergamon Press, New York, 1959.

[4] Feltner, C. E. and Landgraf, R. W., "Selecting Materials to Resist Low Cycle Fatigue," *Paper No. 69-DE-59*, American Society of Mechanical Engineers, May, 1969.

[5] Landgraf, R. W., Morrow, JoDean and Endo, T., "Determination of the Cyclic Stress-Strain Curve," *Journal of Materials*, JMLSA, Vol. 4, No. 1, 1969, pp. 176–188.

[6] Halford, G. R. and Manson, S., "Application of a Method of Estimating the High Temperature, Low Cycle Fatigue Behavior of Materials," *Transactions*, American Society for Metals, Vol. 61, 1968, pp. 94–102.

[7] Morrow, JoDean, "Cyclic Plastic Strain Energy and Fatigue of Metals," *Internal Friction, Damping and Cyclic Plasticity, ASTM STP 378*, American Society for Testing and Materials, 1965, pp. 45–87.

[8] Feltner, C. E., "Dislocation Arrangements in Aluminum Deformed by Repeated Tensile Stresses," *Acta Metallurgica*, AMETA, Vol. 11, No. 7, July, 1963, pp. 817–828.

[9] Feltner, C. E. and Sinclair, G. M., "Cyclic-Induced Creep of Close-Packed Metals," *Joint International Conference on Creep*, Institute of Mechanical Engineers, London, 1963, Session 3–9.

[10] Feltner, C. E., "A Debris Mechanism of Cyclic Strain Hardening for F.C.C. Metals," *Philosophical Magazine*, Vol. 12, 1965, p. 1229.

[11] Feltner, C. E. and Laird, C., "Cyclic Stress-Strain Response of F.C.C. Metals and Alloys—I. Phenomenological Experiments," *Acta Metallurgica*, AMETA, Vol., 15, Oct., 1967, pp. 1621–1632.

[12] Feltner, C. E. and Laird, C., "Cyclic Stress-Strain Response of F.C.C. Metals and Alloys—II. Dislocation Structures and Mechanisms," *Acta Metallurgica*, AMETA, Vol. 15, Oct, 1967, pp. 1633–1653.

[13] Laird, C. and Feltner, C. E., "The Coffin-Manson Law in Relation to Slip Character," *Transactions*, American Institute of Mining and Metallurgical Engineers Vol. 239, July, 1967, pp. 1074–1083.

[14] Mitchell, M. R. and Feltner, C. E., "Direct Measurement and Control of Inelastic Strain," Report No. SL-68-36, Scientific Laboratory, Ford Motor Co., Dearborn, Mich., 1968.

[15] Feltner, C. E. and Jackobs, J. A., "Automatic Area Compensator for Constant Stress Cycling," *Review of Scientific Instruments*, Vol. 34, No. 12, 1963, pp. 1360–1363.

[16] Feltner, C. E., "An Extensometer for Use at Low Temperatures," Report No. 64-37, Scientific Laboratory, Ford Motor Co., Dearborn, Mich., 1964.

[17] Mitchell, M. R. and Feltner, C. E., "Cyclic Deformation and Fracture Behavior of Gray Cast Iron," in preparation.

M. H. Hirschberg[1]

A Low Cycle Fatigue Testing Facility

REFERENCE: Hirschberg, M. H., "**A Low Cycle Fatigue Testing Facility,**" *Manual on Low Cycle Fatigue Testing, ASTM STP 465,* American Society for Testing and Materials, 1969, pp. 67–86.

ABSTRACT: The equipment and methods for low cycle fatigue testing used at the National Aeronautics and Space Administration (NASA) Lewis Research Center are presented. These include the design of the specimens, grips, and loading frame, as well as the hydraulic system and console which are capable of operating several testing machines simultaneously. The methods of measuring and controlling load, strain, and temperature are also included. Emphasis is placed on those items or procedures used in our laboratory but not commonly used by others.

KEY WORDS: materials tests, fatigue tests, fatigue (materials), mechanical properties stress cycle, strain measurement, low cycle fatigue, tests

The low cycle fatigue facility of the NASA-Lewis Research Center is used by a number of different investigators for a wide variety of research programs [*1–7*][2]. For this reason we have standardized the equipment and procedures wherever this was possible without affecting the desired testing versatility. We have accomplished this goal by running all of our axial low cycle fatigue machines (currently numbering eight) from a central console with as many components as possible common to all machines. Each machine is capable of performing any of our desired tests. It is the ease of operation of these machines from a central location and the fact that all the necessary peripheral equipment (for example, recorders, function generators, hydraulic supply, etc.) is always available for immediate use with any of the machines that we refer to this as a "facility" rather than a laboratory. This paper is a description of the equipment and procedures used at NASA-Lewis for conducting low cycle fatigue research programs. Emphasis is placed on those items or procedures used here but not commonly used by others, as well as the reasons for adopting those items or procedures.

[1] Head, Fatigue Research Section, Lewis Research Center, National Aeronautics and Space Administration, Cleveland, Ohio 44135. Personal member ASTM.

[2] The italic numbers in brackets refer to the list of references at the end of this paper.

Specimen Design

The specimen design used in any particular program depends on the information or data required. We have standardized our specimens to the extent that they have either of two end designs for gripping in our machines. These are a buttonhead as in Figs. 1(*a*) and (*b*) or a threaded end as in Figs. 1(*c*) and (*d*). Four standard specimens using these ends are also shown in this figure. They are (*a*) the solid cylindrical buttonhead specimen for ambient and elevated temperature tensile testing, (*b*) the solid, hourglass, buttonhead specimen for most of our ambient temperature fatigue programs, (*c*) the solid, notched, threaded specimen for ultrasonic crack detection work, and (*d*) the tubular, hourglass, threaded specimen for elevated temperature fatigue work. These figures include typical dimensions, surface finishes, and the location of the critical surfaces that are necessary for proper specimen alignment.

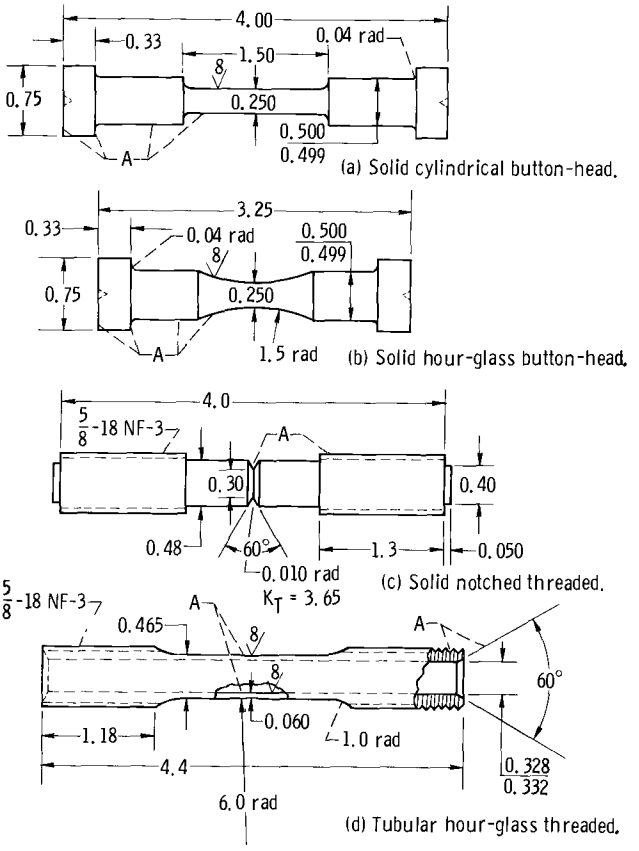

FIG. 1—*Standard specimen configurations.*

Many low cycle fatigue investigations incorporate notches in the specimen design. We have used two different types of notches, both having distinct advantages for specific investigations. These notch configurations are shown in Fig. 2 and are (*a*) the circumferential "V" notch and (*b*) the side or tangential slot notch. Typical dimensions are given on the figure.

The circumferential "V" notch is used in programs in which nominal stress rather than strain is to be controlled and in programs in which fatigue crack initiation data are to be obtained by an ultrasonic sensor rather than by visual observation. Considerable work has been done in our laboratory using ultrasonics for the detection of crack initiation and the measurement of crack growth rates. Ultrasonics as well as electrical potential and compliance measurements are sensitive to crack area rather than crack depth. It is therefore desirable to have as large a crack area as

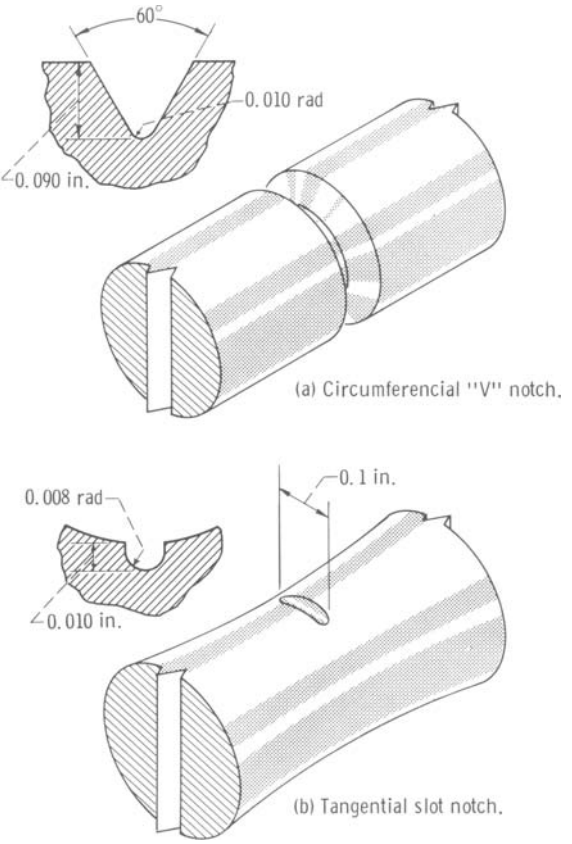

FIG. 2—*Fatigue specimen notch geometries.*

possible associated with a small crack depth if these methods are to be used to their greatest advantage. This is best accomplished with circumferential notches. It has been our experience [*1*] that in low cycle fatigue tests the crack front generally progresses uniformly inward around the specimen circumference at the notch, resulting in an appreciable crack area for a shallow crack depth. Localized cracks which start from point defects or slot notches would have to grow to a much greater depth before the same first detectable crack area would be produced.

Specimens with slot notches are used in programs in which nominal strain control is desired. Inasmuch as the slot notch removes a very small percentage of the specimen cross-sectional area and does not cover much of the minimum section circumference, it is possible to place a diametral extensometer across the unaffected portion of the specimen diameter and still obtain meaningful strain measurements. The slot notch is also very useful when visual observation of crack initiation is desired. Since the maximum strain concentration is at the geometric center of the slot notch, optical equipment can be focused easily at this point and crack initiation observed. When a circumferential notch is used, observation is made more difficult since the maximum strain occurs along a line around the entire circumference.

All specimens have a code letter and number stamped on both ends. The letter identifies the material and the number identifies the specimen in that material series. After failure of the specimen, both pieces are stored for possible future metallographic examination and can be easily identified from the coding.

Specimen Grips

In order to accommodate the two types of specimen ends, two different types of loading rods are used. The buttonhead and threaded types are shown in Figs. 3 and 4. A set of each type of loading rods is available for each of the fatigue machines and a change from one type to the other can be accomplished in a few minutes.

The buttonhead loading rods are connected to the buttonhead-type specimen by means of a split grip. Solid metal-to-metal contact between the specimen and the loading rods is obtained through the use of a set of tapered wedges. The wedges are driven into position while a tensile preload of approximately 200 lb is beeing applied (the dead weight of the lower platen, load cell, etc.). The integrity of the assembly is maintained during testing by a metal hose clamp that is tightened over the tapered retaining ring and bears against the protruding ends of the tapered wedges. Figure 3 shows the split grip, wedges, and final assembly for connecting the speci-

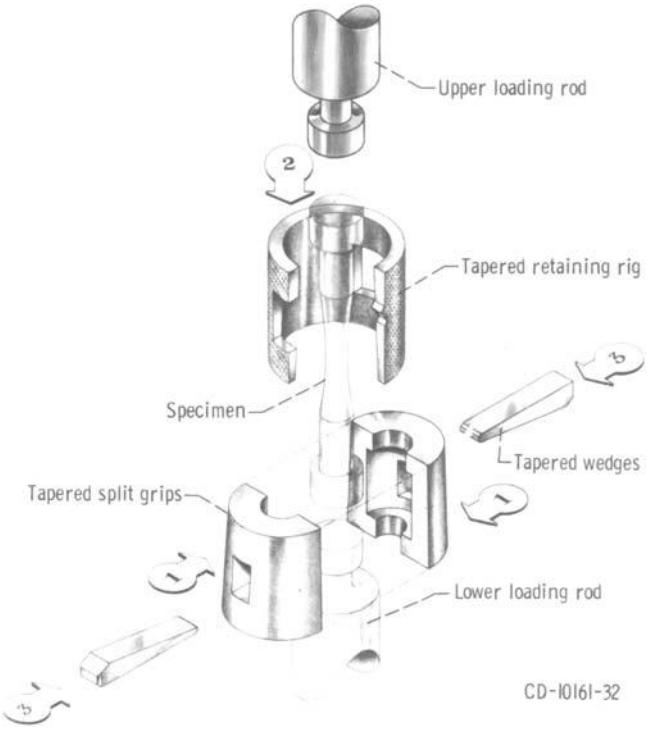

FIG. 3—*Split grip for use with buttonhead specimens.*

men to the lower loading rod. Another such assembly (not shown) is needed to connect the specimen to the upper loading rod.

The threaded loading rods are in three, rather than two, sections as seen in Fig. 4. The upper rod *A* and the lower rod *C* are connected to the frame of the fatigue machine. The specimen is screwed into the upper rod *A* and the center rod *B*. Lock nuts *D* are used to eliminate backlash from the machine threads. Final assembly is obtained by connecting loading rods *B* and *C* with the same kind of split grip described above since both of these rods have buttonhead ends. The use of the split grip at this point simplifies final assembly and does not load the specimen, a possibility when final assembly is achieved by tightening threaded members. Figure 4 shows the final assembly of a threaded specimen loading system.

The loading rods for the threaded specimens have an opening just beyond the ends of the specimen. These openings permit easy access to the ends of the specimens during testing and are currently being used for, (*a*) electrical connections to heating elements inserted into the hollow type

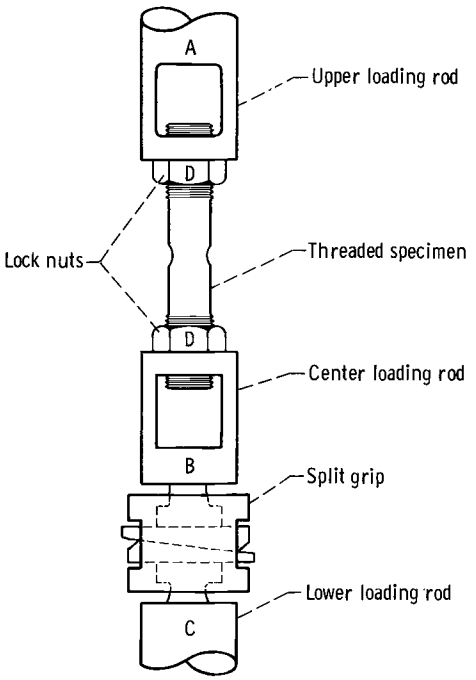

FIG. 4—*Loading assembly for threaded specimens.*

specimens and (*b*) for the attachment of ultrasonic crystals to the ends of solid notched specimens used in fatigue crack growth investigations. These ports might also be used to pass a cooling fluid through tubular specimens should external specimen heating and an associated method of providing rapid cooling be considered.

Loading Frame

The loading frame (Fig. 5) for all eight of our low cycle fatigue machines are identical and were designed and built at NASA. They are rated for ± 20,000-lb loads and differ from available commercial equipment in that a die set is used to maintain rig alignment during specimen compression. The frame consists of a base *A*, four support posts *B*, an upper support plate *C*, a hydraulic cylinder *D* having a 6-in. bore and a 6-in. stroke, and a load sensor *E* located between the die set and the piston rod of the hydraulic cylinder. The upper platen of the die set *F* is connected to the upper support plate, while the lower movable portion of the die set *G* is connected to the top of the load sensor. The loading rods *H* are located between the die platens, which are supported and guided by the die posts *J*.

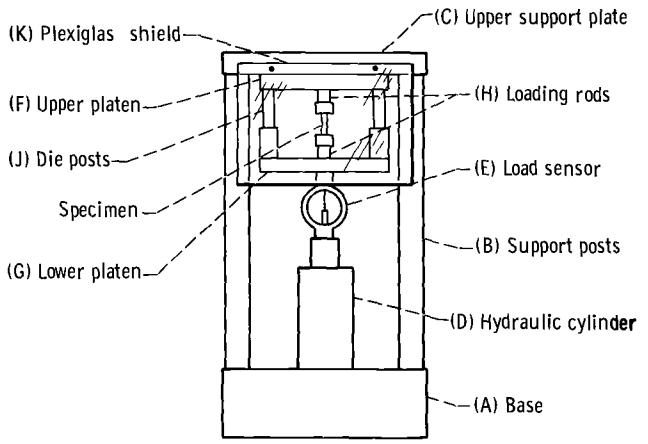

FIG. 5—*Schematic of loading frame.*

The use of the die set has disadvantages as well as advantages. The major disadvantage results from the large opening between the die set that produces a large elastic deflection of the loading linkages. This deflection requires the piston in the hydraulic cylinder to move farther, thereby increasing the oil flow requirements and reducing the frequency response of the machine. With the hydraulic system being used (discussed in a later section) the equipment is limited to 2-Hz operation. At this frequency it takes approximately 14 h to accumulate 10^5 cycles.

The advantages of using the die set are that it aids in maintaining the alignment of the loading rods, thereby decreasing the possibility of bucking in compression. The appreciable opening between the platens allows for a large working space while conducting tests and permits great flexibility in testing procedures. Space is available for microscopes and photographic equipment. Heating as well as cooling arrangements can be flexible and there is adequate room for mounting strain-measuring devices.

Before a machine is placed in operaton, two plexiglas shields *K* are mounted over the front and rear of the die set openings. These shields serve to protect laboratory personnel from equipment or specimen failure and act to insure the integrity of the test as well. High temperature tests are protected from drafts thus minimizing temperature fluctuations. The strain sensor and its associated lead wires are also protected from any accidental disturbance which could produce erroneous data and cause premature specimen failure.

Measurements and Observations

It is our philosophy that one should obtain as much information as possible from each test. On a macroscale this entails a complete history of

loads or stresses, displacements or strains, temperature, as well as the size and shape of cracks. This complete history would involve continuous measurements throughout each loading cycle from the first cycle to the time of failure. Since material behavior seldom changes very rapidly or erratically, the volume of data necessary for obtaining maximum information may be reduced effectively by taking data for preselected well-spaced cycles. The primary sensors used in our laboratory for obtaining this information are described below.

Load Measurement

A proving ring load sensor, shown in Fig. 6, is mounted in the loading frame as previously described and shown in Fig. 5. The ring is designed for ±20,000-lb operation and the relative axial movement of points *A* and *B* (Fig. 6) is approximately 0.001 in./1000 lb of load. A linear variable differential transformer (LVDT) is mounted in the opening of the ring as indicated in the figure and produces an electrical signal proportional to displacement, and therefore to load.

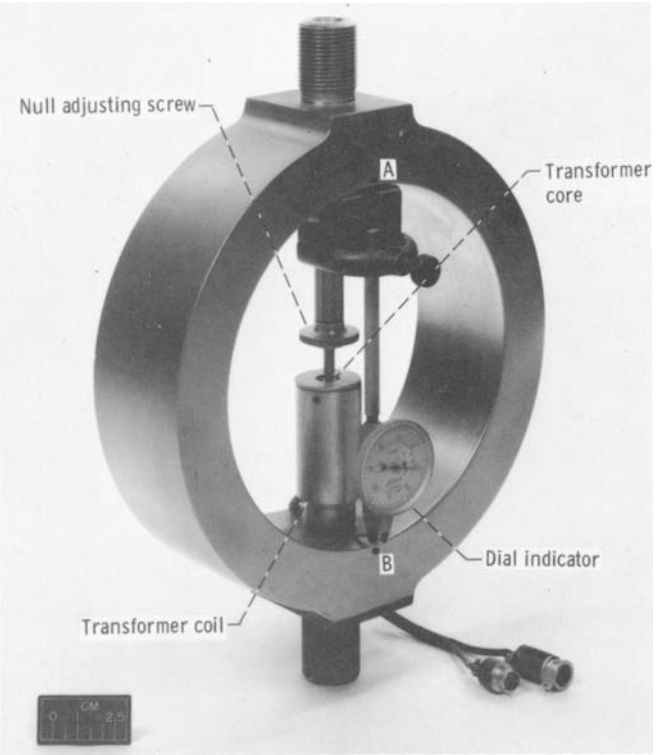

FIG. 6—*Proving ring load sensor.*

The advantages of the proving ring-LVDT method of measuring load over the more conventional load cells are: (1) There is almost no chance of damaging the sensor in the event of side loads, and (2) inasmuch as we use LVDT's to measure displacements, it is convenient to use the same type of transducer for load measurements as well. The transformers and the signal conditioning equipment are thus identical and hence interchangeable, resulting in easier maintenance.

The proving ring, with its linear deflection with applied load, provides a convenient place for obtaining a mechanical check on the electronic load calibration. Each of our proving rings has attached across points *A* and *B* a dial indicator on which the smallest division on the scale indicates approximately 100 lb of applied load. The dial indicators are not kept in position at all times since they are not meant for continuous cyclic operation, but rather they are placed in position periodically. The dial indicator reading of load is then compared with the readout from the load portion of the servo control equipment.

Strain Measurement

We have chosen to measure and control diametral rather than longitudinal strain. The extensometer used is of our own design and is illustrated in Fig. 7. Diametral extensions or contractions of the specimen *A* are transferred to the extensometer through the knife edges *B* to the support arms *C*. This displacement causes the support arms to rotate about the center of the flex spring pivot *D*, resulting in relative motion of the core *E* and the transformer *F* of the LVDT. The null adjustment screw *G* is used to position the core for zero output voltage when no axial load is being applied to the specimen. A small diametral tension spring *H* is mounted across the end of the gage to assure a small positive pressure and hence knife-edge contact on the specimen throughout the loading cycle.

In order that the extensometer not slip or rotate on the specimen during a test, it is supported by the eight springs *J*. The tension in each spring is individually adjusted by the turnbuckle *K* so that the gage is held horizontally and at the minimum section of the specimen.

It has been our experience that with the gage and supporting method described, knife-edge indentation of the specimen is not a problem and test results have not been affected by the presence of the gage. This has been assured by taking precautions in both the knife-edge design and in the choice of the diametral spring tension. The knife edge is not sharp, but rounded as shown in Fig. 7. This allows for large reductions in contact stresses for even small surface deformation. Contact stresses are initially kept at a minimum by supplying just enough spring force to keep

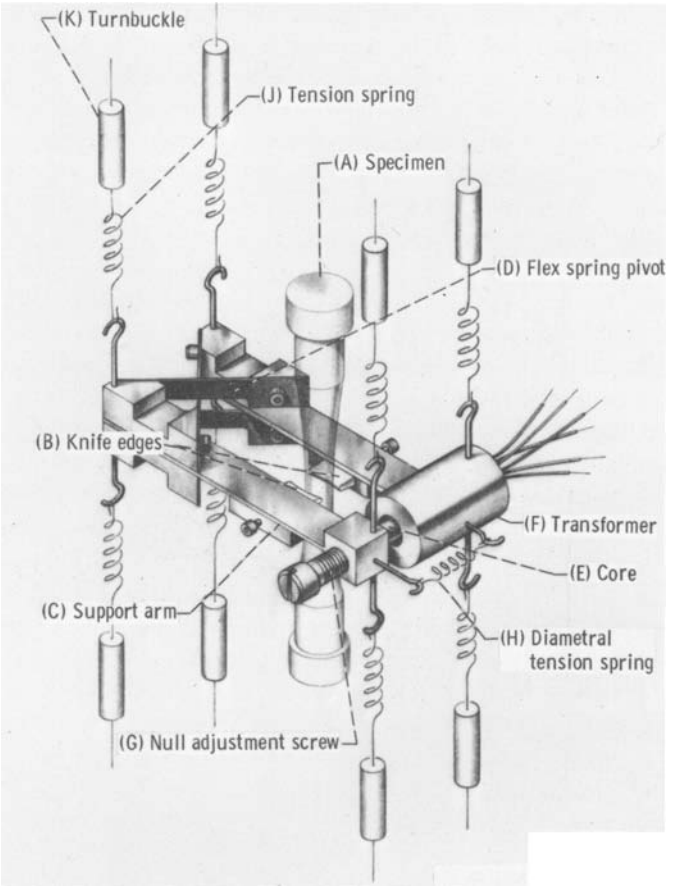

FIG. 7—*Diametral strain gage and supports.*

the knife edges following the specimen surface. The eight axial springs assist in minimizing the required diametral spring force since frictional forces between the specimen and the knife edges are not needed for supporting the gage.

There are a number of advantages as well as disadvantages associated with choosing a diametral measurement over a longitudinal measurement. Some of these are discussed by the other contributors to this publication. The major reason for our choice of a diametral measuring technique is our requirement that the same equipment be used for a wide variety of tests. The two tests that virtually demand diametral strain measurements are: (1) very low-life strain cycling tests in which the loads exceed the ultimate strength and necking occurs, and (2) high temperature tests.

The only possible way of obtaining meaningful strain measurements or control in the low-life strain cycling tests is to measure the specimen diameter at the plane of necking. A longitudinal reading across this necked section would result in erroneous data. In high temperature testing it might be difficult to maintain constant temperature over the gage length. A "hot spot" within the gage length will act the same as a strain concentration point. The temperature distribution on the plane of the minimum section of an hourglass specimen will tend to be uniform due to the symmetry of the structure. In the event that temperature variations with time are desired, as in a thermal fatigue test, it is just about impossible to have the entire longitudinal gage section vary in temperature at the same rate, whereas the minimum section of an hourglass specimen can maintain very nearly a zero temperature gradient.

Note that when a specimen is cycled and the diametral strain range $\triangle\epsilon_d$ is controlled and maintained constant, it does not necessarily mean that the longitudinal strain range $\triangle\epsilon_l$ is also maintained constant. This can be seen from the following equation relating these strain ranges.

$$\Delta\epsilon_l = 2\Delta\epsilon_d + [(1 - 2\nu)(\Delta P/AE)] \quad (1)$$

where:

$\Delta\epsilon_l$ = longitudinal strain range,
$\Delta\epsilon_d$ = diametral strain range,
ΔP = load range,
ν = Poisson's ratio,
E = Young's modulus of elasticity, and
A = nominal cross-sectional area of the specimen.

For a constant diametral strain range, the longitudinal strain range remains constant only if the load range also remains constant. Low cycle fatigue testing generally causes materials to either cyclically strain harden or strain soften [6, 7], which is another way of saying that $\triangle P$ either inincreases or decreases. However, under these conditions the term of the equation involving $\triangle P$ generally makes up only a small portion of the longitudinal strain range.

For the many materials we have tested under conditions of constant diametral strain cycling, the longitudinal strain range has varied by no more than 15 percent and this occurred for materials exhibiting extremes in cyclic strain hardening or softening. These variations occurred within the first 20 percent of the life of the specimen, and for the remainder of the life the diametral as well as the longitudinal strain ranges were constant. In the event that longitudinal strain cycling data were desired and that the small deviation from constancy resulting from running constant

diametral cycling tests were not acceptable, then either longitudinal strain cycling tests would have to be performed or an analog computer could be incorporated into the equipment. The computer can make it possible to maintain a constant longitudinal strain range while controlling on the diameter. Such a procedure is described in one of the other contributions to this publication [Slot et al, pp. 100-128].

There is one other condition that makes longitudinal rather than diametral strain cycling more desirable. This occurs when anisotropic materials are tested. Wells discusses this problem in his contribution to this publication, pp. 87-99.

Temperature Measurement

Our choice of a diametral, strain-controlled, tubular, hourglass specimen in conjunction with an internal heater has simplified the problem of temperature measurement. The test temperature of interest is at the minimum section where the heat is intentionally concentrated and the temperature is therefore the highest. Hence, we are not hampered by having to measure temperatures along a uniform gage length where thermal gradients would occur to varying degrees, particularly during nonisothermal testing. Nevertheless, with the internal heating element presently in use, we still encounter some temperature differential through the relatively thin (0.060 in.) specimen wall. The magnitude depends upon the thermal characteristics of the specimen material and the overall temperature level.

Our practice is to calibrate specimens of each material over a range of temperatures to determine the temperature difference through the wall at the minimum section as well as the temperature at points on the outside surface located $\pm\frac{1}{8}$ in. from the minimum section. These locations are then used as the control locations for spot-welding two small Chromel-Alumel thermocouples, one for the feedback control of the temperature servo system and the other for direct measurement with a portable potentiometer. Each thermocouple is not individually attached as a single bead, but rather one lead is welded to one side of the specimen while the other is welded at the diametrally opposed position. Thus an average of the two-spot location temperatures is indicated. The advantages of this overall arrangement, which is shown in Fig. 8, are twofold. First, the thermocouples are not attached in the zone of high strain, thereby avoiding the problem of having the spot-weld influence the fatigue life. Second, the use of the two thermocouples placed equidistant from the test section enables the operator manually to position the internal heating element until it is thermally centered in the specimen. This condition is achieved when the two thermocouples produce the same output. In addition to the readings taken with the portable potentiometer, the temperature as sensed

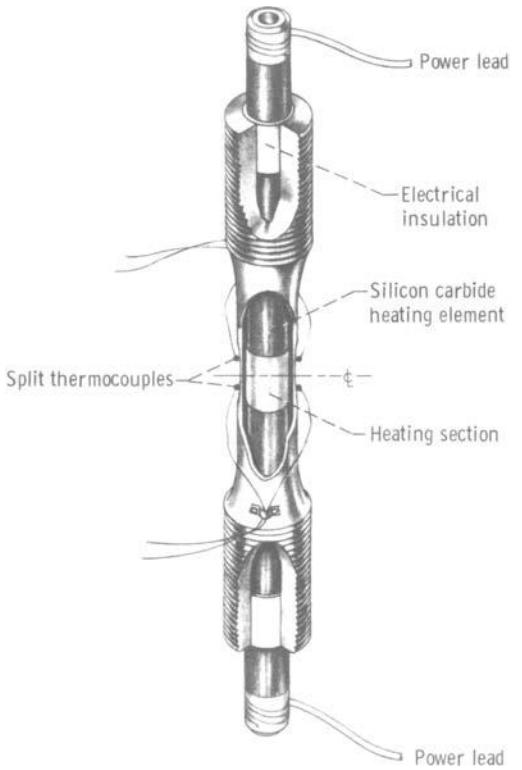

FIG. 8—*Instrumented high temperature specimen.*

by the control thermocouple can be recorded on a strip chart and can also be accurately read from the oscilloscope on the control console.

To achieve the desired specimen temperature, electric power is fed to a silicon carbide heating element through a step-down transformer. Approximately 300 W are required for maintaining a test section temperature of 1400 F. The input to the transformer is controlled by a commercial power regulator which in turn is controlled by a commercial temperature controller. Interchangeable thermocouple range cards are available to cover a wide variety of testing conditions. A drum-type curve follower is available for programming the temperature as a function of time, as is the case when conducting thermal fatigue tests.

Crack Initiation Measurement

We are currently employing two methods to determine the initiation of fatigue cracks. Both methods require notched specimens. The first is an optical method and uses a 30-power stereo zoom microscope mounted on

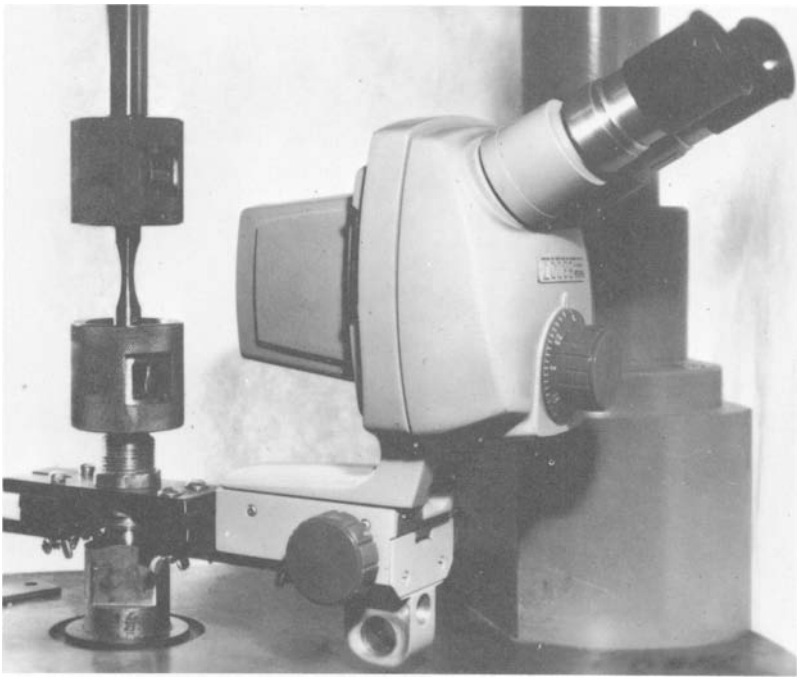

FIG. 9—*Setup for observing crack initiation at notch root.*

the fatigue machine and focused on the center of the slot notch described earlier. The experimental setup is shown in Fig. 9 and described in more detail in Ref *2*. With this arrangement it is possible to observe cracks 0.001 to 0.003 in. in depth and determine the number of cycles required to initiate them.

Another method being used to determine crack initiation and propagation involves the use of ultrasonics. In this method ultrasonic waves travel the length of the specimen while it is cycled. Changes in the reflected signal are a measure of the crack growth at the root of the circumferentially notched specimens. The test setup is shown in Fig. 10 and is described in greater detail in Ref *1*. This method has been used to detect cracks less than 0.001 in. in depth.

Console

The central control console contains all the electronic equipment necessary for the control of the fatigue machines as well as all the readout equipment. Many of these components are common to the eight machines with one set of readout instruments capable of recording data from any

one machine at a time. A more detailed description of the central control console follows.

Closed-Loop Servo Control Equipment

A commercial servo control unit is used for each of the fatigue machines. Each unit consists of a controller for the hydraulic system capable of closed-loop load, strain, or stroke control as well as a temperature controller operating off a Chromel-Alumel thermocouple between 0 and 2000 F. A schematic of the complete system is shown in Fig. 11. A more

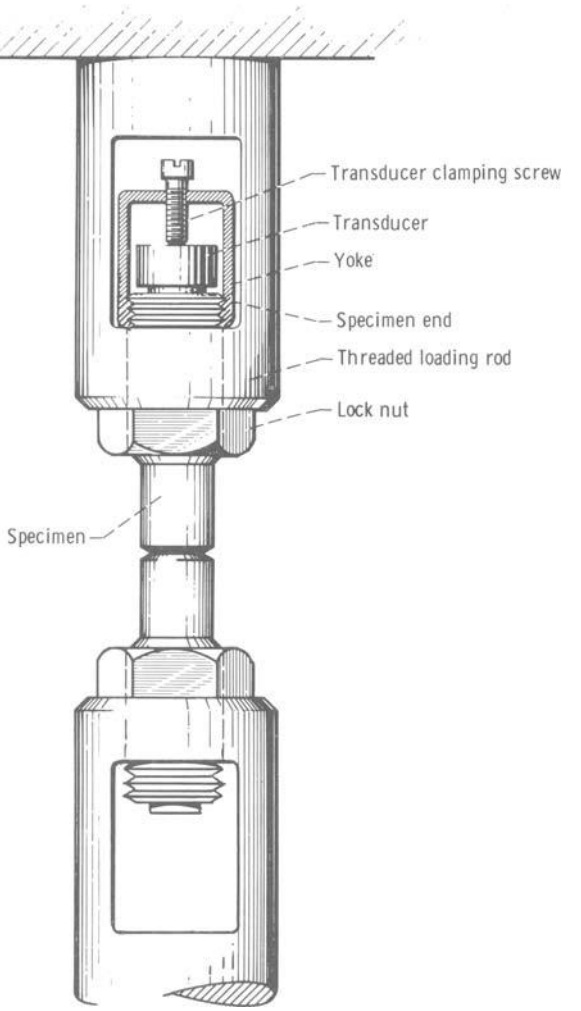

FIG. 10—*Setup for ultrasonic crack detection.*

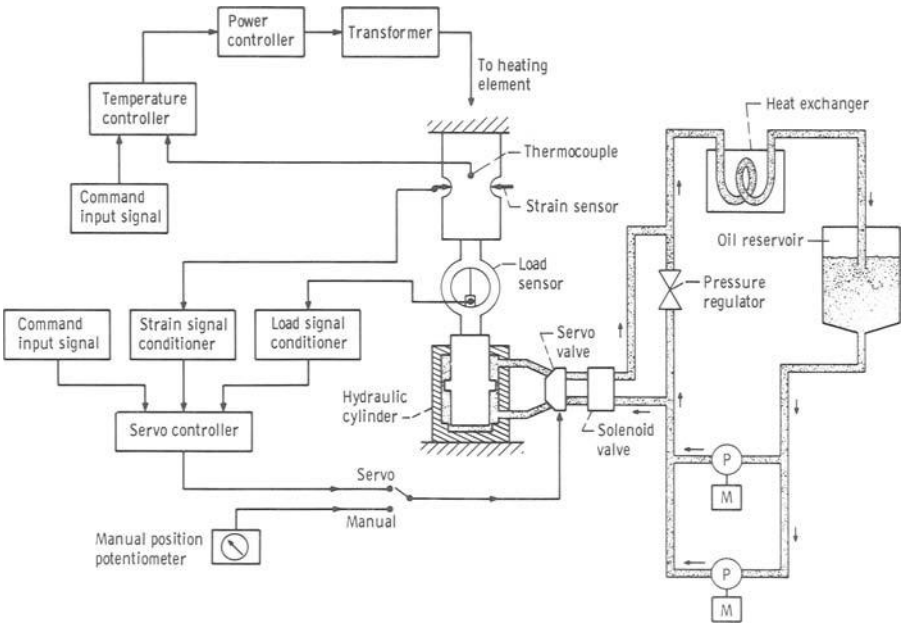

FIG. 11—*Schematic of electromechanical closed-loop servo system for material testing.*

complete description of the ways in which these pieces of equipment may be operated is described in the section, "Modes of Operation."

Command Input Signals

The command input signal is the electrical signal that the servo system is made to follow. Three types of function generators are available for the operation of any or all of the fatigue machines. They are: (1) a commercial low frequency function generator, (2) a NASA-designed ramp generator, and (3) a commercial drum-type curve follower.

The low frequency function generators (we use three) are used for the generation of sine, saw-tooth, and square waves. The most commonly used functions for fatigue testing in our laboratory are sine waves for room temperature testing and saw-tooth waves for the high temperature testing. The latter type function is desirable when loading rate or strain rate becomes an important test parameter.

The ramp generator is primarily used for controlled tension testing. It has the capability of producing an increasing or decreasing voltage, and can be switched to a hold position at any time. The ramp rate and direction can be changed manually at any time during a test.

The commercially available drum-type curve followers (we have four) are used when either the desired function frequency is below that obtainable from a low frequency function generator or when a command signal other than a standard sine, saw-tooth, or square wave is desired. These units are also used for programming temperature variations with time.

Measurements of Test Conditions.

Measurements of load, strain, temperature, cycle count, and elapsed time are available from each of the fatigue machines. When one of the machines is selected with the rig selector switch, the load, strain, and temperature signals from that machine are made available for readout on a differential input oscilloscope, strip chart recorders, and an *X-Y* recorder.

Three strip chart recorders are available for the purpose of determining the load, strain, and temperature as a function of time. The *X-Y* recorder is used for recording load versus strain (hysteresis loops). Load or strain versus temperature loops may also be recorded for tests in which the temperature is cycled and either the load or strain is held constant.

The differential input scope is used for dynamic measurements of load, strain, and temperature by comparing the desired signal with a known percentage of our standard reference voltage. The system voltage levels (±5 V) and the scope settings are such that it is possible to see variations in signal amplitudes and relate these variations to percentages directly.

A preset cycle counter is available for each of the machines and is actuated in the following manner: A mechanical linkage (Fig. 12) is set up between the platens *C* and *D* of the die set, which produces a lever arm *B* tip deflection that is approximately ten times the deflection between the platens. A microswitch *G* is tripped by the adjustment screw *F* at the end of the lever arm once in each cycle. This lever system is also used for

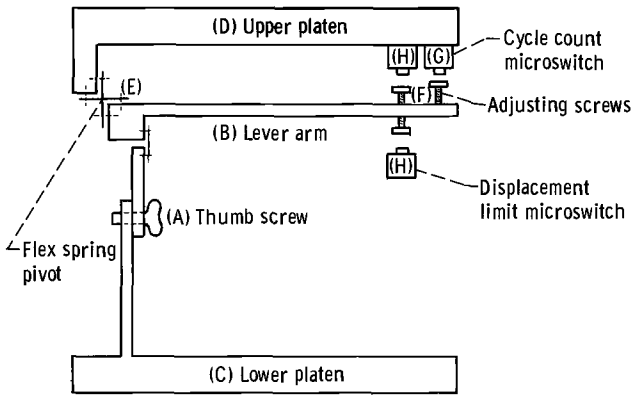

FIG. 12—*Lever system for mechanical cycle counting and displacement limiting.*

limit shutoff of the machines, as will be discussed later in the section dealing with the hydraulic system. When a test is about to be started, the thumb screw *A* is locked so that the lever arm is horizontal. Any relative motion of the platens rotates the lever arm about the flex spring *E* causing the adjustment screw to trip the microswitch. This results in a pulse to the counter and permits recording of that cycle. The counters are of the preset type meaning that a cycle number can be preset in the counter before the test is started. When the actual cycle reaches the preset number, a relay is tripped and the fatigue machine is shut off.

A reset clock is connected to each of the machines. These clocks are reset to zero at the time of the first cycle and indicate the elapsed time of operation in tenths of a minute. When the machine is shut down for any reason, the clock is stopped.

Hydraulic System

The hydraulic supply system (also shown in Fig. 11) is common to all eight fatigue machines. Two motor (*M*)-pump (*P*) units, each capable of supplying 5 gal/min, are connected in parallel and can be operated either separately or simultaneously. The hydraulic servo control valves are of the one-gal/min type, therefore an 8-gal/min oil supply system is sufficient for all our machines. The oil is continuously circulated, cooled by a heat exchanger to between 90 and 110 F, and filtered to the cleanliness specified by the manufacturer of the servo valves. Each of the machines has a solenoid valve in its hydraulic lines, thereby making it possible to isolate it from the hydraulic supply. The solenoid valves are used for on-off control for each machine and are also closed when either the tension or compression limit microswitch is tripped. These two limit switches are seen as parts *H* of Fig. 12. This method of shutting off a machine does not interfere with the hydraulic supply system, the control electronics, or any of the readout equipment common to other machines.

Modes of Operation

The fatigue machines can be operated manually or by the electronic servo equipment. The manual mode of operation is accomplished at the loading frame rather than from the console. This is done by switching the electrical input to the servo control valve from the servo controller to a separate d-c supply. This positions the servo valve with the turn of a potentiometer as shown schematically in Fig. 11. This mode of operation makes it very simple to install and remove specimens from the machine.

The thermal and hydraulic control systems are very versatile and can be used for a wide variety of closed-loop, servo-controlled modes of operation. These include:

1. Isothermal tension or compression testing under conditions of controlled loading or straining rate.

2. Conventional stress-rupture and creep testing at constant temperature. This is accomplished by maintaining a constant load on the specimen and recording strain as a function of time as well as time to failure.

3. Conventional relaxation testing at constant temperature. In these tests the strain is held constant and the load is recorded as a function of time.

4. Conventional isothermal fatigue testing where either the load or strain is used as the controlled variable.

5. Thermal fatigue testing in which the temperature as well as either the load or strain are controlled throughout the test.

6. Cyclic creep testing. These tests are run by servo controlling a constant load until a desired strain limit is reached at which time the load is reversed and the specimen allowed to creep to the negative strain limit. These cycles are repeated until failure occurs. Recordings of creep strain as a function of time and applied cycles as well as time and cycles to failure are kept.

7. Cumulative fatigue testing may be accomplished by either programming step changes in the applied load or strain range, or by applying a random variation in either amplitude or frequency of excitation, or both, in place of discrete step changes.

8. Any of the cyclic tests can be run with different wave shapes of the controlled variable. These include sine, saw-tooth, and square wave as well as any more general repetitive wave shape that one might want to draw on a drum-type curve follower.

9. With the inclusion of some additional electronic equipment such as an analog or small digital computer, it is possible to control from a computed rather than measured value. Such additional equipment would permit testing under conditions of constant plastic strain range, for example, or permit tests in which true stress rather than load could be controlled or maintained. One example of the application of this concept is described by Slot et al, pp. 100-128.

10. Cryogenic testing may also be incorporated in a low cycle fatigue laboratory provided a cryostat is available for the testing machine and all the additional equipment is installed for the handling of the cryogenic fluids. NASA-Lewis has developed the capacity of doing extensive cryogenic low cycle fatigue testing [*8*] but inasmuch as one of the cryogenic fluids used is liquid hydrogen, safety considerations did not permit the incorporation of this equipment with our ambient and elevated temperature testing equipment.

The above listed flexibility in modes of testing is a very desirable feature for any fatigue testing laboratory since it permits the generation of a wide variety of test data in one machine and from the same size and type of specimen, thus eliminating some of the variables affecting the correlation of material behavior. This cannot help but aid in the understanding of material behavior.

References

[1] Klima, S. J. and Freche, J. C., "Ultrasonic Detection and Measurement of Fatigue Cracks in Notched Specimens," *NASA TN D-4782,* National Aeronautics and Space Administration, 1968.

[2] Manson, S. S. and Hirschberg, M. H., "Low Cycle Fatigue of Notched Specimens by Consideration of Crack Initiation and Propagation," *NASA TN D-3146,* National Aeronautics and Space Administration, 1967.

[3] Manson, S. S., "A Simple Procedure for Estimating High-Temperature Low-Cycle Fatigue," *Experimental Mechanics,* EXMCA, Vol. 8, No. 8, 1968, pp. 349–355.

[4] Manson, S. S., Freche, J. C. and Ensign, C. R., "Application of a Double Linear Damage Rule to Cumulative Fatigue, *"Fatigue Crack Propagation," ASTM STP 415,* American Society for Testing and Materials, 1967, pp. 384–414.

[5] Manson, S. S., "Interfaces Between Fatigue, Creep, and Fracture," *International Journal of Fracture Mechanics,* IJFMA, Vol. 2, No. 1, 1966, pp. 327–363.

[6] Manson, S. S., "Fatigue: A Complex Subject—Some Simple Approximations," *Experimental Mechanics,* EXMCA, Vol. 5, No. 7, 1965, pp. 193–226.

[7] Smith, R. W., Hirschberg, M. H. and Manson, S. S., "Fatigue Behavior of Materials Under Strain Cycling in Low and Intermediate Life Range," *NASA TN D-1574,* National Aeronautics and Space Administration, 1963.

[8] Nachtigall, A. J., Klima, S. J. and Freche, J. C., "Fatigue of Liquid Rocket Engine Metals at Cryogenic Temperatures to —450 F (4 K)," *NASA TN D-4274,* National Aeronautics and Space Administration, 1967

C. H. Wells[1]

Elevated Temperature Testing Methods

REFERENCE: Wells, C. H., "**Elevated Temperature Testing Methods,**" *Manual on Low Cycle Fatigue Testing, ASTM STP 465*, American Society for Testing and Materials, 1969, pp. 87–99.

ABSTRACT: Techniques of axial strain-controlled fatigue testing at elevated temperature are described. The specimen design incorporates thin ridges for attaching the extensometer arms; details of the design are provided to avoid premature failure at these discontinuities. Special problems of specimen gripping, alignment, and break detection at high temperature are discussed for both mechanical and closed-loop hydraulic testing machines.

KEY WORDS: metals, fatigue (materials), fatigue tests, high temperature, strain control, extensometry, alignment, stress concentration, size effect, specimen grips, tests

It is important to emphasize at the outset that there is no single "best" test of low cycle fatigue behavior at elevated temperature. Obviously the kind of information sought will govern the selection of the specimen design and test procedure and may run the gamut from the prediction of the lifetime of a structure to basic materials studies. Accuracy of lifetime data dictates that the service cycle be simulated as completely as possible, whereas the understanding of the fatigue problem must be based upon simpler tests that allow separation of cause and effect.

Two types of low cycle fatigue problem may be identified in the aircraft gas turbine. The first comprises parts in which the stresses are nominally in the elastic range but which contain sources of strain concentration, such as attachments to disks or oil holes through shafts. For reasons of economics and low weight the local strains in these regions may be well into the plastic range. The second type of problem involves rapid heating and cooling wherein most of the strain is caused by transient temperature gradients. This is, of course, the problem of thermal fatigue, which is considered in detail in another chapter. In cases of thermal fatigue, for example piping and turbine vanes, plastic deformation may be more gen-

[1] Assistant director, Advanced Materials Research and Development Laboratory, Pratt & Whitney Aircraft, Middletown, Conn. 06457. Personal member ASTM.

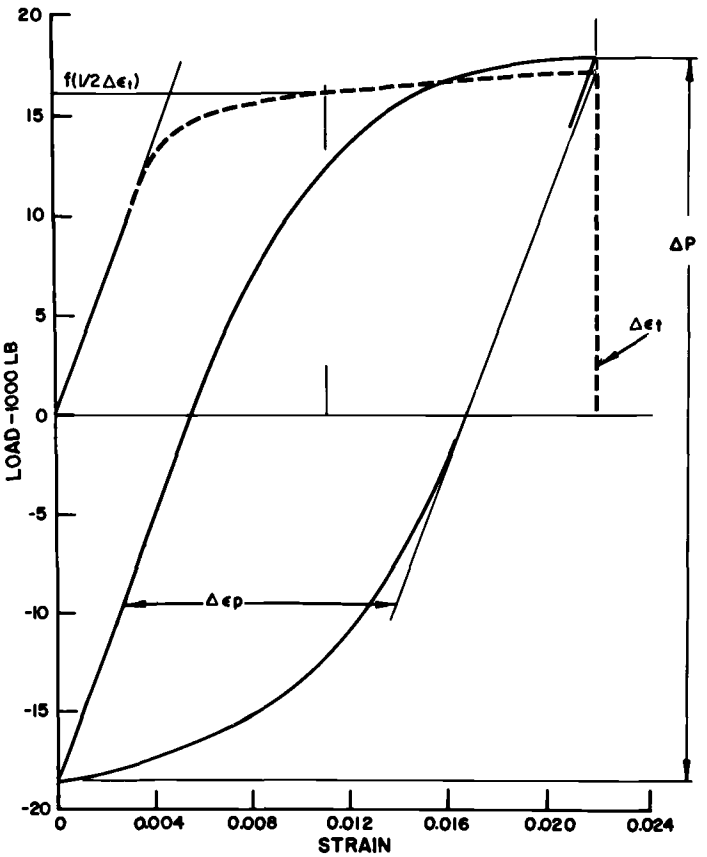

FIG. 1—*Typical strain cycle. Taken from Ref* 1.

eral, and in contrast to examples of the first type, growth and distortion of the part may be strongly influenced by the cyclic behavior of the material.

Our objectives in low cycle fatigue testing have been to generate both cyclic stress-strain data for design purposes and to determine the dependence of cycles to crack initiation on strain range, temperature, and hold time. The first requirement necessitates the simultaneous measurement of stress and strain, which cannot be accomplished with a notched specimen. The initial problem of interest was the description of material behavior in critical areas of compressor and turbine disks [*1–4*].[2] The nominal stress field is essentially tensile and, by virtue of the extremely small growth of the disk tolerated in each cycle, elastically reversible. The strain cycle at the

[2] The italic numbers in brackets refer to the references at the end of this paper.

surface of a notch or hole was accordingly approximated by the zero-to-maximum cycle indicated in Fig. 1. As we did not wish to include geometric and machining variables in these investigations, a right-circular cyclindrical specimen with an electropolished surface was chosen. This design, which is described in detail below, allowed the study at high magnifications of the mechanisms of microcrack initiation and linking and established a basis from which the effects of residual stress, cold work, surface finish, coatings, edge radii, strain gradients, etc., could be evaluated. At the same time, the cyclic variation of the stress range, mean stress, and hysteresis loop size and shape could be directly measured. It was hoped, and subsequently established, that the observations of all these variables, both mechanical and metallographic, would explain the dependence of crack initiation lifetime on strain range, temperature, and hold time. That is to say, the uniaxial test of a smooth specimen provides the maximum information concerning the behavior of the material in a localized region.

If, on the other hand, we had wished to obtain only lifetime data for a certain geometry, machining procedure, and surface condition, particularly where the number of cycles to the observation of a macrocrack of a certain length was the critical result, a much more direct and simple route would have been a cyclic load test on a specimen of the same notch configuration and processing as the component of interest.

The testing procedure was subsequently extended to materials and temperatures appropriate to turbine blade and vane design [*5–8*]. The strain cycle of Fig. 1 is usually not realized in problems of thermal fatigue —it is more common to find the mean strain near zero—and in complex alloys it may happen that any isothermal low-cycle fatigue test drastically overestimates the crack initiation life under cyclic heating and cooling. A discussion of the relevance of isothermal to thermal fatigue testing is outside the scope of this paper.

Specimen Gripping

The necessity to cycle from tension into compression entails two principal problems in gripping the specimen: The grips must be stiff enough to maintain alignment in compression, and all threaded connections must be preloaded beyond the minimum test levels to prevent backlash. One additional consideration—and an overriding one—imposed by the requirement of testing temperatures up to 1800 F was that the specimen be readily removable after prolonged exposure to oxidation. The requirements have been met by the configuration shown in Fig. 2, which accomplishes preloading via an extra-fine threaded coupling and alignment through two pairs of accurately ground, flat surfaces. The end faces of the grips, square with the grip centerline, are installed in the machine concentric within

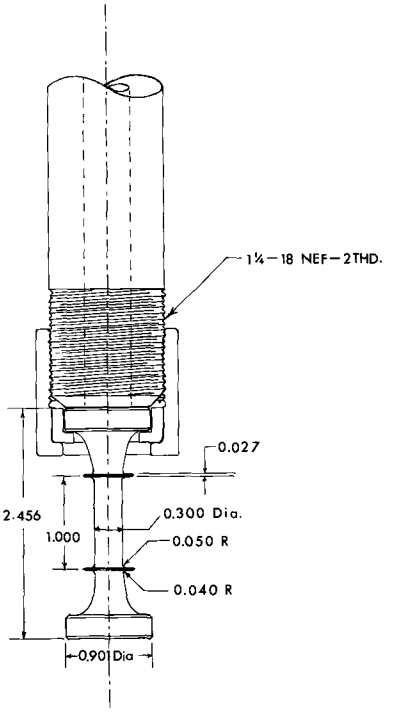

FIG. 2—*Specimen grip assembly.*

about 0.005 in. and parallel to each other such that when, without the specimen, they are brought together until lightly touching, no gap is visible front to back or side to side when a strong light is shown from the side opposite the operator. In this manner the operator can easily detect a deviation of 0.0005 in. from parallel. The end faces of the specimen are similarly ground flat, parallel and square with the centerline of the gage length. With appropriate precautions observed during installation, as outlined below, the bending stress[3] in a ⅜-in.-diameter steel specimen does not exceed 2000 psi. To minimize galling of the threads during disassembly, which initially led to the removal of many couplings by the cutoff wheel, the use of one or more "chipways"—grooves cutting the threads parallel to the centerline and extending slightly below the root diameter of the grip—is emphatically recommended. Incidentally, high temperature lubricants or parting agents of all types were tried with generally disastrous re-

[3] With stiff grips, the alignment is not expressible in terms of an initial eccentricity, with the percent bending stress proportional to the ratio of eccentricity to specimen radius. Rather, it is in the form of an initial "clamping stress" that changes little over the elastic range of loading.

sults, either severe contamination or galling. The best antigalling agent was found to be the natural oxide layer forming on the grips at elevated temperature (our grips, split rings, and couplings are machined from Udimet 500 or 700). In fact it is desirable to oxidize new hardware prior to testing to ensure easy disassembly.

The center holes through the grips were originally provided to reduce heat conduction; their effectiveness is questionable, but they are of possible use for instrumentation or cooling when testing tubular specimens.

Occasionally, insufficient material is available for full-size, 0.900-in.-diameter specimens. Threaded collars have been used with ⅝-in.-diameter stock to allow testing of the same gage geometry, Fig. 3. Left-handed threads are required on one coupling and grip to allow tightening of the couplings. Buttonheads of standard specimens have also been employed as adapters for miniature, ⅛-in.-diameter by ½-in. gage length specimens, Fig. 4.

The procedure for installation is, first, to install split rings and securely tighten one end of the specimen to its grip (the torque varies from 50 to 100 lb • ft, depending upon the build of the technician). Then the free end of the specimen is brought to bear upon the other grip with a load of a few pounds, and the gap between the mating surfaces checked by eye.

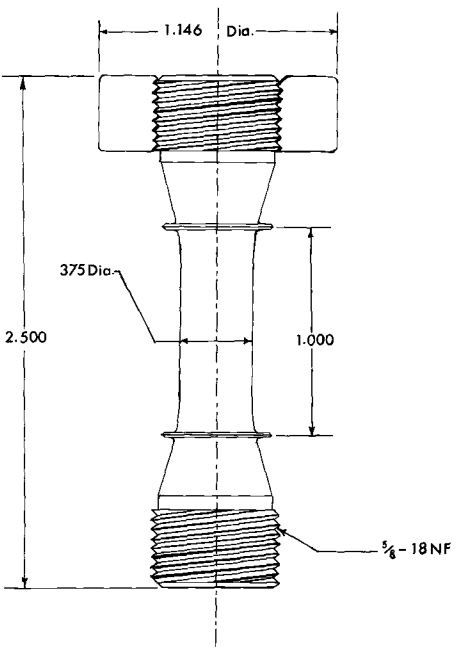

FIG. 3—*Thread-end specimen and adapter, 5/8-in. diameter.*

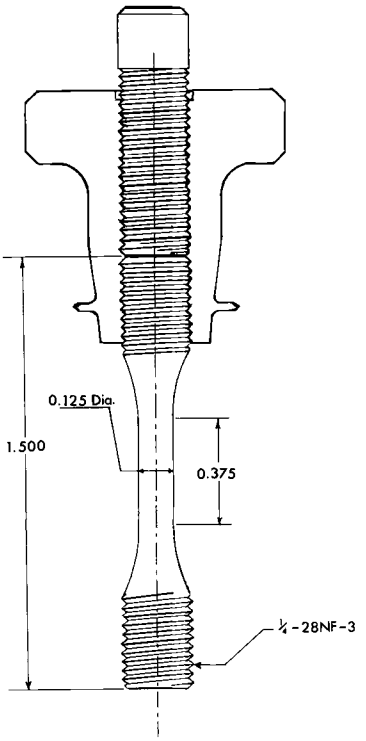

FIG. 4—*Thread-end specimen and adapter, 1/4-in. diameter.*

If the alignment is satisfactory, the split rings and coupling are attached and gently tightened. Then the specimen is loaded in tension to about one half the proportional limit and reloaded the same amount in compression. Under the compressive load the couplings are tightened to the maximum torque.[4] This procedure assures the elimination of backlash and prevents the transfer of torque during wrenching to the specimen gage length.

Extensometry

We elected to measure and control axial rather than diametral strain for several reasons. First, a larger displacement was available. Second, the axial strain was the independent variable and was desired to be maintained as accurately as possible. Diametral strain must be varied as the

[4] One further precaution must be followed when installing a specimen in a MTS machine to avoid large clamping stresses. The hydraulic ram has elastomeric seals and a relatively low transverse spring constant. Thus it has been found necessary to couple the specimen first to the grip mounted on the ram and then, in load control, to tighten the opposite coupling against the fixed grip.

hysteretic behavior of the material changes if the axial strain is to be maintained constant. The axial strain must be calculated from the diametral strain with known values of Poisson's ratio; in the case of some highly anisotropic materials of interest [9], Poisson's ratio was known only from a theoretical calculation. Finally, a constant diameter section without any mechanical contact was desired for ease of specimen replication and to obviate the possibility of crack initiation at points of contact. As shown in Fig. 2, the measurement of elongation was approached through thin ridges ground at either end of the specimen gage length.

This choice was not without disadvantages, for the discontinuity in the smooth specimen surface was expensive[5] and prone to premature crack initiation, which subject is related to the notch sensitivity of the material and would in its own right constitute a research paper. We shall be content to list here the successful designs for the several materials and temperatures investigated and the general principles we believe to be applicable.

The basic concept upon which this ridge design is based is that of a size effect in fatigue crack initiation: crack initiation is governed not by a maximum concentrated stress alone, but by a concentrated stress acting over some region of an extent comparable to the scale on which cracking initiates. In the case of materials that deform heterogeneously by coarse slip—that crack along slip bands, for example—this region is approximately equal to the grain diameter, and it is relatively easy to grind the radius at the base of the ridge smaller than the maximum grain diameter in the gage section. We believe that in such materials the rate of cracking is related to the range of shear displacement across a slip plane; the displacement is proportional to the product of total strain and grain diameter. This concept appears to be valid for the wrought, recrystallized nickel-base alloy Udimet 700 and for the α-β titanium alloy Ti-6Al-4V. For the latter, the critical dimension is thought to be the length of primary α platelets. In both cases ridge cracking was suppressed by sharpening the transition between the ridge and the gage length (Table 1).

What about materials in which crack initiation is obviously on too small a scale to be approached by machine shop practice? The ridge design is much less satisfactory, for now the maximum value of strain must be kept below that in the gage section, and this necessitates large blend radii between the gage section and the ridge. This approach had to be adopted for a single crystal nickel-base alloy at 1700 F (Fig. 2 and Table 1) although the other design was satisfactory for this material at lower temperatures. The deformation mode changes from heterogeneous to homo-

[5] Specimens finish ground from 1-in.-diameter bar stock were obtained for about $50 to $60 each in small lots, exclusive of material and heat treating. We are now preparing these specimens by electrochemical grinding.

TABLE 1—*Range of test conditions resulting in center fractures in specimens with extensometer ridges.*

Material	Reference	Temperature, deg F	Extensometer Ridge: Width, in.	Extensometer Ridge: Root radius, in.	Gage Diameter, in.	Minimum Total Strain Range for Center Fracture[b]
Udimet 700	[1]	70	0.050	0.015 to 0.025	0.375	0.008
	[2]	1400	...	...	...	0.012
	[6]	1400	0.025	0.015 max	...	0.009
	[6]	1700	...	...	...	0.004
Ti-6Al-4V	[4]	70	0.025	0.015 max	0.375	0.009
Ni-2% Th[a]	...	70	0.025	0.015 max	0.375	0.0075
		1800	...	...	...	0.002
Mar-M200, single and columnar grained	[7]	70	0.025	0.015 max	0.350	0.009
	[8]	1400	...	...	...	0.009
	[8]	1700	...	...	...	>0.016
	[8]	1700	...	0.040 to 0.050 (Fig. 2)	0.300	<0.016

[a] G. R. Leverant, Pratt & Whitney Aircraft, unpublished research.

[b] The incidence of cracking at the base of the extensometer ridge was significant below this strain range and was negligible at this range.

geneous at the high temperature [8]. The scale of crack initiation may also be greatly reduced at low amplitudes, particularly if second-phase particles are present. Table 1 lists the lowest total strain ranges at which the designs proved satisfactory.

The ridge serves as an extremely stable attachment for the extensometer clamp. The latter is V-notched and held in place on the ridge by a bar, a nut, and a bolt. The extension arms are aluminum oxide for stiffness, absence of distortion at high temperature, and for minimum thermal expansion. They are glued into the clamps with Ceramabond 503[6] high temperature cement and aligned in a jig under heat until the cement has hardened. The point of contact between the upper and lower halves of the measuring unit, where the relative motion is measured, is located on the centerline of the specimen. The advantages of this arrangement are that it is mechanically averaging and that it is not subject to error resulting from small sideways deflections. The basic design has been incorporated into our high temperature creep extensometers [10].

[6] Aremco Products, Inc.

The extensometer assembly performs equally well inverted (Fig. 5); this attachment permits a very simple approach to liquid environment testing, for example, sealing a beaker about the lower coupling with wax.

Strain and Temperature Control

Both closed- and open-loop strain control have been employed with equal success. In the case of the MTS[7] equipment, a Collins 10101B linear motion transducer (G. L. Collins Corp., Long Beach, Calif.) is mounted in line with the specimen without mechanical magnification of the core displacement (Fig. 5). The saw-tooth wave form is normally selected. A

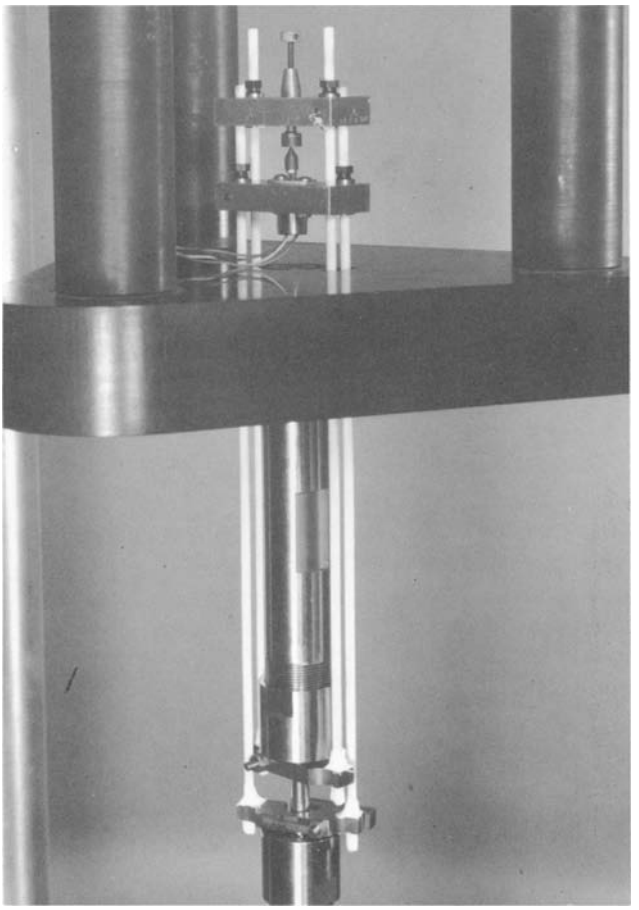

FIG. 5—*View of inverted extensometer assembly in MTS machine.*

[7] MTS Systems Corp., Minneapolis, Minn.

digital load indicator is installed for accuracy in measuring the load range and for convenience in setting up a test. The test is stopped by the dynamic response of the linear variable differential transformer (LVDT) at fracture, which usually triggers the error detector. However, if the material is very soft, or crack propagation very slow, the error detector is incapable of determining rupture of the specimen. In general the error detector will work only if unstable crack propagation occurs.

The other testing machine is a Wiedemann-Baldwin (SATEC Systems, Inc., Grove City, Pa.) 25,000-lb. capacity "Mark G" load frame comprising gear-driven, preloaded ball screws and SR-4 load cells. The load indicator incorporates switches for load control. The LVDT is a Wiedemann-Baldwin microformer; the measuring unit retains the 3-to-1 magnifying lever, fulcrum, and knife edge of the Wiedemann-Baldwin PSH-8MS extensometer. The knife edge bears on a glass rod, and the point of contact lies on the specimen centerline. The LVDT is mounted horizontally and off the centerline; however, the unbalance has not been a problem. Strain is controlled by electronic limit switches on the y-axis of a Moseley 2D recorder (Hewlett-Packard, Palo Alto, Calif.). The pen motion is geared to the rotation of the core rod of a slave LVDT. The core rod is carried on a screw thread; thus the recorder magnification is determined by fixed gear ratios. Break detection in strain control is provided by the adjustable tension load limit switch. At the peak tensile strain the motor is normally reversed by a series of relays. The control circuit is wired such that when the tension strain limit switch is closed, current must flow through the tension load limit switch. If the indicated load is below the set point, the motor stops and is not reversed. This machine will also combine load or strain holding in a strain cycle. During this period of creep or relaxation the x-axis of the recorder is switched from load to time base, and strain versus time is plotted. Electronic limit switches and an auxiliary low speed control can maintain constant strain for increasing or decreasing load.

In both machines the specimens are heated by 3-zone split resistance furnaces. The Kanthal A elements total 8 in. in length and have an inner diameter of 3 in. About 1½ h are required to preheat and stabilize at 1700 F. Chromel-Alumel thermocouples are tied to the gage length with prebaked silica thermocouple insulation. Temperature control is from a heavy-gage thermocouple in the furnace wall, rather than from the specimen. This procedure has been most satisfactory for long-time stability, and with the Barber-Colman 350 and 477 controllers (Barber-Colman Co., Industrial Instruments Div., Rockford, Ill.) it has been observed that the temperature remains constant within about ± ½ F, until the specimen is cycled. The thermoelastic effect, heating of a metal in compression and cooling in tension, has caused as much as a ± 3 F cycle in phase with the

load at a frequency of 2 cpm. This amplitude has been in agreement with the equation [*11*]

$$\Delta T = \frac{-\alpha T \Delta \sigma}{\rho C_p J}$$

where T is the absolute temperature, α the coefficient of thermal expansion, ρ the density of the material, C_p its specific heat, and J the mechanical equivalent of heat.

Interpretation of Results

From a practical standpoint it is desirable to express crack initiation lifetime as a function of total strain. In the absence of accurate theories of cyclic plasticity, only the range of total strain in a structure can be calculated or measured with any degree of confidence. This is especially true in gas turbine applications, in which temperature and strain exhibit complex histories and where the plastic strain range is usually smaller than or comparable to the elastic strain range. Also, changes in the flow stress of the material accompanying cyclic deformation can significantly change the plastic strain range during a test.

The reproducibility of lifetime under the experimental conditions described above is excellent and adequate to discriminate between different theories of low cycle fatigue damage. For example, Fig. 6 indicates a cor-

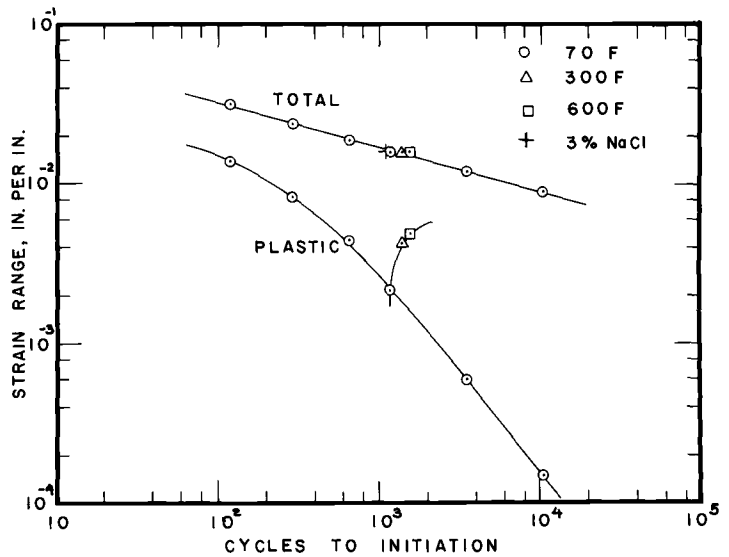

FIG. 6—*Total strain range versus lifetime for Ti-6Al-4V. Taken from Ref. 4.*

relation of lifetime with total, rather than with plastic, strain range for Ti-6Al-4V alloy [*4*]. We believe the reason for this correlation is the proportionality between slipband displacement and total strain range [*6*] and have argued that there is little significance of plastic strain range, averaged over the specimen gage length, for materials that deform heterogeneously.[8] Consequently, we have chosen to express low cycle fatigue results in terms of total strain range for both practical and theoretical reasons. In contrast, at high temperatures the strain range versus lifetime correlation may exhibit the more usual knee, as in the case of wrought Udimet 700 at 1700 F [*6*], where plastic deformation is much more homogeneous. Crack initiation at elevated temperature is determined from a decrease in slope of the load range versus cycles curve; the crack length corresponding to this change of slope is approximately 1/16 in.

Attempts [*12*] to interpret the effects of creep and relaxation on cyclic life in terms of cumulative life fraction or increase in the plastic strain range have not met with success. It appears that the mechanisms of grain-boundary cracking may differ in that there is very little driving force for crack propagation in static creep relative to fatigue. This area, together with the attendant effects of temperature cycling, present the greatest challenge and opportunity for studying the high temperature fatigue behavior of materials.

Acknowledgments

The author is indebted to his colleagues, M. L. Gell, G. R. Leverant, and especially C. P. Sullivan, for countless valuable discussions of low cycle fatigue.

Of the many persons who assisted in the development of testing procedures, particular thanks are due E. D. Johnson and S. W. Hopkins for refinements in extensometry and machine control.

References

[*1*] Wells, C. H. and Sullivan, C. P. "Low-Cycle Fatigue Characteristics of a Nickel-Base Superalloy at Room Temperature," *Transactions Quarterly*, American Society for Metals, ASMQA, Vol. 57, 1964, p. 841.

[2] Wells C. H. and Sullivan, C. P. "Low-Cycle Fatigue Damage of Udimet 700 at 1400 F," *Transactions Quarterly*, American Society for Metals, ASMQA, Vol. 58, 1965, p. 391.

[*3*] Wells, C. H. and Sullivan, C. P. "The Effect of Temperature on the Low-Cycle Fatigue Behavior of Udimet 700," *Transactions Quarterly*, American Society for Metals ASMQA, Vol. 60, 1967, p. 217.

[8] This is clearly the case at elevated temperature, where surface crack initiation takes place in oxide layers or protective coatings.

[4] Wells, C. H. and Sullivan, C. P. "Low-Cycle Fatigue Crack Initiation in Ti-6A1-4V," *Transactions Quarterly*, American Society for Metals, ASMQA, Vol. 62, 1969, p. 263.

[5] Leverant, G. R. and Sullivan, C. P. "The Effect of Dispersed Hard Particles on the High-Strain Fatigue of Nickel at Room Temperature," *Transactions of the American Institute of Mining and Metallurgical Engineers*, TAMMA, Vol. 242, 1968, p. 2347.

[6] Wells, C. H. and Sullivan, C. P. "Low Cycle Fatigue of Udimet 700 at 1700 F," *Transactions Quarterly*, American Society for Metals, ASMQA, Vol. 61, 1968, p. 149.

[7] Gell, M. and Leverant, G. R. "Fatigue of the Nickel-Base Superalloy MAR-M200 in Single Crystal and Columnar Forms at Room Temperature," *Transactions of the American Institute of Mining and Metallurgical Engineers*, TAMMA, Vol. 242, 1968, p. 1869.

[8] Leverant, G. R. and Gell, M. "The Elevated Temperature Fatigue of a Nickel-Base Superalloy in Conventionally Cast and Directionally Solidified Forms," *Transactions of the American Institute of Mining and Metallurgical Engineers*, Vol. 245, 1969, in press.

[9] Wells, C. H. "The Elastic Constants of a Directionally Solidified, Nickel-Base Superalloy, MAR-M200," *Transactions Quarterly*, American Society for Metals, ASMQA, Vol. 60, 1967, p. 270.

[10] Tishler, D. N. and Wells, C. H. "An Improved High-Temperature Extensometer," *Materials Research and Standards*, American Society for Testing and Materials, MTRSA, Vol. 6, Jan. 1966, p. 20.

[11] Swalin, R. A. *Thermodynamics of Solids*, Wiley, New York, 1962, p. 25.

[12] Wells, C. H. and Sullivan, C. P. "Interactions Between Creep and Low-Cycle Fatigue in Udimet 700 at 1400 F," *Fatigue at High Temperature, ASTM STP 459*, 1969, pp. 59–74.

T. Slot,[1] *R. H. Stentz,*[2] *and J. T. Berling*[2]

Controlled-Strain Testing Procedures

REFERENCE: Slot, T., Stentz, R. H. and Berling, J. T., "**Controlled-Strain Testing Procedures,**" *Manual on Low Cycle Fatigue Testing, ASTM STP 465,* American Society for Testing and Materials, 1969, pp. 100–128.

ABSTRACT: Experimental procedures are described for conducting fatigue investigations at high temperatures on servo-controlled testing machines. Specially developed equipment permits programming of push-pull tests on hourglass specimens with closed-loop control of either stress, axial strain, transverse strain, or plastic strain at the minimum diameter of the specimen.

KEY WORDS: fatigue tests, fatigue (materials), high temperature, hydraulic testing machine, servo control, strain measurement, cyclic loading, stress, strain

Nomenclature

σ Axial Stress
ϵ Axial strain
ϵ_p Plastic component of axial strain
ϵ_e Elastic component of axial strain
ϵ_d Diametral strain (transverse strain)
ϵ_{dp} Plastic component of diametral strain
ϵ_{de} Elastic component of diametral strain
ν_p Poisson's ratio for plastic deformation
ν_e Poisson's ratio for elastic deformation
E Modulus of elasticity
K Compliance constant ($K = \nu_e/AE$)
A Minimum cross-sectional area of test specimen
F Force on specimen

In this paper the authors have chosen to place the primary emphasis on the technique of testing. For this reason much attention is given to the method of loading a fatigue specimen, the measurement of test parameters, and the control of test conditions, whereas little or no attention is given

[1] Knolls Atomic Power Laboratory, General Electric Co., Schenectady, N. Y. 12301; formerly Nuclear Systems Programs, General Electric Co., Cincinnati, Ohio.
[2] Nuclear Systems Programs, General Electric Co., Cincinnati, Ohio 45215.

to the equally important subjects of specimen fabrication, metallographic and fractographic analysis, and fatigue data reduction. More information on the latter subjects may be found in some of the other papers contained in this publication, or in the literature cited there.

The technique of testing employed at the authors' laboratory was developed for a research program on the low cycle fatigue properties of various heat-resistant metals and alloys at elevated temperatures up to 1000 C. Objectives of this test program, which has been sponsored at Nuclear System Programs by the U.S. Atomic Energy Commission[3] since 1964, are to gain a better understanding of the mechanical and metallurgical behavior of structural materials under cyclic loading at temperatures in the creep range, and to generate low cycle fatigue data for use in the design of structural components of high performance nuclear reactor systems. Materials that have been tested with the equipment to be described include: AISI 304, 316, and 348 stainless steel, Incoloy 800, Inconel 718, A-286, and several high strength pressure vessel steels (maraging, precipitation-hardened, quenched and tempered).

Versatility and reliability characterize the testing procedures and equipment in the authors' laboratory. Test parameters that can be programmed in a fatigue test are stress, transverse strain, axial strain, plastic strain, and actuator displacement. The mode of cycling can be varied with respect to wave form, frequency, and the duration of hold periods within each cycle. Perhaps it should be stressed here that the experimental procedures were largely selected to permit tests to be conducted with large strain amplitudes, low strain rates, and long hold periods. Typically, the equipment has been used to perform fatigue tests with strain amplitudes in the range from 0.25 to 3 percent, strain rates from 10^{-5} to 10^{-2} s^{-1}, hold times from 0 to 3 h, and temperatures from 25 to 1000 C [*1–4*][4].

In essence, the experimental approach to be described consists of subjecting a specimen with an hourglass-shaped gage section to programmed push-pull loading on a servo-controlled, hydraulic fatigue machine, while the specimen is being heated by means of an induction coil around the gage section. Test parameters measured in this approach are the (uniaxial) stress and the transverse strain at the minimum diameter, as well as the temperature in the gage section. A load cell mounted in series with the specimen and a diametral displacement sensor positioned at the minimum diameter furnish electrical analogs of the measured stress and transverse strain. Used as feedback signals, the analogs permit tests to be programmed

[3] Fuels and Materials Branch, Division of Reactor Development and Technology, Contract AT(40-1)-2847.

[4] The italic numbers in brackets refer to the list of references at the end of this paper.

with control of either stress or transverse strain. With the aid of a specially developed analog computer circuit, an analog signal is also obtained for the axial strain at the minimum diameter. This feature permits a fatigue test to be performed on an hourglass specimen with control of axial strain. Because an analog signal proportional to the plastic component of strain is obtained in the process of converting transverse strain to axial strain, programming of plastic strain is still another available mode of testing.

Testing Equipment and Experimental Procedures

Experimental Approach

Two basic considerations have influenced the development of the controlled-strain testing procedures described in this paper. The first is the definition and measurement of the strain in the specimen, the second the control of that strain during the fatigue test. Adhering to this distinction, subjects related to the techniques of producing and measuring strain are covered in this section, while those related to the special techniques of programming and controlling strain are treated in the next section. However, a brief discussion of the overall testing system at this point will be helpful so that the various interactions between topics covered in the two sections may be better appreciated.

It is important to distinguish between the different types of strain control utilized by various investigators in low cycle fatigue testing. Apart from basic differences associated with the method of loading a specimen (for example, push-pull, bending, torsion), confusion sometimes arises because the connotations "controlled strain" and "strain cycling" are used rather loosely to describe widely different control techniques. For instance, some investigators load the specimen by cycling at a constant rate between limits on the displacement of the mechanical or hydraulic actuator of the testing machine. This technique, however, does not assure a constant strain amplitude, nor does it assure a controlled strain rate. With such a control system, any redistribution of elastic and plastic strain caused by cyclic strain hardening or softening, relaxation during hold periods, or changes in mean stress in tests with mean strain, will result in deviations from a constant strain amplitude. Also, even though the actuator moves at a constant rate, the strain rate in the specimen will vary when the specimen deforms plastically. Similarly, a sinusoidal or other periodic variation of the actuator motion will not produce the same periodic variation in the strain.

Other investigators use the testing machine in a somewhat different manner. Here, the reversal of loading is controlled by limits set on the output of the strain-measuring device, which is mounted on the gage sec-

tion of the specimen. This technique is an improvement over the precious one in that it will maintain the amplitude of strain averaged over the length of the gage section. Again, however, the intracycle variation of strain is not controlled. Therefore, a constant velocity of the actuator will not give a constant strain rate because of plastic deformation.

The highest degree of precision of testing and flexibility of programming is achieved with servo-controlled testing machines operated in closed loop. The closed-loop technique requires the availability of a so-called "feedback signal" that is representative of the test parameter concerned (for example, strain, stress, temperature). This signal is continuously compared to a programmed "demand signal," to provide an instantaneous correction to the applied load. With this technique, control is continuous, so that both amplitude and rate can be programmed. Electrohydraulic components provide the response, precision, and loading capability needed to take advantage of the technique.

It can be said that the testing procedures described in this paper were all selected and developed to take advantage of the closely controlled test conditions that can be achieved on hydraulic fatigue machines equipped with a closed-loop servo control system. One of six such machines in use at the authors' laboratory is shown in Fig. 1. This particular machine was built from commercially available hydraulic and electronic components and mechanical and electronic components made in-house. However, complete testing machines of this type can be procured from several manufacturers.

The fatigue machine shown in Fig. 1 has a rugged three-column load frame that is complete with a vertically adjustable center column, loading fixtures, and a hydraulic actuator, the latter hidden behind the panel containing a pressure gage. Also hidden behind the panel are the servovalve and other hydraulic components that make up the hydraulic system. Somewhat difficult to recognize in the photograph is a transparent plastic enclosure that surrounds the testing space. It protects the test environment from air currents in the laboratory and permits a test to be conducted in an inert atmosphere. On the left of the loading frame is a console that holds all the electronic control components and some of the recording equipment. Not visible in the photograph are a 450-kilocycle high frequency generator and standard temperature control and recording equipment used for heating the specimen by induction. A block diagram of the control system is shown in Fig. 2.

It is not practical within the scope of this paper to include a comprehensive description of the operational and functional characteristics of the electrohydraulic system that constitutes the servo-controlled testing machine. The best source for detailed information on this subject is found in the manuals prepared by the manufacturers of servo control equipment

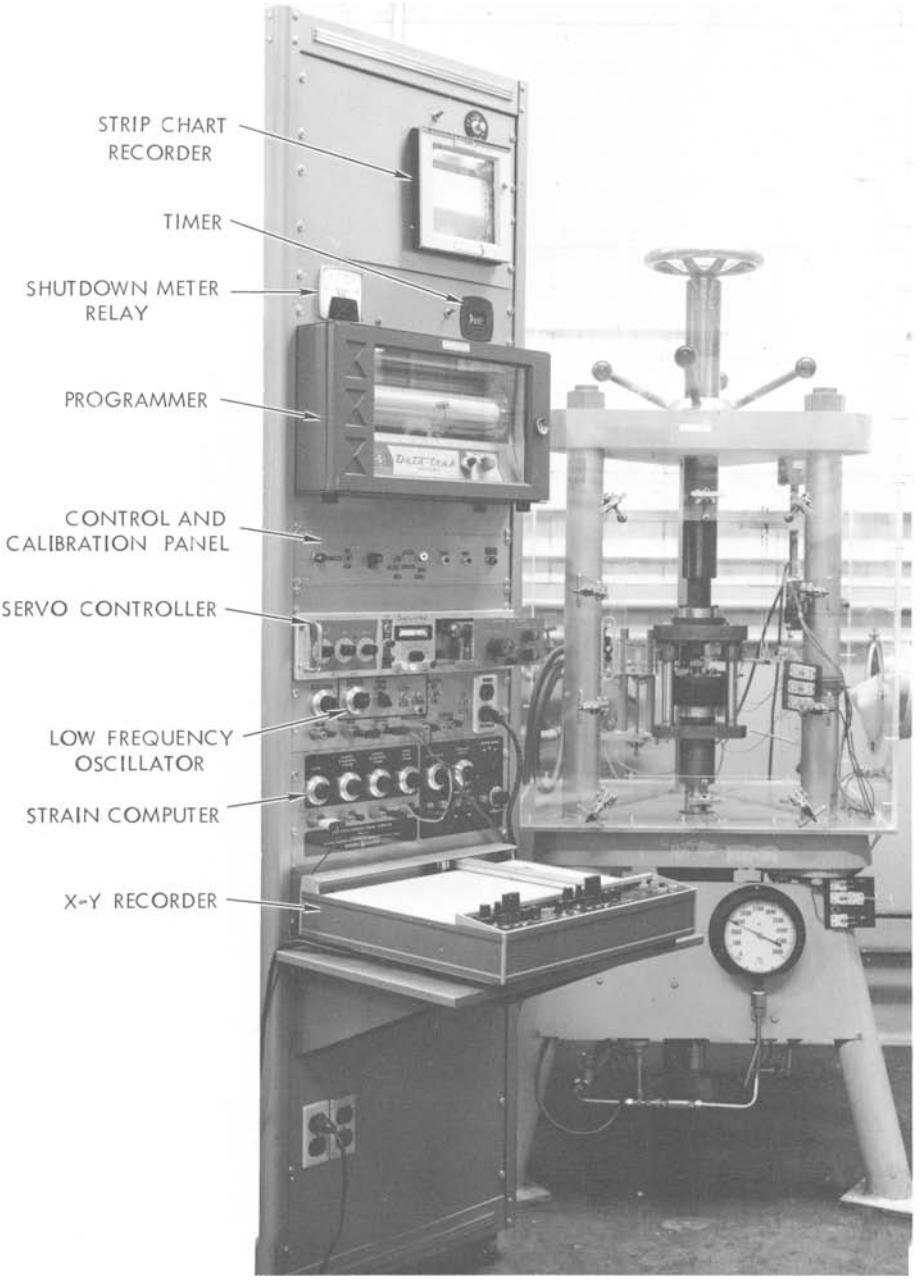

FIG. 1—*Servo-controlled, hydraulic fatigue machine.*

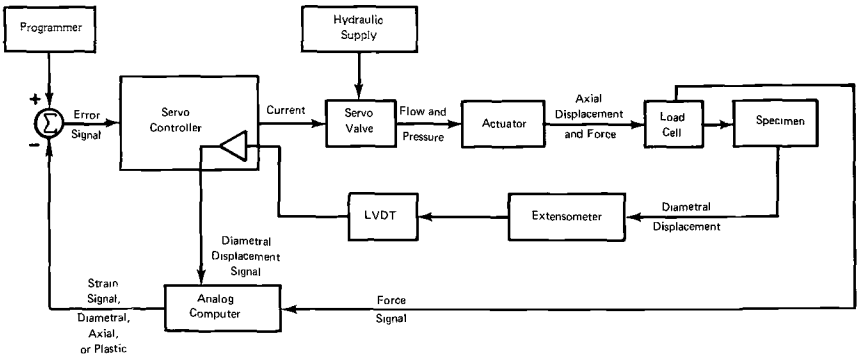

FIG. 2—*Block diagram of control system.*

and complete materials testing machines. Rather, the authors intend to discuss the function of each component identified in Figs. 1 and 2 in general terms in the course of describing various testing procedures in this section and the next one.

In Fig. 2, the programmer in the system is the device which furnishes an electrical analog or demand signal for the test parameter to be programmed in a given fatigue experiment. Generally, this is a time-varying signal of a specific wave form, which in a strain-controlled test determines both strain amplitude and strain rate. Figure 1 shows two programmers in the control console, one marked "programmer" and one marked "low frequency oscillator." The former is a programmer of the curve-follower type. It provides a signal proportional to the lateral displacement of a stylus that is electrically forced to follow a curve drawn on the revolving drum visible in the photograph. A programmer of this type is used when the specific wave form of interest is of arbitrary shape. The frequency of revolution can be varied and an extension drum is available for the design of experiments in which the wave form is not repetitive.

The oscillator is used to generate an accurate, triangular wave form for the demand signal. It was developed for the purpose of conducting tests with constant strain rate at low frequencies (0.001 to 1 cycle/s). Also, it has the built-in feature that permits a test to be started in tension or compression with the proper wave form from the first instant. With commercially available oscillators, it is usually necessary to select a frequency and then start the test by gradually increasing the amplitude to the desired value. (Results presented in the Discussion indicate that, at least for short tests, the starting mode can have an effect on the outcome of the test.) Additional programmers, not visible in Fig. 1, have been developed for

testing with hold times. These devices are essentially motor-driven function potentiometers which are electrically connected to adjustable timer relays. They permit tests to be conducted with independent control of the hold periods in tension and compression [*4*].

The output of the programmer is compared at a summing junction with a feedback signal representative of the actual value of the test parameter. The summing junction can also be used to sum more than one demand signal, which permits cyclic tests to be conducted with a mean value superposed on the alternating value of the test parameter being controlled. Any difference between the demand signal and the feedback signal provides an error signal to the servo controller, the central electronic component which initiates corrective action. The servo controller supplies a current to the servovalve, which in turn controls the flow of high pressure fluid to the hydraulic actuator. This is the device that imparts load and displacement to the specimen to obtain the desired value of the test parameter.

As indicated in the block diagram, two signals are generated at the specimen. One signal is obtained from a load cell, the other from an extensometer that measures diametral displacement. These signals are fed to a small analog computer which converts them into electrical analogs of axial strain, diametral strain, and plastic strain, for comparison with the output of the programmer. The conversion circuits are based on the computation of engineering stress and engineering strain. This is considerably simpler than working with true stress and true strain, and the differences are negligible as long as the strain range is small, say $\triangle\epsilon$ less than 5 percent.

Test Specimen

In fatigue testing, the choice of specimen geometry is governed by the type of test to be performed and the experimental data to be acquired. It is generally recognized that testing round specimens in a push-pull mode is superior to other testing methods when complete information is desired on the history of stress and strain during the test. This is particularly true when fatigue is to be investigated in the low cycle range, where plastic deformation in each cycle of loading complicates the relationship between stress and strain. The push-pull mode is considered essential for successfully executing the types of tests that will be referred to in the Discussion.

Accepting the push-pull mode, a choice must be made between specimens with a cylindrical gage section and specimens with a gage section in the shape of an hourglass. These will be referred to as cylindrical and hourglass specimens, respectively. Typically, the former require measurement of axial strain over a portion of the uniform gage section, whereas the latter require measurement of transverse strain across the minimum diameter of the gage section.

The hourglass specimen is preferred by the authors over cylindrical specimens for the following advantages:

1. The strain can be measured and controlled at the cross section where fracture will occur.
2. Relatively large compressive strain can be produced in the material without buckling of the specimen.
3. Local heating of the specimen is readily accomplished, as the axial temperature profile needs to be flat over only a relatively short length of specimen adjacent to the minimum diameter.
4. A diametral displacement sensor is easily positioned on the specimen.
5. Internal and surface flaws are less likely to affect the outcome of the test since only a small portion of the specimen is exposed to maximum strain.

Disadvantages of the hourglass specimen are:

1. The diameter changes to be measured are usually considerably smaller than the axial changes measured on cylindrical specimens, so that precision requirements for strain measurement are more exacting.
2. The test parameter generally of primary interest, the axial strain in the specimen, is not measured directly, but indirectly via transverse strain and load measurements, so that programming of axial strain requires a conversion circuit to be added to the electronic control system.
3. The specimen geometry is not suited to testing of anisotropic materials on account of the difficulty of relating transverse and axial strain when the cross section does not remain circular under axial loading. Only the latter disadvantage amounts to a serious obstacle to the use of the hourglass specimen. For testing of isotropic materials, the authors developed an accurate transverse strain sensor and a conversion circuit to circumvent the other two disadvantages mentioned above. Anisotropic materials in general require the use of cylindrical specimens.

Figure 3 gives the dimensions of the standard specimen used by the authors. It has an hourglass gage section characterized by a contour radius of 1½ in. and a minimum diameter of ¼ in. The ends of the specimen are of the buttonhead type. These are preferred over threaded ends for the following reasons: (1) The specimen as shown in Fig. 3 can be machined in one setup on a centerless grinding machine, a procedure that yields specimens of uniform quality at low cost, and (2) clamped connections are less prone than threaded connections to develop backlash or misalignment problems from wear or tolerances that are too wide.

There have been a few cases where, under certain unfavorable test conditions, the use of the standard specimen resulted in fatigue fracture under the buttonheads rather than in the gage section. In these instances, the problem was eliminated by reducing the minimum diameter to 3/16 in., leaving all other dimensions the same. Of course, an alternative would be

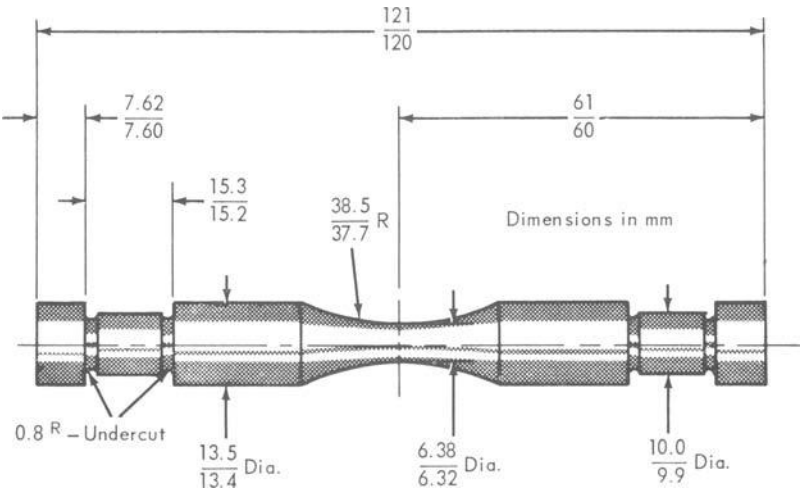

FIG. 3—*Fatigue specimen.*

to strengthen the buttonhead by enlarging its dimensions, but this option is not always available because of size limitations imposed by the available material stock.

Surface finish and heat treatment are important parameters to be considered in specimen design and fabrication. With the standard specimen in Fig. 3, the gage section is ground to a smooth finish using low-stress grinding techniques. This is followed by a polishing operation that leaves finishing marks in the axial direction rather than in the circumferential direction. Depending on the condition in which a given material is to be tested, fabrication of the specimen may be followed by an annealing heat treatment, a stress-relief heat treatment, or no heat treatment at all. In any case, the purpose of such a final heat treatment is to eliminate or reduce any residual stresses left in the material after machining.

Loading Fixtures

The accuracy attained in a fatigue experiment is in no small measure dependent on the proper mounting of the test specimen in the fatigue machine. It is important that the specimen be rigidly held and accurately aligned for the duration of the experiment. The fixture should not impede proper load and strain measurement or interfere with the chosen method of heating. It is important also that the specimen be readily installed and removed without upsetting the precision of the alignment of the fixture or machine.

Figure 4 shows a photograph of the fixture designed and built to meet these requirements. A sketch of the principal parts is shown in Fig. 5. It

should be evident from the sketch that the ends of the specimen are pressed into a three-post die set with the aid of split conical collars that fit under the buttonheads. Clamping plates maintain the buttonheads in a state of compression throughout the loading cycle, thus preventing any backlash during load reversal. The guide rods preserve the alignment of the specimen while the test is in progress, without reliance on the alignment and rigidity of the loading frame. It should be noted that the load cell in this arrangement measures the force on the specimen independent of any friction in the bushings of the die set. To install the specimen in the fixture, it is first assembled into the lower mounting plate before the plate itself is connected to the load cell adapter. This adapter, the load cell, and the base plate with guide rods are permanently attached to the hydraulic actuator. After placing the induction coil over the specimen, the upper mounting plate is put in place and lowered until the split conical collar can be inserted under the upper buttonhead. After tightening of the upper clamping plate, the actuator is brought up hydraulically to complete the connection between the upper mounting plate and the adapter that is attached to the loading frame. To avoid inadvertent loading of the specimen, the load cell signal is monitored during the installation.

FIG. 4—*Close-up view of loading fixture and induction coil.*

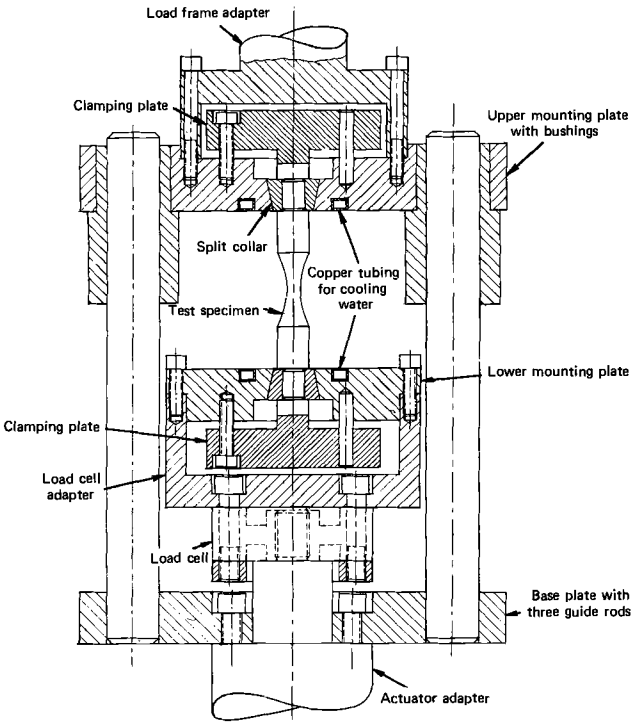

FIG. 5—*Assembly drawing of loading fixture with internal load cell.*

All parts of the fixture are precision made, with tool steel used almost throughout. The mounting plates are water-cooled to prevent thermal distortion due to the heat generated in the test sample. With the temperature of the specimen as high as 1000 C, the temperature rise in the mounting plates is minimal.

Load and Strain Measurement

To measure accurately the dynamic load on the specimen in a fatigue experiment, a load cell must be selected that possesses a high degree of structural rigidity and meets stringent requirements of sensitivity, linearity, and reliability. A compact, stiff structure is needed to avoid improper loading of the specimen due to flexibility of the load cell. When the load cell signal is used not only for recording purposes but also for controlling test conditions, reliability of the load cell becomes especially important. In other words, the calibration of the load cell may not change during such a test, if the test results are to be meaningful.

The recently developed flat load cell [5] is ideally suited for the experimental approach described in this paper. As may be appreciated from the dashed outlines shown in Fig. 5, such a load cell is exceptionally compact and rugged. These qualities made it possible to mount the load cell in series with the specimen within the confinement of the loading fixture, rather than external to it, as was the case with the earlier fixture sketched in Fig. 6. The flat load cell is essentially a thick, circular disk that consists of a rim and hub separated by a section of reduced thickness. To measure the load transferred from one component to another, the load cell is installed in such a way that the hub is connected to one component and the rim to the other. An electrical signal proportional to the load on the cell is generated by means of strain gages positioned in radial holes in the midplane of the reduced section. A special physical arrangement of the strain gages results in a load cell with identical sensitivity in tension and compression [5].

A diametral displacement sensor developed for the measurement of transverse strain at the minimum diameter of the specimen is shown in Fig. 7. Adjustable sensing arms capable of withstanding high temperature

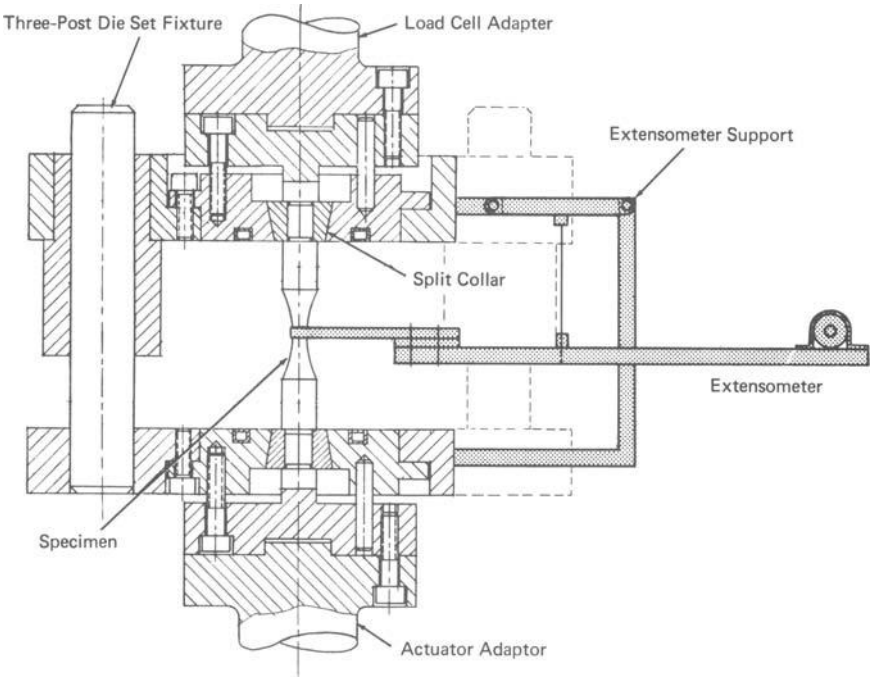

FIG. 6—*Assembly drawing of loading fixture with external load cell.*

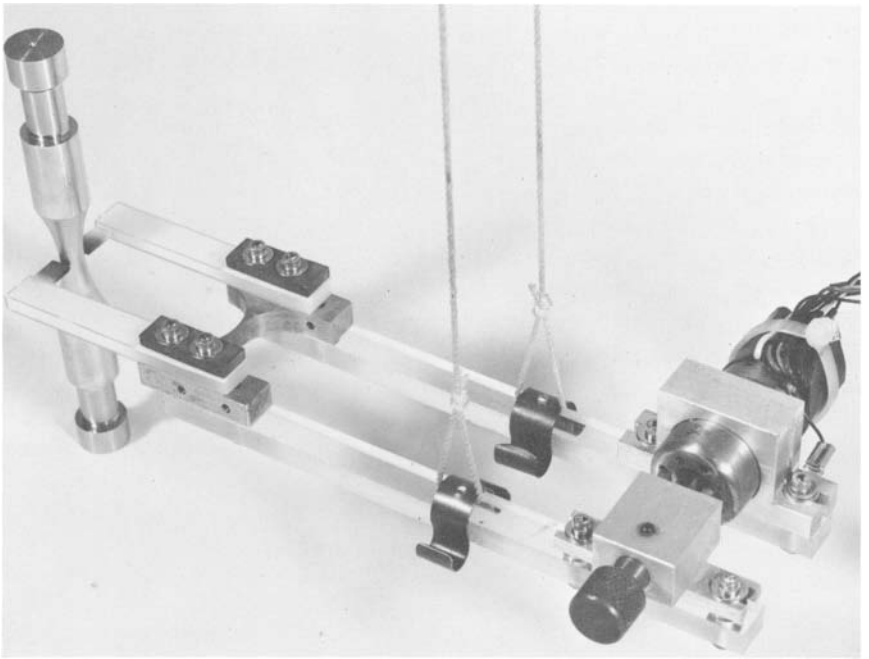

FIG. 7—*Extensometer for transverse strain measurement.*

are connected to a bracket consisting of two parallel beams joined by a flexible ligament that acts as an elastic hinge. The geometry of the ligament is formed by two arcs of 0.5-in. radius that leave a ligament with a minimum width of 0.020 in. between them. Diameter changes sensed at the knife edges are magnified before they are measured at the other end of the extensometer by a sensitive and magnetically shielded linear variable differential transformer (LVDT). Transformer and armature of the LVDT are mounted on opposite beams and the position of the armature relative to the transformer may be adjusted after the test specimen has been brought to the desired temperature level. The output signal of the LVDT is proportional to the diameter change in the specimen and is used in the servo control loop of the fatigue machine.

In normal use the hinge is only lightly strained, and the contact force exerted by the knife edges is quite low, just enough to prevent slipping. The spring constant of the strain sensor, defined as the ratio of force and displacement of the knife edges, was measured to be 4 g/0.001 in. It is obvious that the distance between knife edges has to be so adjusted that contact with the specimen is maintained during the complete strain cycle, the contact force reaching a minimum at peak tension in the specimen. To allow for unrestrained flexing of the hinge, as well as for free vertical

motion of the knife edges with the specimen, the sensor is suspended from long, flexible strains. Figure 6 shows a support arrangement whereby the whole sensor moves in unison with the minimum diameter of the specimen. It was originally thought that this type of support would be necessary [*1*]; however, experience has proved that suspending the sensor with strings from a stationary stand is adequate.

A narrow, elongated sensor design was chosen to separate the LVDT from the high temperature environment and to minimize potential experimental error from thermal distortion in the sensor. To avoid such thermal distortion, the sensor should be made of materials that are poor heat conductors and that have low coefficients of thermal expansion. The sensor seen in Fig. 7 has Invar for the flexible ligament, quartz for the beams, and Lucalox[5] for the sensing arms.

The calibration fixture used for calibrating the strain sensor is shown in Fig. 8. To ensure precision, the sensor is supported in identical fashion as on the fatigue machine. Displacement between the knife edges is produced by spreading two halves of a 0.25-in.-diameter pin cut along an axial plane. One of the pin halves is fixed and the other can be displaced a known amount by means of the micrometer. The fixture permits linearity of the sensor to be established and calibration to be obtained to the nearest 10 μin., the smallest increment that can be read on the micrometer. For most work, the authors calibrate on the basis of a displacement of 5000 μin., so the error in calibration of the strain sensor is very small. Used in conjunction with the electronic control and recording equipment, the sensor is capable of 1-μin. resolution. However, the accuracy of the strain produced in the test specimen depends also on the stability of the electronic components and the precision of temperature control. A reasonable estimate of the accuracy of strain control on the equipment described in this paper is 100 μin./in. in terms of the axial strain range. This amounts to an error of 1 percent when the strain range is 10,000 μin./in., which for many materials tested at room temperature produces fracture in 10,000 cycles of loading.

Hydraulic Equipment

The hydraulic equipment consists of the components identified in Fig. 9. Hydraulic fluid is supplied from a central source outside the laboratory in which the fatigue machines are located. All machines are operated off the same source, which makes for a more efficient arrangement than provided by individual units for each machine. Supplying the fluid from an external location has the additional advantage of excluding unwanted noise and vibration from the laboratory environment.

[5] General Electric Co. trademark for commercial polycrystalline alumina.

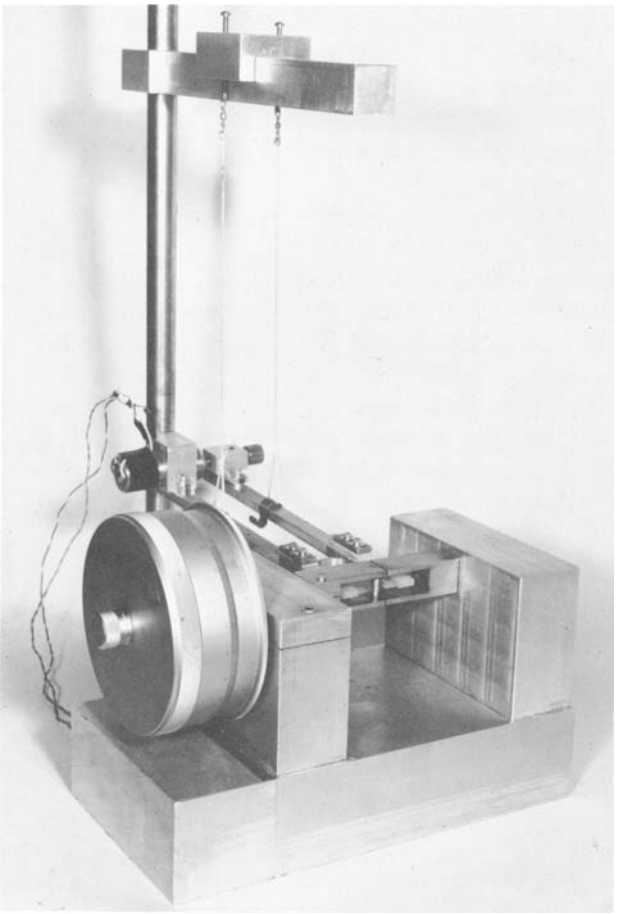

FIG. 8—*Fixture for calibration of extensometer.*

As shown in the block diagram, the machines can be disconnected from the central supply by means of shutoff valves in the forward and return line. Reverse flow is prevented by a check valve in the return line. A replaceable (10-μm) filter strains the fluid for protection of the servovalve and actuator and a gas-cushioned accumulator provides pressure isolation between fatigue machines. The pressure reducing valve is used to attenuate the pressure of the supplied fluid to a level that is adequate for the test. A pressure higher than needed leads to unnecessary wear of the servovalve and actuator seals.

A critical component in the hydraulic system is the servovalve. This is a precision flow-control device which consists of an electrical torque motor

and two stages of hydraulic power amplification. The output of the servo-controller is applied to the torque motor of the valve, which indirectly causes a four-way sliding spool to move relative to the null position. This spool then provides flow to one side of the hydraulic actuator, while providing a path for the return flow from the other side. Because of the extremely small movements required of the actuator and servovalve spool in low cycle fatigue testing, a superimposed a-c signal is also applied to the torque motor by the servo controller. The signal frequency is about 400 Hz and although above the frequency response of the system, it does reduce the effect of static friction and improves the system resolution.

Another important component is the hydraulic actuator. For best results, a high-quality actuator capable of sustaining small oscillating motions for long periods of time should be used. The symmetric, double-ended variety is preferable, for it provides bearing support of the actuator rod on both sides of the piston and thus minimizes any tendency for lateral flexibility. Also, symmetry of flow characteristics in tension and compression greatly facilitates the tuning of the electronic control system. To permit easy installation of test specimens, the actuator should have ample travel. The authors use actuators with a 6-in. stroke. For testing with axial displacement control, actuators with a built-in displacement transducer are commercially available.

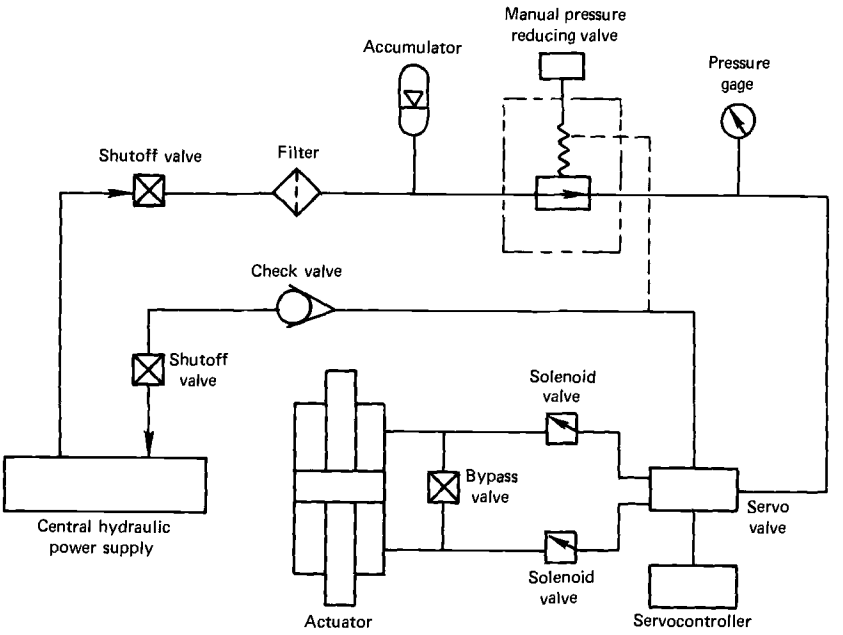

FIG. 9—*Block diagram of hydraulic system.*

Attention is called to the location of the solenoid valves. When the error signal to the servo controller exceeds a preset limit, the shutdown relay in the console (Fig. 1) will trigger instant closing of these valves, so that no further motion of the actuator rod is possible. This feature ensures stoppage of the test upon fracture of the specimen. Tripping of the relay also stops the programmer, timer, and recorders, and shuts down the heating system. The purpose of the bypass valve is to permit opening the solenoid valves without producing a surge through the control system. With the control system poised for closed-loop control the system is energized with the bypass valve open. The valve is then gradually closed before the programmer is engaged to start the fatigue test.

Recording Equipment

Signals that can be recorded are the electrical analogs of load (stress), elastic strain (proportional to load), plastic strain, and total strain. The manner in which these signals are generated is discussed in the section describing the computer module.

Two types of recorders are normally needed: strip chart recorders to obtain the variation of test parameters as a function of time, *X-Y* recorders to calibrate the control system and to analyze the relationship between two test parameters at certain times in the test. During a standard test, two strip chart recorders are usually employed to record the complete history of load and axial strain and an *X-Y* recorder is used to record hysteresis loops, first continuously in the early part of the test and then periodically thereafter. Typical records of this type may be found in earlier papers by the authors [*1, 2*] and in the papers in this publication by Feltner and Mitchell, Morrow and Raske, and Lord and Coffin.

In interpreting the results of low cycle fatigue tests, a suitable criterion for defining fatigue failure would be the number of cycles required to initiate a propagating crack. However, fatigue life based on such a criterion is difficult to measure in practice, even on a laboratory specimen when tested at elevated temperature in an oxidizing environment. For this reason, the authors define fatigue life as the number of cycles to that point in the test where, due to the presence of one or more cracks, the load range has fallen off by a certain percentage from its stationary value [*1–4*]. The continuous load record is used for this purpose.

Specimen Heating

In the authors' experience, the induction method has been simple and accurate for heating the test specimen. With this particular method, heating of the specimen results from circumferential eddy currents induced in the specimen by a high frequency current that flows through a

coil surrounding the gage section. The coil, visible in Fig. 4, is made of copper tubing. It is water-cooled and the individual windings are sheathed in fiber glass braiding to prevent short-circuiting.

The geometry of the coil was developed to furnish a flat temperature profile along the gage section of the specimen, while at the same time leaving sufficient room for measurement of the diametral strain at the minimum diameter. Basically, the coil consists of two separated parts, each with four windings. The temperature profile can be shaped by adjustment of the distance separating the two parts. Figure 10 gives typical axial temperature distributions obtained on a stainless steel specimen at different temperature levels, using the same coil. Temperature measurements made with a thermocouple inside the specimen through a small axial hole produced no evidence of a radial temperature gradient. Outside the coil windings the temperature in the specimen falls off sharply. This is apparent from the infrared photograph shown in Fig. 11, made with the specimen at 800 C. The black bands are the windings with the fiber glass braiding removed.

In a fatigue test, the specimen is instrumented with three Chromel-Alumel thermocouples spot-welded at a distance of 3/16 in. from the mid-position. Two of the thermocouples, on opposite sides of the mid-position, are used to balance the temperature profile. Before the fatigue test is started, the induction coil is adjusted vertically until the two thermocouples register the same temperature. The third thermocouple is

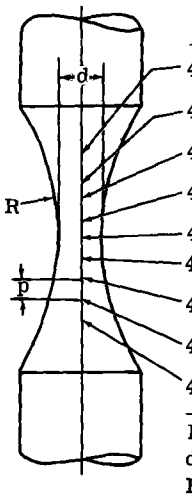

403	507	621	723	833	946
418	525	629	746	858	973
426	533	646	758	868	982
427	536	648	762	869	977
427	538	649	760	871	981
425	536	648	762	869	979
422	532	646	760	869	984
414	523	637	746	863	987
403	509	621	736	846	972

Legend:
d = minimum diameter = 1/4 in.
R = profile radius = 1-1/2 in.
p = thermocouple spacing = 1/8 in.

FIG. 10—*Temperature distribution in fatigue specimen (AISI 304 stainless steel).*

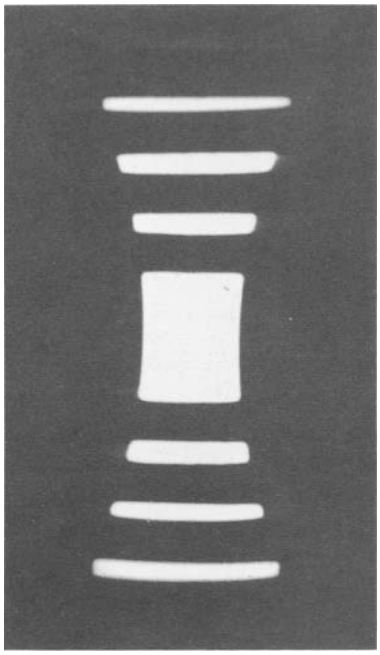

FIG. 11—*Infrared photograph of fatigue specimen at 800 C (AISI 304 stainless steel).*

used for temperature control. It causes the temperature indicator on a standard commercial recorder-controller to move relative to the temperature set-point indicator. When the two indicators do not coincide, an error signal is generated which results in corrective action through the induction generator.

Several makes of induction generators are commercially available and the manufacturers are an excellent source of information on the components necessary to obtain closed-loop temperature control with their equipment. The authors did not consider it worthwhile, therefore, to describe in detail the particular temperature control system used in their laboratory.

Computer Module for Optional Modes of Strain Control

Figure 12 shows the front panel of the computer module built for the purpose of providing a choice between programming diametral (transverse) strain, axial strain, plastic strain, or load in the fatigue experiments. Its operational features will be described below with the aid of the block diagram shown in Fig. 13 and the network schematic presented in Fig. 14.

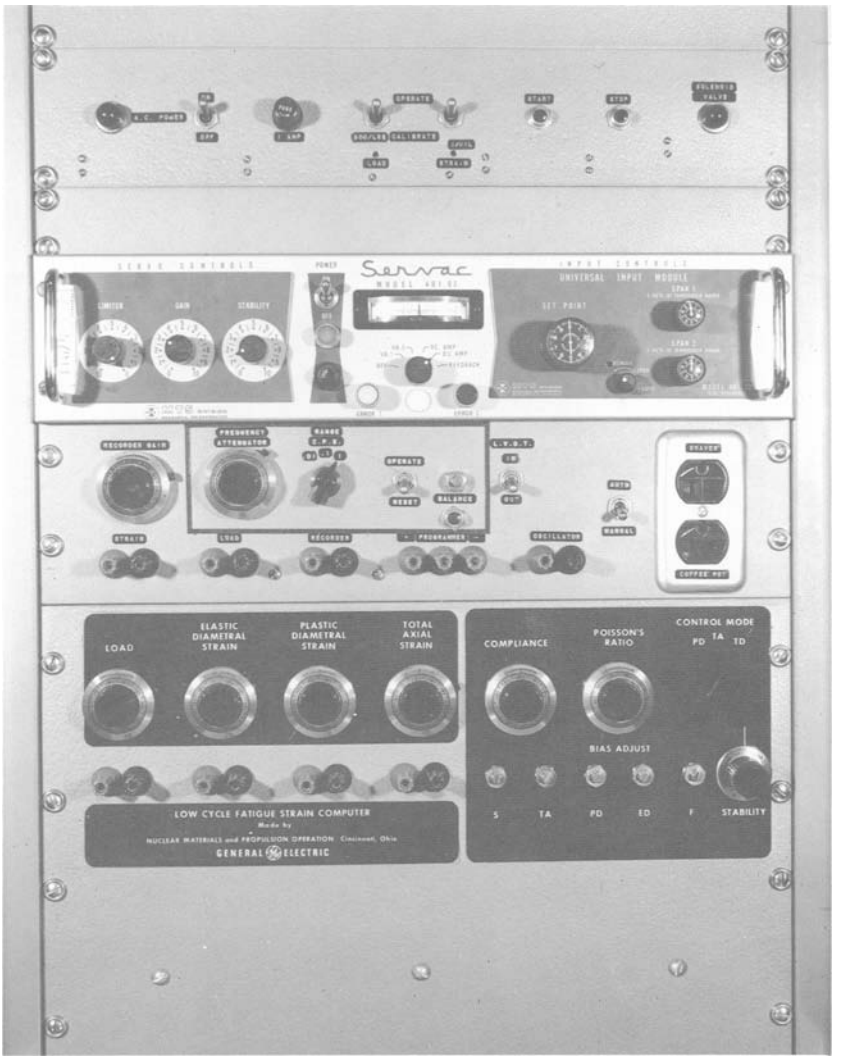

FIG. 12—*Close-up view of strain computer.*

Computer Circuit

The conversion from diametral strain to axial strain requires the determination of the elastic and plastic components of the diametral strain. From these the elastic and plastic components of the axial strain can be computed and then combined to give the total axial strain. The pertinent relationships needed for the conversion are:

$$\epsilon = \epsilon_e + \epsilon_p,$$

$$\epsilon_d = \epsilon_{de} + \epsilon_{dp},$$

$$\epsilon_{de} = -\nu_e \epsilon_e,$$

$$\epsilon_{dp} = -\nu_p \epsilon_p, \text{ and}$$

$$\epsilon_e = F/AE.$$

These expressions may be rearranged to give:

$$\epsilon_{de} = -KF, \text{ where } K = \nu_e/AE = \text{a constant},$$

$$\epsilon_{dp} = \epsilon_d - \epsilon_{de}, \text{ and}$$

$$\epsilon = -\epsilon_{de}/\nu_e - \epsilon_{dp}/\nu_p.$$

The computer generates the electrical analogs of ϵ_{de}, ϵ_{dp}, and ϵ. To accomplish this, analogs of ϵ_d and F must be supplied as inputs. As indicated in Fig. 13, the lateral strain sensor and the load cell furnish these signals. The values of the constants ν_e and K must be inserted by means of two potentiometers, located to the right in Fig. 12. The value of ν_p is fixed at 0.5 in accordance with the constant-volume condition associated with plastic deformation of isotropic materials.

In Fig. 14 it can be seen that Amplifier 1 operates as a differential amplifier to increase the level of the load cell signal. The signal is then attenuated by a calibration potentiometer to produce a properly scaled analog of ϵ_{de} at the output of Amplifier 2. Amplifier 3 is used to subtract ϵ_{de} from ϵ_d to give ϵ_{dp}, while Amplifier 4 sums ϵ_{de}/ν_e and ϵ_{dp}/ν_p to produce the analog of ϵ. Switch S1 maintains the proper phase relationship

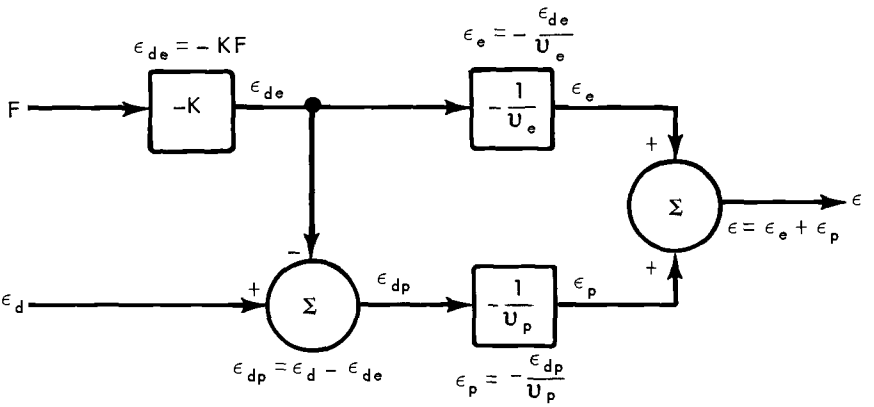

FIG. 13.—*Block diagram of strain computer.*

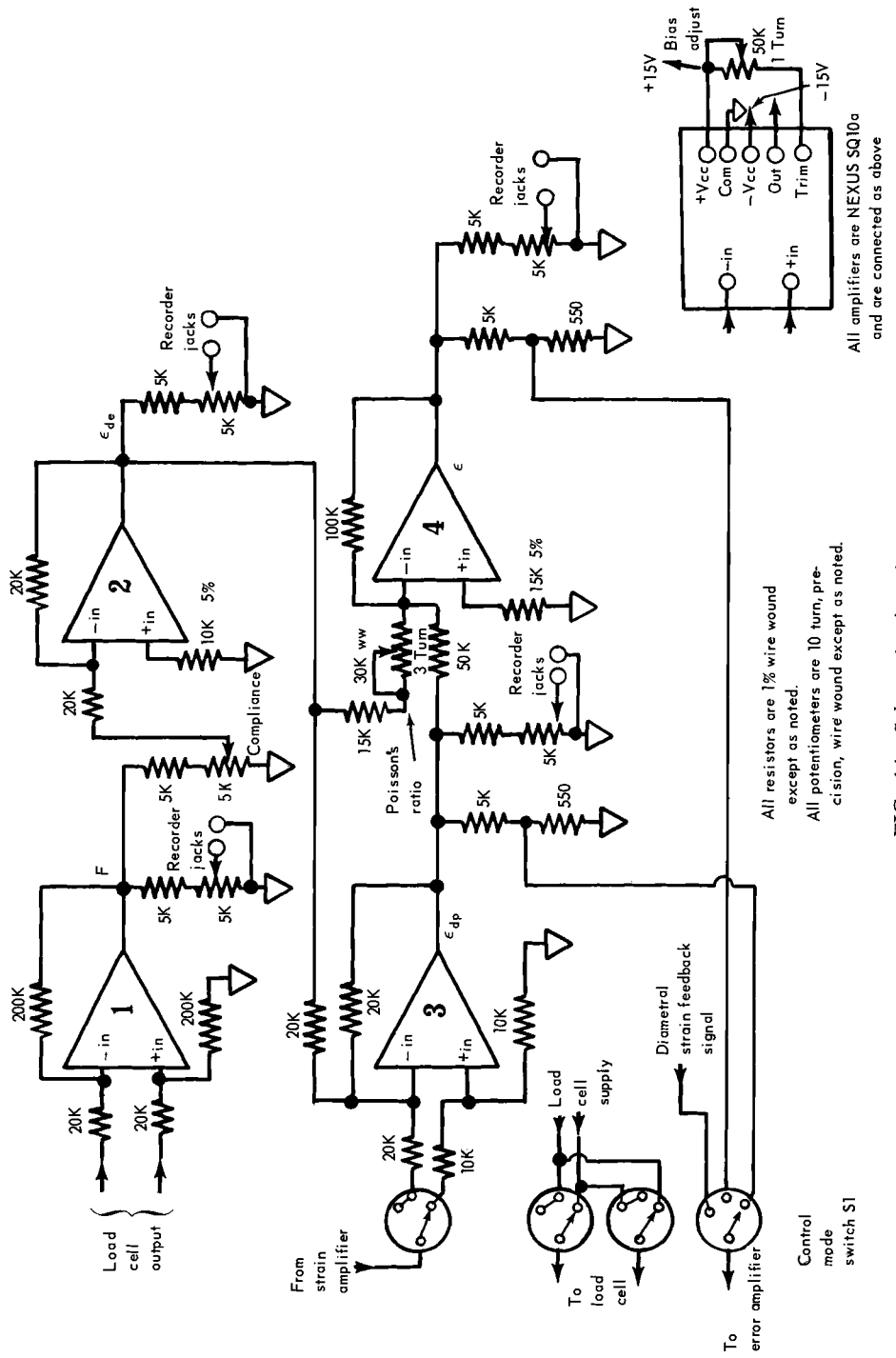

FIG. 14—*Schematic of strain computer.*

between all three modes of control, that is, control of ϵ_{dp}, ϵ_d, and ϵ. The switch positions are denoted in Fig. 12 as *PD*, *TD*, and *TA*, respectively. (Control of ϵ_{dp} also implies control of ϵ_p, since $\epsilon_p = -\epsilon_{dp}/\nu_p = -2\epsilon_{dp}$.) It is appropriate to mention that with control of plastic strain some system dead band cannot be avoided upon strain reversal. This occurs because no dynamic control of the plastic strain is possible while the specimen is unloading elastically. Therefore, trial runs may be necessary under some test conditions to evaluate system performance with this mode of control.

Fewer amplifiers could have been used to obtain ϵ, but only by sacrificing the low-impedance signals desired for maximum flexibility of recording and control. Figure 12 shows that recording signals are directly available for F, ϵ_{de}, ϵ_{dp}, and ϵ. Four 10-turn potentiometers are provided to facilitate the selection of recorder scales. Note that ϵ_e and ϵ_p are also readily recorded, for they differ from ϵ_{de} and ϵ_{dp} only by simple scale factors.

Load control of the fatigue experiment is also available, since the load cell signal makes up part of the axial strain signal. It is only necessary to remove the diametral strain signal from the computer and place the selector switch in the total-axial-strain position. A simple modification of the circuit would be needed to permit load control without removing the diametral strain signal.

Bias-adjustment potentiometers found on the front panel of the computer module serve the purpose of assuring a zero output from each of the amplifiers when all inputs are zero. Adjustments are needed only occasionally.

Stability Circuit

The computer module also contains a rate-feedback stability circuit, added to the control system of the fatigue machine to improve performance. Experience has shown that instability problems are sometimes encountered with high-gain servo systems when using hourglass specimens and diametral-strain measurements as feedback signals. Certain combinations of specimen material, temperature, strain amplitude, and strain rate can result in unwanted strain excursions within each cycle.

To understand the reasons for such instabilities requires a brief discussion of the specimen as a component of the servo system. In order to strain the specimen at a desired rate, the hydraulic actuator has to supply both a variable force and a variable displacement. Unfortunately, the force and displacement rates are not the same above and below the proportional limit of the material. This nonlinear behavior can result in an intracycle gain change of an order of magnitude or more. In addition, the

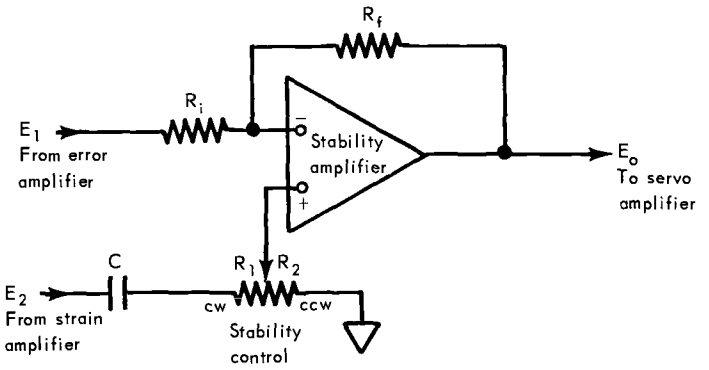

$$E_o = \frac{\frac{R_2}{R_i}[R_i + R_f]CS}{(R_1+R_2)CS+1} E_2 - \frac{R_f}{R_i} E_1$$

where $R_i = 10\,K\,\Omega$
$R_f = 1$ meg Ω
$R_1 + R_2 = 50\,K\,\Omega$
$C = 0.1\,\mu f$

FIG. 15—*Stability circuit.*

creep or relaxation characteristics of the specimen can introduce a time effect which results in a lag in the system time response. These two effects can easily cause unstable system operation unless some type of compensation is introduced.

The circuit shown in Fig. 15 and modifications thereof have been used to minimize the effects of the specimen behavior on system stability. It serves as a so-called derivative-lag network that consists of a feedback loop around all system components, except the error amplifier and the computer circuit. This technique of using an inner loop within a larger system is a common means for minimizing the detrimental effects of a nonlinear element, in this case the specimen. The gain of this loop can be adjusted by turning a potentiometer available as a front panel control on the computer module. It should be noted that the values of the components of the circuit of Fig. 15 are consistent with the components in the authors' control system and should not be assumed to be universal by any standard.

Operating Procedure

In the case of axial strain control, programming the testing machine requires the calibration of the computer to establish the proper values for

K and ν_e. Four steps are needed to accomplish this for K, as follows:

1. Allow the specimen and servo system to reach equilibrium at the test temperature of interest. During heating the specimen should be allowed to expand freely and assume a steady-state temperature distribution. The electronic components must also be allowed to warm up and stabilize.

2. Obtain closed-loop control of the machine in the diametral strain mode (Switch S1 on *TD*).

3. Cycle the specimen within the linear, elastic range of the material.

4. Monitor the output signal of ϵ_{dp} with a high-gain recorder and adjust the compliance potentiometer on the computer panel to give a zero readout. This procedure establishes the proper value of K in the system.

It should be noted that by this calibration procedure K is automatically adjusted to its proper value, while no effort is made to determine its actual value.

The value of ν_e is determined by recording ϵ_{de} versus F on an X-Y recorder while the specimen is cycled in the elastic range, as in Step 3 above. The slope of the straight line so obtained gives ϵ_{de}/F, which in turn yields ν_e through the relationship $\nu_e = -AE\epsilon_{de}/F$, where A and E must assume the values applicable to the temperature of interest. A tension test is required to determine E.

In the case of diametral strain control, the analog computer is bypassed when the selector switch S1 is in the *TD*-position. Consequently, the values of K and ν_e are not needed for controlling the machine in this mode. In the case of plastic strain control, it suffices to establish only the value of K. Inspection of the block diagram in Fig. 13 shows that once the computer has been calibrated for K, a correct signal for ϵ_{dp} is available for control purposes. Hence, tests with control of diametral strain or plastic strain can be performed without knowledge of the elastic constants of the material. Of course, it is good practice to obtain complete calibration of the computer regardless of the desired mode of control, so that all strain signals are available for recording purposes.

It was assumed above that the recording equipment is calibrated for strain. For this purpose, the electronic control console contains a calibration switch which can insert an artificial diametral-strain signal into the system. Since it enters the computer network without a corresponding force signal, it appears as all plastic strain. Consequently, the strain equivalence of the calibration switch is twice as high for axial strain as for diametral strain. The artificial diametral strain signal is set with the aid of the calibration device shown in Fig. 8. Calibrating the recording equipment for load is accomplished in a similar manner, that is, by means of a switch that can insert an artificial load signal of known magnitude.

The switches are located in the panel above the servo controller, as may be observed in Figs. 1 and 12.

Once the computer has been calibrated, it remains to select a command signal program, set timers for tests with hold times, and start the test. Automatic shutdown of the equipment, including the heating system, is accomplished when the system error signal exceeds a preset limit. The limits are manually set by adjusting the limit switches on the meter relay after the test is started.

Discussion

It is apparent from the experimental approach described in this paper that the authors have a strong preference for using hourglass specimens in their low cycle fatigue research at elevated temperature. This preference originates from the advantages associated with this type of specimen, as discussed earlier. Many other investigators have used the hourglass specimens for the same reasons. In the past, however, testing of hourglass specimens was generally executed with control of either load, transverse strain, or actuator displacement. Because the axial strain is usually the test parameter of primary interest, the authors pursued the development of testing procedures that would permit programming of the axial strain in the hourglass specimen, as described in the preceding pages.

The purpose of this discussion is to review the benefits gained from controlling axial strain rather than transverse or diametral strain. Before proceeding with the review it is necessary to present several relationships between the test parameters in the push-pull test. The relationship involving the parameters σ, ϵ, and ϵ_d is expressed by the following equation:

$$\epsilon = (1 - \nu_e/\nu_p)\,\sigma/E - \epsilon_d/\nu_p \quad \ldots\ldots (1)$$

This equation is readily derived by eliminating ϵ_p from the basic relations $\epsilon = \epsilon_p + \epsilon_e$, $\epsilon_d = -\nu_p\epsilon_p - \nu_e\epsilon_e$, and $\sigma = E\epsilon_e$, where $\nu_p = 0.5$.

Denoting the maximum and minimum axial strain magnitudes by ϵ_1 and ϵ_2, respectively, and subscripting the corresponding stress and diametral strain magnitudes accordingly, one may write:

$$\epsilon_1 = (1 - \nu_e/\nu_p)\,\sigma_1/E - \epsilon_{d1}/\nu_p \quad \ldots\ldots (2)$$

$$\epsilon_2 = (1 - \nu_e/\nu_p)\,\sigma_2/E - \epsilon_{d2}/\nu_p \quad \ldots\ldots (3)$$

Now let $\Delta\sigma = |\sigma_1 - \sigma_2|$, $\Delta\epsilon = |\epsilon_1 - \epsilon_2|$, and $\Delta\epsilon_d = |\epsilon_{d1} - \epsilon_{d2}|$, where Δ denotes the range traversed by the associated parameter. Then, stress and strain ranges are related as follows:

$$\Delta\epsilon = (1 - \nu_e/\nu_p)\,\Delta\sigma/E + \Delta\epsilon_d/\nu_p \quad \ldots\ldots (4)$$

Next, symbols R and R_d are introduced to define test conditions encountered when an alternating strain is superposed on a mean strain:

$$R = \epsilon_1/\epsilon_2 = \frac{(1 - \nu_e/\nu_p)\,\sigma_1/E - \epsilon_{d1}/\nu_p}{(1 - \nu_e/\nu_p)\,\sigma_2/E - \epsilon_{d2}/\nu_p} \quad \ldots\ldots (5)$$

$$R_d = \epsilon_{d1}/\epsilon_{d2} \quad \ldots\ldots (6)$$

With the aid of the above equations it is now possible to point to several obvious advantages to be gained by programming the axial strain in an hourglass specimen:

1. The wave form is programmed for the test parameter of primary interest, the axial strain. Inspection of Eq 1 shows that programming ϵ_d with a certain wave form would not result in the same wave form for ϵ. An illustrative example of the difference was shown in an earlier paper [*2*].

2. Many materials exhibit cyclic strain hardening or softening in strain-controlled fatigue experiments. An example of such behavior is seen in Fig. 16, taken from another paper [*3*]. The diagram shows a variation in the stress range as the test progresses. Such a variation is accompanied by a redistribution between elastic and plastic strain. Consequently, with a fixed diametral strain range, the axial strain range increases with cyclic hardening and decreases with cyclic softening. This observation may be verified by inspection of Eq 4. Being able to program axial strain is clearly advantageous when the materials tested exhibit cyclic hardening or softening.

3. A given ratio of alternating axial strain and mean axial strain is readily programmed. It can be deduced from Eqs 5 and 6 that this ratio is not the same as the corresponding one for diametral strain. Therefore, it is difficult with diametral strain control to select that value of R_d which

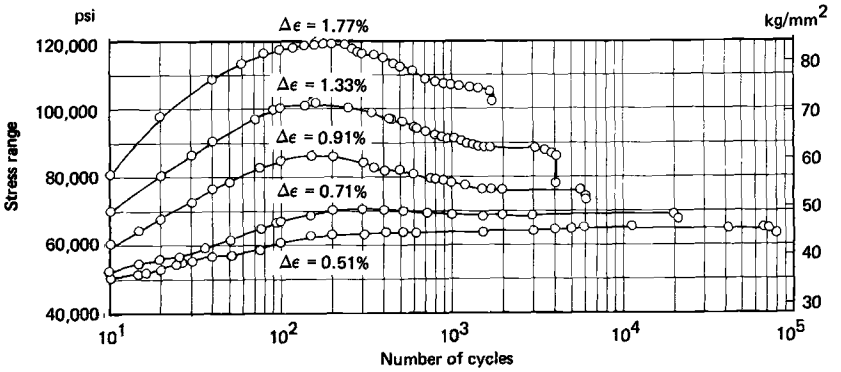

FIG. 16—*Stress range versus loading cycles for AISI 316 stainless steel at 430 C (axial strain rate 0.004 s^{-1}).*

will produce the desired value of R in the test. Also, with a fixed value for $R_{\bar{a}}$, cyclic hardening or softening would result in a variable value for R.

4. At temperatures in the creep range, holds in the strain cycle result in stress relaxation during the hold periods. Relaxation is accompanied by a decrease in elastic strain and hence by an increase in plastic strain when the total strain is held constant. It is apparent from Eqs 2 and 3 that a hold on diametral strain will not result in a true hold on axial strain. A true hold on axial strain in the hourglass specimen can only be obtained by programming the axial strain.

In conclusion, there is one additional testing consideration that deserves to be mentioned, the manner of starting a test. Test results presented in Table 1 show that in tests with large strain amplitudes, the fatigue life may depend on whether the test is started in tension or compression. A similar finding was reported recently by Tilly [*6*]. As a matter of standard laboratory practice, tests performed in the authors' laboratory are always started in compression [*1–4*].

TABLE 1—*Fatigue test*[a] *results for annealed Type 304 stainless steel at* 800 *C.*

Axial Strain Range ($\Delta\epsilon$), %	Axial Strain Rate ($\dot{\epsilon}$), s^{-1}	Stress Range ($\Delta\sigma$), kg/mm^2	Starting[b] Condition	Frequency, cycles/min	Cycles to Failure
3.0	3×10^{-3}	36	c	3	265
3.1	3×10^{-3}	37	c	3	280
3.1	3×10^{-3}	38	t	3	258
3.1	3×10^{-3}	37	t	3	241
1.6	3×10^{-3}	39	c	6	683
1.6	3×10^{-3}	39	c	6	685
1.7	3×10^{-3}	39	t	6	516
1.7	3×10^{-3}	38	t	6	545

[a] Mode shape: triangular, with zero mean strain.
[b] Test started in compression (c) or tension (t).

Acknowledgment

The authors gratefully acknowledge the extensive and valuable technical participation of D. Stratton in the development of the testing equipment described in this paper.

References

[*1*] Slot, T., "Experimental Developments in Low Cycle Fatigue Research on Pressure Vessel Steels at Elevated Temperatures," presented at Symposium on Low Cycle and Thermal Stress Fatigue, General Electric Research and Development

Center, Schenectady N. Y., June 1966: *General Electric Report GE-TM 66-6-11; Clearinghouse for Scientific and Technical Information Report CONF-660647-1*, Springfield, Va.

[2] Slot, T. and Stentz, R. H., "Experimental Procedures for Low Cycle Fatigue Research at High Temperatures," *Experimental Mechanics*, EXMCA, Vol. 8, No. 3, 1968, pp. 107-114.

[3] Berling, J. T. and Slot, T., "Effect of Temperature and Strain Rate on Low Cycle Fatigue Resistance of AISI 304, 316, and 348 Stainless Steels," *Fatigue at High Temperature, ASTM STP 459*, American Society for Testing and Materials, 1969, pp. 3–30.

[4] Berling, J. T. and Conway, J. B., "Effect of Hold Time on the Low Cycle Fatigue Resistance of AISI 304 Stainless Steel at 1200 F," presented at First International Conference on Pressure Vessel Technology, Delft, Holland, Sept. 1969.

[5] Kutsay, A. U., "Flat Load Cells," *Instruments and Control Systems*, INCSA, Vol. 39, No. 2, 1966, pp. 123-125.

[6] Tilly, G. P., "Strain and Rupture Behavior Under High-Stress Reversals," *Journal of Strain Analysis*, Institution of Mechanical Engineers, Vol. 2, No. 3, 1967, pp. 220-225.

D. C. Lord[1] *and L. F. Coffin, Jr.*[1]

High Temperature Material Behavior

REFERENCE: Lord, D. C. and Coffin, L. F., Jr., **"High Temperature Materials Behavior,"** *Manual on Low Cycle Fatigue Testing, ASTM STP 465*, American Society for Testing and Materials, 1969, pp. 129-148.

ABSTRACT: The purpose of this paper is to describe the equipment and procedures developed at the General Electric Research and Development Center for testing and evaluating materials at elevated temperature under uniaxial controlled cyclic strain. Items considered include specimen design and surface finish, grip design and specimen assembly, extensometer design and operation, instrumentation, heating and temperature control, test operation, and failure interpretation and data reduction.

KEY WORDS: fatigue (materials), fatigue tests, low cycle fatigue, high temperature fatigue, mechanical tests, metals, high temperature tests

This paper presents information on the limit-controlled, uniaxial cyclic strain testing procedures employed at the General Electric Research and Development Center. These procedures have been and continue to be evolutionary in nature and are subject to modification as improved techniques, design, or instrumentation become available. The present report describes the current status of these procedures as they exist in conjunction with screw-driven constant crosshead rate testing machines, but do not reflect the methods introduced with the advent of servo-controlled closed-loop testing machines in the authors' testing activities.

The testing philosophy for which the experimental program was designed was to provide basic material information on structural materials useful for machines and components manufactured by the General Electric Co. and whose service requirements subjected them to low cycle fatigue. The interest in these experiments was centered primarily on the material rather than on the specific component, and, to make the work of general interest, the conditions of the tests were such that the results

[1] Technical specialist and mechanical engineer, respectively, Research and Development Center, General Electric Co., Schenectady, N. Y. 12301. Dr. Coffin is a personal member ASTM.

could be applied to complex structural configurations through appropriate engineering judgment. Hence the loading was uniaxial, such that the applied stress could be found at all times from the measured load and the instantaneous specimen diameter.

Further, the experiments were conducted under controlled strain range rather than the earlier and more common procedure of employing controlled stress or load limits. This was done to relate the work more closely to the real problem to which the results could be applied, as for example where the cyclic conditions were primarily a result of thermal cycling or of load cycling of elastic structure containing small local plastic regions such as filets or other stress concentrations.

The limited life regime was of primary interest in the experimental program. Fatigue failures of the test specimens were investigated in the range of 1 to 10^5 cycles, or more generally, where measurable plastic strain could be obtained on each cycle. In other words, the regime of interest was when stress and strain were nonlinearly related.

Specimen shape is of considerable importance in these experiments and more detailed information will be provided in the body of this report. A primary purpose of the program is to provide information on the cyclic strain and fatigue behavior of a specific material where failure may result in a very few cycles. This requires sufficiently close monitoring of the specimen deformation throughout its life such that the actual stress and strain existing in well-defined locations can be measured and controlled. In uniaxial loading this can only be done with the so-called "hourglass" test specimen, in which only a small region at the minimum diameter of the specimen is subjected to the maximum stress and strain conditions. Control of strain range of this element is effected by continuously monitoring the minimum diameter of the specimen. In contrast to the broad strain ranges to which the hourglass specimen can be employed, use of other specimen shapes, such as uniaxially loaded, uniform gage length specimens, is limited to strain ranges where progressive local shape changes in the gage length region do not give rise to erroneous strain information.

Since material behavior at elevated temperatures is of prime importance to this program, means for producing and maintaining the desired temperature constant in the test area of the specimen is a basic requirement. Measurement and control of temperature without compromising life, such as by fatigue crack nucleation at thermocouples located in the test region, require special attention. Also localization of the high temperature to the general test area and away from the specimen grips and load cell requires adequate water-cooling of the grips. It is particularly important for reliable load measurement that the load cell remain under isothermal

conditions during the life of the test. Careful control of temperature is required to insure reliable load and strain records.

Diametral strain range control requires an extensometer whose prime function is to indicate the diameter limits of the cycle for purposes of reversing the direction of loading. Continuous monitoring of the diameter change is highly desirable, so that, in conjuction with the instantaneous load, hysteresis loops of load versus diameter change can be recorded during the test. Until a suitable alternative can be devised, direct contact of the extensometer with the surface of the specimen is necessary. The localized contact pressure acting in conjunction with the applied cyclic plastic strain can produce progessive indentation of the specimen especially for low strain hardening metals [*1*],[2] and cause premature crack initiation. Attention must therefore be given to minimizing the contact pressure of the extensometer.

Under fully reversed strain conditions, compressive loads are encountered which are equal in magnitude to the tensile loads. Buckling of the specimen is always a possibility and requires special attention. Particular attention must be given to the shape and dimensions of the test specimen, the initial alignment of the grips, and their movement during the test. Features of the specimen and grip design and of the testing machine to implement stability will be discussed.

Continuous recording of temperature, load and diameter change versus time and the recording of load versus diameter change throughout a particular test give a complete picture of the material response to controlled cyclic strain and serve as valuable tools in the interpretation of the test. Additional observations such as surface changes in the specimen, crack nucleation, and crack propagation can be made to suit the needs of the investigation.

With these observations much can be learned regarding the cyclic strain and fatigue response of metals. Several investigations of the authors have been published [*2–6*] and these provide additional information on testing procedures as well as on material behavior under conditions of controlled cyclic strain applicable to the design of real structures.

Specimen Design

The general design of the hourglass specimen is based on the concept of localizing the strain to the area where it can be controlled, while minimizing the constraint effects of the notch arising from the hourglass shape, consistent with resistance to buckling during the test. From experience the specimen shape, defined in terms of the ratio of the radius of curva-

[2] The italic numbers in brackets refer to the list of references at the end of this paper.

ture of the notch, r, to the minimum radius of the specimen, R, depends on the maximum strain range required in a particular program. For example, for diametral strain ranges not exceeding 0.02, the ratio, r/R, employed was 12. For very large strain ranges, in the order of 0.2, $r/R = 6.67$.

Detailed dimensions of the test specimen most commonly used are shown in Fig. 1. Figure 2 shows several typical test specimens used in various experimental programs. Specimen 2 is that detailed in Fig. 1, while Specimen 4 was designed for high buckling resistance where large compression strains are encountered.

Specimen Preparation

Since test results are very sensitive to the surface of the specimen, some detail is required of the method involved for surface finishing. The specimen is first rough-finished in the hourglass region leaving 0.005 in. on the minimum diameter. It is then mounted between centers in a cylindrical grinder. The wheel spindle is aligned at 90 deg to the specimen axis and positioned at its mid-point. The specimen is rotated at 325 rpm while its axis is translated back and forth in a direction perpendicular to the wheel spindle. With a grinding wheel of appropriate radius operating at 5150 rpm, about 0.0002 in. is removed per pass until the finished diameter +0.001 in. is reached.

The specimen is then mounted on ball-bearing fixtures and held against a buffing wheel at a slight angle, about 10 deg, to the buffing wheel plane. This imparts a rotating movement to the specimen which can be braked by the operator with his thumb. Three different polishing wheels are used,

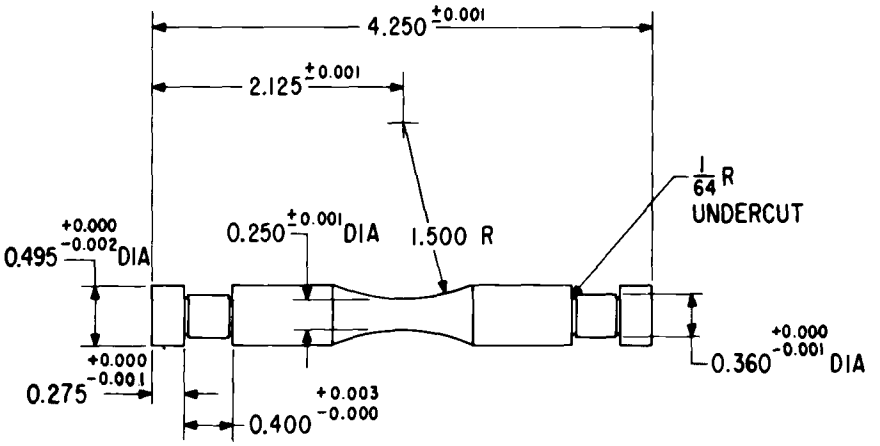

FIG. 1—*Standard low cycle fatigue specimen detail.*

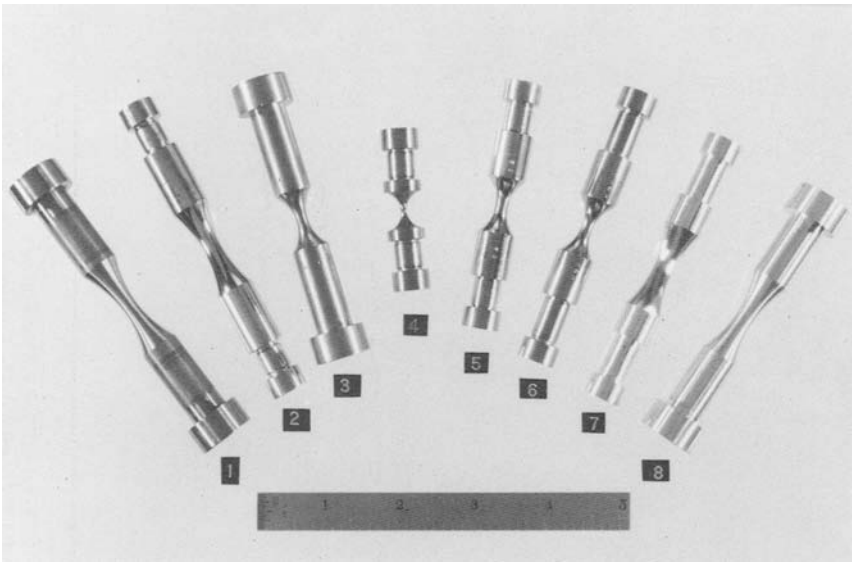

FIG. 2—*Various test specimen configurations.*

each charged with the proper polishing agent to impart a surface finish which is polished in appearance and measures on an average of a 3 to 4 μin. surface roughness. All the grinding lines and polishing marks are longitudinal, and all circular machining marks are removed. A surface so prepared minimizes any influence of specimen preparation on the test results.

Following this the specimen is degreased and then heat treated. The heat treating is conducted in such a way as to avoid any surface damage and a protective atmosphere is employed to eliminate surface oxidation. The minimum diameter is then measured by optical means to eliminate any contact and possible marking of the sample.

Two thermocouples are attached at a location ¼ in. from the minimum diameter. Ten-mil Chromel-Alumel wires are welded to form a 0.04-in.-diameter bead which is pinched flat with pliers to about 0.015 in. and then carefully spot-welded to the specimen. This procedure results in a strong attachment that is highly resistant to mechanical failure, yet does not influence the fatigue life of the specimen.

Grip Design

The grip assembly is shown in Fig. 3. Details of the design include two pairs of split gripping collars which fit snugly to the specimen (two styles are shown in the figure), two retaining rings, two water-cooled grip housings, and pull-down bolts to clamp the split collars firmly to the

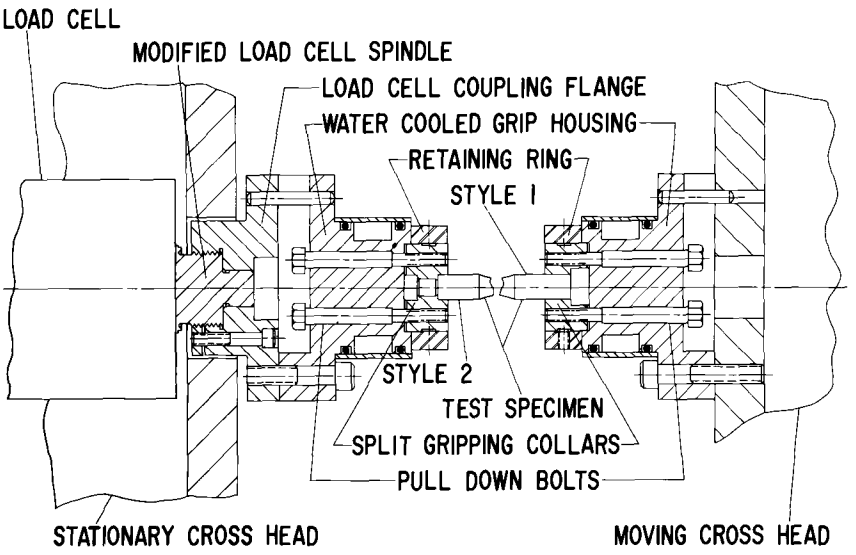

FIG. 3—*Section view of testing assembly.*

housings. One housing is attached to the moving crosshead of the testing machine, the other to a load cell coupling flange. Features of this design include: rigid support of the test specimen against tensile and compressive forces as well as bending movements, firm clamping of the specimen and split collars to the housing for effective heat transfer in tension as well as compression, precision in alignment, and ease in assembly.

Alignment is very important. Aside from careful machining of the several parts described above, the following was done. An Instron GR[3] load cell was made with a special spindle containing a pilot stud as an integral part of the spindle. After installing and bolting the load cell in place, the load cell coupling flange was attached and locked. Alignment was assured by the pilot stud and by threading the coupling flange to the spindle shoulder. The upper housing was then firmly bolted to this flange and the lower housing was loosely mounted to the moving crosshead. Both pairs of split couplings were bolted into their respective counter bores without a specimen, the gap between them reduced to zero, and with one retainer ring in place, the lower housing was moved about until the ring slid easily from the upper to lower split coupling. At this point the lower housing was firmly bolted to the moving crosshead. In the installation of the specimen, care must be taken to prevent loading of the specimen while tightening the pull-down bolts.

[3] 20,000-lb reverse stress cell; Instron Corp., Canton, Mass.

It should be understood that, prior to clamping of the specimen rigidly in the machine, the load recording system must be calibrated by conventional methods and the zero load point positioned mid-scale on the recorder.

Extensometer

Figure 4 shows the diametral strain transducer. A structural frame of Invar is balanced about a single fulcrum point screw. This frame provides the support for two quartz gage rods that contact the minimum diameter of the specimen at diametrically opposite points. A pivot point is attached to the frame and the entire extensometer carefully balanced on this point. This arranagement allows only very small restrictive forces to be applied to the specimen. One gage rod is fixed in the frame assembly. The other gage rod is movable and is supported by means of two thin elastic phosphor bronze leaf springs. Attached to the transducer assembly is a standard Instron (Catalog G-51-16) ½ in. gage length strain gage extensometer. This extensometer measures the relative movements of the two gage rods and hence the diameter of the specimen. The Invar and quartz materials used in the transducer were chosen to provide good dimensional stability independent of small ambient temperature changes. In connection with elevated temperature experiments where a portion of the gage rods are at specimen temperature, quartz offers the additional advantage of oxidation resistance. The elastic leaf springs minimize frictional effects that would otherwise lead to backlash in the performance of the transducer. The contact pressure against the specimen is quite low.

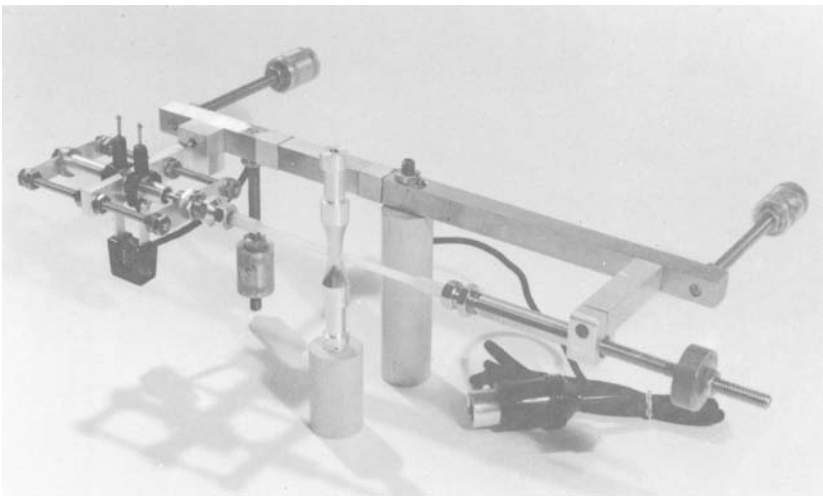

FIG. 4—*Diametral extensometer.*

This was achieved by reducing the spring force to a few tenths of a pound and by contouring the gage rod contacts more nearly to match the curvature of the specimen.

Maximum sensitivity of the strain transducer is such that 0.0002 in. of diameter change in the specimen is equivalent to full-scale deflection of a strain recorder to be described later. In a specimen with a minimum diameter of 0.25 in., a diametral strain of 8 μin./in. is then equal to 1 percent of full scale on this strain recorder. The transducer has been used to control an experiment in which the diametral changes were as little as ± 60 μin. This was equivalent to a diametral strain range of 0.0008 in./in. in a specimen with a nominal diameter of 0.15 in. During several days of continuous operation in conducting this experiment, stability checks were made. No significant change in calibration, point of reference, or controlled diametral range was observed.

Controlled Constant Strain Range Experiments

The electrical signal from the strain transducer is amplified and recorded by associated equipment. The equipment consists of a carrier frequency amplifier and strip chart recorder. These components are located in the diametral strain range control console shown in Fig. 5. Only minor modifications to these components are required to facilitate coupling them electrically to other equipment to be described.

Calibration of the overall measuring system is then made with a Boeckeler Instrument Co. micrometer head which can be read to 10 μin. The extensometer is attached to the calibration stand such that the movable end is displaced a known amount by the micrometer and the full scale of the recorder so determined. The extensometer is then mounted on the specimen such that it is carefully balanced at the minimum diameter position. This position is determined on the recorder by applying a small vertical oscillation to the extensometer. The recorder pen is then centered on the chart.

When it is desired to conduct experiments in which the controlled function is a constant diametral strain range, finite changes in diameter may be specified by the following relationships:

$$\Delta d_c = d_0[\exp(\tfrac{1}{2}\Delta\epsilon_d) - 1] \quad (1)$$

$$\Delta d_t = d_0[1 - \exp(-\tfrac{1}{2}\Delta\epsilon_d)] \quad (2)$$

where:

$\Delta\epsilon_d$ = diametral strain range,
d_0 = original specimen diameter,
Δd_c = limiting specimen diameter change in compression, and
Δd_t = limiting specimen diameter change in tension.

FIG. 5—*Diametral strain range control console.*

Two limit switches are installed in this strip chart recorder (hereafter called "the diametral range recorder"). These limit switches are then independently adjusted to settings equivalent to the values determined by Eqs 1 and 2. When the test is in progress, these switches are alternately actuated when the continuous specimen diameter indication equals their settings. It is of importance to note that this control system regulates machine loading direction from specified strain limits only. While the true strain rate of the specimen is not controlled (crosshead rate is), a fair approximation of its value may be determined from the data. Crosshead rate is controlled independently by a selsyn control system incorporated in the Instron machine.

Heating System and Control

The specimen is heated by induction using a small water-cooled work coil as shown in Fig. 6. Maximum temperature and its uniformity depend on coil design and good coupling with the specimen. Although the thermocouple wires were contained within the coil, experiments showed that the radio frequency field (500 kHz) did not influence the tempera-

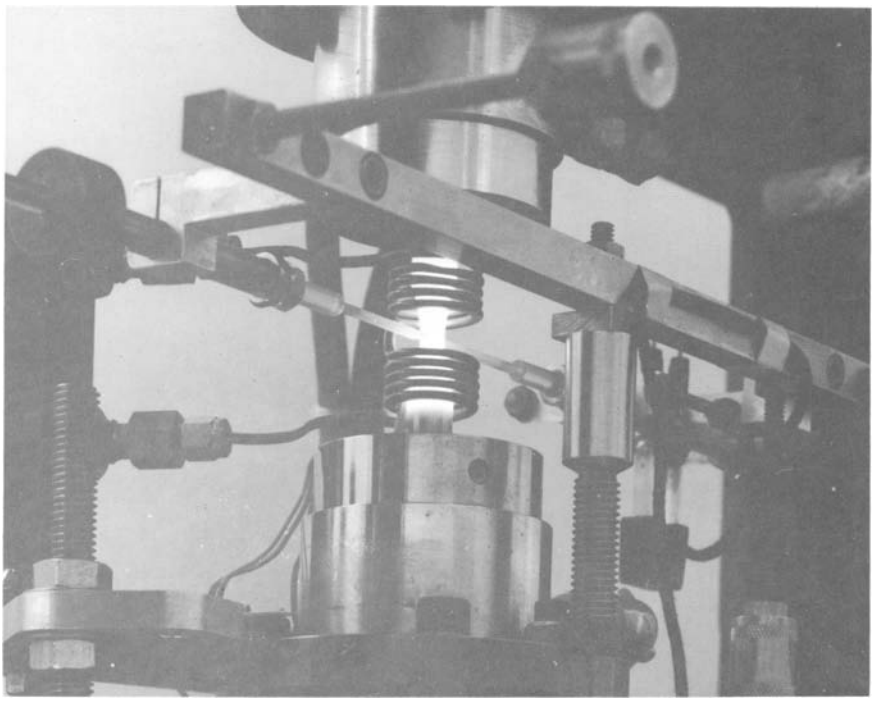

FIG. 6—*View of test assembly with high temperature test in progress.*

ture measurements. Similarly, measurement of the vertical temperature distribution revealed satisfactory uniformity of temperature in the test region.

A 4-kW power supply was employed, installed with a variable coupling feature for better coupling of a wide variety of test materials to the heating system. Specimen temperature is maintained by a system consisting of a three-action temperature controller, one thermocouple, and the power supply. The other thermocouple is fed into a potentiometer to establish the actual test temperature desired.

In bringing the temperature of the specimen up to the test conditions, care must be exercised to prevent excessive compression of the specimen as a result of differential thermal expansion. During this period the load on the specimen is closely watched and the crosshead adjusted accordingly to keep the specimen load near zero while equilibrium conditions are being established. Details of this procedure may vary depending on the discretion of the investigator.

Experience is required in achieving the best control of temperature. It is highly desirable that temperature oscillations be minimized and that the coupling between the specimen temperature and the system response be very close. Observe that the temperature tends to vary with change in load. This arises primarily because of variation in heat transfer in the specimen and grip connection between tension and compression. The effect is minimized by firm clamping and rapid response in the control system to temperature change.

Testing Machine

The testing machine used in these investigations was an Instron Model TTD-L having a load capacity of ±20,000 lb. Crosshead rates could be varied in steps from 0.0002 to 2 in./min. Range in the strip chart speeds of all recorders was from 0.02 to 5 in./min and instruments were provided with event markers for close matching of load and diameter change and for cycle determination in long tests.

Experimental Measurements and Automatic Operations

The useful data produced by this cyclic strain experimental equipment include measurements of force, diameter, cyclic rate, time, temperature, and number of cycles. The values of some of these quantities for a typical cyclic strain experiment (of constant strain range) appear in various recorded combinations in the equipment, such as force time in Fig. 7*a*, diametral range time in Fig. 7*b*, and temperature time. The cross-plotting of force and diameter change on a Cartesian coordinate graph displays in Fig. 7*c* the particular hysteresis loops selected for the

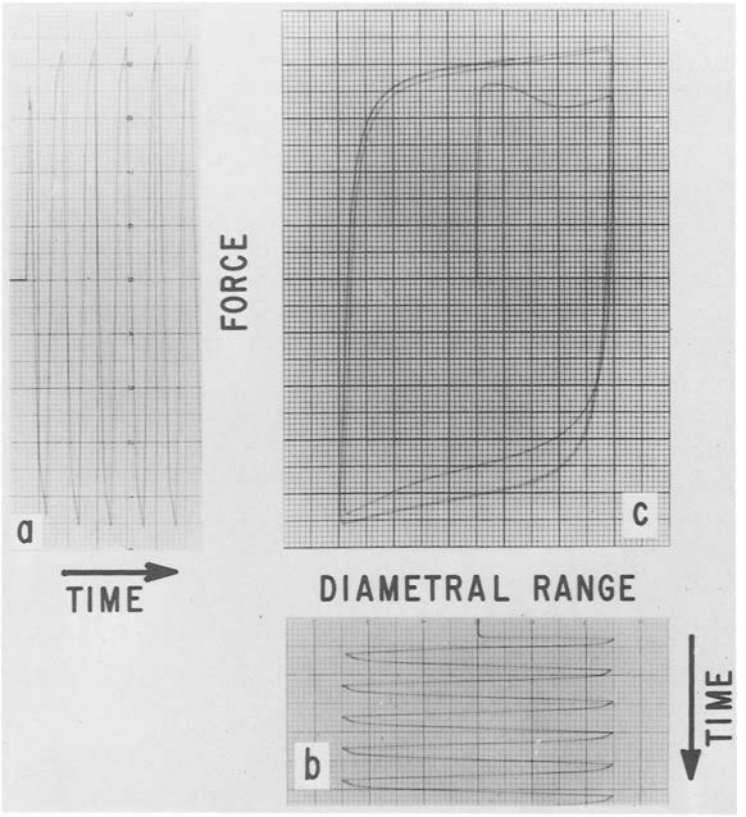

(*a*) Force time.
(*b*) Diametral range time.
(*c*) Diametral change force.

FIG. 7—*Typical cyclic strain data*

experiment in progress. This is accomplished with a Model 7000 A Moseley *X-Y* recorder also shown in Fig. 5. This particular model was selected because it offers the advantage in this application of minimum electrical circuit losses through its high signal input impedance.

In order to obtain representative hysteresis loops throughout a given test without continuous writing of the *X-Y* recorder, an event programmer was built which actuates the stylus for the duration of one cycle. Setting the programmer to a specific position determines the cyclic interval between recorded hysteresis loops. The programmer is shown in Fig. 5 to the left of the main chassis.

There are several automatic shutdown provisions available in the equipment. At some point in the course of any type of experiment when

the formation of a crack has reduced the cross-sectional area of the specimen, the force associated with the tensile half of a cycle will be somewhat less than that for the uncracked specimen. This low tensile force then initiates an automatic shutdown by causing the moving crosshead to be stopped. A "force level" switch is installed in the force-time recorder for this purpose. This force level switch is connected into the moving crosshead reversing electrical control circuit. The reversing sequence is therefore interrupted at the Δd_t limit when the tensile force of the specimen is less than the selective value of the force level switch. When the moving crosshead of the machine has been stopped for a selected period of time, a timer will then turn off the electrical power which supplies the equipment, if desired. This set of shutdown provisions protects the specimen from the total separation and preserves it for further study.

Facility Component Arrangement

The overall view of the cyclic strain test facility is shown in Fig. 8. The diametral strain control console located to the left in the view contains, in a top-to-bottom order, the temperature-time recorder, temperature reference supply, calibration controls associated with the total diam-

FIG. 8—*Cyclic strain test facility.*

eter change-time recorder [7], the diametral range recorder, the Instron a-c bridge amplifier associated with the diametral range recorder, the cyclic strain programmer described elsewhere [7], and the shutdown circuit controls. The force-diametral change recorder is on the left side of the console. The testing machine straining frame with the test fixtures installed is located in the center of the figure. The Instron machine control console is located farther to the right. The force-time recorder is a part of this console. The specimen heater-controlling equipment is not included in this photograph.

Operation

Having stabilized the temperature such that there is no load or diameter change response and with load and diameter change recorders centered and at appropriate scale span, the test can be started. Depending on the crosshead rate, some overshooting of diameter change can occur at the limit points and this must be carefully watched in the early stages of the test. The limit positions are adjusted to insure that the diameter limits remain constant during the test. Overshooting is a dynamic problem arising both in the machine and the sample as the straining direction is reversed. When tests are conducted in the creep range, overshooting in diameter can also occur during holding or unloading because of creep of the specimen under the applied load.

Fatigue Failure

Since fatigue crack initiation and propagation to failure are major considerations in these tests, observations of these effects can be made in many ways. In terms of the load versus time and load versus diameter records, there are changes in pattern which are useful indicators of the presence of a fatigue crack. With reference to Fig. 9, the effect is seen in the load-diameter change record as a small cusp at the compression load reversal point. This cusp grows in magnitude with continued cycling. At the same time a small spike appears on the load-time curve which also grows in intensity as cycling proceeds. These indications reflect the presence of a crack which is open except for the interval of the spike when it closes to increase the net cross-sectional area of the specimen.

With further cycling the crack grows in size and the tensile load reduces in magnitude, slowly at first and then near the end of the test very rapidly. It is in this region that the shutdown provision operates. By adjustment of the force level switch position relative to the maximum tensile load carried by the specimen, the crack length can be made to be small or large as desired.

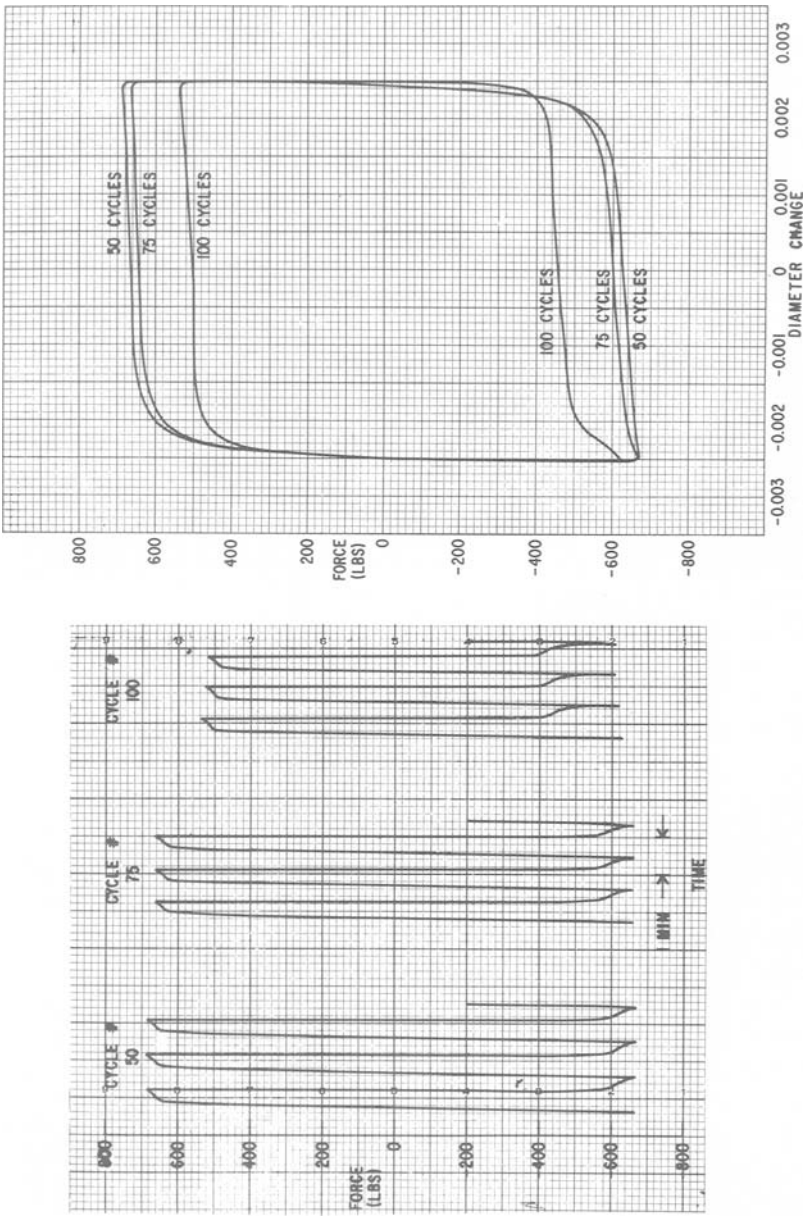

FIG. 9—*Progressive changes in force-diameter change and force-time records.*

Data Reduction

Depending on the specific requirements of the test, reduction of data can take a variety of forms. By way of illustration an example will be used here which describes how the authors treat an elevated temperature, low cycle fatigue test. The general procedure is to develop a program for a time-sharing computer system such that test information can be fed into the program and the tabulated results returned as output. Figure 10 gives the time-sharing program using "basic" language; definitions of the symbols used are found in the appendix. Figure 11 gives the tabulated output. Tabulated results are obtained from the indicated calculations and include the true tensile stress (line 00260), the true compressive stress (line 00280), the stress range (line 00300), the mean stress (line 00320), the longitudinal plastic strain range (line 00340), and the total strain range (line 00360). For a specific test, the diameter limits as obtained from the diameter change chart, the initial diameter, the elastic modulus, Poisson's ratio, the cycle number, the tensile load, and the compressive load are inputs from which the stresses and strains can be calculated. The load quantities are obtained by measurement from the test records at the same cycle number for each test.

Additional input information includes the test number, test temperature, material, and crosshead rate. The program calculates the frequency and period of the cycle when the maximum tensile load occurs. As a separate determination, the cycle when the tensile load has decreased to 75 percent of the peak value is obtained from a plot of tensile load versus cycle number. This is the failure definition employed for this investigation, although other failure definitions can be introduced. The cycle for failure so determined is tabulated in Fig. 11.

Acknowledgment

The authors are indebted to the many people in the Research and Development Center of the General Electric Co. who, over a period of several years, have been most helpful in establishing these testing procedures. Included are R. F. Berning and his staff in the Mechanical Testing Laboratory, and W. A. Reed, foreman, Mechanical Equipment Shop. The assistance of G. Jernakoff and W. N. Coffey of Design Engineering and Instrumentation is also acknowledged. Finally, the authors are appreciative of the support and encouragement of D. W. Lillie, manager, Physical Metallurgy Branch.

```
$LIST
08/11/69    11:46

00010 READ T,H,D1,D2,X,D0,M,M1,F,F1,N,N1,T1
00020 LET K1=(L0G(1+(D2/D0))-L0G(1-(D1/D0)))/2
00030 LET K1=INT((K1+5E-7)*1E6)/1E6
00040 PRINT
00050 PRINT "TEST N0"T
00060 PRINT
00070 PRINT " NICKEL A AT"H"CENT"
00080 PRINT " K1"K1
00090 PRINT " X'HD RATE"X"IN/MIN"
00100 PRINT " 0RIG DIA"D0"IN"
00110 PRINT " ELASTIC M0DULUS"M
00120 PRINT " P0ISS0N RATI0"M1
00130 PRINT
00140 PRINT
00150 PRINT TAB(7);"PLASTIC";TAB(17);"T0TAL"
00160 PRINT " CYC";TAB(7);"STRAIN";TAB(17);"STRAIN";TAB(27);"TEN";
00170 PRINT TAB(35);"C0MP";TAB(43);"STRESS";TAB(51);"MEAN"
00180 PRINT " N0";TAB(7);"RANGE";TAB(17);"RANGE";TAB(27);"STRESS";
00190 PRINT TAB(35);"STRESS";TAB(43);"RANGE";TAB(51);"STRESS"
00200 PRINT
00210 F0R I=1 T0 F
00220 DIM N(50),T(50),C(50)
00230 READ N(I),T(I),C(I)
00240 NEXT I
00250 F0R I=1 T0 F
00260 LET S1=T(I)/(((D0*EXP(-K1))↑2)*.7854)
00270 LET 01=INT(.1*(S1+5))*10
00280 LET S2=C(I)/(((D0*EXP(K1))↑2)*.7854)
00290 LET 02=INT(.1*(S2+5))*10
00300 LET S3=S1+S2
00310 LET 03=INT(.1*(S3+5))*10
00320 LET S=(S1-S2)/2
00330 LET 0=INT(.1*(S+5))*10
00340 LET E3=4*(K1-M1*S3/(2*M))
00350 LET 04=INT((E3+5E-6)*1E5)/1E5
00360 LET E=E3+S3/M
00370 LET 05=INT((E+5E-6)*1E5)/1E5
00380 PRINT N(I); TAB(6);04; TAB(16);05; TAB(26);01;
00390 PRINT TAB(34);02; TAB(42);03; TAB(51);0
00400 NEXT I
00410 PRINT
00420 PRINT
00430 LET I=F1
00440 LET S3=((T(I)/((D0*EXP(-K1))↑2))+(C(I)/((D0*EXP(K1))↑2)))/.7854
00450 LET E3=(2*(2*K1-M1*S3/M))/(.5*T1)
00460 LET 04=INT((E3+5E-7)*1E6)/1E6
00470 PRINT " CYCLE N0 AT MAX TEN"N
00480 PRINT " CYC N0 AT .75 MAX TEN"N1
00490 PRINT " TIME/CYCLE"T1"MIN"
00500 PRINT " CYCLES/MIN"1/T1
00510 PRINT " PLASTIC STRAIN RATE"04"IN/IN/MIN"
00520 PRINT " CALC T0TAL TIME"N(I)*T1"MIN"
99999 END

READY
```

FIG. 10—*Data reduction computer program.*

```
$LIST *(90000,90040)
08/11/69    11:42

90000 DATA 965,750,.00258,.00255,.05,.2481,155E5,.3,22,17,52,101.5,.936
90010 DATA 0,480,575,1,610,615,2,630,630,3,640,630,4,640,635,5,645,640
90020 DATA 6,650,640,7,650,640,9,655,645,11,660,650,14,665,650,18,670,68
90030 DATA 23,675,660,29,680,670,36,685,670,46,690,670,52,690,670
90040 DATA 60,685,665,75,670,660,90,615,660,110,440,575,125,310,230

READY

$BASIC
08/11/69    11:42



TEST NØ 965

 NICKEL A AT 750 CENT
 K1 0.01034
 X'HD RATE 0.05 IN/MIN
 ØRIG DIA 0.2481 IN
 ELASTIC MØDULUS 15500000
 PØISSØN RATIØ 0.3


      PLASTIC    TØTAL
CYC   STRAIN     STRAIN     TEN      COMP     STRESS   MEAN
NØ    RANGE      RANGE      STRESS   STRESS   RANGE    STRESS

0     0.04052    0.04192    10140    11650    21790    -760
1     0.04038    0.04201    12880    12460    25340     210
2     0.04035    0.04203    13300    12760    26070     270
3     0.04034    0.04204    13520    12760    26280     380
4     0.04034    0.04204    13520    12870    26380     320
5     0.04033    0.04205    13620    12970    26590     330
6     0.04033    0.04205    13730    12970    26690     380
7     0.04033    0.04205    13730    12970    26690     380
9     0.04032    0.04205    13830    13070    26900     380
11    0.04031    0.04206    13940    13170    27110     380
14    0.04031    0.04206    14040    13170    27210     440
18    0.04029    0.04207    14150    13370    27520     390
23    0.04029    0.04207    14250    13370    27630     440
29    0.04028    0.04208    14360    13580    27940     390
36    0.04027    0.04208    14470    13580    28040     450
46    0.04027    0.04209    14570    13580    28150     500
52    0.04027    0.04209    14570    13580    28150     500
60    0.04028    0.04208    14470    13470    27940     500
75    0.04029    0.04207    14150    13370    27520     390
90    0.04034    0.04204    12990    13370    26360    -190
110   0.04055    0.0419     9290     11650    20940   -1180
125   0.04093    0.04165    6550     4660     11210     940


 CYCLE NØ AT MAX TEN 52
 CYC NØ AT .75 MAX TEN 101.5
 TIME/CYCLE 0.936 MIN
 CYCLES/MIN 1.06838
 PLASTIC STRAIN RATE 0.086048 IN/IN/MIN
 CALC TØTAL TIME 48.672 MIN
```

FIG. 11—*Typical tabulation of test results.*

APPENDIX

Definitions of Symbols Used in Fig. 10

C(I)	Compressive force at Datum Point I, lb
DO	Initial specimen diameter, in.
D1	Limiting specimen diameter change in tension, in.
D2	Limiting specimen diameter change in compression, in.
E	Total longitudinal true strain range, in./in.
E3	Plastic longitudinal true strain range, in./in.
F	Total number of data points taken at various cycles
F1	Datum point number of cycle containing maximum tensile force
H	Test temperature, deg C
I	Index or datum point number
K1	One half of the diametral strain range, in./in.
M	Elastic modulus, psi
M1	Poisson's ratio
N	Number of cycle containing maximum tensile force
N1	Number of cycle containing 75 percent of maximum tensile force
N(I)	Cycle number at Datum Point I
O	Rounded-off value of S, psi
O1	Rounded-off value of S1, psi
O2	Rounded-off value of S2, psi
O3	Rounded-off value of S3, psi
O4	Rounded-off value of E3, in./in.
O5	Rounded-off value of E, in./in.
S	True mean stress, psi
S1	True tensile stress, psi
S2	True compressive stress, psi
S3	True stress range, psi
T	Test number
T1	Time per cycle at maximum tensile force, min
T(I)	Tensile force at Datum Point I, lb
X	Crosshead rate, in./min

References

[1] Coffin, L. F. Jr., "The Stability of Metals under Cyclic Plastic Strain," *Journal of Basic Engineering, Transactions, Series D,* American Society of Mechanical Engineers, JBAEA, Vol. 82D, 1960, pp. 671–682.

[2] Tavernelli, J. F. and Coffin, L. F. Jr., "Cyclic Straining and Fatigue of Metals," *Transactions,* American Institute of Mining and Metallurgical Engineers, TAMMA, Vol. 215, 1959, pp. 794–807.

[3] Tavernelli, J. F. and Coffin, L. F. Jr., "The Cyclic Strain Aging and Fatigue of a Low Carbon Steel," *Proceedings, Joint International Conference on Creep,* Institution of Mechanical Engineers, London, Vol. 1, 1963, pp. 3-63 to 3-70.

[4] Coffin, L. F. Jr., "The Effects of Quench Aging and Cyclic-Strain Aging on a Low Carbon Steel," *Journal of Basic Engineering, Transactions, Series D,* American Society of Mechanical Engineers, JBAEA, Vol. 87D, 1965, pp. 351–362.

[5] Coffin, L. F. Jr., "Cyclic Strain and Fatigue Study of a 0.1% C-2.0% Mo Steel," *Transactions,* Amercian Institute of Mining and Metallurgical Engineers, Vol. 230, 1964, pp. 1690–1699.

[6] Coffin, L. F. Jr., "An Investigation of the Cyclic Strain and Fatigue Behavior of a Low-Carbon Manganese Steel at Elevated Temperature," *International Conference on Thermal and High Strain Fatigue,* The Metals and Metallurgy Trust, London, 1967, pp. 171–197.

[7] Lord, D. C., "New Uniaxial Cyclic Strain Test Equipment," *Report 67-C-195,* General Electric Co., Research and Development Center, Schenectady, N. Y., May 1967.

M. R. Gross[1]

Engineering Materials Evaluation by Reversed Bending*

REFERENCE: Gross, M. R., "**Engineering Materials Evaluation by Reversed Bending,**" *Manual on Low Cycle Fatigue Testing, ASTM STP 465*, American Society for Testing and Materials, 1969, pp. 149–162.

ABSTRACT: A method for conducting low cycle fatigue tests by reversed bending is described. The advantages of bend (flexure) testing lie in its simplicity, specimen stability at high strain levels, and minimal equipment costs. Description of the method includes (1) types of specimens, (2) equipment construction and operation, (3) stress and strain measurements, and (4) data output, presentation, and analysis.

KEY WORDS: fatigue (materials), fatigue tests, fatigue (low cycle), stress measurement, metals, bending (flexure), tests, evaluation

Nomenclature

P	Load, lb
ΔP_t	Total load range, lb
S	Stress, psi
S_P	Load-based stress, psi
S_ϵ	Strain-based stress, psi
ϵ	Strain, in./in.
$\Delta\epsilon_e$	Elastic strain range, in./in.
$\Delta\epsilon_p$	Plastic strain range, in./in.
$\Delta\epsilon_t$	Total strain range, in./in.
E	Modulus of elasticity, psi
a	Moment arm, in.
c	Distance from neutral axis to outermost fiber, in.
I	Moment of inertia, in.^{4}
N	Number of cycles to failure

[1] Metallurgist, Metals and Composites Dept., U.S. Naval Ship Research and Development Laboratory, Annapolis, Md. 21402.

* The opinions or assertions made in this paper are those of the author and are not to be construed as official or reflecting the views of the Department of the Navy or the naval service at large.

Over 95 percent of our knowledge of the fatigue behavior of materials has developed from laboratory tests of relatively simple test specimens. Some 200 laboratories in the United States are engaged in fatigue studies. The number outside the United States is estimated to be even larger. In spite of all the information developed, the fatigue behavior of metals is not completely understood. The subject is highly complex and to a great extent continues to remain empirical in nature.

A high percentage of the fatigue data developed in laboratory tests is obtained under cyclic bending (flexural) conditions. The advantages of flexure testing lie in its simplicity, specimen stability at high strain levels, and minimal equipment costs. A disadvantage is that the stress and strain are not uniform throughout the cross section and therefore not amenable to rigorous analysis. Of particular concern is the finite life region wherein specimen failure may entail plastic deformation in the test section. Despite these difficulties, information applicable to materials evaluation and structural design can be developed from flexure tests. The procedure used in carrying out low cycle flexure fatigue tests at the Naval Ship Research and Development Laboratory in Annapolis, Md., will be described.

Specimens

The specimen selected was originally developed by Lehigh University [*1*][2] for the study of pressure vessel steels. The dimensions of the smooth specimen are shown in Fig. 1*a*. The short end of the specimen is held stationary, while the long end is cyclically flexed. The maximum stress or strain occurs in the reduced section in close proximity to the minimum cross section. A biaxial stress of 2:1 ratio is produced in this region. The design of the specimen effectively eliminates the formation of corner cracks which frequently occur in rectangular specimens having uniform thickness throughout their length.

Modifications to the specimens may take the form of mechanical notches as shown in Fig. 1*b* or the introduction of weld metal as shown in Fig. 2. The advantage of the longitudinal weld is that it simultaneously subjects weld metal, base metal, and heat-affected zone to cyclic stressing. The theoretical stress concentration factor K_t for the notched specimens can be estimated from tables and graphs derived by Neuber and published on pp. 60 and 61 of *Manual on Fatigue Testing, ASTM STP 91*. The case of a centrally located notch is not covered, but it can be assumed that the results would be similar to the full-width surface notch. The estimated K_t for the notch dimensions shown in Fig. 1*b* is approximately 3.

[2] The italic numbers in brackets refer to the list of references at the end of this paper.

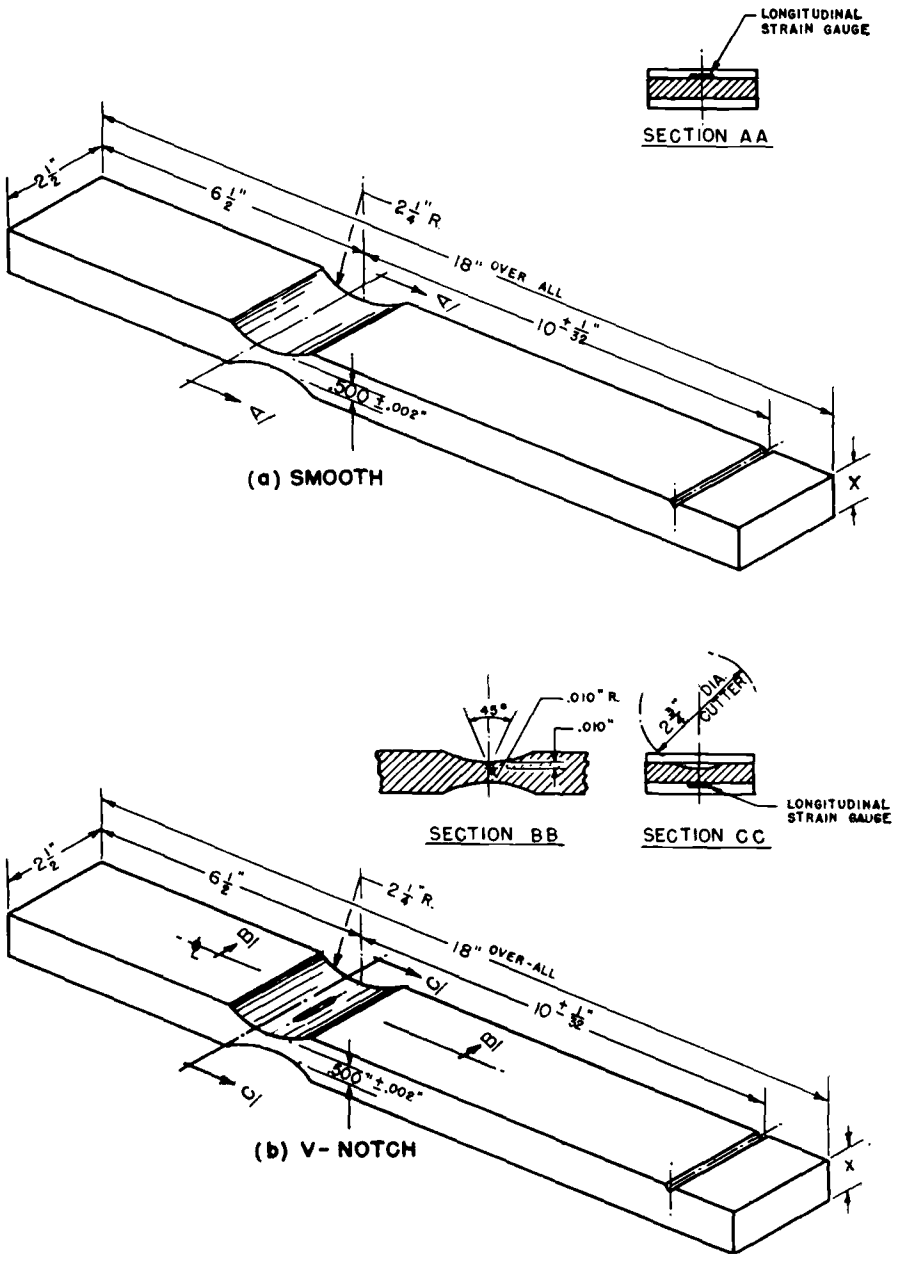

FIG. 1—*Low cycle fatigue specimens.*

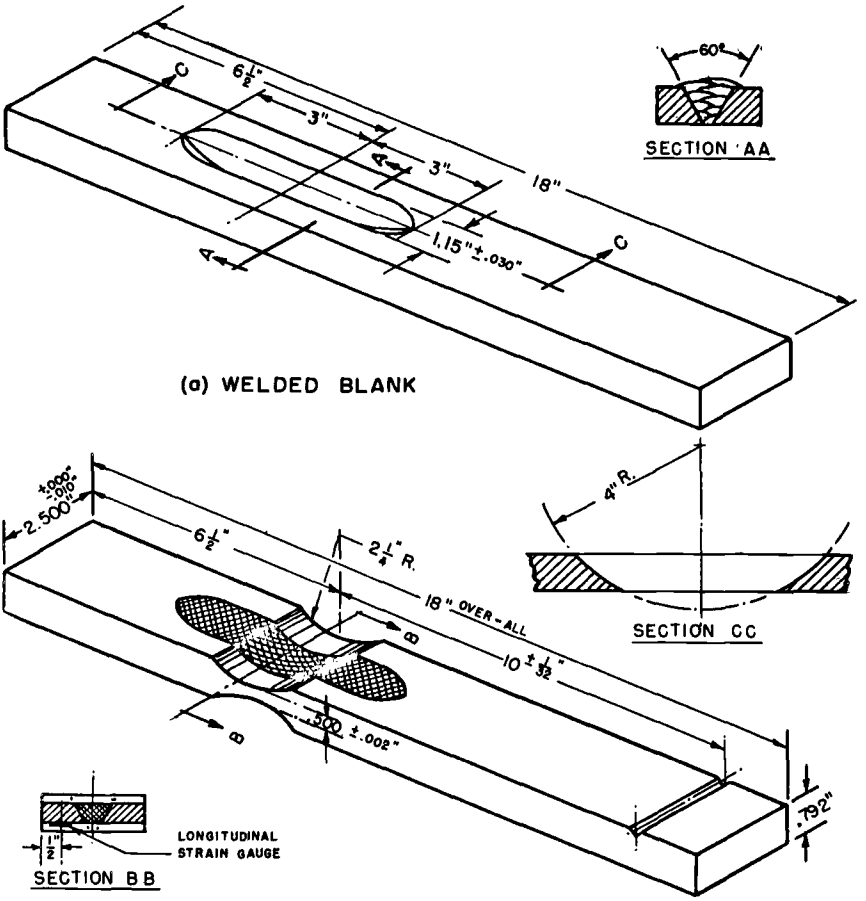

FIG. 2—*Welded low cycle fatigue specimens.*

Test Machines

The flexural fatigue testing machines shown in Fig. 3 were designed and constructed specifically for studying the behavior of materials when subjected to cyclic strains in the low cycle region. Figure 4 is a schematic drawing of one test machine. Figure 5 is a close-up view of the specimen and some of the associated equipment. The short end of the test specimen is rigidly fixed to the base of the machine. A bending moment is applied through a weighbar or load cell to the free end by a double-acting, 2-in.-stroke hydraulic cylinder. The direction of the cylinder is controlled by a four-way solenoid reversing valve. The reversing valve is actuated

either by electrical contacts or by a timer, depending upon whether a saw-tooth or a square-wave type of strain-time response is desired. The control of the test machine will be discussed in greater detail in a later section.

The speed of the test is about 5 cpm max and is regulated by the precision control valve visible in Fig. 5. Each cycle is recorded on an electrical counter. Although each test unit is operated independently, hydraulic pressure for all six machines is supplied by a single 1000-psi, 0.75-gal/min hydraulic power unit. This unit is visible to the right of the machines in Fig. 3.

Measurements

The cyclic strains developed in the test section of the fatigue specimens are measured with resistance-type strain gages. Although various backing materials and cements have been tried, the greatest success has been with paperbacked foil gages similar to Baldwin-Lima-Hamilton Corporation Type FAP-25-12 applied with SR-4 or Duco cement in accordance with the manufacturer's instructions. The SR-4 precoat is not generally used. However, it is required for titanium specimens. Gages should be applied

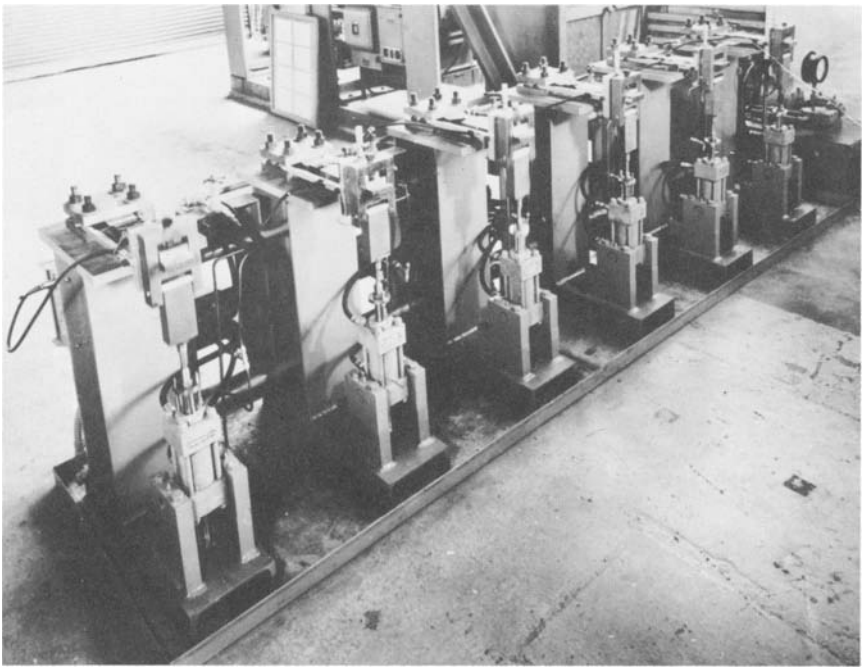

FIG. 3—*Low cycle fatigue test machines.*

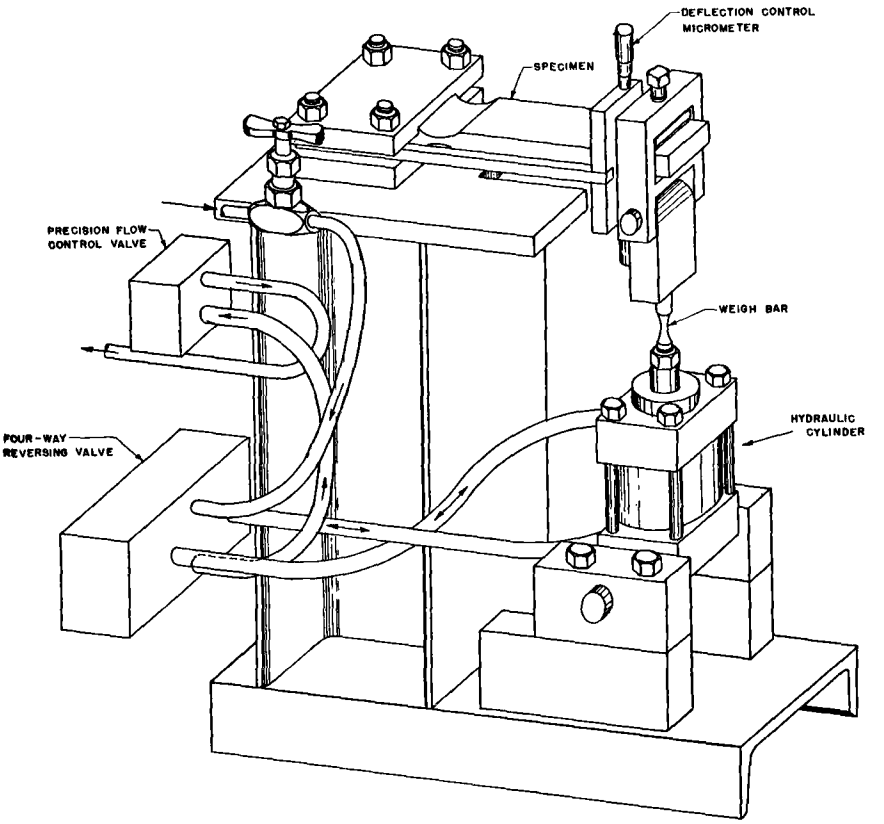

FIG. 4—*Low cycle fatigue test machine.*

to the specimens well in advance of actual testing to permit complete drying. In this connection the quick-setting Eastman 910 cement is *not* satisfactory for low cycle fatigue work.

The FAP-25-12 is a 120-Ω gage having ¼-in.-gage length. The gages are applied longitudinally with the transverse center line of the gage located at the minimum cross section. Observations on smooth specimens have shown that fatigue cracks do not occur at a precise location but tend to fall in about a ¼-in.-wide band extending across the specimen. Elastic stress calculations show a variation of approximately 4 percent in the maximum longitudinal stress in this region.

The strain gage is sometimes offset from the longitudinal center line of the specimen to the extent shown in Section *B-B* in Fig. 2. Experiments have shown no significant difference in longitudinal strain as a result of offsetting.

The magnitude of the applied bending load is determined by resistance-type strain gages attached to a weighbar. The dimensions and strength of the weighbar selected should be such that only elastic strains occur within the load range of the machine. Commercial load cells such as Series 22 of Transducers, Inc., have also been found to be satisfactory for the purpose.

The strain measuring gage on the specimen and load measuring gages on the weighbar are connected into separate Wheatstone bridge circuits having a fixed shunting resistance for calibration. The load versus strain hysteresis loop is plotted directly on a Moseley (Hewlett-Packard Corp.) Model 2D-2 two-axis recorder.

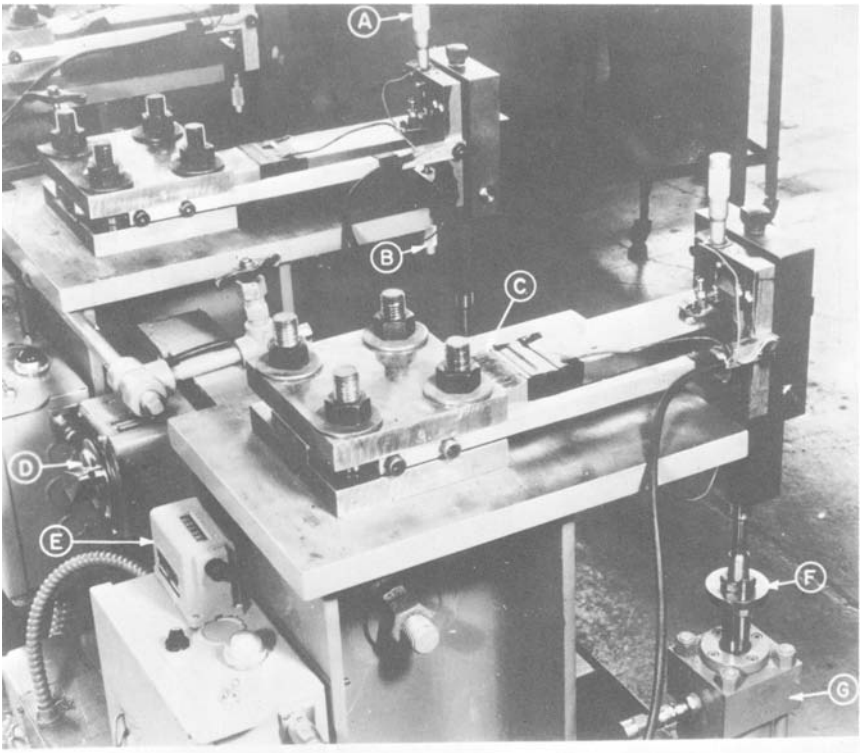

FIG. 5—*Close-up view of specimen and controls.*

Operation

Control is maintained over the deflection of the movable end of the specimen. As mentioned previously, this can be accomplished either by electrical switching or mechanical stops. Figure 5 shows the electrical contact type of control system consisting of two insulated micrometer heads mounted in a supporting yoke. The yoke is supported by an arm which is attached directly to the fixed end of the specimen. The setting of the upper and lower micrometer heads establishes the control and maximum deflection of the specimen. The electrical shock hazard is eliminated by using an auxiliary 6-V a-c relay circuit to actuate the 110-V a-c reversing valve. Mechanical stops are used to back up the electrical control in the event of circuit failure. When a square-wave type of response is desired, these same mechanical stops are used to control the deflection of the specimen. Reversal of the load is then accomplished by an electrical timer inserted in the electrical control circuit.

One problem in testing flexure specimens at low cycling rates concerns the definition of what constitutes failure. The problem arises from the fact that stress and strain are not uniform throughout the cross section. Accordingly, as the crack depth approaches the neutral axis, the crack propagation rate decreases and the specimens tend to "hang on" indefinitely. Therefore, complete fracture is not a satisfactory end point at low cycling rates. In the case of smooth specimens, an arbitrary failure criterion has been defined as the development of one or more surface cracks 3/16 to 1/4 in. in length. In notched specimens, failure is defined as one or more surface cracks 1/8 to 3/16 in. in length, extending from the ends of the notch.

Using the above criteria it is possible to introduce an automatic shutdown capability into the electric control circuit. This is done by cementing a No. 36 polyvinyl formal insulated copper wire grid to the surface of a smooth specimen as shown in Fig. 6. The grid consists of a series of hairpin loops spaced about ¼ in. apart and extending across the test section. Ordinary Duco cement is used to hold the grid in place against the specimen surface. The grid is in series with the 6-V a-c control circuit and thus the breaking of the grid as a result of a crack will stop cyclic operation and the hydraulic cylinder will come to rest against one of the mechanical stops. Only a single loop placed about ⅛ in. from each end of the notch is necessary for shutting down the notch specimen.

It is often desirable to conduct rests in environments other than air. In the case of saltwater environment, the salt water is dripped on the top and sides of the test section at a rate of 2 or 3 drops per minute as shown in Fig. 7. The bottom side of the test section and the remainder

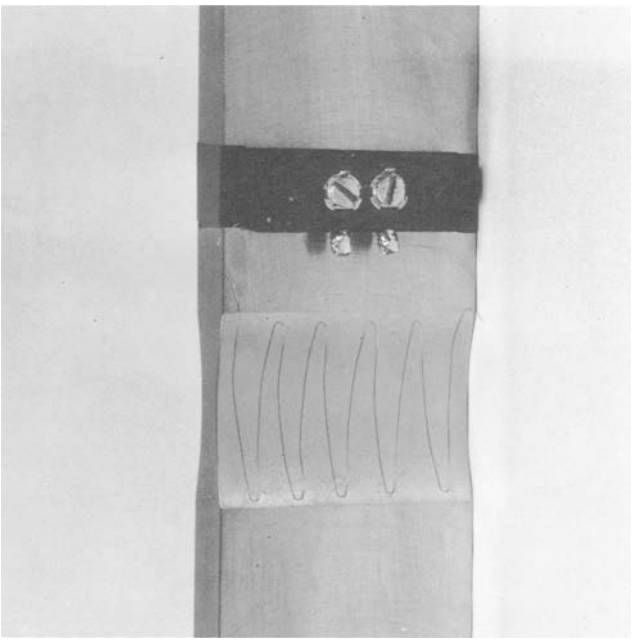

FIG. 6—*Shutdown control grid cemented to specimen.*

of the specimen are protected against the environment with 3M Brand EC-612 putty. The automatic shutdown control described in the previous paragraph cannot be used under these conditions. Instead, the end point of the test is determined by periodic visual examination of the test surface.

Data Output

Although the outputs of the load and strain bridges can be indicated and recorded in a variety of ways, relationships during the course of a cycle are best depicted by an X-Y recording. When plasticity is present, the output after the first cycle will take the form of a mechanical hysteresis loop as shown in Fig. 8. The parameters of major interest are the total load range, ΔP_t, and the total strain range, $\Delta \epsilon_t$. One might think that the plastic strain range, $\Delta \epsilon_p$, could be obtained by measuring the width of the loop in Fig. 8. This is not the case for flexure specimens inasmuch as the surface strain is not necessarily zero when the applied load is zero. This results from the development of a nonlinear strain gradient through the specimen. This permits a residual strain to exist at the surface when the applied load is zero.

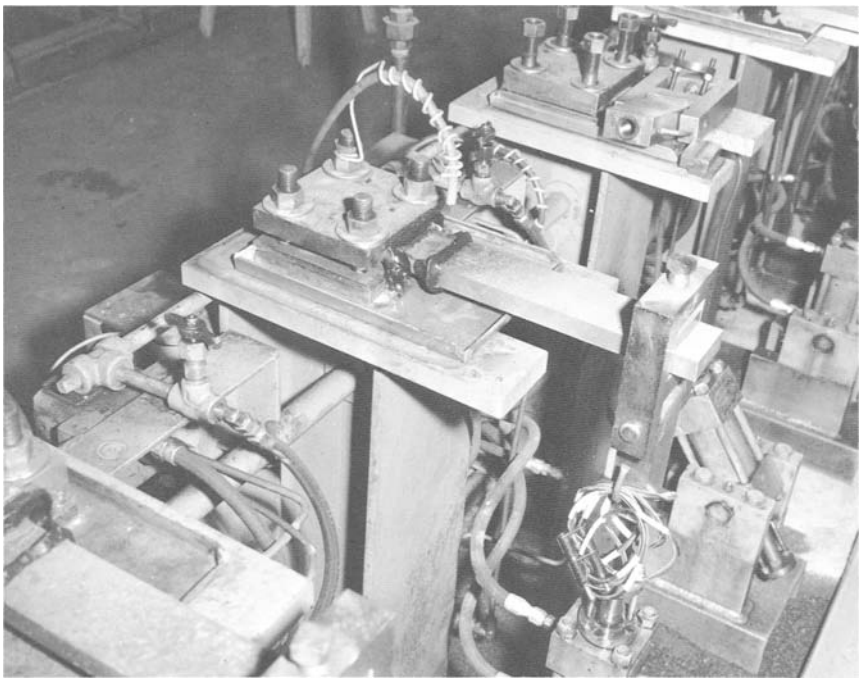

FIG. 7—*Corrosion-fatigue specimen.*

The parameters in Fig. 8 undergo changes during the early stages of strain cycling. The magnitude and direction of these changes depend upon the degree to which the material "cyclic strain hardens" or "cyclic strain softens." It has been observed that for cyclic strain ranges above 0.001 in./in., the shape and size of the loop tend to stabilize within 10 cycles. For cyclic strain ranges below 0.001 in./in., however, complete stabilization may not occur for 100 or more cycles. It is highly desirable to have early stabilization inasmuch as the fatigue life of the strain sensing gage may be quite short. To provide consistency, all of the parameters are measured on the tenth cycle loop. In the case of saltwater tests, the hysteresis loops are developed while the specimen is exposed to air. The strain sensing gage is removed from the test surface before saltwater exposure begins.

The stress amplitude for flexure specimens can be calculated from either the load or the strain. We shall call the former "load-based stress amplitude, S_P" and the latter "strain-based stress amplitude S_ϵ." In simple beam calculations using elastic formulas, $S_P = ac\,\Delta P_t/2I$, where ΔP_t is

the total applied range, a is the distance from the point of load application to stress point, c is the distance from the neutral axis to the outermost fiber, and I is the moment of inertia of the section. When plastic yielding occurs, however, S_P becomes invalid because the outermost fibers no longer resist a proportional share of the applied moment. As a consequence, large increases in surface strain can occur with little increase in nominal stress level. To overcome this difficulty, low cycle fatigue data are frequently presented in terms of strain-based stress, using the relationship $S_\epsilon = \Delta\epsilon_t E/2$, where $\Delta\epsilon_t$ is the measured total strain range and E is the modulus of elasticity. The advantage of this approach is that it permits the data to be presented as a "stress," a term with which designers are familiar, even though the parameter actually being considered is strain. It is obvious that in the presence of large strains, the values of S_ϵ become fictitiously high.

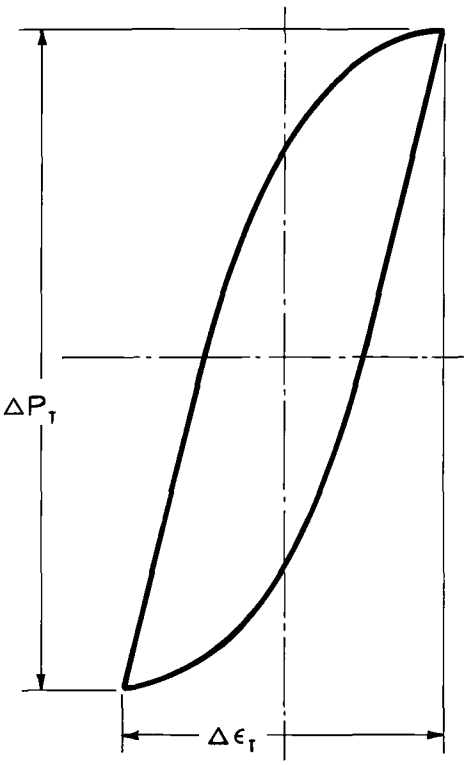

FIG. 8—*Typical mechanical hysteresis loop and parameters.*

Presentation and Analysis of Data

It is generally agreed that low cycle fatigue life is strain-range dependent. Discussions do arise as to whether the plastic strain range $\Delta\epsilon_P$ or the total strain range $\Delta\epsilon_t$ is controlling. However, if one considers the relationship $\Delta\epsilon_t = \Delta\epsilon_e + \Delta\epsilon_p$, it is apparent that $\Delta\epsilon_t \approx \Delta\epsilon_p$ in the very low cycle region where $\Delta\epsilon_p \gg \Delta\epsilon_e$, and that $\Delta\epsilon_t \approx \Delta\epsilon_e$ in the high cycle region where $\Delta\epsilon_p \approx 0$. It is apparent that $\Delta\epsilon_t$ is the sole parameter which has continuity over a broad spectrum of fatigue life. This is fortunate from a practical standpoint inasmuch as $\Delta\epsilon_t$ can be directly measured by strain sensing devices.

Figure 9 shows a typical log-log relationship between S_ϵ and N obtained from flexure specimens. The relationship is nearly linear over the life range considered. Many investigators show a continuous curvilinear relationship. For some materials, however, there is a question whether S_ϵ is in fact a continuous function of fatigue life. It is apparent that if more than one basic mechanism can cause fatigue failure, then discontinuities in the curve can exist. Wood et al [2] have identified several mechanisms which produce discontinuities in the fatigue life curve. The question of discontinuities is probably academic from an engineering standpoint, but occasions do arise in the presentation of low cycle fatigue data where a series of straight lines appear to provide a better fit to the data.

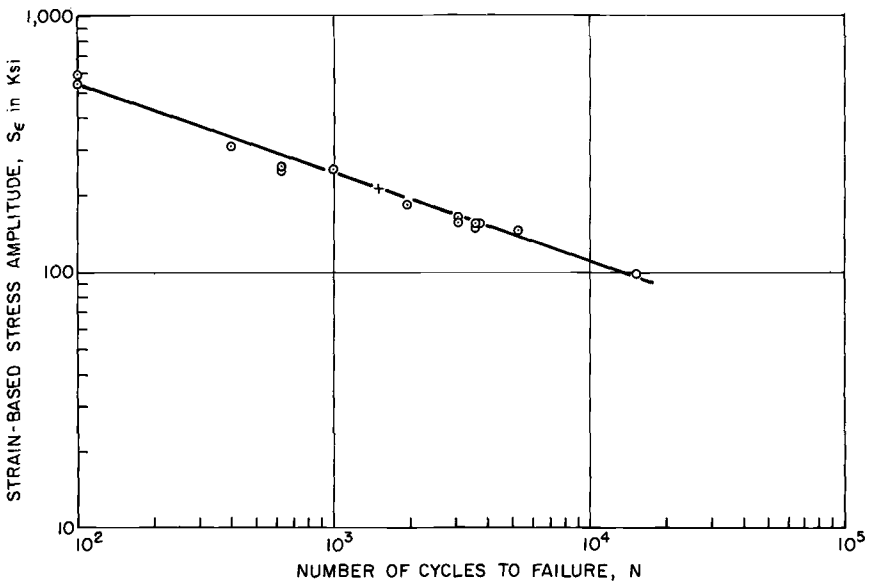

FIG. 9—*Flexural fatigue results for a 100-ksi yield strength steel.*

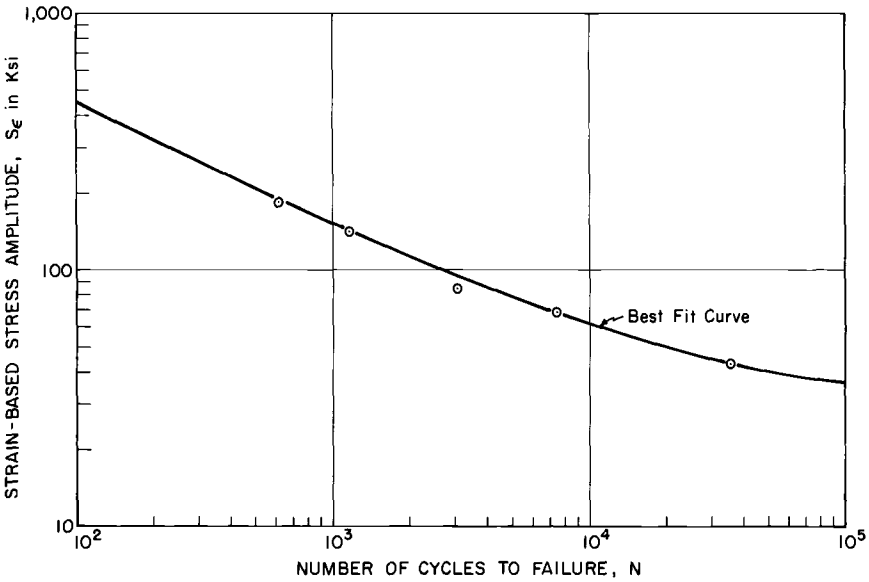

FIG. 10—*Comparison of flexural fatigue results with best-fit curve developed by Gibbons for 70-30 cupronickel. Taken from Ref* 3.

The question naturally arises whether flexural fatigue tests and direct stress fatigue tests provide a similar evaluation of materials. Insofar as known, the answer is yes. On several occasions where the same materials have been evaluated by both types of tests, the results have shown excellent agreement, not only with respect to order of merit, but also with respect to the amount of strain for a given life. For example, Fig. 10 shows the best-fit curve determined by Gibbons [*3*] for 70-30 cupronickel based on 33 direct stress fatigue tests. The points on the graph represent data obtained on the same material using the flexure test method described herein. It is apparent that the data obtained by the two methods are, for all practical purposes, identical.

References *4* through *8* contain a substantial quantity of low cycle flexural fatigue data for various metallic materials.

References

[*1*] Gross, J. H., Gucer, D. E. and Stout, R. D., "Plastic Fatigue Strength of Pressure Vessel Steels," *Welding Journal,* WEJUA, Vol. 33, No. 1, Jan. 1954, pp. 31-s–39-s.

[*2*] Wood, W. A., Cousland, S. McK. and Sargant, K. R., "Systematic Microstructural Changes Peculiar to Fatigue Deformation," *Acta Metallurgica,* AMETA, Vol. 11, July 1963, pp. 643–652.

[3] Gibbons, W. G., "Strain-Cycle Fatigue of 70-30 Copper Nickel," *Transactions of the American Society of Mechanical Engineers, Series D,* TASMA Vol. 88, No. 2, June 1966, pp. 552–554.

[4] Gross, M. R., "Low-Cycle Fatigue of Materials for Submarine Construction," *Naval Engineers Journal,* NVEJA, Vol. 75, No. 5, Oct. 1963, pp. 783–797.

[5] Gross, M. R. and Schwab, R. C., "Fatigue Properties of Nonferrous Alloys for Heat Exchangers, Pumps, and Piping," *Transactions of the American Society of Mechanical Engineers, Series A,* TASMA, Vol. 89, No. 3, July 1967, pp. 345–352.

[6] Gross, M. R. and Czyryca, E. J., "Effect of Notches and Saltwater Corrosion on the Flexural Fatigue Properties of Steel for Hydrospace Vehicles," *Naval Engineers Journal,* NVEJA, Vol. 79, No. 6, Dec. 1967, pp. 1003–1013.

[7] DePaul, R. A., Pense, A. W. and Stout, R. D., "The Elevated Temperature Fatigue Properties of Pressure Vessel Steels," *Welding Journal,* WEJUA, Vol. 44, No. 9, Sept. 1965, pp. 409-s–416-s.

[8] Hickerson, J. P., Pense, A. W., and Stout, R. D., "The Influence of Notches on the Fatigue Resistance of Pressure Vessel Steels," *Welding Journal* WEJUA, Vol. 47, No. 2, Feb. 1968, pp. 63-s–71-s.

A. E. Carden[1]

Thermal Fatigue Evaluation

REFERENCE: Carden, A. E., **"Thermal Fatigue Evaluation."** *Manual on Low Cycle Fatigue Testing, ASTM STP 465*, American Society for Testing and Materials, 1970, p. 163–188.

ABSTRACT: A test method for performing uniaxial low cycle thermal fatigue tests on ductile metals is described. The test method is built around the Instron[2] testing machine. Both temperature and crosshead extension are programmed and the test cycle can be designed for either tensile or compressive loading at the maximum temperature.

The test method is described for hollow, tubular, threaded-end specimens, resistance heating and compressed air cooling, linear heating and cooling rates, and air environment. The stress dependence of the thermal coefficient of expansion causes no special problem in the determination of the strain values.

A strain measuring system is described that eliminates the thermal component of strain from strain record. Employment of such a system allows a direct recording of load versus mechanical deformation. From these hysteresis loops the pertinent information of the cycle can be determined.

KEY WORDS: thermal fatigue, thermal cycling, fatigue tests, strain measurement, elevated temperature, test methods, fatigue (materials), temperature measurement, tests

Nomenclature

E	Modulus of elasticity
T	Temperature
N_f	Cycles to failure
K	Calibration constant of extensometer, 10^{-6} in./in. mV
e	Voltage output of extensometer, mV
R	Ratio of plastic strain range to total strain range
W_p	Plastic strain energy
σ	Normal stress
ϵ	Normal strain
μ	Poisson's ratio (elastic strain only)

[1] Research associate, Metallurgy Dept., School of Engineering, The University of Connecticut, Storrs, Conn. 06268. Formerly associate professor, Department of Mechanical Systems Engineering, University of Alabama. Personal member ASTM.

[2] Instron Corp., Canton, Mass.

μ^*	Effective Poisson's ratio
α	Thermal coefficient of expansion
C_p,c	Specific heat, heat transfer coefficient
τ	Time constant
$\Delta()$	Range of values
d,∂	Differential and partial differential operator

Subscripts

r,θ,l	Coordinate directions: radial, tangential, longitudinal
e,p,T,m	Strain component: elastic, plastic, thermal, mechanical

Thermal fatigue, as defined herein, is that process by which cracks originate and are propagated in materials that have both cyclic temperature and cyclic mechanical strain at a critical location. Mechanical components of strain are those which are associated with stress. They may be elastic, inelastic, or viscoelastic, or all three. Both temperature and strain vary with time in a thermal fatigue cycle. In 1952 Thielsch [*1*][3] discussed a number of factors related to the problem of thermal fatigue. At that time no thermal fatigue test method was available to evaluate quantitatively the thermal fatigue resistance of materials. It was not until 1954, when Coffin and Wesley [*2, 3*] published the description of a test method, that our understanding of thermal fatigue was to be empirically shaped. The results of tests made on austentic steel presented a quantitative description of the material in terms of strain range versus fatigue life. Actually, no strain measurements were obtained. The calculations of strain were deduced from the thermal cycle and the stiffness and geometry of the system. The test method developed by Coffin was used extensively in this country and abroad. Yen [*4*] and Glenny [*5*] published reviews of the thermal fatigue literature in 1961. One of the severe criticisms of Yen's review was the deficiency of the available methods of strain calculations. An analysis of the mechanics of the Coffin-type thermal fatigue test [*6*] showed how a hysteresis loop of load versus multiple thermocouple output could be used to better deduce the strain values. Later, strain measuring techniques were employed [*7, 8*]. Other thermal fatigue test methods have been developed using circular disks [*9–12*], thick-walled cylinders [*13*], beams [*14*], thin plates [*15*], and thin-walled tubes [*16, 17*]. A survey of test methods was included in the London International Conference in 1967 [*18*]. Two bibliographies on fatigue [*19, 20*] also catalog numerous references to thermal fatigue.

[3] The italic numbers in brackets refer to the references at the end of this paper.

Some of the recent thermal fatigue test methods require strain measurements and some do not. One of the limitations of most of the referenced test methods is their inherent inability to alter the stress temperature arrangement of the fatigue cycle. Some of the stress-temperature arrangements of the thermal fatigue tests are shown in Fig. 1. The stress-temperature cycles of *c*, *d*, *e*, and *f* of Fig. 1 require two separate and synchronous programs: one of temperature and one of deformation. The cycles of *e* and *f* require that load or strain be held constant with constant temperature during part of the cycle. One advantage of such a thermal fatigue test facility is versatility: one disadvantage is complexity and cost.

The purpose of this paper is to describe one of the test methods that can be used to study the uniaxial thermal fatigue of ductile metals. The test method is one which has two programmed variables: (1) crosshead extension and (2) specimen temperature. The test method allows flexibility in the selection of the stress-temperature-time cycle. A unique strain-measuring system is used to allow a strain output that is independent of the thermal component of strain. The primary limitations of the test method are: (1) sheet and thin plate materials cannot be tested, (2) only low cycle frequencies can be used (0.02 Hz or less), and (3) very high strain levels are generally accompanied by tendencies toward geometric instability.

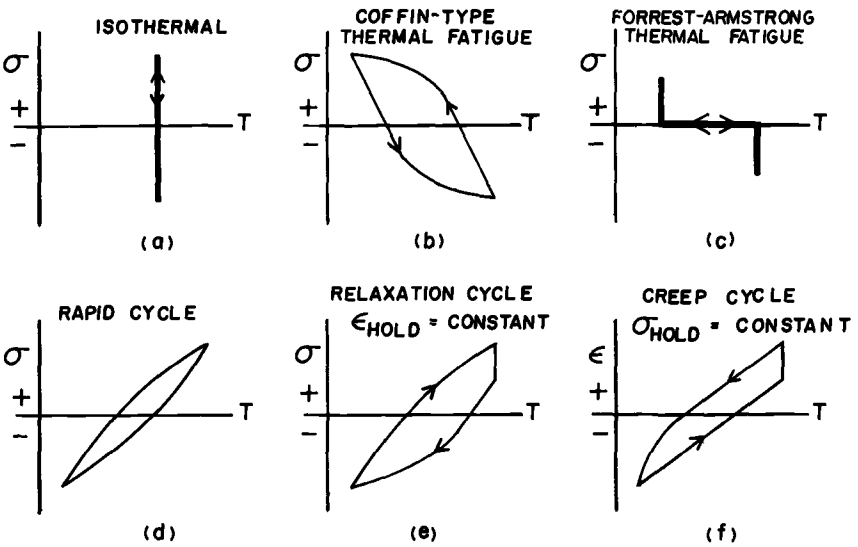

FIG. 1—*Stress-temperature cycles for several types of thermal fatigue test methods.*

Test Method

The test method described in this paper allows the selection of one of three stress-temperature arrangements: positive, negative, or isothermal. The stress-strain and stress-temperature paths for these fatigue cycles are

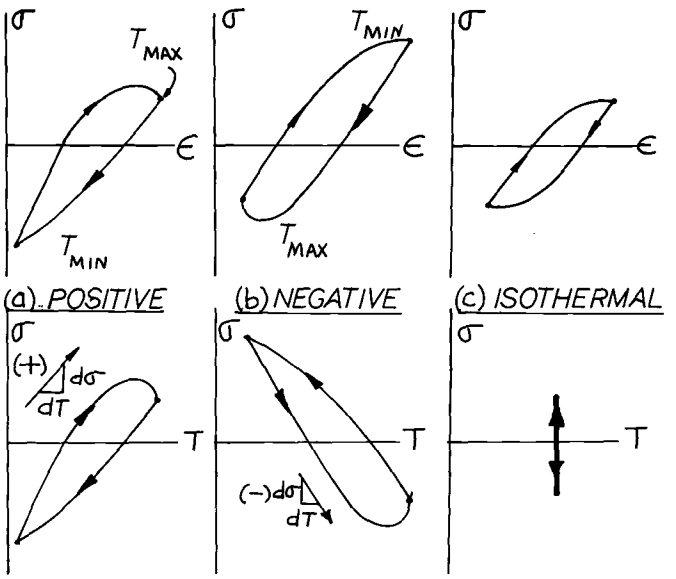

FIG. 2—*Stress-temperature cycles for the thermal fatigue test method of this paper.*

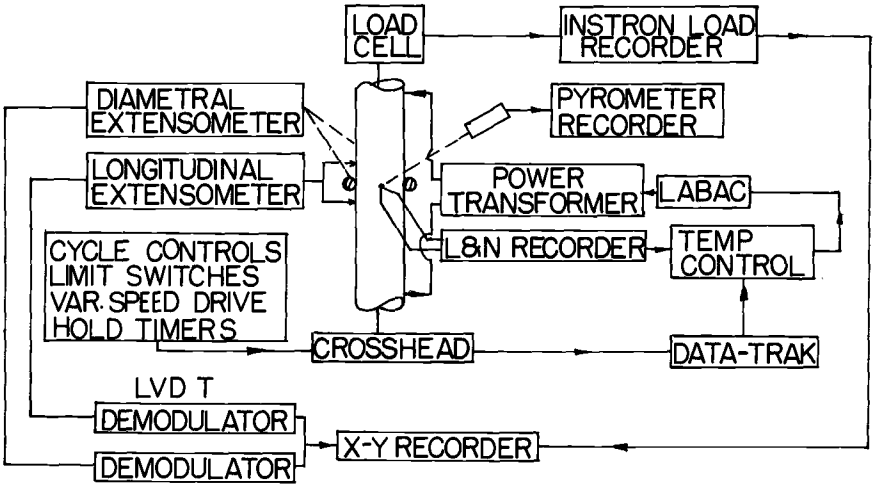

FIG. 3—*Schematic of the elements in the thermal fatigue test facility.*

shown in Fig. 2. The positive loop means that the stress is changing in a positive (tensile) sense when the temperature is increasing. The converse is true for the negative-type test. Hold time under constant load or constant extension can be programmed into the cycle.

A schematic of the test system is shown in Fig. 3 and photographs of the Instron test facility are shown in Figs. 4 and 5. Two extensometers are used: (1) a longitudinal strain extensometer, and (2) a diametral strain transducer. A temperature program control and feedback system comprises the thermal system. As a backup, an optical pyrometer is used for temperature measurement. A hollow tubular specimen is heated by the use of a low voltage welding transformer; compressed air is used to cool the specimen. An X-Y recorder is used to obtain hysteresis loops.

FIG. 4—*Thermal fatigue test facility. Load cell calibration weights are visible.*

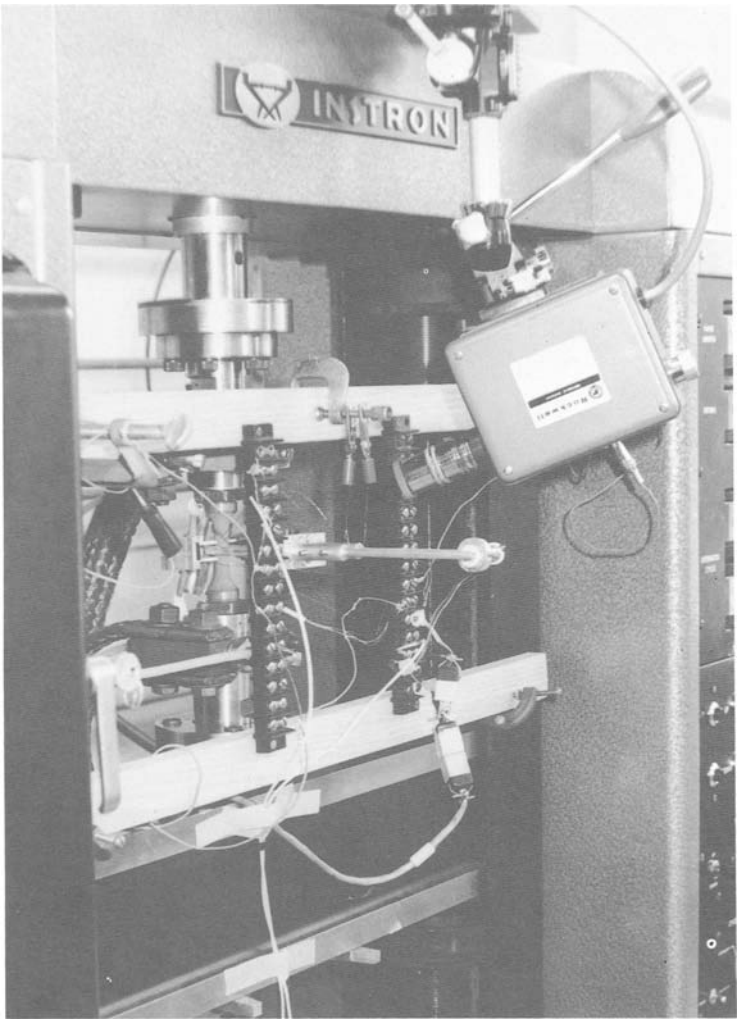

FIG. 5—*Section of apparatus in vicinity of test specimen and grips.*

Specimen and Gripping Arrangement

Typical specimen dimensions are shown in Fig. 6. Other specimen designs can be used but hollow specimens are required for the present method of cooling. Numerous tests have been performed with hollow specimens using wall thickness from 0.020 to 0.120 in. To obtain small radial temperature gradients, thin-walled specimens are preferred. For maximum stability the larger wall thicknesses are preferred. A good compromise is obtained if the wall thickness is between 0.030 and 0.060 in.

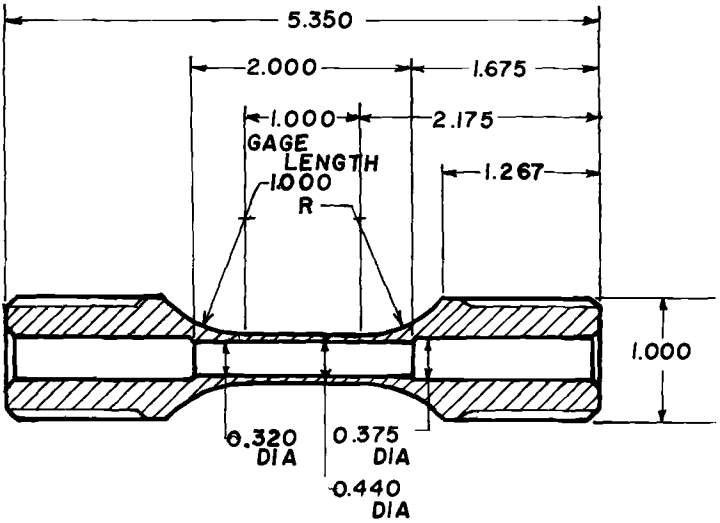

FIG. 6—*Thermal fatigue test specimen dimensions.*

The stability of the specimen is not necessarily improved when solid hourglass specimens are used. Materials that are susceptible to cyclic instability in the thermal fatigue test using hollow tubes are also unstable in the solid specimen geometry. As a proof of this statement observe the three specimens shown in Fig. 7. A sample of Hastelloy N and of stainless steel were subjected to a large thermal cycle. The Hastelloy N specimen grew a little in the middle but the fracture occurred in this volume of deformed material. The stainless specimen, however, greatly increased in diameter, formed two necks, and failed one of the necks.

Because the specimens are resistively heated the gripping system must be water-cooled and designed to carry several thousand amperes of current. A schematic of the gripping system is shown in Fig. 8. Because of the heating method several factors must be given special consideration. The gripping system must be electrically isolated from the rest of the testing machine. This is accomplished by insulation (*1* in Fig. 8) on both the upper and lower grip. Because a threaded-end specimen, *7*, is used, special precautions must be taken to reduce the electrical resistance of the threads and to insure against a differential thermal expansion that would loosen the connection. A cylindrical insert of copper, *5*, works well. The copper has good conductivity, can mate with the bottom of the grip and the bottom of the specimen, and has a higher thermal expansion than either the grip material or the specimen. This differential thermal expansion guarantees a large locking force on the threads, decreases the

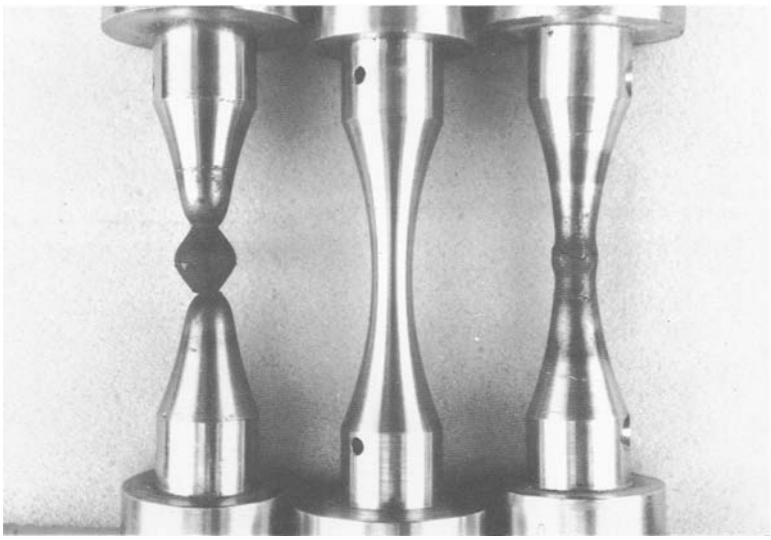

FIG. 7—*Three 0-gage-length (solid) specimens:* (left) *304 stainless (badly deformed);* (center) *virgin sample;* (right) *Hastelloy N (slight bulge). The two failed samples were tested at strain levels of greater than 10 percent per cycle.*

electrical resistance between the specimen and the grip, and provides a good heat conduction path from the specimen to the heat sink.

Large water-cooled copper connections form the electrical connection and the heat sink. (These, with the electrical leads, can be seen in Fig. 9.) The cooling air enters a hole in one grip, *3*, passes through the specimen, *7*, and exits through a connection in the other grip. The lower grip is attached to the crosshead, *8*, by passing a 1-in.-diameter rod through the crosshead. When the lower locking nuts, *9*, are removed and the crosshead is moved down, the specimen is free to expand and contract under no load. The total thermal expansion of the specimen and grips is measured by a dial gage. The dial gage is attached to the Instron frame and touches the bottom of the lower grip rod, *10*.

For alignment the whole system is assembled and attached to the Instron crosshead, while the load cell is disconnected from the machine frame. Pieces of shim stock are placed underneath the load cell at 90 deg locations. The crosshead is moved down until the load cell output indicates a slight load (20 lb). The shims are examined for tightness. When the load cell can be brought against the testing machine frame and all of the shims remain equally tight, the load cell is then bolted to the frame. After this initial alignment only the lower grip is disconnected from the testing machine.

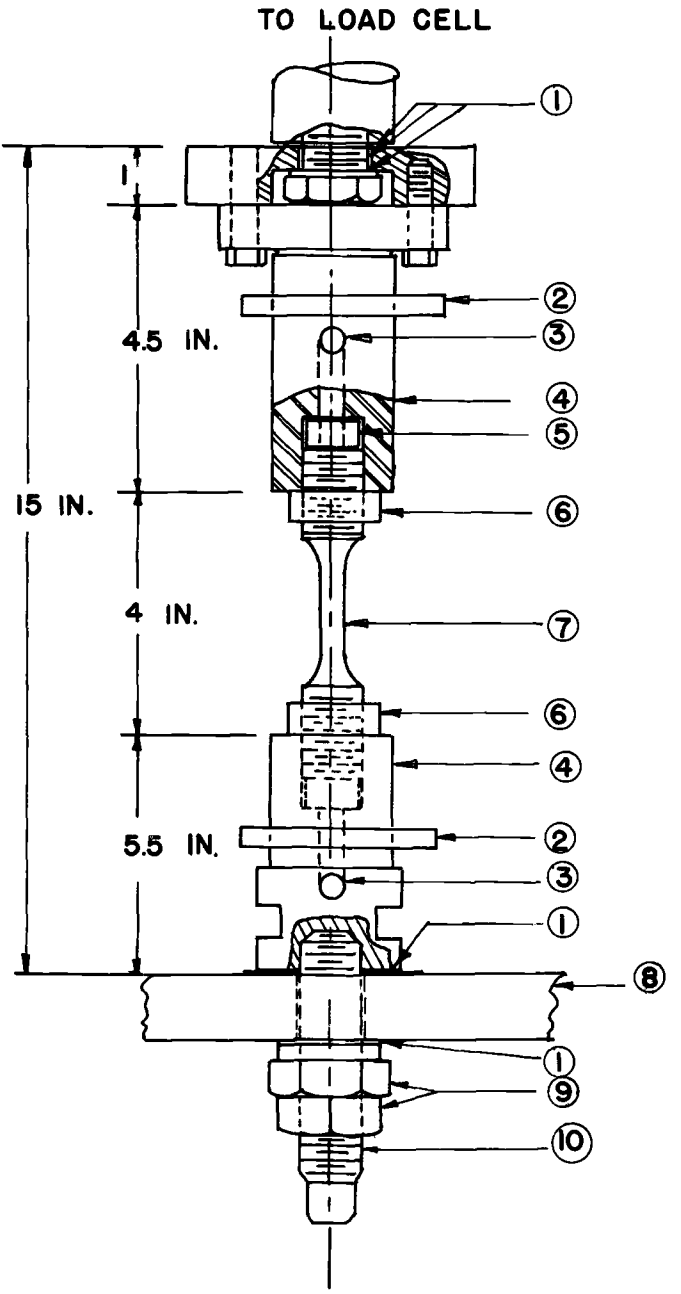

FIG. 8—*Schematic of gripping system. See text for description of numbered elements.*

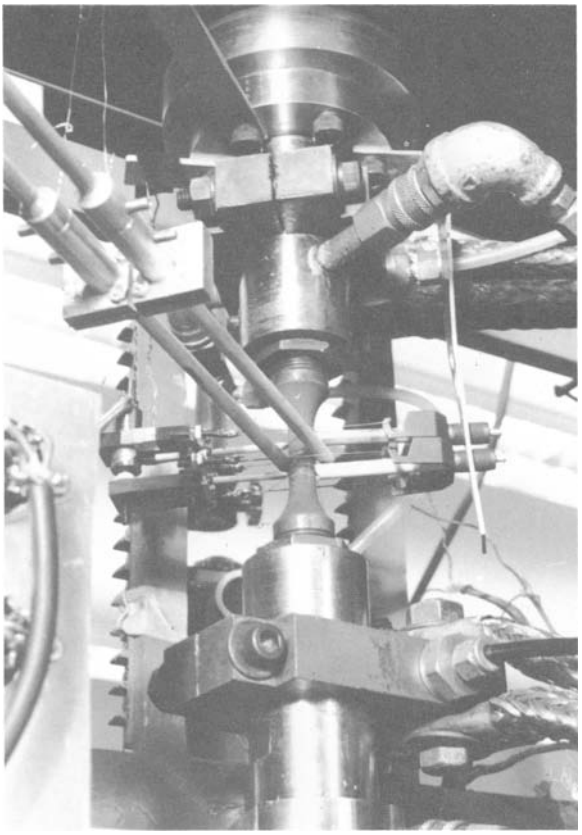

FIG. 9—*Thermal fatigue test specimen. A ½-in. gage length extensometer is on the left. Part of the diametral extensometer is visible in the upper left.*

During assembly the specimen is threaded into the upper grip against the copper insert, and the specimen lock nut, *6*, is tightened. The lower grip is threaded onto the specimen and the lower nut, *6*, is tightened. The strain and temperature measuring devices are mounted and the specimen is ready for test.

The calibration of the load cell is accomplished by using dead weights and two aluminum I beams to span the specimen grip regions. The beams rest on the upper collar of the specimen grip (see Fig. 4). Half of the weights are visible, the other half are not. The lower specimen grip must be disconnected from the crosshead for calibration.

Thermal Components

A schematic of the thermal components of the system are shown in Fig. 10. The temperature control system consists of a program device,

a feedback element, and a controller. Resistance heating of the specimen is used for several reasons. To obtain strain and temperature measurements a number of items must be mounted physically on the outer surface of the specimen. An open space on the specimen surface is required for viewing with the optical pyrometer. When induction heating is used, there is usually a skin effect to the heat generation; also, the induction coil must be located around and in close proximity to the specimen surface. The presence of the induction coils greatly hinders the mounting of the strain and temperature transducer elements.

The power transformer shown in Fig. 10 is an 8-kVA welding transformer. A 220-V a-c primary circuit and a 3-V secondary circuit are common values for this transformer. Because large currents are generated in the secondary circuit, it is necessary to use large flexible copper cables for the transmission lines and joints. These cables must be joined to the secondary circuit and to the specimen grips with large clamping forces. All contact surfaces must be kept clean. It is also necessary to insulate electrically the top and bottom grips from the testing machine to prevent a parallel path for the current (see Fig. 8). Actually, only one grip needs to be insulated, but the additional effort to insulate the other grip is worthwhile.

The temperature program and control depend on the program device, a specimen temperature feedback element, and a control facility (see

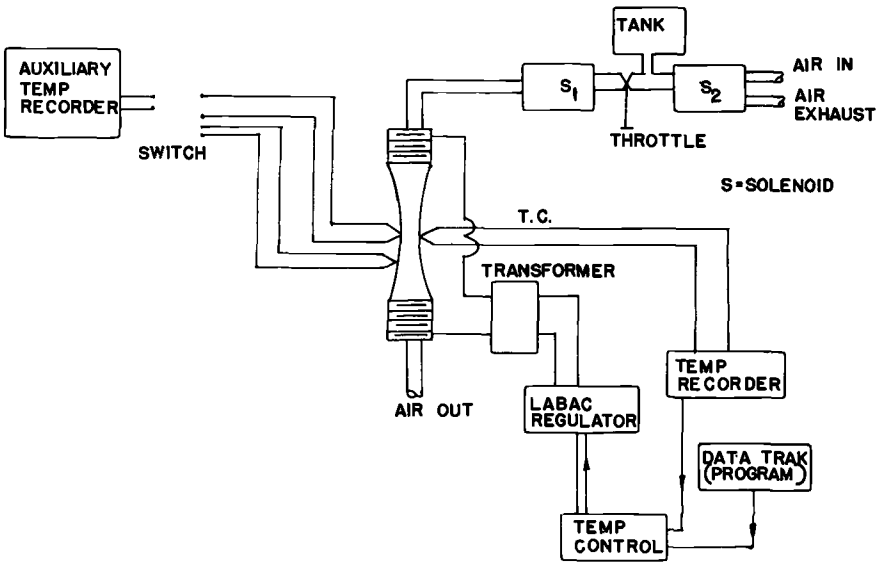

FIG. 10—*Schematic of the thermal components of the thermal fatigue test facility.*

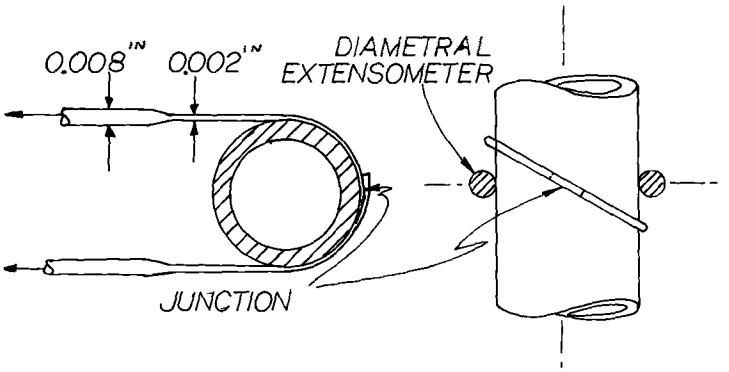

FIG. 11—*Schematic of thermocouple location. This scheme is used only when welding the thermocouple to the specimen is detrimental to the fatigue behavior.*

Fig. 10). A Data-Trak[4] with a program profile drawn on a metalized sheet and mounted on a rotating drum is used. The feedback element is the thermocouple. A Leeds and Northrup[5] CAT (current adjust type) control unit is the temperature controller. The d-c current from the Leeds and Northrup CAT unit controls a silicon controller a-c power regulator (LABAC)[4]. The power regulator supplies the primary voltage for the power transformer.

The primary temperature measurement is obtained by small thermocouple wires that are either welded to the specimen surface or attached by specially prepared thermocouple wires wrapped helically around the specimen and pulled taut. The junction of the helically wound thermocouple is in close proximity but is not truly at the specimen surface (see Fig. 11), causing a greater dynamic response problem. The limitation of low cycle frequencies and the attendant low heating and cooling rates are necessary in order to minimize these dynamic errors.

On materials that show a deterioration of fatigue resistance when the thermocouple is welded to the surface (that is, when the crack originates at the weld region) the thermocouple junction first must be formed and the junction must be placed at the specimen surface. The intrinsic (welded) junction gives far superior response but sometimes it is excluded because the welding operation impairs the fatigue behavior. Another potential source of thermocouple error results when the small Chromel-Alumel wires (0.008-in.-diameter wire) are used at 1600 F or above for an extended time. At 1800 F for about 100 h a complete deterioration of the couple occurs. When the helically wound thermocouple

[4] Research, Inc., Minneapolis, Minn.
[5] Leeds and Northrup Co., North Wales, Pa.

is used there is no problem in changing the thermocouple, but there may be a significant layer of oxide between the new thermocouple and the metallic surface. The present technique is to use two junctions in parallel for control and another for auxiliary recording (see Fig. 10). The result well justifies the expense and trouble. The auxiliary thermocouple can show differences, if any, and the two thermocouples in parallel are good insurance against loss of control due to a thermocouple failure. The time constant, τ, of the junctions is defined as the time to reach 63 percent of the temperature difference between the junction and the source temperature, where

$$\tau = \frac{(\text{mass of junction})\ (C_p \text{ of } TC \text{ material})}{(\text{area of junction for heat transfer})\ (C)},$$

C is a heat transfer coefficient, and C_p is the heat capacity of the thermocouple material. The time constant (and the lag of the junction output relative to a dynamic temperature) can be minimized by reducing the numerator and increasing the denominator.

Thermocouple Manufacture

Reducing the time constant is accomplished by proper design and manufacturing techniques. Small thermocouple wires are flattened between two hardened blocks in a testing machine. These flattened regions are cut and the two dissimilar materials are laid one on top of the other. An energy discharge weld joins the two regions. The flat portion is placed in intimate contact with the specimen surface, which maximizes the area, and the wires are pulled taut, which maximizes the conduction mode of heat transfer. The wires are as small as practical, initially, to minimize heat storage in the junction (see Fig. 11). This technique may sound complicated but it is considerably easier to master than, say, cementing strain gages on flat surfaces.

The optical pyrometer is an auxiliary instrument for temperature measurement. The pyrometer is a solid state infrared system and has relatively high response. The transducer in the pyrometer is a photon detector and has a time constant of less than 2 μs. The emissivity of the specimen surface, however, must be set into the pyrometer. With some materials the value of the emissivity changes with surface oxidation and stress. For this reason the pyrometer readings are usually only relative temperature measurements. With proper calibration and use the absolute readings can be obtained, but their accuracy is lower than comparable thermocouple readings. The cycle-to-cycle repeatability is certainly useful information, especially at the maximum temperature. The system,

when properly calibrated, will show less than ±5-F variation at a peak temperature of, say, 1600 F.

The specimen does not follow exactly the command signal. This dynamic response of the system is not severe if the heating and cooling rates are low. For a heating rate of about 20 F/s the lag in temperature is about 5 F.

The most severe temperature gradient in this type of test is longitudinal. The effect of temperature gradient on the strain measurement is not severe if the extensometer gage length is small. The calculations of strain obtained from load, temperature, and longitudinal strain (½-in. gage length or less) show little differences from those obtained from load, temperature, and diametral extensometers. In fact, diametral transducers at the center and at the upper end of a ½-in. gage length have been used to observe the longitudinal distribution of strain. For most nickel-base alloys the strains are very uniformly distributed.

The longitudinal temperature gradient can cause significant problems in relaxation cycling. The temperature system controls the temperature at only one point, that of the thermocouple junction. Under a temperature cycling program, the specimen temperature profile is dynamic. If the specimen is brought to a hold condition of temperature, the longitudinal temperature profile will continue to change for about 60 s [*8*]. The increase of the thermal length of the specimen during temperature holds means that for tests that have constant crosshead positions there will be a tendency for the specimen to be loaded or unloaded, depending on whether the specimen is held at a compressive or tensile load during this period. The thermal length of the specimen can be controlled, approximately, if numerous thermocouples are placed along the length of the specimen, connected in parallel, and used as the control feedback signal. The specimen length should be divided into several segments, each having the same length. A thermocouple is placed in the center of each of these segments and is used to indicate the temperature of that segment. When this technique is used the *average* temperature of the specimen is programmed, not the maximum temperature.

Within the limitations stated above, almost any temperature program can be drawn on the Data-Trak program paper and synchronized with the crosshead program of the testing machine.

Synchronization of the Thermal and Extension Program

The Instron machine has a constant crosshead speed which is selected through change gears and a variable speed drive. Limit switches on the extension cycling cams are used to reverse the direction of loading. Timers

are available so that a number of possible extension, load, creep, and relaxation cycles can be programmed into the crosshead cycle. Relays in the Instron are relied upon to activate the temperature program on each cycle of loading. The temperature program is obtained from the Data-Trak drum rotation. A limit switch is set to stop the drum rotation at the end of each cycle. The drum rotation stops until the Instron relay contacts and indicates the initiation of a new cycle and a secondary circuit activates the continued rotation of the drum.

Determination of the Mechanical Extension of the Specimen

Prior to the clamping of the specimen to the crosshead the thermal cycle is operated, and although the crosshead is operated, it is mechanically disconnected from the specimen. The operation of the testing machine crosshead during the "free-cycling" period is required because of the dependence of the Data-Trak rotation on crosshead operation. A dial gage is used to determine the amount of total thermal expansion in the specimen grip assembly. The amount of deformation sustained by the specimen in the form of mechanical loading will be the difference between this thermal expansion and the extension range of the Instron crosshead.

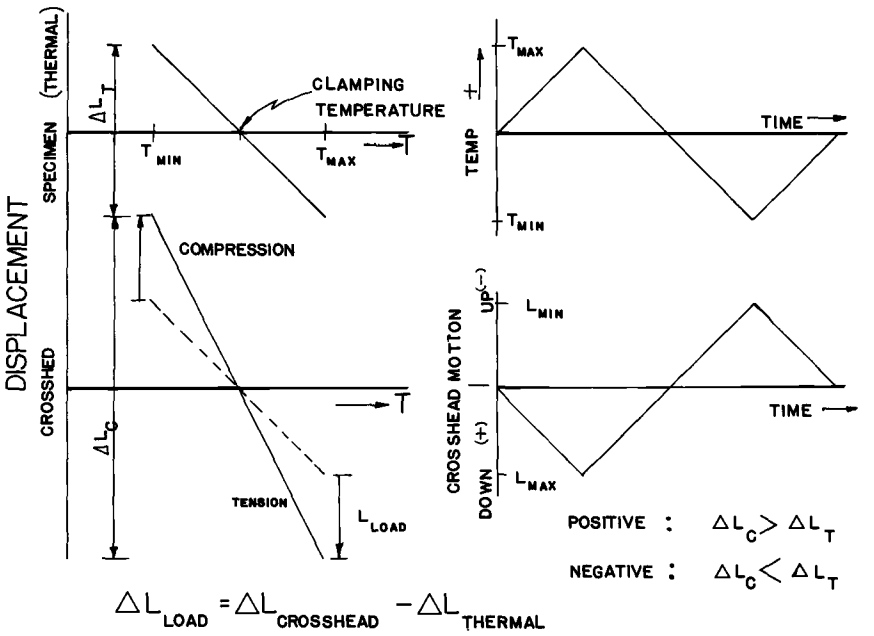

FIG. 12—*Schematic of crosshead and specimen-thermal displacements. Crosshead displacement shown here is for a positive-type thermal fatigue cycle.*

When the two displacements are exactly equal and in phase, the specimen thermally cycles without sustaining any load. A schematic of the displacements (specimen-thermal and crosshead versus temperature) and of the two programs (temperature and crosshead) as functions of time are shown in Fig. 12. Thus, with this test method the maximum and minimum temperatures can be kept constant while the deformation range is varied from test to test. The deformation range is the difference of the specimen-thermal deformation range and the extension range of the crosshead. This is called "effective deformation range." When the maximum and minimum temperatures and the specimen geometry are kept constant, a log plot of "effective deformation range" versus cycles to failure will give a smooth curve and can be used to select crosshead extension ranges for specified (expected) life values. As already defined, when the Instron extension is greater than the thermal expansion range, the specimen is placed in tension at the maximum temperature. A schematic of the three types of thermal-mechanical cycles was shown in Fig. 2. When the test conditions are changed from one type of cycle to another (positive, negtive, or isothermal) an appropriate change in the relationship of effective deformation versus cycles to failure can be expected.

Strain Measurements and Hysteresis Loops

Extensometers

Drawings of the longitudinal and diametral extensometers are shown in Figs. 13 and 14. A linear variable differential transformer (LVDT) is

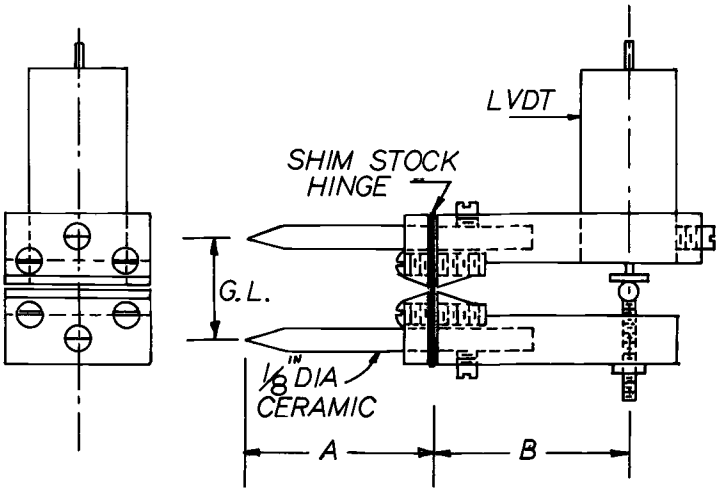

FIG. 13—*Schematic of longitudinal extensometer.*

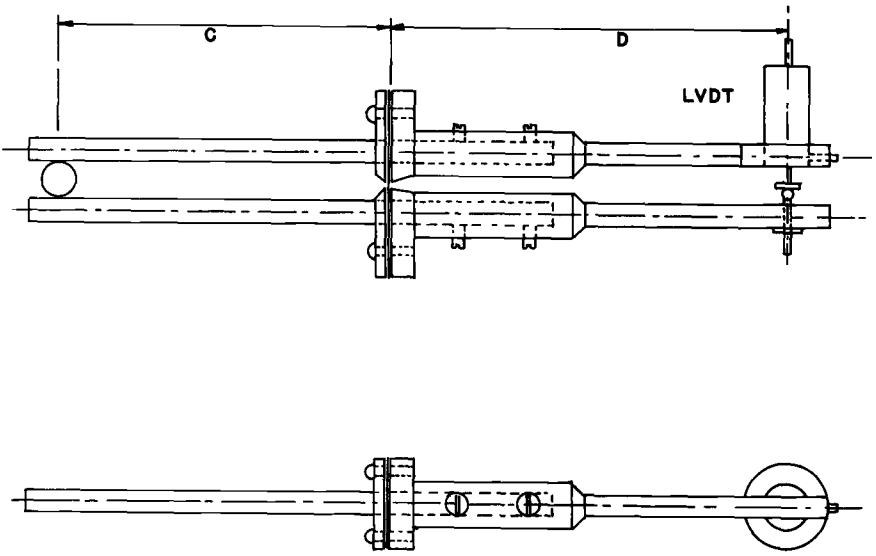

FIG. 14—*Schematic of diametral extensometer.*

used for displacement measurements. The choice of the particular LVDT (Atcotran 6233A)[6] and signal conditioning equipment (Atcotran 6101E) was based on the following requirements: high strain sensitivity (10^{-6} in. or better), stable zero setting, light weight, small size, and excitation and demodulation system that would allow cancelling of the strong 60-cycle signal induced by the heater current, and an infinitely variable attenuation setting. Two 0.3-in. gage length extensometers mounted on opposite faces of the specimen are shown in Fig. 15. These two extensometers have shorter gage lengths and give greater output than the one shown in Fig. 9.) Two extensometers average the strain on the two sides of the specimen.

With a properly designed extensometer the fulcrum plates must be frictionless, the clamping force for each ceramic rod must be small and colinear with the rod axis, the weight must be counterbalanced, the ceramic rods must be sharp, there must be no drag of the LVDT core on the transformer housing, and the strain transfer device must have no nonlinearities. In the vertical mounting position gravity is usually sufficient to maintain the core extension rod against the opposite lever arm. In the horizontal position (Figs. 15 and 16) a small spring is required to maintain contact.

[6] Automatic Timing and Control Co., King of Prussia, Pa.

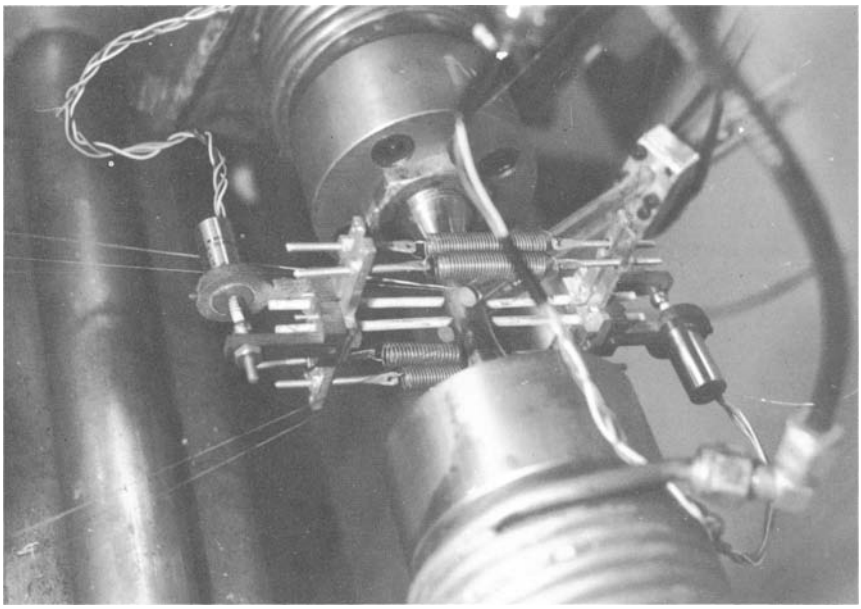

FIG. 15—*Twin 0.3-in. gage length extensometers. In this test facility the specimen is horizontal. The diametral extensometer rods are oblique to the specimen axis.*

Strain Measurement

The calibration data of the transducers and the setting of the attenuator on the exciter-demodulator unit can be used to set the condition for eliminating the thermal component from the recorded value of strain. The equations for the output of the two transducers measuring strain between two points on a hysteresis loop are:

$$K_l e_l = \Delta\epsilon_{el} + \Delta\epsilon_{pl} + \alpha_l \Delta T \quad (1)$$

$$K_\theta e_\theta = -\mu\, \Delta\epsilon_{el} - \tfrac{1}{2}\Delta\epsilon_{pl} + \alpha_\theta \Delta T \quad (2)$$

Note that the difference of the two transducers is

$$K_l e_l - K_\theta e_\theta = \Delta\epsilon_{el}(1 + \mu) + \Delta\epsilon_{pl}(1.5) + (\alpha_l - \alpha_\theta)\Delta T \quad (3)$$

If the thermal expansion coefficients are equal and if the two calibration constants of the two transducers are equal, then the expression is

$$K(e_l - e_\theta) = \Delta\epsilon_{ml}[(1 + \mu)(1 - R) + 1.5R] \quad (4)$$

where $R = (\Delta\epsilon_{pl}/\Delta\epsilon_{ml})$

and letting

$$(1 + \mu^*) = [(1 + \mu)(1 - R) + 1.5R] \quad (5)$$

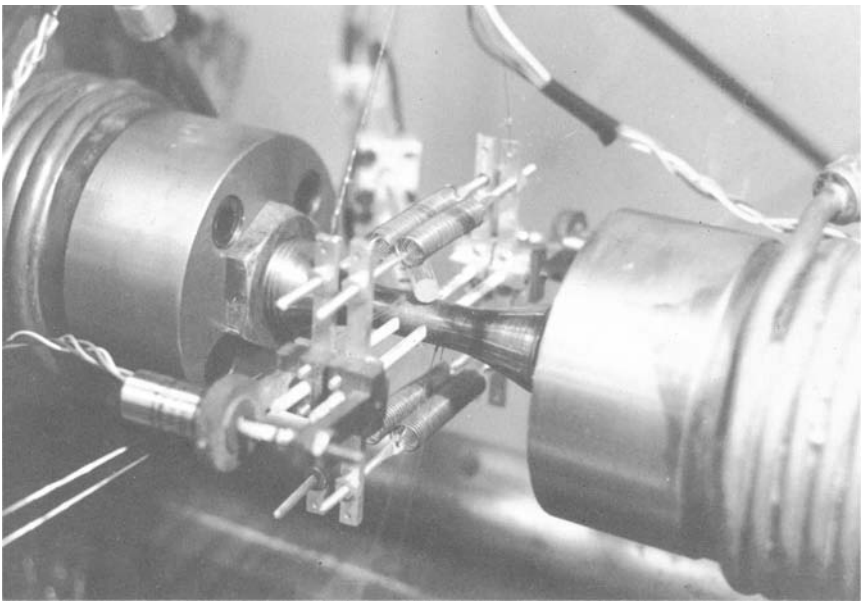

FIG. 16—*Twin 0.3-in. gage length extensometers. The helically wound thermocouple leads are partly visible.*

then

$$K(e_l - e_\theta) = (1 + \mu^*)\Delta\epsilon_{ml} \quad \ldots\ldots\ldots\ldots\ldots\ldots\ldots\ldots (6)$$

Hysteresis Loops

A plot of load versus the difference-of-transducer output will be analogous to a stress-mechanical strain hysteresis loop. The output of the difference of transducers is not strain directly but must be divided by $(1 + \mu^*)$ as shown by Eq 6. The value μ^* takes values of from μ to 0.5 and the values of $(1 + \mu^*)$ vary linearly with R from values of $(1 + \mu)$ at $R = 0$ (elastic strains only) to 1.5 for $R = 1.0$ (fully plastic case). A typical value of μ for the elastic strain component at elevated temperature is 0.3. Measurements over large temperature changes do not show μ (based on the definition of Poisson's ratio determined from elastic strain only) to be temperature dependent. For the Eqs 4 and 6 to be true, there must be a uniform distribution of strain and temperature in the longitudinal and circumferential directions. If there are highly local phenomena, then the values obtained are only average values.

A typical hysteresis loop taken from a thermal fatigue test is shown in Fig. 17. This plot, load versus difference-of-transducer output, is for a negative-type loop of 1600 to 600 F. The temperature points (100-F in-

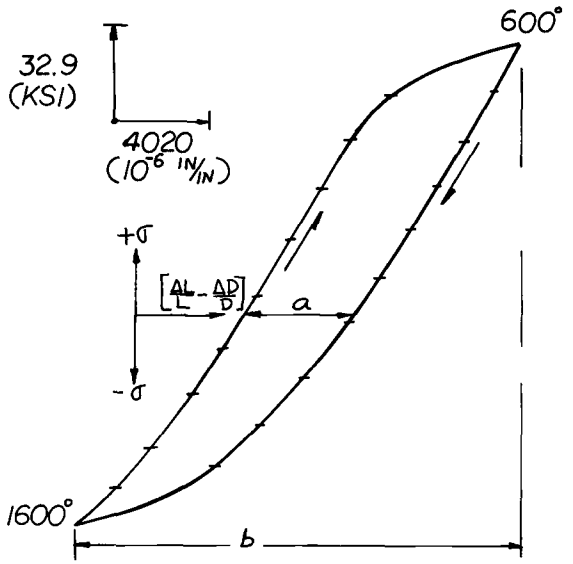

FIG. 17—*Typical load versus difference-of-transducer hysteresis loop, 1600–600 F, negative-type loop.*

crements) are marked around the loop. The curvature of the elastic unloading line is due to the change of modulus of elasticity during cooling and heating. The plastic strain range (at the zero load location) is: (the output in millivolts times the calibration constant) ÷ 1½. The value of $(1 + \mu^*)$ is 1.5 because the two points on the hysteresis loop have no elastic strain content. The R value for the extreme points is about 0.24 (the ratio of a to b), which gives a value of 1.35 for $(1 + \mu^*)$. The calculations for the pertinent values of this loop are summarized as:

$$\Delta\epsilon_m = 0.0138,$$

$$\Delta\epsilon_p = 0.0029,$$

$$\Delta\epsilon_e = 0.0109,$$

$$\Delta\sigma = 167 \text{ ksi}$$

$$\Delta\sigma/\Delta\epsilon_e = 15.3 \ (10^6 \text{ psi}),$$

$$d\sigma/d\epsilon \ (\text{at } \sigma = 0) = 18.9 \ (10^6 \text{ psi, and}$$

$$W_p \text{ in·lb/in.}^3 = 187 \text{ (compressive), } 277 \text{ (tensile).}$$

The hysteresis loops of Figs. 17 and 18 were obtained from a plot of load versus transducer-difference output. The numbers indexed around the loop are indications of hundred-degree-F temperature points. The

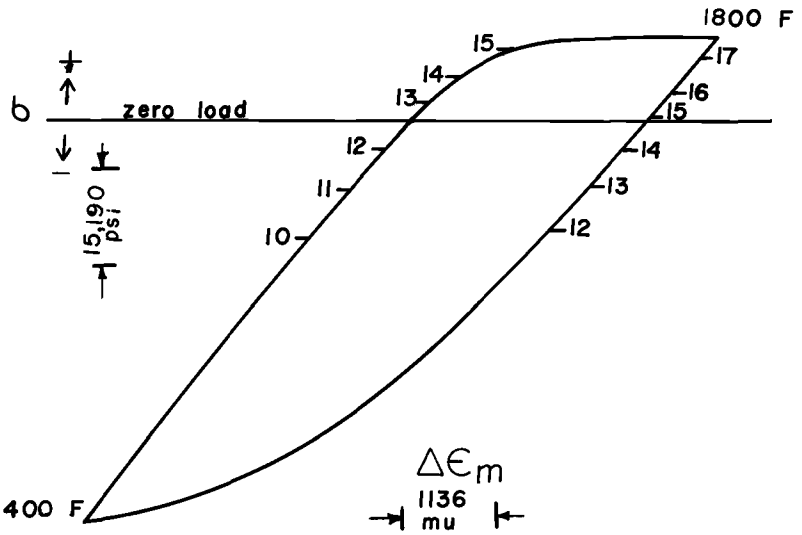

FIG. 18—*Load versus difference-of-transducer hysteresis loop, 400–1800 F, positive-type thermal fatigue cycle. This loop and the one shown in Fig. 19 were obtained from the same test.*

loops are not symmetrical with regard to the zero-load abscissa. Strain hardening is evident during the loading period at the minimum temperature, while strain softening is observed at the other extreme (Fig. 18 only). The maximum tensile stress in one of the loops occurs prior to the end of heating-and-extension cycle. The specimen passes through zero load at temperatures above the mean temperature of the cycle. The lack of symmetry does not imply a mean strain. Technically, there is a mean stress, but this inequality of stress is required for no mean plastic strain because of the difference in strength at the two temperature extremes. The integration of the area inside the hysteresis loop will be proportional to the plastic work per cycle.

In contrast to this method of strain measurement, consider the load versus diametral strain loop of Fig. 19. The loops of Figs. 18 and 19 were taken from the same test. Note the following facts related to the kind of loop shown in Fig. 19: The internal width of the loop is not proportional to the plastic strain range; the external width of the loop is not proportional to the mechanical strain range; the integration of the area within the loop is not proportional to the plastic strain energy of the loop; strain hardening is not discernible from the shape of the loop; and although the strain output is positive for increasing stress, the diametral elastic and plastic strains are negative.

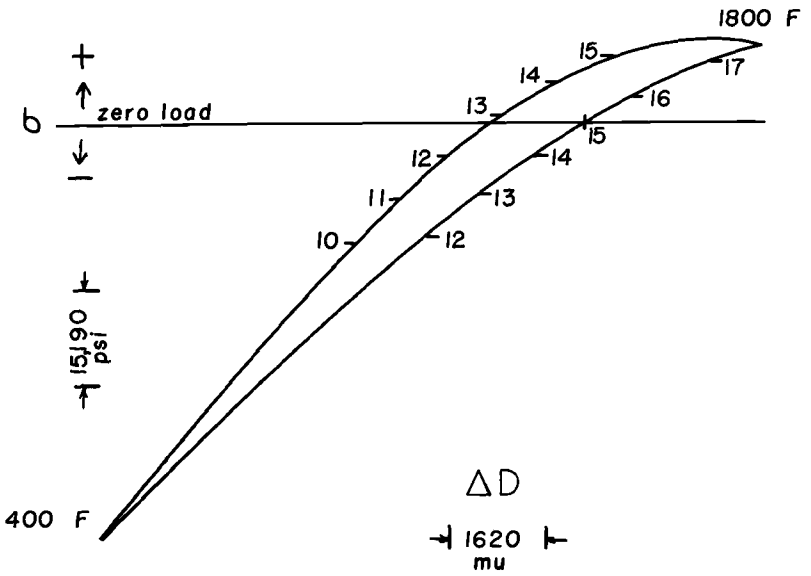

FIG. 19—*Load versus diametral extensometer hysteresis loop.*

The primary advantage of the foregoing technique for eliminating the thermal component of strain is that the most urgently needed data can be directly recorded. An appreciation for the amount of data reduction saved by this method of strain measurement can be obtained by considering the amount of calculation required to transform the loop of Fig. 19 to a load versus mechanical component of strain loop. The third variable of temperature must be precisely known and the mechanical properties of modulus of elasticity, Poisson's ratio, and thermal coefficient of expansion must be known as functions of temperature. Further consideration of this problem will also reveal the great sensitivity of the resulting transformation to the accuracy of the temperature measurement.

Recording of Data

A number of the test parameters are recorded as functions of time throughout the test: load, temperature (both thermocouple and optical pyrometer measurements), and possibly strain. Periodically the load is plotted as a function of the strain transducer output on an *X-Y* recorder.

The load-difference-of-transducer output record is the primary record of the test. If sufficient numbers of these records are collected during the test, strain hardening, creep (during periods of constant load), or relaxation (under periods of constant crosshead extension) can be observed.

Definition of Failure

With regard to crack detection and a definition of failure, failure is defined as the condition where a crack propagation occurs over one half of the periphery of the specimen. We have no automatic crack detection device but if possible we like to terminate the test before the specimen is completely fractured.

Analysis of Thermal and Mechanical Cycling

A number of questions can be raised with regard to the definitions of the thermal and mechanical components of strain during thermal-mechanical loading. Semantics, perhaps, have caused some of the misunderstanding. Let us assume that strain is a function of stress, time, and temperature, and possibly other variables. For the uniaxial loading case the normal strain in the longitudinal direction is

$$\epsilon_l = F(\sigma_l, T, t, \ldots\ldots) \quad (7)$$

The total differential of the strain is

$$d\epsilon_l = (\partial\epsilon/\partial\sigma)\, d\sigma + (\partial\epsilon/\partial T)\, dT + (\partial\epsilon/\partial t)\, dt \quad (8)$$

where:

$(\partial\epsilon/\partial\sigma)\, d\sigma$ = elastic,
$(\partial\sigma/\partial T)\, dT$ = thermal, and
$(\partial\epsilon/\partial t)\, dt$ = time.

or

$$d\epsilon = (1/E)\, d\sigma + \alpha dT + \dot{\epsilon}\, dt \quad (9)$$

The first partial derivative is the reciprocal of the modulus of elasticity, the second is the thermal coefficient of expansion, and the third is the creep coefficient. The modulus of elasticity, creep coefficient, and thermal expansion coefficient are temperature dependent. What additional strain components will accompany a change of temperature besides the value represented by αdT? Taking the partial derivative of the elastic component (uniaxial) with respect to temperature and multiplying this value by the differential change in temperature gives

$$(\partial/\partial T)\,(\partial\epsilon/\partial\sigma) = (-1/E^2)\,(dE/dT) \quad (10)$$

and

$$(\partial/\partial T)\,(\epsilon_{el})\, dT = -(\sigma/E^2)\,(dE/dT)\, dT \quad (11)$$

Thus this component of strain (and it is properly called a thermal component) occurs when there is an elastic component of strain, when the

modulus of elasticity is temperature dependent, and when there is a temperature change. If the difference of this component of strain is needed between two points on a stress-temperature excursion, the term on the right of Eq 11 can be integrated, keeping in mind that the stress, the value of the modulus of elasticity, and its temperature derivatives are functions of and change with temperature and must be explicitly shown before integration. Thus, if the time dependent component of strain is neglected, the elastic, thermal (ordinary), and thermal (stress dependent part) components of strain are

$$d\epsilon_l = (d\sigma/E) + \alpha dT - (\sigma/E^2)\,(dE/dT)\,dT \quad \text{.....(12)}$$

or for a range of values

$$[\Delta\epsilon_l]_{1-2} = \int_1^2 \frac{d\sigma}{E} + \int_1^2 \alpha\, dT - \int_1^2 \frac{\sigma}{E^2}\left(\frac{dE}{dT}\right) dT \quad \text{.....(13)}$$

The *sum* of the thermal and the elastic strain components is independent of the path taken. The individual values of these components, however, are path dependent.

The amount of elastic or thermal strain change observed on unloading from one point of stress and temperature to another cannot be determined without specifying the path of unloading. The semantics are confusing. Even though the term shown in Eq 11 is truly a thermal component it represents the *change* of the *elastic* strain during a temperature change (because E changes). The common name given to this effect is "the stress dependence of the thermal coefficient of expansion" [*21*]. The name implies that the effect is tied to stress rather than strain. If a bi-axial stress case is selected for discussion it is obvious that the effect just described is not present in some situations, even though there are stresses present. Note the case where the circumferential stress is equal to the longitudinal stress divided by Poisson's ratio. The elastic strain component in the longitudinal direction is

$$\epsilon_l = [(\mu\sigma_\theta)/E] - (\mu/E)\,(\sigma_\theta) \quad \text{.....(14)}$$

where $\sigma_l = \mu\,\sigma_\theta$ and $\sigma_r = 0$. On heating there will be no longitudinal thermal component except for $\int \alpha dT$ because there is no elastic strain component in this direction. The general form of this effect can be described [*22*] but has no particular use for uniaxial loading.

For practicality, all of this discussion can be summarized by the following. The sum of the elastic and thermal strain components is independent of the path taken. A bar loaded and heated is the same length

as that of an identical one heated and then loaded, or of another loaded and heated simultaneously (assuming the same temperature change and no plastic or viscoelastic strain components are present). For low cycle thermal fatigue the stress dependence of the thermal expansion coefficient causes no problem in the determination of the strain values.

Summary

A thermal fatigue test method has been described that has the capability of several stress-temperature-time cycles for thermal fatigue studies. Strain measurements were obtained from the specimen and although the temperature was found to vary in the cycle, one method of strain measurement allowed direct recording of the mechanical component of strain.

Reasonably precise temperature measurement was obtained without welding a thermocouple to the specimen. The stress dependence of the thermal expansion coefficient caused no great problem in the determination of the strain.

Acknowledgment

The test method described in this report was developed over a period of years as a part of sponsored research performed at the University of Alabama. The Metals and Ceramics Division of the Oak Ridge National Laboratory (operated by Union Carbide Corp. for the U. S. Atomic Energy Commission) initiated and guided the work for six years. Other work was part of a thermal fatigue study of superalloys made for Pratt & Whitney Aircraft, a Division of United Aircraft Corp.

The author is indebted to numerous laboratory assistants and graduate students. The results in a special measure rest on the able leadership and encouragement given by W. D. Jordan, head of the Department of Mechanical Systems Engineering, University of Alabama.

References

[*1*] Thielsch, H., "Thermal Fatigue and Thermal Shock," *Bulletin No. 10*, Welding Research Council, WRCBA, 1952.

[*2*] Coffin, L. F., Jr. and Wesley, R. P., "Apparatus for the Study of Effects of Cyclic Thermal Stresses on Ductile Metals," *Transactions*, American Society of Mechanical Engineers, TASMA, Vol. 76, 1954, p. 923.

[*3*] Coffin, L. F., Jr., "A Study of the Effects of Cyclic Thermal Stresses on a Ductile Metal," *Transactions*, American Society of Mechanical Engineers, TASMA, Vol. 76, 1954, p. 931.

[*4*] Yen, T. C., "Thermal Fatigue—A Critical Review," *Bulletin No. 72, Welding Research Council*, WRCBA, 1961.

[*5*] Glenny, E., "Thermal Fatigue," *Metallurgical Reviews*, MREVA, Vol. 6, No. 24, 1961, p. 387.

[6] Carden, A. E., "Thermal Fatigue—Part I. An Analysis of the Conventional Experimental Method," *Proceedings*, American Society for Testing and Materials, ASTEA, Vol. 63, 1963, p. 735.

[7] Foley, D. D., Hallander, J. M. and Horton, K. E., "Thermal Stress and Low Cycle Fatigue Data on Typical Materials, *Preprint 65-GTP-13*, American Society of Mechanical Engineers, 1965.

[8] Kawamoto, M., Tanaka, T. and Nakajima, H., "Effects of Several Factors on Thermal Fatigue," *Journal of Materials*, JMLSA, Vol. 1, No. 4, 1966, pp. 719–758.

[9] Glenny E. and Taylor, T. A., "A Study of the Thermal Fatigue Behavior of Metals," *Journal of the Institute of Metals*, London, Vol. 88, 1959-60, p. 449.

[10] Rostoker, W., "Thermal Fatigue Resistance of Martensitic Steels," *Journal of Materials*, JMLSA, Vol. 4, No. 1, 1969, pp. 117–144.

[11] Aramayo, G. A., "A Study of the Thermal Fatigue Behavior of Thin Circular Discs," *Thesis*, University of Alabama, 1965.

[12] Doughty, L. E., "An Investigation of the Thermal Fatigue Failure of Circular Discs by Cyclic Thermal Stress," *Thesis*, University of Alabama, 1965.

[13] Keyes, J. J., Jr. and Krakoviak, A. I., "High Frequency Surface Thermal Fatigue Cycling of Inconel at 1405 F," *Nuclear Science and Engineering*, NSENA, Vol. 9, 1961, p. 462.

[14] Forest, P. G. and Penfold, A. B., "New Approach to Thermal Fatigue Testing," *Engineering*, ENGNA, Vol. 192, 1961, pp. 522–523.

[15] Stetson, A. R., "Thermal Fatigue Tests of Diffusion Coated Alloys," *Report to Ad Hoc Committee of ASTM-C22 RDR-1399*, American Society for Testing and Materials, 1966.

[16] Avery, L. R., Carayanis, G. S. and Michky, G. L., "Thermal-Fatigue Tests of Restrained Combustor-Cooling Tubes," *Experimental Mechanics*, EXMCA, Vol. 7, No. 6, 1967, pp. 256–264.

[17] Harman, D. G., *Thermal Fatigue of Rocket Nozzle Cooling Tubes*, Oak Ridge National Laboratory, ORNL TM 2089, 1969.

[18] King, R. H. and Smith, A. I., *Thermal and High-Strain Fatigue*, International Conference Metals and Metallurgy Trust of the Institute of Metals and the Institution of Metallurgists, London, 1969, pp. 364–378.

[19] Carden, A. E., *Bibliography of the Literature on Thermal Fatigue*, N68-23652 (NASA-CR-94605), University of Alabama, 1967. (Available from Clearinghouse for Federal Scientific and Technical Information, Springfield, Va.)

[20] *Bibliography on Low Cycle Fatigue, ASTM STP 449*, American Society for Testing and Materials, 1969.

[21] Rosenfield, A. R. and Averbach, B. L., "Effects of Stress on the Expansion Coefficient," *Journal of Applied Physics*, JAPIA, Vol. 27, No. 2, 1956, pp. 154–156.

[22] Wang, A. J. and Prager, W., "Thermal and Creep Effects in Work-Hardening Elastic-Plastic Solids," *Journal of the Aeronautical Sciences*, JASCA, Vol. 21, No. 5, 1954, pp. 343–344, 360.

INDEX

APPLICATION FOR 1970 ASTM ORGANIZATIONAL MEMBERSHIP

Extracts from Charter and Bylaws and Dues Schedule on REVERSE SIDE of this application

Application is made for membership in the American Society for Testing and Materials in the class of (check one):

☐ **SUSTAINING MEMBER** ☐ **INDUSTRIAL MEMBER** ☐ **INSTITUTIONAL MEMBER**

and if elected the applicant agrees to be governed by the Charter and Bylaws of the Society, and to further its objectives as laid down therein. (This membership includes: opportunities for participation of the Official Representative of the membership in the general and District activities of the Society, and for him [or others in the member organization whom he designates] to make application for participation on its technical committees; subscription(s) to **Materials Research & Standards**; parts of the **Book of Standards**; member discounts on publications; and other benefits and privileges.)

FORMAT FOR LISTING THE ASTM MEMBERSHIP

Please complete the grid below. PRINT or TYPE. Leave a space between words. Use no punctuation marks or special characters, except the ampersand (&). Use initials and abbreviations where necessary.

Line 1:—List the PARENT ORGANIZATION.
Line 2:—If applicable, list the FACILITY which will HOLD THE MEMBERSHIP.
Line 3:—Beginning in 8th position, list LAST NAME, FIRST NAME and MIDDLE INITIAL of the OFFICIAL REPRESENTATIVE who will exercise membership privileges.
Line 4:—TITLE of the Official Representative and DEPARTMENT
Line 5:—STREET ADDRESS or P. O. BOX for the MEMBER FACILITY
Line 6:—CITY (leave 1 space) STATE (leave 2 spaces) ZIP CODE

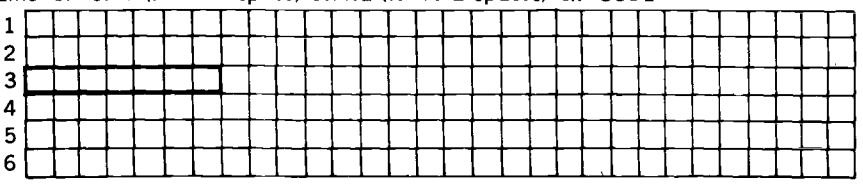

Major Product.....
(Or service performed by firm or organization)

Representative's Major Field of Interest.....
Examples: chemical research/civil engineering

Specific Application of Effort.....
Examples: polymer plastics/construction

ASTM MEMBERSHIP POLICY — The development of organization memberships and management understanding are vital to the Society's ability to serve the economy effectively in the future. The Society hopes that major organizations will help support its activities with one or more Sustaining Memberships. ASTM also offers inexpensive Industrial and Institutional memberships, providing substantial publications and participating benefits, to help small organizations or subdivisions benefit from affiliation with ASTM.

Each company should be concerned with the number and the classes of membership it maintains. Memberships should be located as needed to take optimum advantage of ASTM's activities. Also, the combination of memberships selected should tend to keep the organization's annual subscription to the Society in line with regard to the benefits it derives from ASTM (in terms of standards, committee participants, etc.) and with the organization's stature in the economy.

Therefore, except for those organizations the Society recognizes as "sister" societies and the agencies of the United States government (each of which may participate on ASTM's Technical Committees with or without a membership in the Society), each organization or major subdivision desiring to obtain publications of the Society at membership prices, or to share in the activities of the Society, should maintain at least one membership in the Society in the name of the organization. The organization's membership may be supplemented by Personal and Associate Memberships as desired.

Name .....
Signature of Person Authorized to Apply for Membership

Position .....

Address .....

SEE REVERSE SIDE FOR DUES AND BENEFITS OF MEMBERSHIP

MAIL TO: American Society for Testing and Materials, 1916 Race St., Philadelphia, Pa. 19103

Application form on reverse side

INFORMATION ON ORGANIZATIONAL MEMBERSHIP FOR 1970

Extract From Charter: The corporation is formed for the promotion of knowledge of the materials of engineering, and the standardization of specifications and the methods of testing.

Extract From Bylaws: ARTICLE 1. Members and Their Election

Sec. 1. . . . . The rights of membership of Institutional, Industrial, and Sustaining Members shall be exercised by the individual who is designated as the official representative of that membership.

Sec. 3. An Institutional Member shall be a public library, educational institution, a nonprofit professional, scientific or technical society, government department or agency at the federal, state, city, county or township level, or separate divisions thereof, meeting the qualifications established by the Board of Directors for this classification.

Sec. 4. An Industrial Member shall be a plant, firm, corporation, partnership, or other business enterprise, or separate divisions thereof, trade association, or research institute meeting the qualifications established by the Board of Directors for this classification.

Sec. 5. A Sustaining Member shall be a person, plant, firm, corporation, society, department of government or other organization, or separate divisions thereof, electing to give greater support to the Society's activities through the payment of larger dues.

SCHEDULE of DUES and BENEFITS of MEMBERSHIP for 1970

Class of Organizational Membership	SUSTAINING	INDUSTRIAL	INSTITUTIONAL
Annual Dues[1]	$500 min.[2]	$125	$35
Participants Allowed on ASTM Technical Committees	No Limit	No Limit	No Limit
33-part **ASTM Annual Book of Standards** Free Parts Allowed (Maximum)[3]	33 Parts	6 Parts	2 Parts
Sets or Parts Available at Discount[4]	No Limit	No Limit	No Limit
Other Publications (Listed with Member Prices) Available at Discount[4]	No Limit	No Limit	No Limit
ASTM Year Book (Abridged Copy to New Members)	1 Free	1 Free	1 Free
Annual **ASTM Proceedings**	$12.00	$12.00	$12.00
Annual Subscriptions to:			
Materials Research and Standards[5]	6 Free[6]	1 Free	1 Free
ASTM News Bulletin[5]	See Limit	See Limit	See Limit
Journal of Materials	$12.00	$12.00	$12.00

[1] Membership year shall commence on the first day of January. Dues are payable in advance. The dues payment retroactive to 1 January must be received to complete a membership. An election to membership shall be voided if payment is not made within three months of notification of election to membership.

[2] Organizations wishing to provide increased support for the operations of the Society may supplement the minimum Sustaining Membership dues by an additional amount in the form of annual payments in such amounts and for such periods as the organization may choose or in the form of a lump sum in anticipation of annual payments of such additional dues.

[3] FREE PARTS of the Book of ASTM Standards are for shipment only to the Official Representative. They must be requested on the copy of the request form provided with the notification of election, and each year thereafter.

[4] Discount on sets or parts of the Book of ASTM Standards approx. 45% off list price. (Discount on other ASTM publications listed with member prices, approx. 20%.) QUANTITY prices are available on request. The member DISCOUNT is allowed ON REQUEST, if the current DUES payment has been received, if the MEMBERSHIP NUMBER is identified, and calls for shipment and billing to, the MEMBERSHIP ADDRESS. An appropriate HANDLING and SHIPPING charge is applied to each order, EXCEPT for the annual pre-publication order for sets or parts of the Book of ASTM Standards on which the PAYMENT in advance ACCOMPANIES the ASTM ORDER FORM (supplied to the Official Representative when the annual dues payment is received).

[5] The ASTM News Bulletin is combined with Materials Research & Standards for distribution to the Official Representative and those designated to receive the allowed subscriptions of MR&S. The ASTM News Bulletin is distributed to the additional individuals the organization designates as its representatives in ASTM's Committee activities. Of the Annual Dues, $5.00 is allocated for each annual subscription to Materials Research & Standards, and $1.00 for each annual subscription to the ASTM News Bulletin for every person designated as eligible to receive copies of one or both magazines, including representatives to the respective committees. (Not deductible.)

[6] ONE subscription to the Official Representative. FIVE subscriptions on request—identify recipients.

NOTE: Benefits of membership and prices of publications are subject to change without notice.

SELECTION OF AN OFFICIAL REPRESENTATIVE: Careful attention should be given the selection of the OFFICIAL Representative of an organizational membership. He should be qualified to exercise the rights and privileges of membership to enhance the overall interests of the organization. This would involve balloting on highly technical matters, and might include participation on technical committees, and selection of other participants for committee work. The Official Representative of an Organization's membership in the Society may be changed as needed.

VOTING RIGHTS: The Official Representative of each organizational membership shall be privileged to cast one ballot in Society matters.

APPLICATION FOR 1970 ASTM INDIVIDUAL MEMBERSHIP

Extracts from Charter and Bylaws and Dues Schedule on REVERSE SIDE of this application
The undersigned hereby applies for membership in the Americon Society for Testing and Moterials in the class of (check one):

☐ **PERSONAL MEMBER** ☐ **SENIOR ASSOCIATE MEMBER** ‡ ☐ **ASSOCIATE MEMBER**

and if elected the applicant agrees to be governed by the Charter and Bylows of the Society, and to further its objectives as laid down therein. (This membership includes: opportunities for the participation of the member in the general and District activities of the Society, and for him to make application for participation on its technical committees; subscription to Materials Research & Standards; member discounts on publications; and other benefits and privileges.)

FORMAT FOR LISTING THE ASTM MEMBERSHIP

Please complete the grid below. PRINT or TYPE. Leave a space between words. Use no punctuation marks or special characters, except the ampersand (&). Use initials and abbreviations where necessary.

Line 1:—List your LAST NAME, FIRST NAME and MIDDLE INITIAL
Line 2:—Beginning in 8th position, your TITLE and DEPARTMENT
Line 3:—List your PARENT ORGANIZATION (or self-employment)
Line 4:—If applicable, list the FACILTY in which you are EMPLOYED.
Line 5:—COMPANY street address or P. O. BOX
Line 6:—CITY (leave 1 space) STATE (leave 2 spaces) ZIP CODE
Line 7:—ADDRESS FOR MAIL (if OTHER than above)
Line 8:—CITY (leave 1 space) STATE (leave 2 spaces) ZIP CODE
Line 9:—LEAVE BLANK (for use by the Society)

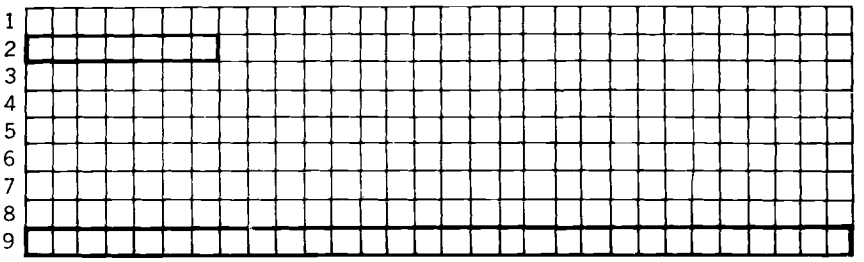

Major Product.....
(Or service performed by your organization or you, if self-employed)

Major Field of Interest.....
Examples: chemical research/civil engineering

Specific Application of Effort.....
Exomples: polymer plastics/construction

Date of Birth: Month.....Day.....Year.....

ASTM MEMBERSHIP POLICY — The development of organization memberships and management understanding are vital to the Society's ability to serve the economy effectively in the future. The Society hopes thot mojor organizations will help support its activities with one or more Sustoining Memberships. ASTM also offers inexpensive Industrial and Institutional memberships, providing substantial publications and participating benefits, to help small organizations or subdivisions benefit from affiliation with ASTM.

Each company should be concerned with the number and the classes of membership it maintains. Memberships should be located as needed to take optimum advontage of ASTM's activities. Also, the combination of memberships selected should tend to keep the organization's annual subscription to the Society in line with regard to the benefits it derives from ASTM (in terms of standards, committee participants, etc.) and with the organization's stature in the economy.

Therefore, except for those organizations the Society recognizes as "sister" societies ond the agencies of the United States government (each of which may participate on ASTM's Technical Committees with or without a membership in the Society), each organizotion or major subdivision desiring to obtain publications of the Society ot membership prices, or to share in the activities of the Society, should maintain at leost one membership in the Society in the name of the organization. The organization's membership may be supplemented by Personal and Associate Memberships as desired.

Applicant's Signature.....

‡Please attoch an outline of your prior ASTM affiliation.

SEE REVERSE SIDE FOR DUES AND BENEFITS OF MEMBERSHIP

MAIL TO: American Society for Testing and Materials,
1916 Race St., Philadelphia, Pa. 19103

Application form on reverse side

INFORMATION ON INDIVIDUAL MEMBERSHIP FOR 1970

Extract From Charter:

The corporation is formed for the promotion of knowledge of the materials of engineering, and the standardization of specifications and the methods of testing.

Extract From Bylaws:

ARTICLE 1. Members and Their Election

Sec. 2. A Personal Member shall be a person meeting the qualifications established by the Board of Directors for this classification. ("The basic qualification . . . shall be that he is interested in the Society's field of activities.")

Sec. 6. An Associate Member shall be a person less than thirty years of age. He shall have the same rights and privileges as a Personal Member, except that he shall not be eligible for office. An Associate Member shall not remain in this category beyond the end of the calendar year in which his thirtieth birthday occurs.

Sec. 8. A Senior Associate Member shall be a person who is fully retired from his regular employment, who has been a member of the Society and/or a participant in an activity of the Society for a total of ten years or more, not necessarily continuously, and who elects to continue his association with the Society through the payment of reduced dues. He shall have the same rights and privileges as a Personal Member, except as may be limited by the Board of Directors for this classification.

SCHEDULE of DUES and BENEFITS of MEMBERSHIP for 1970

Class of Individual Membership	PERSONAL	ASSOCIATE	SENIOR ASSOCIATE
Annual Dues[1]	$20	$10	$10
Member's Participation on ASTM Technical Committees	No Limit	No Limit	No Limit
33-part **ASTM Annual Book of Standards**			
Free Parts Allowed[2]	1 Part	None	None
Parts Available at Discount (Maximum)[3]	2 Parts	2 Parts	2 Parts
Other Publications (Listed with Member Prices)			
Available at Discount[3]	No Limit	No Limit	No Limit
ASTM Year Book (Abridged Copy to New Members)	1 Free	1 Free	1 Free
Annual **ASTM Proceedings**	$12.00	$12.00	$12.00
Annual Subscriptions to:			
Materials Research & Standards[4]	1 Free	1 Free	1 Free
ASTM News Bulletin[4]	1 Free	1 Free	1 Free
Journal of Materials	$12.00	$12.00	$12.00
Registration (badge and program) at ASTM National Meetings	. . .	. . .	Free

[1] Membership year shall commence on the first day of January. Dues are payable in advance. The dues payment retroactive to 1 January must be received to complete a membership. An election to membership shall be voided if payment is not made within three months of notification of election to membership.

[2] The FREE PART of the Book of ASTM Standards must be requested on the copy of the request form provided with the notification of election and each year thereafter.

[3] Discount on the two PARTS of the Book of ASTM Standards, approx. 45% off list price. (Discount on other ASTM publications listed with member prices, approx. 20%.) The two PARTS can be obtained at member prices ONLY if ordered on, and paid for with the ASTM ORDER FORM (supplied to the member when the annual dues payment is received). The member DISCOUNT is allowed ON REQUEST, if the current DUES payment has been received, if the MEMBERSHIP NUMBER is identified, and calls for shipment and billing to, the MEMBERSHIP ADDRESS. An appropriate HANDLING and SHIPPING charge is applied to each order, EXCEPT for the annual pre-publication order for parts of the Book of ASTM Standards on which the PAYMENT in advance accompanies the ASTM ORDER FORM.

[4] The ASTM News Bulletin is combined with Materials Research & Standards for distribution to the individual members of the Society. Of the Annual Dues, $5.00 is allocated for each annual subscription to Materials Research & Standards, and $1.00 for each annual subscription to the ASTM News Bulletin. (Not deductible.)

NOTE: Benefits of membership and prices of publications are subject to change without notice.

VOTING RIGHTS: Each member shall be privileged to cast one ballot in Society matters, and may apply for participation in any of the Technical Committee activities of the Society. Individual memberships in the Society are non-transferable.